RESEARCH REPORT

HEALTH EFFECTS INSTITUTE

Number 212
July 2022

Mortality–Air Pollution Associations in Low Exposure Environments (MAPLE): Phase 2

Michael Brauer, Jeffrey R. Brook, Tanya Christidis, Yen Chu, Dan L. Crouse, Anders Erickson, Perry Hystad, Chi Li, Randall V. Martin, Jun Meng, Amanda J. Pappin, Lauren L. Pinault, Michael Tjepkema, Aaron van Donkelaar, Crystal Weagle, Scott Weichenthal, Richard T. Burnett

Includes a Commentary by the Institute's Low-Exposure Epidemiology Studies Review Panel

ISSN 1041-5505 (print)
ISSN 2688-6855 (online)

Mortality–Air Pollution Associations in Low Exposure Environments (MAPLE): Phase 2

Michael Brauer, Jeffrey R. Brook, Tanya Christidis, Yen Chu, Dan L. Crouse, Anders Erickson, Perry Hystad, Chi Li, Randall V. Martin, Jun Meng, Amanda J. Pappin, Lauren L. Pinault, Michael Tjepkema, Aaron van Donkelaar, Crystal Weagle, Scott Weichenthal, Richard T. Burnett

with a Commentary by HEI's Low-Exposure Epidemiology Studies Review Panel

---

Research Report 212

Health Effects Institute

Boston, Massachusetts

Trusted Science · Cleaner Air · Better Health

Publishing history: This document was posted at *www.healtheffects.org* in July 2022.

Citation for document:

Brauer M, Brook JR, Christidis T, Chu Y, Crouse DL, Erickson A, et al. 2022. Mortality–Air Pollution Associations in Low Exposure Environments (MAPLE): Phase 2. Research Report 212. Boston, MA: Health Effects Institute.

Cover paper: made with at least 55% recycled content, of which at least 30% is post-consumer waste; free of acid and elemental chlorine. Text paper: made with 100% post-consumer waste recycled content; acid free; no chlorine used in processing. The book is of permanent archival quality.

CONTENTS

ABOUT HEI

The Health Effects Institute is a nonprofit corporation chartered in 1980 as an independent research organization to provide high-quality, impartial, and relevant science on the effects of air pollution on health. To accomplish its mission, the Institute

- Identifies the highest-priority areas for health effects research
- Competitively funds and oversees research projects
- Provides intensive independent review of HEI-supported studies and related research
- Integrates HEI's research results with those of other institutions into broader evaluations
- Communicates the results of HEI's research and analyses to public and private decision makers.

HEI typically receives balanced funding from the U.S. Environmental Protection Agency and the worldwide motor vehicle industry. Frequently, other public and private organizations in the United States and around the world also support major projects or research programs. HEI has funded more than 340 research projects in North America, Europe, Asia, and Latin America, the results of which have informed decisions regarding carbon monoxide, air toxics, nitrogen oxides, diesel exhaust, ozone, particulate matter, and other pollutants. These results have appeared in more than 260 comprehensive reports published by HEI, as well as in more than 2,500 articles in the peer-reviewed literature.

HEI's independent Board of Directors consists of leaders in science and policy who are committed to fostering the public–private partnership that is central to the organization. The Research Committee solicits input from HEI sponsors and other stakeholders and works with scientific staff to develop a Five-Year Strategic Plan, select research projects for funding, and oversee their conduct. For this study, a special panel — HEI's Low-Exposure Epidemiology Studies Oversight Panel — worked with the Research Committee in project selection and oversight. The Review Committee, which has no role in selecting or overseeing studies, typically works with staff to evaluate and interpret the results of funded studies and related research. For this study, a special review panel — HEI's Low-Exposure Epidemiology Studies Review Panel — fulfilled this role.

All project results and accompanying comments by HEI's Low-Exposure Epidemiology Studies Review Panel are widely disseminated through HEI's website (*www.healtheffects.org*), reports, newsletters and other publications, annual conferences, and presentations to legislative bodies and public agencies.

ABOUT THIS REPORT

Research Report 212, *Mortality–Air Pollution Associations in Low Exposure Environments (MAPLE): Phase 2,* presents a research project funded by the Health Effects Institute and conducted by Dr. Michael Brauer of The University of British Columbia, Vancouver, BC, Canada, and his colleagues. The report contains three main sections.

The HEI Statement, prepared by staff at HEI, is a brief, nontechnical summary of the study and its findings; it also briefly describes the Low-Exposure Epidemiology Studies Review Panel's comments on the study.

The Investigators' Report, prepared by Brauer and colleagues, describes the scientific background, aims, methods, results, and conclusions of the study.

The Commentary, prepared by members of the Low-Exposure Epidemiology Studies Review Panel with the assistance of HEI staff, places the study in a broader scientific context, points out its strengths and limitations, and discusses remaining uncertainties and implications of the study's findings for public health and future research.

This report has gone through HEI's rigorous review process. When an HEI-funded study is completed, the investigators submit a draft final report presenting the background and results of the study. This draft report is first examined by outside technical reviewers and a biostatistician. The report and the reviewers' comments are then evaluated by members of an independent Panel of distinguished scientists who are not involved in selecting or overseeing HEI studies. During the review process, the investigators have an opportunity to exchange comments with the Panel and, as necessary, to revise their report. The Commentary reflects the information provided in the final version of the report.

CONTRIBUTORS

LOW-EXPOSURE EPIDEMIOLOGY STUDIES OVERSIGHT PANEL

Jonathan M. Samet, Chair *Dean of the Colorado School of Public Health, University of Colorado–Denver*

Amy H. Herring *Sara & Charles Ayres Professor of Statistical Science and Global Health, Duke University, and member of the HEI Research Committee*

Jay H. Lubin *Senior Research Scientist (retired), National Cancer Institute, Division of Cancer Epidemiology & Genetics, Biostatistics Branch*

Fred W. Lurmann *Chairman / Manager of Exposure Assessment Studies, Sonoma Technology, Inc.*

LOW-EXPOSURE EPIDEMIOLOGY STUDIES REVIEW PANEL

Sverre Vedal, Chair *Professor, Environmental and Occupational Health Sciences, University of Washington*

Sara D. Adar *Associate Professor, Epidemiology, School of Public Health, University of Michigan*

Benjamin Barratt *Senior Lecturer in Chinese Environment, King's College, London, United Kingdom*

Kiros T. Berhane *Professor of Biostatistics and Director of Graduate Programs in Biostatistics and Epidemiology, Department of Preventive Medicine, Keck School of Medicine, University of Southern California, and member of the HEI Review Committee*

Christopher J. Paciorek *Adjunct Professor, Statistical Computing Consultant, Department of Statistics, University of California–Berkeley*

Jennifer L. Peel *Professor of Epidemiology, Colorado School of Public Health and Department of Environmental and Radiological Health Sciences, Colorado State University, and member of the HEI Review Committee*

Gavin Shaddick *Chair of Data Science and Statistics, Department of Mathematics, University of Exeter, United Kingdom*

HEI PROJECT STAFF

Hanna Boogaard *Consulting Principal Scientist (Study Oversight)*

Martha Ondras *Research Fellow (Report Review and Commentary)*

Eva Tanner *Staff Scientist (Report Review and Commentary)*

Eleanne van Vliet *Staff Scientist (Report Review)*

Kristin Eckles *Senior Editorial Manager*

Hope Green *Editorial Project Manager*

Carol Moyer *Consulting Editor*

PREFACE

HEI's Program to Assess Adverse Health Effects of Long-Term Exposure to Low Levels of Ambient Air Pollution

INTRODUCTION

Levels of ambient air pollution have declined significantly over the last few decades in North America, Europe, and in other developed regions. Despite the decreasing levels of air pollution, several large epidemiological studies published in the early 2010s reported associations between adverse health effects and exposure to air pollution. These studies found associations between exposure to fine particulate matter ($PM_{2.5}$*) and mortality at levels below the then-curent ambient air quality standards (e.g., Beelen et al. 2014a, b; Crouse et al. 2012; Hales et al. 2012; Preface Figure 1). In order to inform future risk assessment and regulation, it is important to confirm whether associations with adverse health effects continue to be observed as levels of air pollution decline still further. It is also important to better understand the shape of the exposure–response function at those low levels. Both issues remain major uncertainties in setting air quality standards.

The growing scientific evidence for effects at pollution levels below current air quality standards, the large overall estimates of the burden of disease attributable to air pollution, and the interest in reducing greenhouse gases suggest that more stringent air quality standards and guidelines may be considered in the future. For these reasons, there was a need for additional investigation to improve our understanding of exposure–response function(s) for mortality and morbidity at low levels of $PM_{2.5}$, ozone (O_3), and other ambient air pollutants. Such studies would inform risk assessors and policy makers regarding exposure–response functions at levels of ambient air pollution currently prevalent in North America, Western Europe, and other high-income regions of the world.

In 2014, HEI issued RFA 14-3, *Assessing Health Effects of Long-Term Exposure to Low Levels of Ambient Air Pollution*, to solicit studies to address these important questions. The main goals of the RFA were to (1) fund studies to assess health effects of long-term exposure to low levels of ambient air pollution, including all-cause and cause-specific mortality and morbidity. Such studies should analyze and evaluate exposure–response function(s) for $PM_{2.5}$ and other pollutants at levels currently prevalent in North America, Western Europe, and other high-income regions and may also address related questions about health effects at low levels of ambient air pollution; and (2) develop statistical and other methodology required for, and specifically suited to, conducting such research including, but not limited to, evaluation and correction of exposure measurement error.

Investigators were asked to pay particular attention to having sufficiently large cohorts and statistical power to detect associations should they exist; having the ability to test various potential confounders of any associations; and to developing exposure assessment approaches and statistical methodology to enable a robust examination of the associations.

Specifically, investigators were asked to propose studies to

1. Compare and contrast alternative analytic models and their uncertainty. For example, compare threshold against nonthreshold models, linear against nonlinear models, and parametric against nonparametric models, to characterize

* A list of abbreviations and other terms appears at the end of this volume.

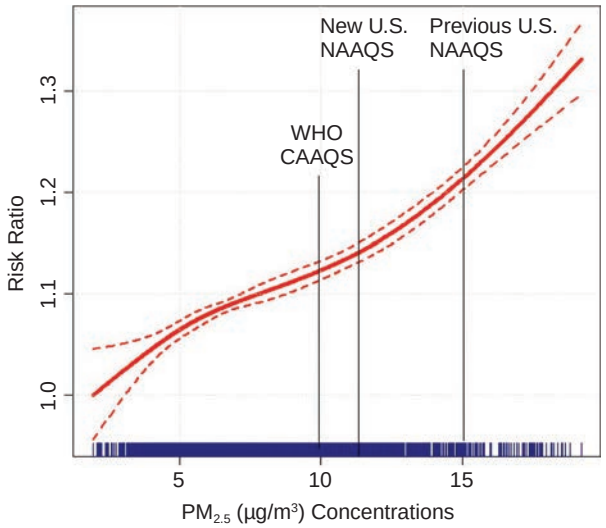

Preface Figure 1. Shape of concentration–response function for mortality associated with fine particulate matter in a Canadian cohort. (Adapted from Crouse et al. 2012, courtesy R. Burnett.)

the exposure–response function(s) at low levels of ambient air pollution.

2. Explore possible variability in estimates of risk at low levels among populations and identify possible contributing factors. Such factors could include age, smoking, socio-economic position, health status, and access to medical care, as well as differences in air pollution sources and time–activity patterns.
3. Develop and evaluate exposure assessment methods suitable to estimate exposure to low levels of air pollution at various spatial and temporal scales in large study populations, including people who reside in areas not covered by routine ground-level monitoring.
4. Develop, evaluate, and apply statistical methods to quantify and correct for exposure measurement error in risk estimates and in characterization of exposure–response relationships.
5. Develop and validate approaches to assess the effects of co-occurring pollutants on any health effect associations at low ambient concentrations.
6. Develop and validate indirect approaches to correct risk estimates for the effects of important potential confounding variables, such as smoking, in the absence of such data at the individual level.
7. Improve techniques for record linkage and methods for disclosure protection for optimal use of large administrative databases in air pollution and health research.

STUDY SELECTION

HEI established an independent Low Exposure Epidemiology Oversight Panel — consisting of outside experts and HEI Research Committee members — to prepare RFA 14-3 and review all applications submitted in response (see Contributors' page). Members of HEI's Research Committees with any conflict of interest were recused from all discussions and from the decision-making process. The HEI Research Committee reviewed the Panel's recommendations and recommended three studies for funding to HEI's Board of Directors, which approved funding in 2015.

This Preface summarizes the three studies, HEI's oversight process, and the review process for the reports.

Preface

OVERVIEW OF THE LOW EXPOSURE EPIDEMIOLOGY STUDIES

After a rigorous selection process, HEI funded three teams — led by Michael Brauer at The University of British Columbia, Canada; Francesca Dominici at the Harvard T.H. Chan School of Public Health, United States; and Bert Brunekreef at the University of Utrecht, the Netherlands — to investigate the health effects of exposure to low levels of air pollution in very large populations in Canada, the United States, and Europe, respectively (see Preface Table and Preface Figure 1). The studies included large population cohorts (with detailed individual information about potential confounders on all or a subset of the cohort) as well as large administrative databases with greater statistical power (albeit with less individual covariate information). Additionally, the three teams employed satellite data and ground-level exposure measurements, used high-quality exposure assessment models at high spatial resolutions, and set out to develop and apply novel statistical methods.

The three studies were expected to inform the scientific community and risk assessors and policy makers regarding exposure–response functions at levels of ambient air pollution currently prevalent in North America, Western Europe, and other developed regions. The full sets of analyses were expected to be completed in 2021 (see below).

CANADIAN STUDY (MICHAEL BRAUER ET AL.)

Brauer and colleagues proposed to assess the relationship between nonaccidental mortality and long-term exposure to low concentrations of $PM_{2.5}$ in four large population-based cohorts, including a careful characterization of the shape of the exposure–response function. The investigators used Canadian census data and had access to a nationally representative population of approximately 8.5 million Canadians (ages 25–90 yr) (Preface Figure 2). The Canadian team proposed developing hybrid models using primarily satellite data, as well as chemical transport models, land use variables, and routinely collected monitoring data for $PM_{2.5}$, as well as estimating exposures for NO_2 and O_3 for Canada and the United States during the period 1981–2016. Additionally, they planned to validate satellite data against ground-based monitors in Canada as part of the SPARTAN network (Snider et al. 2015).

Preface Table. HEI's Research Program to Assess Adverse Effects of Long-Term Exposure to Low Levels of Ambient Air Pollution

Investigator (institution)	Study Title	Phase 1 Report	Final Report Published
Brauer, Michael (University of British Columbia, Canada)	Mortality–Air Pollution Associations in Low Exposure Environments (MAPLE)	HEI Research Report 203 (2019)	HEI Research Report 212 (July 2022)
Brunekreef, Bert (Utrecht University, the Netherlands)	Mortality and Morbidity Effects of Long-Term Exposure to Low-Level $PM_{2.5}$, BC, NO_2, and O_3: An Analysis of European Cohorts in the ELAPSE Project	None	HEI Research Report 208 (September 2021)
Dominici, Francesca (Harvard T.H. Chan School of Public Health, USA)	Assessing Adverse Health Effects of Long-Term Exposure to Low Levels of Ambient Air Pollution	HEI Research Report 200 (2019)	HEI Research Report 211 (January 2022)

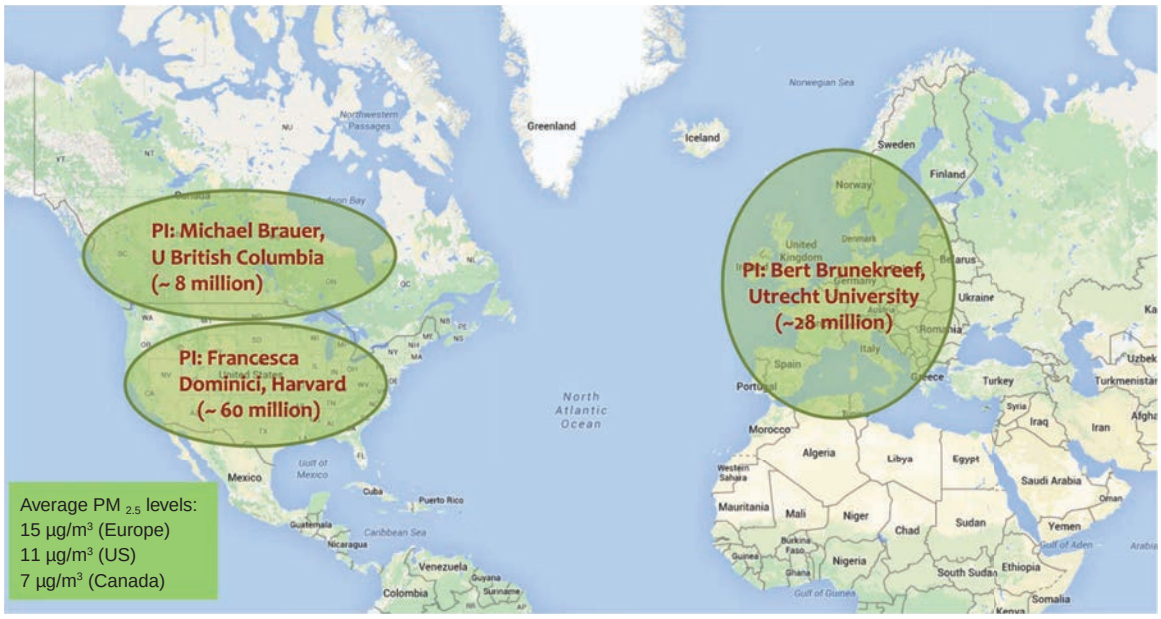

Preface Figure 2. Geographical areas and populations covered by HEI's Research Program to assess adverse effects of long-term exposure to low levels of ambient air pollution.

The exposure models were to be applied to estimate effects of air pollution exposure on all-cause and cause-specific mortality in four Canadian cohorts:

1. About 2.6 million subjects who completed the 1991 census long-form of the Canadian Census Health and Environment Cohorts (CanCHEC),
2. About 3.5 million subjects who completed the 1996 CanCHEC census long-form,
3. About 3.5 million subjects who completed the 2001 CanCHEC census long-form, and
4. About 540,000 subjects who participated in the Canadian Community Health Survey (CCHS) between 2001 and 2012, and reported individual-level risk factors, including smoking.

EUROPEAN STUDY (BERT BRUNEKREEF ET AL.)

Brunekreef and colleagues based their study on the European Study of Cohorts for Air Pollution Effects (ESCAPE), which started about a decade ago; its results have been published widely (e.g., Beelen et al. 2014a, b; Cesaroni et al. 2014; Eeftens et al. 2012a, b). In the current HEI-funded study, the investigators proposed to analyze pooled data from 10 ESCAPE cohorts (instead of the cohort-specific approach they used previously). In addition, they planned to use data from six large administrative cohorts to yield a total study population of approximately 28 million Europeans (Preface Figure 2). They proposed developing hybrid Europewide and location-specific exposure models that would utilize land use information, dispersion modeling, satellite data, ESCAPE monitoring data, and routinely collected monitoring data for $PM_{2.5}$, NO_2, O_3, and black carbon at high spatial resolution (residential address level; such detailed information is very difficult to obtain in the United States).

Brunekreef and colleagues proposed to investigate the following health outcomes: all-cause and cause-specific mortality, incidence of coronary and cerebrovascular events, and lung cancer incidence. The incorporation of ESCAPE cohorts with individual covariate information as well as very large administrative cohorts (albeit with less detailed information) will provide new insights into the merits of both approaches.

UNITED STATES STUDY (FRANCESCA DOMINICI ET AL.)

Dominici and colleagues proposed to evaluate Medicare and Medicaid data for a study population of approximately 60 million Americans (Preface Figure 2). They planned to develop hybrid exposure models that incorporate satellite data, chemical transport models, land use, and weather variables, and routinely collected monitoring data for $PM_{2.5}$ and its components, NO_2, and O_3, at high spatial resolution (1-km^2 grid) for the continental United States during the period 2000–2014. Exposure models were to be applied to estimate adverse health effects of air pollution in three cohorts:

1. Medicare enrollees (28.6 million elderly enrollees per year, 2000–2014);
2. Medicaid enrollees (28 million enrollees per year, 2010–2014); and
3. Medicare Current Beneficiary Survey enrollees (nationally representative sample of approximately 15,000 enrollees per year with rich individual-level risk factor information, including smoking).

Dominici and colleagues planned to analyze the following health outcomes: time to hospitalization by cause, disease progression (time to rehospitalization), and time to death. They proposed developing and applying new causal inference methods to estimate exposure–response functions to adjust for confounding and exposure measurement error. Additionally, they proposed developing tools for reproducible research including approaches for data sharing, record linkage, and statistical software.

STUDY OVERSIGHT

HEI's independent Low Exposure Epidemiology Oversight Panel provided advice and feedback on the study designs, analytical plans, and study progress throughout the duration of the research program (see Contributors' page).

Given the substantial challenges in conducting a systematic analysis to assess health effects of long-term exposure to low levels of ambient air pollution, HEI worked actively with the study teams to coordinate their efforts and ensure the maximum degree of comparable epidemiological results at the end of this research effort. To this end, HEI regularly held investigator workshops and site visits, among other activities. In addition, the studies were subject to HEI's special quality assurance procedures that included an audit by an independent audit team (see *www.healtheffects.org/research/quality-assurance*).

REVIEW OF PHASE 1 AND FINAL (PHASE 2) REPORTS

To inform the ongoing review of the U.S. National Ambient Air Quality Standards (NAAQS) for $PM_{2.5}$ and O_3 during 2019–2020, HEI requested Phase 1 reports based on the research completed during the first two years of the Canadian and U.S. studies. Thus, the Phase 1 reports by Drs. Brauer and Dominici provided summaries of results to date, including those published in journal articles, with accompanying Commentaries by an independent Special Review Panel. These Phase 1 reports provided an opportunity to review the results to date and evaluate their strengths and weaknesses, a process normally performed after a study has been completed.

As is common for major research programs, HEI convened a Special Review Panel to independently review the Phase 1 reports by Drs. Brauer and Dominici. The Panel consists of seven experts in epidemiology, exposure assessment, and biostatistics (see Contributors' page). The Panel also reviewed the final (Phase 2) reports of the three studies.

The three studies commenced in Spring 2016 and were completed at different times in 2020, with final reports published during 2021. In addition, further analyses, for example to compare approaches among the three teams, are ongoing and are expected to be completed in 2022.

REFERENCES

Beelen R, Raaschou-Nielsen O, Stafoggia M, Andersen ZJ, Weinmayr G, Hoffmann B, et al. 2014a. Effects of long-term exposure to air pollution on natural-cause mortality: An analysis of 22 European cohorts within the multicentre ESCAPE project. Lancet 383:785–795.

Beelen R, Stafoggia M, Raaschou-Nielsen O, Andersen ZJ, Xun WW, Katsouyanni K, et al. 2014b. Long-term exposure to air pollution and cardiovascular mortality: An analysis of 22 European cohorts. Epidemiology 25:368–378; doi: 10.1097/EDE.0000000000000076.

Cesaroni G, Forastiere F, Stafoggia M, Andersen ZJ, Badaloni C, Beelen R, et al. 2014. Long term exposure to ambient air pollution and incidence of acute coronary events: Prospective cohort study and meta-analysis in 11 European cohorts from the ESCAPE project. BMJ 348:f7412; doi: 10.1136/bmj.f7412.

Crouse DL, Peters PA, van Donkelaar A, Goldberg MS, Villeneuve PJ, Brion O, et al. 2012. Risk of nonaccidental and cardiovascular mortality in relation to long-term exposure to low concentrations of fine particulate matter: A Canadian national-level cohort study. Environ Health Perspectives 120:708–714.

Eeftens M, Beelen R, de Hoogh K, Bellander T, Cesaroni G, Cirach M, et al. 2012a. Development of land use regression models for $PM_{2.5}$, $PM_{2.5}$ absorbance, PM_{10} and PM_{coarse} in 20 European study areas: Results of the ESCAPE project. Environ Sci Technol 46:11195–11205; doi: 10.1021/es301948k.

Eeftens M, Tsai MY, Ampe C, Anwander B, Beelen R, Bellander T, et al. 2012b. Spatial variation of $PM_{2.5}$, PM_{10}, $PM_{2.5}$ absorbance and PM_{coarse} concentrations between and within 20 European study areas and the relationship with NO_2: Results of the ESCAPE project. Atmos Environ 62:303–317.

Hales S, Blakely T, Woodward A. 2012. Air pollution and mortality in New Zealand: Cohort study. J Epidemiol Community Health 66:468–473; doi: 10.1136/jech.2010.112490.

Snider G, Weagle CL, Martin RV, van Donkelaar A, Conrad K, Cunningham D, et al. 2015. SPARTAN: A global network to evaluate and enhance satellite-based estimates of ground-level particulate matter for global health applications. Atmos Meas Tech 8:505–521; doi.org/10.5194/amt-8-505-2015.

HEI STATEMENT

Synopsis of Research Report 212, Phase 2

Mortality–Air Pollution Associations in Low-Exposure Environments (MAPLE): Phase 2

BACKGROUND

Growing scientific evidence indicates that effects of air pollution on health are observed at concentrations below current air quality standards. Combined with the large burden of disease attributed to air pollution exposure, this is resulting in consideration of more stringent air quality standards and guidelines. To improve our understanding of exposure–response functions for mortality and morbidity at low concentrations of fine particulate matter ($PM_{2.5}$), nitrogen dioxide, ozone, and other ambient air pollutants, HEI issued RFA 14-3, *Assessing Health Effects of Long-Term Exposure to Low Levels of Ambient Air Pollution*. Three studies based in the United States, Canada, and Europe were funded. The studies used state-of-the-art exposure assessment methods with large cohorts in high-income countries where ambient concentrations are generally lower than current air quality guidelines and standards for Europe and the United States. HEI convened an independent Low-Exposure Epidemiology Studies Review Panel to evaluate the studies' strengths and weaknesses. This Statement highlights results from the study in Canada.

What This Study Adds

- The MAPLE study evaluated whether exposure to fine particulate matter ($PM_{2.5}$) at concentrations below current air quality standards was associated with an increased risk of nonaccidental death among 7.1 million Canadian adults.
- Combining satellite data, air monitor sampling, and atmospheric modeling, the investigators estimated outdoor $PM_{2.5}$ exposures across Canada from 1981 to 2016.
- They applied comprehensive epidemiological analyses in a large representative sample of Canadian adults to evaluate the risk of death at different $PM_{2.5}$ exposure ranges and to identify the lowest concentration at which associations with health effects could be detected.
- Long-term outdoor $PM_{2.5}$ exposures as low as 2.5 μg /m^3 were associated with increased risk of death, with variation across different geographical regions and with smaller effects when adjusted for ozone concentrations.
- This study identified associations with health effects at $PM_{2.5}$ concentrations below the current U.S. ambient air quality standard of 12 μg/m^3, suggesting that lowering the standard could yield further health benefits.

APPROACH

The Mortality–Air Pollution Associations in Low-Exposure Environments (MAPLE) study by Brauer and colleagues aimed to characterize the association between long-term exposure to outdoor $PM_{2.5}$ and death in a nationally representative sample of Canadian adults, with a focus on $PM_{2.5}$ concentrations below current air quality standards. They created $PM_{2.5}$ exposure estimates across North America from 1981 to 2016 that incorporated satellite, ground monitor, and atmospheric modeling data. The study had the following objectives:

1. To evaluate the association between long-term outdoor $PM_{2.5}$ exposure and total and cause-specific nonaccidental death, including assessments among people with exposures below the current U.S. air quality standard
2. To evaluate these associations across regions of Canada with different atmospheric conditions while accounting for exposure to the co-occurring pollutant ozone
3. To examine whether the association between $PM_{2.5}$ exposure and death changed over different exposure ranges
4. To identify the $PM_{2.5}$ concentration below which there was no association with increased risk of death.

This Statement, prepared by the Health Effects Institute, summarizes a research project funded by HEI and conducted by Dr. Michael Brauer at The University of British Columbia, School of Population and Public Health, Vancouver, BC, Canada, and colleagues. Research Report 212 contains both the detailed Investigators' Report and a Commentary on the study prepared by the Institute's Low-Exposure Epidemiology Studies Review Panel.

The investigators assembled a census-based cohort that combined three cycles of the Canadian Census Health and Environment Cohort. It comprised 7.1 million people and recorded 1.3 million deaths over the 25-year study period (1991–2016). They estimated outdoor $PM_{2.5}$ concentrations averaged over 10 years at a 1×1 km resolution and then assigned exposure for each participant based on home postal codes and accounted for address changes. They used Cox hazards regression to assess the overall average association of the assigned $PM_{2.5}$ exposure with death. In addition, they used the Shape Constrained Health Impact Function model to examine the shape of the association over the full range of exposures as well as whether the association changed over different exposure ranges. The analyses were adjusted for the region of Canada, census year, and many individual- and community-level sociodemographic factors. The specific causes of death evaluated were death from cardiovascular disease, cerebrovascular disease, ischemic heart disease, heart failure, diabetes, nonmalignant respiratory disease, chronic obstructive pulmonary disease (COPD), pneumonia, lung cancer, and kidney failure.

KEY RESULTS

Long-term outdoor $PM_{2.5}$ exposure was associated with increased total nonaccidental death (hazard ratio per 4.16 μg/m³ = 1.034; 95% confidence interval = 1.030–1.039). In other words, an interquartile range increase in $PM_{2.5}$ exposure from the 25th to 75th percentile was associated with 32 more deaths for every 100,000 people each year when compared with the average annual death rate over the 25-year study period. Given Canada's population in 2016, this rate equates to 7,848 more deaths every year. In cause-specific analyses, higher $PM_{2.5}$ exposure was also associated with increased risk of death due to cardiovascular disease, ischemic heart disease, cerebrovascular disease, diabetes, pneumonia, respiratory disease, and COPD.

The shape of the association between $PM_{2.5}$ and death was nonlinear; this means that the association varied for different concentrations of $PM_{2.5}$ exposure (Statement Figure). The relative risk of death increased rapidly from the minimum $PM_{2.5}$ concentrations of 2.5 μg/m³. At $PM_{2.5}$ concentrations of 5 μg/m³ and above, the relative risk of death increased linearly at a shallower slope. The investigators did not detect a definitive $PM_{2.5}$ concentration below which no health effects were observed; they observed positive associations with risk of death near the lowest $PM_{2.5}$ exposure in this study, 2.5 μg/m³.

Results were similar when limiting the analysis to people with $PM_{2.5}$ exposure below 12 μg/m³, the current U.S. air quality standard. In contrast, there was no association when limiting the analysis to people with $PM_{2.5}$ exposure below the former Canadian standard of 10 μg/m³. Brauer and colleagues suggested that higher exposures were influential in deriving the statistical estimates of the association between $PM_{2.5}$ and death. However, they noted that limiting the exposure concentration to 10 μg/m³ resulted in a sample group of people

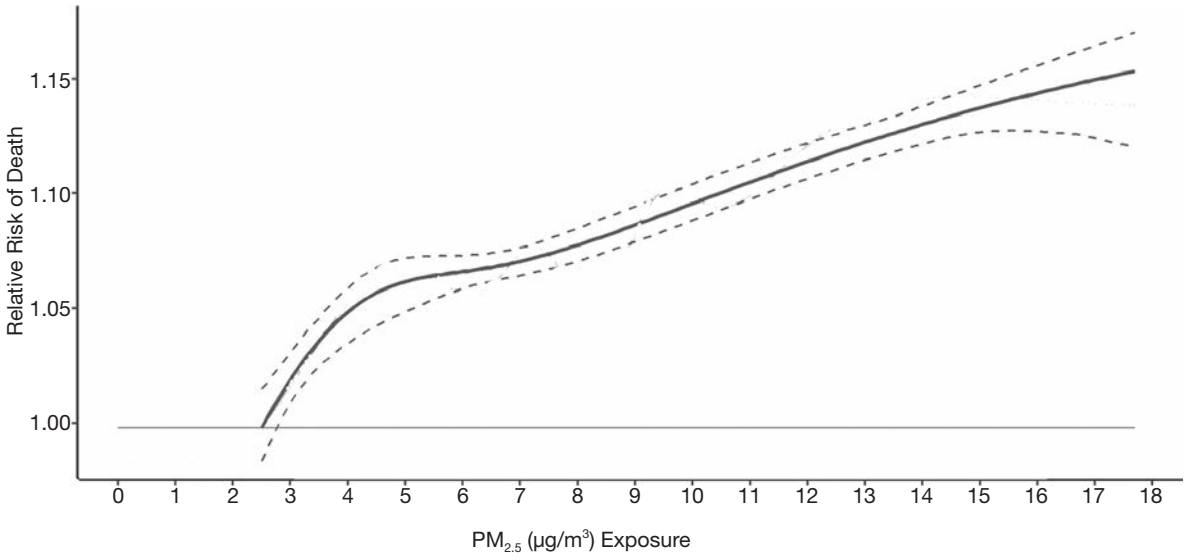

Statement Figure. Shape of the association between outdoor $PM_{2.5}$ exposure and nonaccidental death. This plot shows how the risk of death changes over different $PM_{2.5}$ exposure concentrations. The relative risk of death compares the lowest observed $PM_{2.5}$ concentration (2.5 μg/m³) to all higher concentrations. (Adapted from Investigators' Report Figure 29.)

who were demographically different from the original nationally representative sample. Therefore, the results from the restricted sample might not apply to the population of Canada as a whole. Furthermore, the association was smaller when adjusting for co-occurring pollutant ozone, and different results were observed for the different regions of Canada. The results were similar after adjusting for lifestyle factors and for regional differences in population characteristics and healthcare access. That suggests that co-occurring pollutants and atmospheric conditions are important determinants of the association between $PM_{2.5}$ and death.

INTERPRETATION AND CONCLUSIONS

This study found that low-level $PM_{2.5}$ exposure was associated with increased risk of total and cause-specific deaths. The results also found that the risk of death is not the same across all $PM_{2.5}$ concentrations. The largest change in the increased risk of death occurred among people with the lowest $PM_{2.5}$ exposure concentrations. The results were largely in agreement with prior studies that have shown increased risk of death for total, respiratory, and cardiovascular-related mortality. This study adds to the growing number of studies that suggest the shape of the association is steepest at lower $PM_{2.5}$ concentrations.

In its independent review of the study, HEI's Low-Exposure Epidemiology Studies Review Panel commended the investigators for assembling such comprehensive data, creating state-of-the-art $PM_{2.5}$ exposure estimates and thorough statistical analyses. However, the Panel noted that some results were difficult to interpret. For example, the Shape Constrained Health Impact Function showed that the shape of the association was largest at lower $PM_{2.5}$ concentrations but limiting the Cox hazards analysis to people with $PM_{2.5}$ exposures below 10 $\mu g/m^3$ showed no association. There were also different results for specific regions of Canada that could not be attributed to measured demographic differences but which might reflect differences in the mixture of air pollutants. Because the study had a large sample size and good statistical power, the Panel concluded that the effects of bias more so than random error could have influenced the results. Sources of bias might include confounding factors that the investigators were unable to control for, such as other copollutants. Exposure measurement error could have also differed across the urban versus rural regions of Canada.

In conclusion, the Panel agreed that this study found evidence of associations between $PM_{2.5}$ and health effects at concentrations well below 12 $\mu g/m^3$, the current U.S. ambient air quality standard. Future work is needed to investigate the influence of other copollutants and atmospheric conditions.

INVESTIGATORS' REPORT

Mortality–Air Pollution Associations in Low Exposure Environments (MAPLE): Phase 2

Michael Brauer[1,2], Jeffrey R. Brook[3], Tanya Christidis[4], Yen Chu[1], Dan L. Crouse[5], Anders Erickson[1], Perry Hystad[6], Chi Li[7], Randall V. Martin[7,8,9], Jun Meng[7], Amanda J. Pappin[4], Lauren L. Pinault[4], Michael Tjepkema[4], Aaron van Donkelaar[7], Crystal Weagle[7], Scott Weichenthal[10], Richard T. Burnett[11]

[1]The University of British Columbia, Vancouver, British Columbia, Canada; [2]Institute for Health Metrics and Evaluation, University of Washington, Seattle, Washington; [3]University of Toronto, Toronto, Ontario, Canada; [4]Health Analysis Division, Statistics Canada, Ottawa, Ontario, Canada; [5]University of New Brunswick, Fredericton, New Brunswick, Canada; [6]Oregon State University, Corvallis, Oregon; [7]Dalhousie University, Halifax, Nova Scotia, Canada; [8]Washington University, Saint Louis, Missouri; [9]Harvard-Smithsonian Center for Astrophysics, Cambridge, Massachusetts; [10]McGill University, Montreal, Quebec, Canada; [11]Population Studies Division, Health Canada, Ottawa, Ontario, Canada

ABSTRACT

INTRODUCTION

Mortality is associated with long-term exposure to fine particulate matter (particulate matter ≤2.5 µm in aerodynamic diameter; $PM_{2.5}$*), although the magnitude and form of these associations remain poorly understood at lower concentrations. Knowledge gaps include the shape of concentration–response curves and the lowest levels of exposure at which increased risks are evident and the occurrence and extent of associations with specific causes of death. Here, we applied improved estimates of exposure to ambient $PM_{2.5}$ to national population-based cohorts in Canada, including a stacked cohort of 7.1 million people who responded to census year 1991, 1996, or 2001. The characterization of the shape of the concentration–response relationship for nonaccidental mortality and several specific causes of death at low levels of exposure was the focus of the Mortality–Air Pollution Associations in Low Exposure Environments (MAPLE) Phase 1 report. In the Phase 1 report we reported that associations between outdoor $PM_{2.5}$ concentrations and nonaccidental mortality were attenuated with the addition of ozone (O_3) or a measure of gaseous pollutant oxidant capacity (O_x), which was estimated from O_3 and nitrogen dioxide (NO_2) concentrations. This was motivated by our interests in understanding both the effects air pollutant mixtures may have on mortality and also the role of O_3 as a copollutant that shares common sources and precursor emissions with those of $PM_{2.5}$. In this Phase 2 report, we further explore the sensitivity of these associations with O_3 and O_x, evaluate sensitivity to other factors, such as regional variation, and present ambient $PM_{2.5}$ concentration–response relationships for specific causes of death.

METHODS

$PM_{2.5}$ concentrations were estimated at 1 km² spatial resolution across North America using remote sensing of aerosol optical depth (AOD) combined with chemical transport model (GEOS-Chem) simulations of the AOD:surface $PM_{2.5}$ mass concentration relationship, land use information, and ground monitoring. These estimates were informed and further refined with collocated measurements of $PM_{2.5}$ and AOD, including targeted measurements in areas of low $PM_{2.5}$ concentrations collected at five locations across Canada. Ground measurements of $PM_{2.5}$ and total suspended particulate matter (TSP) mass concentrations from 1981 to 1999 were used to backcast remote-sensing-based estimates over that same time period, resulting in modeled annual surfaces from 1981 to 2016.

Annual exposures to $PM_{2.5}$ were then estimated for subjects in several national population-based Canadian cohorts using residential histories derived from annual postal code entries in income tax files. These cohorts included three census-based cohorts: the 1991 Canadian Census Health and Environment Cohort (CanCHEC; 2.5 million respondents), the 1996 CanCHEC (3 million respondents), the 2001 CanCHEC

This Investigators' Report is one part of Health Effects Institute Research Report 212, which also includes a Commentary by the Low-Exposure Epidemiology Studies Review Panel and an HEI Statement about the research project. Correspondence concerning the Investigators' Report may be addressed to Dr. Michael Brauer, The University of British Columbia, School of Population and Public Health, 366A – 2206 East Mall, Vancouver, BC V6T1Z3, Canada; e-mail: *michael.brauer@ubc.ca.* No potential conflict of interest was reported by the authors.

Although this document was produced with partial funding by the United States Environmental Protection Agency under Assistance Award CR–83467701 to the Health Effects Institute, it has not been subjected to the Agency's peer and administrative review and therefore may not necessarily reflect the views of the Agency, and no official endorsement by it should be inferred. The contents of this document also have not been reviewed by private party institutions, including those that support the Health Effects Institute; therefore, it may not reflect the views or policies of these parties, and no endorsement by them should be inferred.

* A list of abbreviations and other terms appears at the end of this volume.

(3 million respondents), and a Stacked CanCHEC where duplicate records of respondents were excluded (Stacked CanCHEC; 7.1 million respondents). The Canadian Community Health Survey (CCHS) mortality cohort (mCCHS), derived from several pooled cycles of the CCHS (540,900 respondents), included additional individual information about health behaviors. Follow-up periods were completed to the end of 2016 for all cohorts. Cox proportional hazard ratios (HRs) were estimated for nonaccidental and other major causes of death using a 10-year moving average exposure and 1-year lag. All models were stratified by age, sex, immigrant status, and where appropriate, census year or survey cycle. Models were further adjusted for income adequacy quintile, visible minority status, Indigenous identity, educational attainment, labor-force status, marital status, occupation, and ecological covariates of community size, airshed, urban form, and four dimensions of the Canadian Marginalization Index (Can-Marg; instability, deprivation, dependency, and ethnic concentration). The mCCHS analyses were also adjusted for individual-level measures of smoking, alcohol consumption, fruit and vegetable consumption, body mass index (BMI), and exercise behavior.

In addition to linear models, the shape of the concentration–response function was investigated using restricted cubic splines (RCS). The number of knots were selected by minimizing the Bayesian Information Criterion (BIC). Two additional models were used to examine the association between nonaccidental mortality and $PM_{2.5}$. The first is the standard threshold model defined by a transformation of concentration equaling zero if the concentration was less than a specific threshold value and concentration minus the threshold value for concentrations above the threshold. The second additional model was an extension of the Shape Constrained Health Impact Function (SCHIF), the eSCHIF, which converts RCS predictions into functions potentially more suitable for use in health impact assessments. Given the RCS parameter estimates and their covariance matrix, 1,000 realizations of the RCS were simulated at concentrations from the minimum to the maximum concentration, by increments of 0.1 μg/m³. An eSCHIF was then fit to each of these RCS realizations. Thus, 1,000 eSCHIF predictions and uncertainty intervals were determined at each concentration within the total range.

Sensitivity analyses were conducted to examine associations between $PM_{2.5}$ and mortality when in the presence of, or stratified by tertile of, O_3 or O_x. Additionally, associations between $PM_{2.5}$ and mortality were assessed for sensitivity to lower concentration thresholds, where person-years below a threshold value were assigned the mean exposure within that group. We also examined the sensitivity of the shape of the nonaccidental mortality–$PM_{2.5}$ association to removal of person-years at or above 12 μg/m³ (the current U.S. National Ambient Air Quality Standard) and 10 μg/m³ (the current Canadian and former [2005] World Health Organization [WHO] guideline, and current WHO Interim Target-4). Finally, differences in the shapes of $PM_{2.5}$–mortality associations were assessed across broad geographic regions (airsheds) within Canada.

RESULTS

The refined $PM_{2.5}$ exposure estimates demonstrated improved performance relative to estimates applied previously and in the MAPLE Phase 1 report, with slightly reduced errors, including at lower ranges of concentrations (e.g., for $PM_{2.5}$ <10 μg/m³).

Positive associations between outdoor $PM_{2.5}$ concentrations and nonaccidental mortality were consistently observed in all cohorts. In the Stacked CanCHEC analyses (1.3 million deaths), each 10-μg/m³ increase in outdoor $PM_{2.5}$ concentration corresponded to an HR of 1.084 (95% confidence interval [CI]: 1.073 to 1.096) for nonaccidental mortality. For an interquartile range (IQR) increase in $PM_{2.5}$ mass concentration of 4.16 μg/m³ and for a mean annual nonaccidental death rate of 92.8 per 10,000 persons (over the 1991–2016 period for cohort participants ages 25–90), this HR corresponds to an additional 31.62 deaths per 100,000 people, which is equivalent to an additional 7,848 deaths per year in Canada, based on the 2016 population. In RCS models, mean HR predictions increased from the minimum concentration of 2.5 μg/m³ to 4.5 μg/m³, flattened from 4.5 μg/m³ to 8.0 μg/m³, then increased for concentrations above 8.0 μg/m³. The threshold model results reflected this pattern with −2 log-likelihood values being equal at 2.5 μg/m³ and 8.0 μg/m³. However, mean threshold model predictions monotonically increased over the concentration range with the lower 95% CI equal to one from 2.5 μg/m³ to 8.0 μg/m³. The RCS model was a superior predictor compared with any of the threshold models, including the linear model.

In the mCCHS cohort analyses inclusion of behavioral covariates did not substantially change the results for both linear and nonlinear models. We examined the sensitivity of the shape of the nonaccidental mortality–$PM_{2.5}$ association to removal of person-years at or above the current U.S. and Canadian standards of 12 μg/m³ and 10 μg/m³, respectively. In the full cohort and in both restricted cohorts, a steep increase was observed from the minimum concentration of 2.5 μg/m³ to 5 μg/m³. For the full cohort and the <12 μg/m³ cohort the relationship flattened over the 5 to 9 μg/m³ range and then increased above 9 μg/m³. A similar increase was observed for the <10 μg/m³ cohort followed by a clear decline in the magnitude of predictions over the 5 to 9 μg/m³ range and an increase above 9 μg/m³. Together these results suggest that a positive association exists for concentrations >9 μg/m³ with indications of adverse effects on mortality at concentrations as low as 2.5 μg/m³.

Among the other causes of death examined, $PM_{2.5}$ exposures were consistently associated with an increased hazard

of mortality due to ischemic heart disease, respiratory disease, cardiovascular disease, and diabetes across all cohorts. Associations were observed in the Stacked CanCHEC but not in all other cohorts for cerebrovascular disease, pneumonia, and chronic obstructive pulmonary disease (COPD) mortality. No significant associations were observed between mortality and exposure to $PM_{2.5}$ for heart failure, lung cancer, and kidney failure.

In sensitivity analyses, the addition of O_3 and O_x attenuated associations between $PM_{2.5}$ and mortality. When analyses were stratified by tertiles of copollutants, associations between $PM_{2.5}$ and mortality were only observed in the highest tertile of O_3 or O_x. Across broad regions of Canada, linear HR estimates and the shape of the eSCHIF varied substantially, possibly reflecting underlying differences in air pollutant mixtures not characterized by $PM_{2.5}$ mass concentrations or the included gaseous pollutants. Sensitivity analyses to assess regional variation in population characteristics and access to healthcare indicated that the observed regional differences in concentration–mortality relationships, specifically the flattening of the concentration–mortality relationship over the 5 to 9 μg/m^3 range, was not likely related to variation in the makeup of the cohort or its access to healthcare, lending support to the potential role of spatially varying air pollutant mixtures not sufficiently characterized by $PM_{2.5}$ mass concentrations.

CONCLUSIONS

In several large, national Canadian cohorts, including a cohort of 7.1 million unique census respondents, associations were observed between exposure to $PM_{2.5}$ with nonaccidental mortality and several specific causes of death. Associations with nonaccidental mortality were observed using the eSCHIF methodology at concentrations as low as 2.5 μg/m^3, and there was no clear evidence in the observed data of a lower threshold, below which $PM_{2.5}$ was not associated with nonaccidental mortality.

INTRODUCTION

Exposure to fine particulate matter ($PM_{2.5}$) is generally accepted as a causal risk factor for mortality and was estimated to be responsible for 4.1 million deaths and 118 million disability-adjusted life years in 2019 (Global Burden of Disease [GBD] 2019 Risk Factors Collaborators 2020). Multiple large epidemiological cohort studies have linked long-term exposure to $PM_{2.5}$ with an increased risk for nonaccidental mortality and chronic diseases such as lung cancer, heart disease, and stroke (Beelen et al. 2014; Burnett et al. 2018; Crouse et al. 2015; Di et al. 2017; Li et al. 2018; Pope et al. 2002; Pun et al. 2017; Yin et al. 2017).

Positive associations between outdoor $PM_{2.5}$ mass concentrations and mortality have also been repeatedly demonstrated in populations living in areas with low $PM_{2.5}$ levels. For example, building on prior analyses of cohorts in Canada (Crouse et al. 2012, 2015; Nasari et al. 2016; Pinault et al. 2016a, 2017; Weichenthal et al. 2017), the MAPLE Phase 1 report and related publications reported an increased risk of nonaccidental mortality (HR = 1.053; 95% CI: 1.041 to 1.065 per 10-μg/m^3 increase) using pooled CanCHEC results and a somewhat higher risk of nonaccidental mortality in a cohort of mCCHS respondents (HR =1.110; 1.040 to 1.180). Understanding the shapes of the concentration–response relationships in areas with low $PM_{2.5}$ concentrations is of particular interest, as many global regions are approaching these lower levels of exposure (Apte et al. 2015). Canada provides an ideal setting to study the shapes of these relationships given the availability of large national cohorts with sufficient sample sizes, detailed information on outdoor air pollution concentrations, and importantly, nearly all Canadians live in areas with relatively low $PM_{2.5}$ concentrations. Specifically, $PM_{2.5}$ median concentrations for the three cycles of CanCHEC in the MAPLE Phase 1 report were 6.4 (2001 CanCHEC), 6.7 (1996 CanCHEC), and 7.4 (1991 CanCHEC) μg/m^3, and 5.5 μg/m^3 in the mCCHS cohort, across all person-years. These levels are below the 2005 World Health Organization Guideline and the current (2021) World Health Organization Interim Target-4 (10 μg/m^3 annual average) and are below the U.S. National Ambient Air Quality Standard (12 μg/m^3) and the Canadian Ambient Air Quality Standard (8.8 μg/m^3) for $PM_{2.5}$. Median concentration of the 2001 CanCHEC are close to the 2021 World Health Organization Air Quality Guideline of 5 μg/m^3 annual average.

In Canada, we previously reported that associations between outdoor $PM_{2.5}$ mass concentrations and cardiovascular, respiratory, and nonaccidental mortality varied across tertiles of outdoor O_x concentrations suggesting that copollutants may influence the shape of concentration–response curves for $PM_{2.5}$ (Weichenthal et al. 2017). As few cohort studies have specifically evaluated interactions between $PM_{2.5}$ and O_x, it isn't clear if this effect modification is caused by a direct effect of O_x on the lungs (e.g., depletion of antioxidants, increased permeability of the lung epithelium barrier) or if O_x is simply a reasonable surrogate for a certain type of air pollution mixture (e.g., a more highly oxidized or aged aerosol) that is more relevant to health (Blomberg et al. 2003; Broeckaert et al. 2000; Ciencewicki et al. 2008; Croberddu et al. 2017; Georas and Rezaee 2014; Kienast et al. 1994; Lakey et al. 2016; Rattanavaraha et al. 2011; Safari et al. 2014). Possible interactions between O_x and $PM_{2.5}$ are of interest for two reasons. First, if O_x directly modifies the health effects of $PM_{2.5}$ (i.e., if $PM_{2.5}$ is more harmful when O_x is higher) this opens up additional regulatory options for reducing the health effects of $PM_{2.5}$ because reductions in O_x would decrease the health effects of $PM_{2.5}$ even if mass concentrations did not change. Alternatively, if O_x is simply a good marker for air pollution mixtures most relevant to health, these areas can be identified and prioritized for

future interventions. In this report we explored this question further by using multiple cohorts as part of Phase 2 of the MAPLE project. As levels of O_x may vary regionally, we additionally evaluated regional population variation and its potential effects on regional variation in the $PM_{2.5}$–mortality relationship as alternative explanations for the observed oxidant effect modification.

STUDY RATIONALE

The aim of this ongoing project, MAPLE, is to provide updated analyses on associations between outdoor fine particulate air pollution and mortality outcomes, using larger and more recent epidemiological cohorts than the 1991 CanCHEC. This project includes the 1991, 1996, and 2001 CanCHEC cohorts and the cohort of CCHS respondents from 2001–2012 (mCCHS), with follow-up to 2016 for all cohorts. A stacked cohort of the three cycles of CanCHECs was also created, where recurring participants were excluded if they were sampled in more than one CanCHEC cycle. For each of these cohorts, we deterministically linked participants to mortality records using individual identifiers (social insurance number), whereas prior analyses used a combination of deterministic and probabilistic linkage, which introduces greater uncertainty.

In the MAPLE Phase 1 report, we assessed associations between outdoor air pollution concentrations and nonaccidental mortality using the three separate CanCHEC cycles (Pappin et al. 2019) and mCCHS (Christidis et al. 2019). A pooled HR estimate was also determined for the three CanCHEC cycles. Similarly, a pooled concentration–response function was also estimated from the shapes of corresponding functions in the three separate CanCHEC cycles. Note that this pooling of HRs from analyses of the three CanCHEC cohorts differs from the approach used in this Phase 2 report, in which individuals were merged into a single stacked cohort. Our Phase 1 analyses incorporated minimally adjusted models, a model informed by a directed acyclic graph to help inform causal relationships, and a fully adjusted model including all individual and contextual available for linkage.

In addition, we evaluated the following during Phase 1:

1. **Refining Spatial Resolution —** MAPLE assigned exposures based on a fine-scale $PM_{2.5}$ model of ~1 km × 1 km resolution that incorporated both remote sensing-based estimates and ground-level observations (Crouse et al. 2020; Pinault et al. 2017).
2. **Residential Mobility at Follow-Up —** MAPLE used a complete annual residential history generated for all cohort members based on a linkage to postal codes from tax records (as in Crouse et al. 2015). Missing postal codes in residential histories were imputed with a probabilistic algorithm (adapted from Finès et al. 2017).
3. **Year-Adjusted Exposure Estimates —** As in Crouse et al. 2015, MAPLE used time-varying exposures based on year-adjusted estimates from 1981 onward. In the case of MAPLE, a new more sophisticated backcasting approach was used in estimating historical exposures (Meng et al. 2019).
4. **Behavioral Covariates —** Parallel analyses were conducted in a new, larger mCCHS cohort, and indirect adjustment for missing behavioral risk factors was also evaluated for application to the CanCHEC cohorts (Christidis et al. 2019; Erickson et al. 2019).
5. **Immigrants** — Most prior analyses excluded all immigrants outright or limited their inclusion based on their time in Canada (e.g., minimum 20 years). In MAPLE we included all immigrant respondents who have been in Canada for at least 10 years prior to the cohort index year. Immigrants who have been in Canada for fewer than 10 years have an unknown prior exposure history (Erickson et al. 2020).

In the Phase 1 report, we focused on examining associations with nonaccidental mortality, and reported a pooled HR of 1.053 (95% CI: 1.041 to 1.065) among the three CanCHECs, and a HR of 1.130 (1.060 to 1.210) in the mCCHS cohort. The shape of the concentration–response curve using the SCHIF indicated a supralinear association in all cohorts. Associations between outdoor $PM_{2.5}$ concentrations and nonaccidental mortality were attenuated with the addition of O_3 or a weighted measure of oxidant gases, O_x. We also found that associations were strengthened with the use of longer moving averages to assign exposures, and smaller spatial scales of exposure estimates. Indirect adjustment for missing behavioral covariates (e.g., smoking and BMI) had very little effect on these associations. The strength of the observed association between outdoor $PM_{2.5}$ and nonaccidental mortality was similar between immigrants and nonimmigrants in Canada.

In this Phase 2 report, we focus on developing a more detailed understanding of these relationships, including analysis of cause-specific mortality, analysis examining the sensitivity of $PM_{2.5}$ associations to the inclusion of O_3 or O_x in the models, and other factors such as regional variation. We present results for both the mCCHS cohort, where behavioral risk factors were measured, and for three separate CanCHEC cohorts. An important update from Phase 1 is the use of a Stacked CanCHEC cohort, where all participants from the three CanCHEC cycles were included together, and participants in repeated, subsequent cycles were excluded. The stacked cohort represented 7.1 million respondents followed over 128 million person-years, or about 20.2% of the population of Canada as of the 2016 census. We also updated our analyses using longer moving average exposures, as sensitivity analyses in Phase 1 indicated that a longer moving average (i.e., 10 years) provided stronger associations with mortality (Crouse et al. 2020). The $PM_{2.5}$ models were further refined from the Phase 1 report by

incorporating an improved representation of aerosol mass scattering efficiency (MSE) for organic and secondary inorganic aerosol. This was based on MAPLE measurements at five sites in Canada of colocated $PM_{2.5}$ mass and chemical composition with AOD. These refined exposure models (V4.NA.02.MAPLE) demonstrated improved performance compared with those used in the MAPLE Phase 1 report (V4.NA.01). For example, at collocated ground-based stations in long-term mean comparisons across the range of observed $PM_{2.5}$, the root mean square difference (RMSD) was reduced from 1.9 to 1.5 μg/m^3, and for the low concentrations directly relevant to this study (e.g., for observed $PM_{2.5}$ <10 μg/m^3 at Canadian sites), RMSD was reduced from 1.7 to 1.4 μg/m^3.

STUDY AIMS

The primary aim of MAPLE is to provide a detailed characterization of the relationship between mortality and exposure to low concentrations of $PM_{2.5}$ in Canada. This work addresses many limitations of prior studies and extends the analyses presented in the Phase 1 report in a number of important ways.

The relationship between $PM_{2.5}$ exposure and nonaccidental mortality was described in our previous report using the three CanCHEC cohorts independently, and then pooled together. Our pooled estimate from three CanCHEC cycles for the association between nonaccidental mortality and $PM_{2.5}$ was HR = 1.053 (95% CI: 1.041 to 1.065 per 10-μg/m^3 increase). In the current report, we remove duplicate respondents who occur in more than one CanCHEC cycle, and determine a new HR based on the combined, or stacked cohort.

Our previous report also described sensitivity analyses of the $PM_{2.5}$ exposure–mortality relationship to different exposure metrics and the effects of including different immigrant groups. In this report, in addition to analyses of nonaccidental mortality we focus specifically on analyses of the relationship between $PM_{2.5}$ exposure and major causes of mortality, using the Stacked CanCHEC cohort. We then provide additional sensitivity analyses of the association between $PM_{2.5}$, O_3 and a weighted oxidative potential (i.e., O_x) for the gaseous pollutants O_3 and NO_2 as well as regional analyses to further investigate the shape of the $PM_{2.5}$–mortality relationship.

Exposure Assignment

As in the MAPLE Phase 1 report, we applied satellite-based $PM_{2.5}$ exposure estimates at a 1 km × 1 km spatial resolution across North America for each year from 1981–2016. These annual estimates are based on a combination of remote-sensing-based AOD, the GEOS-Chem, land use information, and ground-monitoring data (Latimer and Martin 2019; van Donkelaar et al. 2019). Estimates have been further refined since the Phase 1 report. Specifically, we

- developed and applied annual average satellite-based estimates of $PM_{2.5}$ across North America at 1 km × 1 km spatial resolution
- evaluated $PM_{2.5}$ estimates using insight gained from comparisons of collocated measurements of $PM_{2.5}$ and AOD with GEOS-Chem simulations of that relationship
- employed a combination of geophysical and statistical methods, together with land use information, to further refine the $PM_{2.5}$ estimates
- used available $PM_{2.5}$ and TSP monitoring data in Canada from 1981–1999, to scale the 1 km × 1 km surface back in time annually over the 1981 to 1999 period, maintaining the 1 km × 1 km grid detail over the 1981–2016 period
- made the refined $PM_{2.5}$ estimates available to other HEI-funded studies that cover Canada and the United States for incorporation into their analyses *https://sites.wustl.edu/acag/datasets/surface-pm2-5/*.

Epidemiological Analysis

We examined the shape of the association between long-term exposure to ambient concentrations of $PM_{2.5}$ and mortality in four large, population-based Canadian cohorts, and a stacked census-based cohort. Specifically, we

- linked the following long form census data cohorts to mortality, vital statistics, and tax records up to December 31, 2016:

  1991 CanCHEC (2.5 million participants); 1996 CanCHEC (3 million participants); 2001 CanCHEC (3 million participants); Stacked CanCHEC (7.1 million unique participants — data came from the 1991, 1996, and 2001 CanCHEC cohorts. Individuals who completed more than one long-form census (i.e., <20% in the next census year) were excluded from subsequent CanCHEC cohorts, ensuring that individuals were not counted more than once; mCCHS (540,900 participants who completed the 2001, 2003, 2005, 2007, 2008, 2009, 2010, 2011, or 2012 CCHS survey panels).
- examined the shape of the association between long-term exposure to ambient concentrations of $PM_{2.5}$ and mortality in all five cohorts using RCS and an extended version of the SCHIF that was first introduced in our Phase 1 report. This new eSCHIF methodology allows us to directly evaluate thresholds, to identify the lowest concentration for which there is evidence of a positive association with mortality and provides functions that are more suitable for benefits analyses.

METHODS

HUMAN STUDIES APPROVAL

The Research Ethics Board of The University of British Columbia determined this study in humans was exempt from ethical review.

EXPOSURE ASSESSMENT

Overview

Several steps are involved in the development of satellite-derived $PM_{2.5}$ estimates for MAPLE as shown in Figure 1. The development process combines daily satellite retrievals of AOD at 1 km × 1 km resolution with simulations of the daily AOD to $PM_{2.5}$ relationship (η) using the GEOS-Chem at 0.5° × 0.67° resolution to produce geophysical $PM_{2.5}$ estimates following the methods described in van Donkelaar and colleagues (2015, 2016). The GEOS-Chem simulation accounts for the relationship between available daily satellite observations and monthly mean concentrations. The next step in Figure 1 shows that geographically weighted regression is applied to statistically fuse monthly mean measurements from $PM_{2.5}$ monitors with the geophysical $PM_{2.5}$ estimates to produce refined hybrid $PM_{2.5}$ estimates. The right panel of Figure 1 shows that these hybrid estimates are backcasted using GEOS-Chem simulations and $PM_{2.5}$, PM_{10}, and TSP measurements to produce estimates for the 1981–1999 period as described later in the report and in more detail by Meng and colleagues (2019). A cross-cutting activity illustrated in the bottom-left of Figure 1 indicates that targeted colocated measurements of $PM_{2.5}$ and AOD were conducted at five measurement sites in Canada and applied to evaluate and refine the simulation of AOD-to-$PM_{2.5}$ as discussed in the next section.

Collection of Measurements

We expanded the Surface PARTiculate mAtter Network (SPARTAN) (Snider et al. 2015) to routinely collect colocated measurements of $PM_{2.5}$, aerosol scatter, and AOD at five sites across Canada. This collection allows us to evaluate and potentially improve simulations of the $PM_{2.5}$ to AOD ratio in regions of low $PM_{2.5}$ mass concentrations. A key source of uncertainty in this relationship is the MSE, the relation between particle

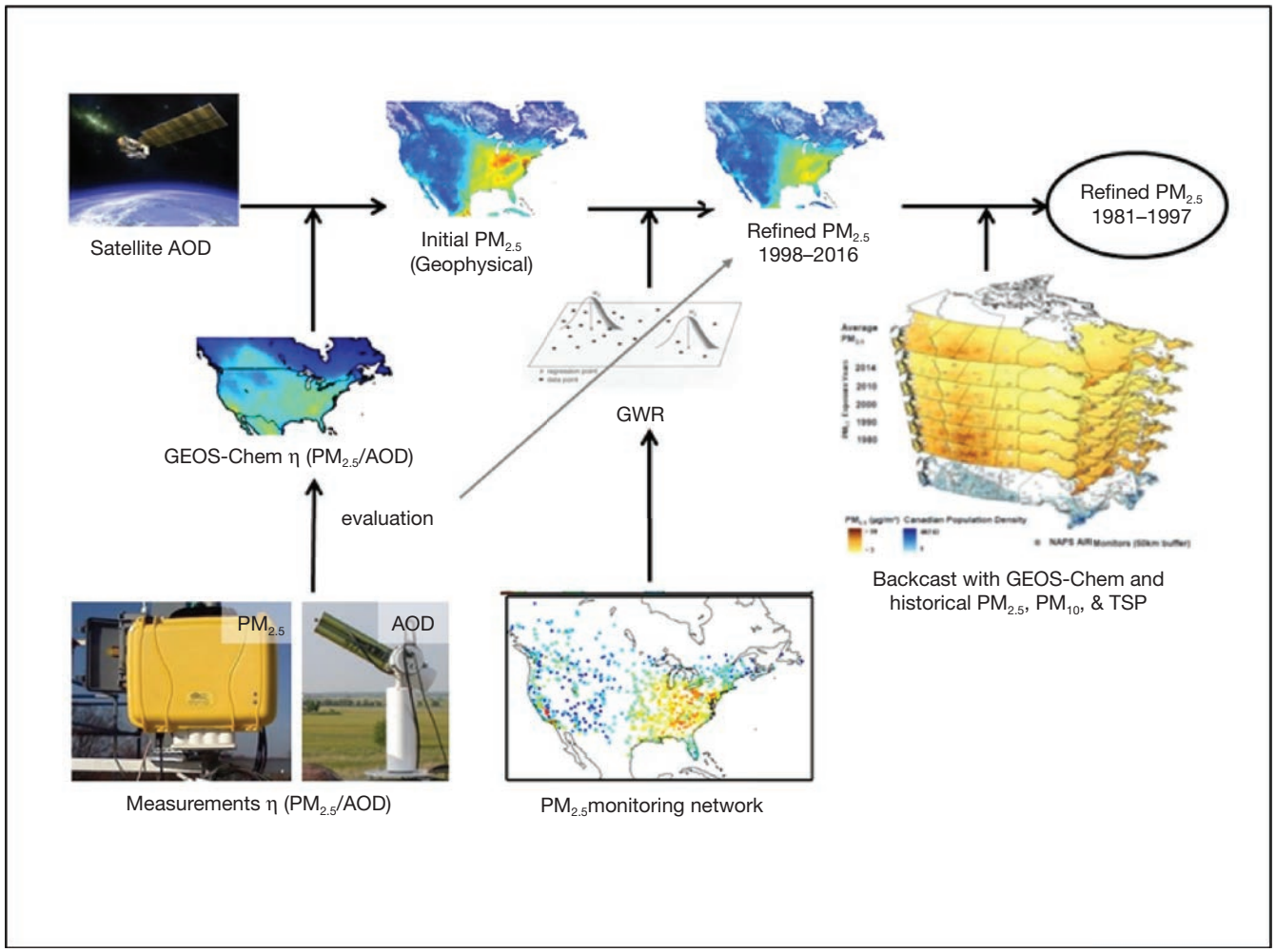

Figure 1. Schematic of the exposure development process for $PM_{2.5}$. GWR = geographically weighted regression.

scatter and $PM_{2.5}$ mass. MSE is fundamental to the measurement of AOD and influences the accuracy of $PM_{2.5}$ estimates as GEOS-Chem simulates the columnar AOD to surface $PM_{2.5}$ relationship. The MSE generally varies smoothly across large distances (Latimer and Martin 2019). Thus, only a moderate number of measurement locations across Canada are needed to evaluate the simulated MSE. As no routinely collected measurements for MSE were available in populated regions of Canada, these targeted ground-based measurements offer the potential to evaluate and improve these estimates.

Measurements include an impaction filter sampler for the analysis of mass and composition, as well as a nephelometer that provides a high temporal resolution for relating observations made during cloud-free conditions at satellite overpass time to the 24-hour averages. The combination of scatter and mass measurements allows for an assessment of the relationship between satellite measurements of backscattered sunlight and the $PM_{2.5}$ mass concentrations. These measurements are compared with GEOS-Chem simulations of the AOD to $PM_{2.5}$ relationship to better understand the geophysical processes affecting the relationship, and in turn to improve the ability of chemical transport models to predict this quantity.

Specifically, we added $PM_{2.5}$ monitors to five ongoing and diverse Canadian sites participating in the global Aerosol Robotic Network (AERONET; *http://aeronet.gsfc.nasa.gov/*) that routinely measure AOD. Figure 2 shows the locations of the collocated $PM_{2.5}$ and AOD measurement sites in Halifax, Nova Scotia; Sherbrooke, Quebec; Downsview, Ontario; Lethbridge, Alberta; and Kelowna, British Columbia.

A detailed explanation of SPARTAN chemical analysis methodology and the filter-based hygroscopicity parameter, κ, are provided by Snider and colleagues (2016). Briefly, all gravimetric analyses were performed in a cleanroom facility with a controlled temperature between 20 to 23°C and a relative humidity of 35 ± 5%, as per U.S. Environmental Protection Agency (U.S. EPA) protocols. Flow rates at ambient pressure and temperature at site locations determine the sampled air volume required to provide $PM_{2.5}$ concentrations in μg/m^3. Black carbon content was estimated from triplicate measurements of surface reflectance using a smoke stain reflectometer (Davy et al. 2017). Filters were subsequently analyzed for trace elements, including dust components (e.g., aluminum, iron, magnesium), via inductively coupled plasma-mass spectrometry and x-ray fluorescence spectrometry and then extracted in methanol and water and analyzed for water-soluble ions (e.g., sulfate, nitrate, ammonium) through ion chromatography. Trace element measurements are described in McNeille and colleagues (2020). As described in Snider and colleagues (2016), the residual matter component, estimated by subtracting the dry inorganic mass and particle-bound water from total $PM_{2.5}$ mass, is treated as predominately organic.

The Downsview MAPLE site was collocated with a National Air Pollution Surveillance (NAPS) site run by Environment and Climate Change Canada that included two sampling stations whose measurements are compared with MAPLE measurements. Comparison of daily $PM_{2.5}$ mass concentration is completed using estimated daily $PM_{2.5}$ from MAPLE versus the NAPS reference method sampler (Partisol). For speciation comparison, NAPS data from the SASS sampler (Met One) are sampled coincidently with the MAPLE integrated filter sample; for example, if a MAPLE filter was sampled August 8–16, 2018, any daily NAPS filter sample(s) from the corresponding time period (e.g., August 9, 12, and 15, 2018) are used to create a mean value.

Creating Refined $PM_{2.5}$ Exposure Estimates

We made further refinements with new information obtained from the ground-based monitoring samples and particle composition analyses. The variance in inferred MSE is smallest for organic and secondary inorganic components, reflecting their dominant contributions to $PM_{2.5}$ mass. The MSE for these two components is also consistent with a compilation of prior measurements by Hand and Malm (2007). We focus on these two components for MAPLE.

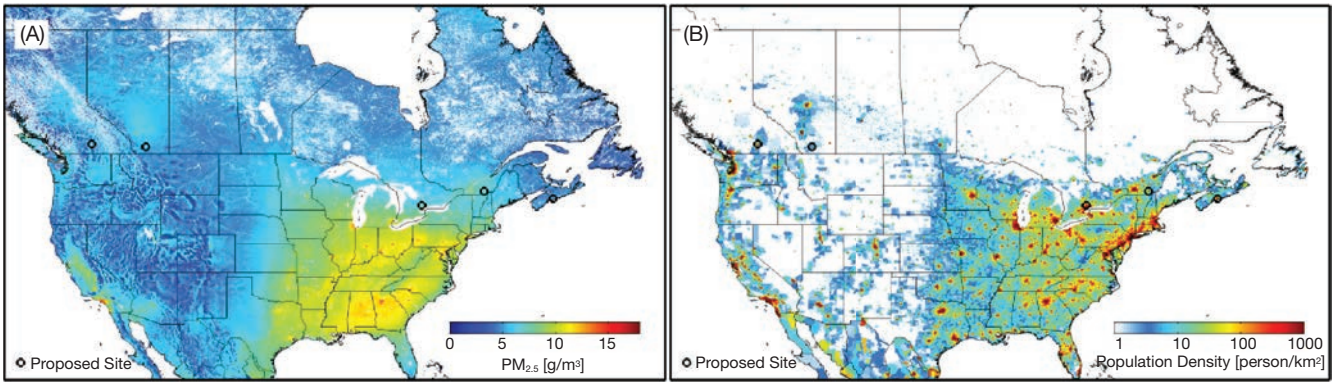

Figure 2. Location of collocated ground-based measurements of $PM_{2.5}$ and AOD. The background shows satellite-based estimates of $PM_{2.5}$ from **(A)** van Donkelaar et al. (2016) and **(B)** population density.

Utilizing the wavelength sensitivity of MSE and Mie calculations, an algorithm was developed and applied that inverts the wavelength-dependent measurements of aerosol scatter for aerosol size-distribution properties (Bissonnette 2019). The dry geometric mean diameter (D_{pg}) of organics and secondary inorganics is found to be 0.56 and 0.62 µm with correspondent geometric mean variance (σ_g) of 1.45 and 1.30 (unitless), respectively. These values are broadly consistent with the upper end of the few $PM_{2.5}$ size distribution measurements and estimates available for North America (e.g., Bissonnette 2019; Cabada et al. 2004). These revised representations of organic and secondary inorganic aerosol MSE and size are applied to refine the satellite-based estimates of $PM_{2.5}$, together with additional algorithmic developments as described later.

The revised exposure dataset for MAPLE (V4.NA.02.MAPLE) builds on specific components of the framework of van Donkelaar and colleagues (2015, 2016) used to create the V4.NA.01 dataset used by the MAPLE project, and the work described earlier. AOD in V4.NA.02.MAPLE is from an ensemble of satellite observations inversely weighted by their error characteristics versus AERONET measurements (van Donkelaar et al. 2019) rather than from a single retrieval as in van Donkelaar and colleagues (2015, 2016). The representation of aerosol hygroscopicity used to relate AOD at ambient relative humidity with $PM_{2.5}$ at controlled relative humidity is informed by a comparison of collocated measurements of aerosol scatter and $PM_{2.5}$ mass conducted for MAPLE as described by Latimer and Martin (2019). The representation of aerosol MSE used to relate aerosol scatter to mass for organic and secondary inorganic aerosol is refined based on an interpretation of MAPLE measurements across Canada (Bissonnette 2019) as summarized in the Results section. The geographic weighted regression used to fuse the satellite-based estimates with ground-based $PM_{2.5}$ mass observations separates the topographic and land-type predictors used in V4.NA.02 (van Donkelaar et al. 2019).

The revised exposure estimates were evaluated with ground-based monitors including RMSD, line of best fit, and coefficient of variation. The RMSD was calculated as

$$\mathrm{RMSD} = \sqrt{\frac{\sum_{i=1}^{N}(x_{e,i} - x_{m,i})^2}{N}}$$

where $x_{e,i}$ and $x_{m,i}$ are the estimated and measured $PM_{2.5}$ concentrations for monitor *i*.

Assigning Exposure Estimates to Cohorts

We applied the revised $PM_{2.5}$ estimates (dataset version V4.NA.02-MAPLE; Dalhousie University Atmospheric Composition Analysis Group) to all epidemiological analyses described in this report. All respondents in each cohort were assigned an exposure estimate based on residential location, defined by postal codes for each year from 1981 through 2016, from the closest 1 km × 1 km grid cell of the $PM_{2.5}$ surface described earlier. Postal codes were geocoded using the Statistic Canada Postal Code Conversion File Plus (PCCF+) containing the June 2017 postal code release with additional postal codes from the May 2011 and August 2015 releases (Statistics Canada 2017a). The PCCF+ contains representative coordinates for current and retired postal codes based on the centroid of a block face, dissemination block, or dissemination area. In Canadian urban areas, postal code locations typically represent one side of a street in a given block or the center of an apartment building and have positional accuracy within ~150 m; there is greater locational uncertainty for rural postal codes (i.e., typically accurate within about 1–5 km) (Khan et al. 2018). Missing postal codes were imputed based on those reported in adjacent years, using a method where the probability of imputation varies depending on the number of adjacent years missing (Finès et al. 2017). However, we refined the assignment of exposure to imputed postal codes implemented in previous publications (e.g., Crouse et al. 2015; Pinault et al. 2017), and for the present analyses required that postal codes available prior to and after a missing code had to have least two digits in common. Exposure was then assigned based on a population-weighted average of the various postal codes covered by these two digits. Previously, in cases where this criterion was not met, we had assigned exposure based on the national population-weighted average for that year.

Older versions of $PM_{2.5}$ data (V4.NA.01) were retained on the analytical files to allow us to conduct a sensitivity analysis comparing the older and newer (V4.NA.02-MAPLE) versions of the $PM_{2.5}$ datasets in epidemiological models, as presented in Appendix Tables A.6 and A.7, available on the HEI website.

Adjustment for NO_2, O_3, and O_x

We estimated ambient NO_2 concentrations at each postal code location based on a national land use regression model that predicted ground-monitoring concentrations for the year 2006 using 10-km^2 gridded remote sensing-derived NO_2 estimates and highly resolved land use data (Hystad et al. 2011). This model has a spatial resolution of 100 m^2. The daily maximum of eight-hour average concentrations of O_3 were estimated based on chemical transport modeling of surface observations in the warm season from 2002 to 2015 (i.e., the average of maximum values within the same 8-hour period each day during the warm season (Environment Canada 2013). From 2002 to 2009 the spatial resolution of the O_3 model was 21 km^2 and was subsequently improved to 10 km^2. Hourly O_3 model output was fused with ground monitor data (Robichaud and Menard 2014; Robichaud et al. 2016) as part of the routine Canadian air quality forecast modeling system. These hourly data were then processed into warm season (May–September) 8-hour daily maximum concentrations and

interpolated to Canadian six-character postal codes by the Canadian Urban Environmental Health Research Consortium (see Pappin et al. 2019).

We applied spatiotemporal adjustments to estimate NO_2 for years prior to 2006 and for O_3 prior to 2002 by first developing an annual time series of both NO_2 and O_3 in 24 of Canada's largest cities, based on available ground-monitoring data for the 1981 to 2016 time period. Among these 24 cities, only cities with data for at least 75% and 40.5% of the days for NO_2 and O_3, respectively, within a given year (i.e., 292 days) were included. For each year, typically 18–24 cities satisfied the criteria. Values were interpolated from adjacent years when data were not available. We then estimated yearly adjustment factors equal to the ratio of the observed concentration in the desired year to the average concentration in the reference year(s) (i.e., 2006 for NO_2 and 2002–2015 for O_3) for each of the 24 cities separately. We scaled the NO_2 concentration estimates per postal code in 2006 over the 1981–2016 period using the annual adjustment factors based on the city most proximate to that postal code location (Weichenthal et al. 2017). A similar time scaling was applied to the 2002–2015 O_3 surface. Although associations between mortality and NO_2 were not examined directly, NO_2 was used to calculate O_x. As in the Phase 1 report and prior publications (Crouse et al. 2020; Weichenthal et al. 2017), O_x was defined using the following equation to approximate redox potentials (Bratsch 1989), calculated at the person-year level based on year-adjusted NO_2 and O_3 estimates:

$$O_x = \frac{((1.07 \times NO_2) + (2.075 \times O_3))}{3.145}$$

EPIDEMIOLOGICAL ANALYSIS

Cohort Creation

As noted earlier, MAPLE incorporates four longitudinal cohorts and one stacked longitudinal cohort that combines three cycles of the CanCHEC. The CanCHEC cycles used individual data from the long form census questionnaire, which includes variables on socioeconomic status such education, income, marital status, ethnicity, immigration status, and employment status. Although some of these variables were measured differently during different census years, all variables were standardized to allow all CanCHEC cohorts to be stacked and the CanCHEC and mCCHS cohorts to be comparable.

1. **1991 CanCHEC —** 2.5 million subjects (after exclusions) over the age of 25 years who completed the 1991 long-form census linked to vital statistics, tax records, and cause of death from census day (June 4, 1991) to December 31, 2016, using methodology previously described in Wilkins and colleagues (2008) and Peters and colleagues (2013).
2. **1996 CanCHEC —** 3 million subjects (after exclusions) over the age of 25 years who completed the 1996 long-form census linked to vital statistics, tax records, and cause of death from census day (May 14, 1996) to December 31, 2016 (Christidis and colleagues 2018).
3. **2001 CanCHEC —** 3 million subjects (after exclusions) over the age of 25 years who completed the 2001 long-form census linked to vital statistics, tax records, and cause of death from census day (May 15, 2001) to December 31, 2016 (Pinault et al. 2017).
4. **Stacked CanCHEC —** 7.1 million subjects (after exclusions) over the age of 25 years who completed one of the three census long-form questionnaires. If the same respondents were included in more than one census year, later census year data were excluded to eliminate duplication of respondents in the sample. Duplicate respondents across census years were identified using records from the Statistics Canada's Derived Record Depository, which compiles individual data on Canadians within a secure computing environment.
5. **CCHS and mCCHS —** 540,900 subjects over the age of 25 years who completed one of the CCHS panels (2001, 2003, 2005, 2007, 2008, 2009, 2010, 2011, or 2012), which are linked to vital statistics, tax records, and cause of death from day of survey completion to December 31, 2016 (Sanmartin et al. 2016). The CCHS is an annual nationally representative interview survey (Statistics Canada 2005). In addition to basic sociodemographic content, the CCHS also includes individual-level information on self-reported health status, such as BMI, and health behaviors, including diet, physical activity, smoking, and alcohol consumption.

Noninstitutionalized respondents to the long form questionnaire who lived in Canada were considered in scope for linkage (Pinault et al. 2016b). To create the cohorts, respondents were linked to death records and residential history through the Statistics Canada Social Data Linkage Environment (Statistics Canada 2017b), which creates linked population data files for social analysis. CCHS respondents were asked at the time of survey if they agreed to record linkage and data sharing, and 95.2% of respondents agreed. Linkage was approved by Statistics Canada and is governed by the Directive on Microdata Linkage. The process begins with linkage to the Derived Record Depository, a highly secure linkage environment comprised of a national dynamic relational database of basic personal identifiers. Survey and administrative data are linked to the Derived Record Depository using G-Link, a SAS-based generalized record linkage software that supports deterministic- and probabilistic-linkage techniques developed at Statistics Canada (Fellegi and Sunter 1969). A list of linked unique individuals was created through linkages that were either deterministic (matching records based on unique identifiers) or probabilistic (matching records based on nonunique

identifiers such as names, sex, date of birth, and postal code and estimating the likelihood that records are referring to the same entity). Through this linkage, we obtained each respondent's annual mailing address postal code (to account for residential mobility in analysis) from tax records. Respondents with no postal code history were excluded from the analysis because we were unable to assign air pollution estimates or neighborhood covariates. Team members received security clearance to conduct all data linkages and analyses at secure Research Data Centers operated by Statistics Canada. Data were anonymized and person-years were rounded to the nearest 100 to prevent individual identification.

Postal code history was not available for each person in every year of follow-up, either because they did not file a tax return or because there were gaps in administrative data. We imputed 2.1% of person-years of missing postal codes if they shared the first two characters (Finès et al. 2017; Pinault et al. 2017), for a total of 89.9% of person-years with a valid postal code after imputation. Person-years were then excluded if they did not have an assigned postal code.

Additional person-years were excluded if respondents immigrated to Canada less than 10 years prior to the survey date (9,364,400 excluded), age during the follow-up period exceeded 89 years (7,357,200 excluded), or postal codes could not be matched to an air pollution estimate (17,814,400), a Can-Marg value (25,613,100), or airshed (25,545,500). Note that these exclusion numbers overlap for many person-years. Finally, the air pollution exposures were based on a 10-year moving average with a one-year lag. Person-years were excluded if the air pollution estimate in a given year was based on fewer than 7 out of 10 years of data (21,751,800).

In stacking three cycles of the CanCHEC, a total of 149,301,100 person-years was available. Finally, to create the Stacked CanCHEC, repeated CanCHEC respondents were excluded, leading to a final number of 128,371,800 person-years for analyses. Person-years excluded because of missing data were associated with persons who: died during follow-up, were age 80–89 years at baseline, reported being a visible minority, reported Indigenous identity, were unemployed, lived in Northern communities, or lived in rural communities.

For the CCHS/mCCHS cohort, response rates varied by cycle (2000/2001 [Cycle 1.1], 84.7%; 2003 [Cycle 2.1], 80.7%; 2005 [Cycle 3.1], 78.9%; 2007–2008, 76.4%; 2009–2010, 72.3%; 2011–2012, 68.4%), as did the numbers of respondents who agreed to data linkage (2000–2001 [Cycle 1.1], n = 117,800 respondents; 2003 [Cycle 2.1], n = 112,900 respondents; 2005 [Cycle 3.1], n = 113,900 respondents; 2007–2008, n = 112,700 respondents; 2009–2010, n = 104,700 respondents; 2011–2012, n = 104,100 respondents). Of those who agreed to linkage, 95.2% were successfully linked to the Social Data Linkage Environment, with 99.8% of relevant deaths linked. There were 540,900 respondents in the cohort with up to 36 years of residential history occurring both before and after the survey date. This was transposed to a file of person-years from entry data to end of follow-up (n = 5,902,100). Of these, a number of person-years were excluded for various reasons (note that totals will exceed number of deleted person-years, given that more than one exclusion criteria may apply to a single person-year), as follows: immigrated to Canada less than 10 years before survey date (n = 541,600 person-years); age during follow-up period exceeded 89 years (n = 161,000); had no postal code (n = 5,009,900); could not be linked to air pollution values (n = 5,711,600); could not be linked to CanMARG values (n = 7,668,000); could not be linked to census metropolitan area (CMA) or census agglomeration (CA) size (n = 4,800,600); could not be linked to airshed (n = 3,500); the 10-year moving average was informed by fewer than 7 years of exposure (n = 39,843); the person-year occurred after the subject death (n = 343,600). The total available person-years for analyses was 4,404,957 after all exclusions.

Description of Covariates

As described in detail in the Phase 1 report, we employed a defined strategy for covariate inclusion and focused our core analyses on two primary models (directed acyclic graph-informed and fully adjusted). In this report we focus on the fully adjusted models. All models were stratified by age (5-year age group), sex, and immigrant status. Respondents who immigrated to Canada 10 or fewer years prior to the index census year were excluded from the analyses, as they had spent most of their lives outside of Canada with unknown exposure. Models for the CCHS and the Stacked CanCHEC cohort also were stratified by the CCHS cycle or census year, respectively.

Subject-Level Risk Factors Available subject-level covariates included income, educational attainment, marital status, Indigenous identity, employment status, occupational class, and visible minority status. Income quintiles were derived by summing total pretax income from all sources for all economic family members or unattached individuals for the year prior to the census and then calculating the ratio of this total income to the Statistics Canada low-income cut-off for the applicable family size, community size group, and year. Weighted quintiles were derived based on this ratio for each CMA, CA area, or provincial residual for each cohort (Statistics Canada 2016). Employment status was defined as employed, unemployed, or not in the labor force (i.e., persons who left on disability, had retired, or had never worked) in the week prior to census day (Statistics Canada 2003). Visible minority status was defined in the Employment Equity Act as "persons, other than Indigenous persons, who were not white in race or color" (Statistics Canada 2003). Furthermore, the CCHS analyses included an additional level of model adjustment, using covariates describing fruit and vegetable consumption, leisure exercise frequency, alcohol consumption behavior, smoking behavior, and BMI categories.

Area-Level Contextual Risk Factors We used the CAN-Marg index (Matheson et al. 2012) to describe socioeconomic characteristics of an individual's home community. CAN-Marg is based on census data and geography; it is used to describe differences in marginalization among areas and to characterize inequalities in various predictors of health and social wellbeing. Derived from principal component analysis, it contains four dimensions of marginalization: material deprivation (e.g., proportion of population with low education, low income), residential instability (e.g., proportion of dwellings that are not owned, proportion of multiunit housing), dependency (e.g., ratio of seniors and youth to working aged population), and ethnic concentration (e.g., proportion of recent immigrants and self-reported visible minorities). We defined CAN-Marg based on census tracts (i.e., neighborhoods) in cities and census subdivisions (i.e., municipalities) outside of larger metropolitan areas. All person-years missing CAN-Marg values were removed from the analysis.

Geographic Identifiers This category includes covariates such as community size, urban form, and airshed. Urban form is a further designation for communities with a population size over 100,000 based on a combination of population density and mode of transit (Gordon and Janzen 2013). We designated communities as one of the following:

- **Active Urban Core** — Active transportation modes used to commute to work at greater than 150% of the metro average and greater than 50% of the national average
- **Transit-Reliant Suburb** — Transit use to commute to work greater than 150% of the metro average and greater than 50% of the national average, active transit use less than 150% of the metro average
- **Car-Reliant Suburb** — Gross population density greater than 150 people per square kilometer and transit use and active transportation use less than 150% of the metro average
- **Exurban** — Gross population density less than 150 people per square kilometer and more than 50% of workers commuting into the metropolitan area.

Airshed was defined by the Canadian Air Quality Management System on the basis of similar air-quality characteristics or dispersion patterns (Crouse et al. 2016). It subdivides the country into six large geographic areas (Figure 3) and adjusts for broad-scale spatial variation in mortality rates not captured by other risk factors.

All missing person-years for geographic identifiers were removed from the analysis. Further, person-years were excluded from the analysis if postal code information was inadequate and could not be linked to air pollution and ecological covariates, or if the air pollution and ecological covariate file did not match with a postal code record.

Analysis Approach

Linear Modeling Our primary statistical model relating exposure to mortality was the Cox proportional hazards model. Participants were at least 25 years of age at the beginning of each cohort, and the time axis was the year of follow-up until 2016. Person-years before census year and after a subject's death year were excluded from the analysis. Events were determined by year of death for nonaccidental and cause-specific mortality, using International Classification of Disease, 10th edition (ICD–10) codes. These include cardiovascular mortality (ICD-10 codes I10 to I69), cerebrovascular mortality (ICD-10 codes I60–I69), heart failure (ICD-10 codes I50.0, I50.1, I50.9), ischemic heart disease (ICD-10 codes I20–I25), diabetes (ICD-10 codes E10–E14), nonmalignant respiratory disease (ICD-10 codes J00–J99), COPD and associated conditions (ICD-10 codes J19–J46), pneumonia (ICD-10 codes J10–J18), lung cancer (ICD-10 codes C33–C34), and kidney failure (ICD-10 codes N18). The Cox model baseline hazard function was stratified by age (5-year groups), sex, and immigrant status. The Stacked CanCHEC and mCCHS were further stratified by census year or survey cycle. In this report we focus on the fully adjusted models introduced in the Phase 1 report. Specifically, models were adjusted for income adequacy quintile, visible minority status, Indigenous identity, educational attainment, labor-force status, marital status, occupation, and ecological covariates of community size, airshed, urban form, and four dimensions of Can-Marg (instability, deprivation, dependency, and ethnic concentration). Subject data were censored at 89 years of age, either at the beginning of each cohort or during follow-up, due to evidence from the 2011 Household Survey of an increased mismatch with increasing age between home address and tax return mailing address (Bérard-Chagnon 2017). We postulate that relatives of elderly people may have been completing their tax returns using a different address. Each of the three CanCHEC cohorts (1991, 1996, and 2001) were examined separately and then stacked to form a single cohort, which formed the basis of the majority of our analyses. Individuals who completed the subsequent long-form census questionnaires were removed, retaining only the first mention of the individual. Individuals who recurred in repeat CanCHEC cycles were identified using a key produced by the Derived Record Depository within Statistics Canada.

The primary exposure time window was a 10-year moving average assigned to the year prior to a given person-year, to ensure that exposures preceded the outcome event. Annual exposures were assigned by converting postal codes to geographic locations (i.e., latitudes and longitudes). However, some postal codes were missing, as not all subjects filed a tax return in each year. These missing postal codes were imputed based on available postal codes prior to and after missing years. Some postal codes could not be imputed with any accuracy and were set to missing. To estimate exposures, 7 years out of each 10-year period must have had available postal codes that were matched to air pollution estimates. We

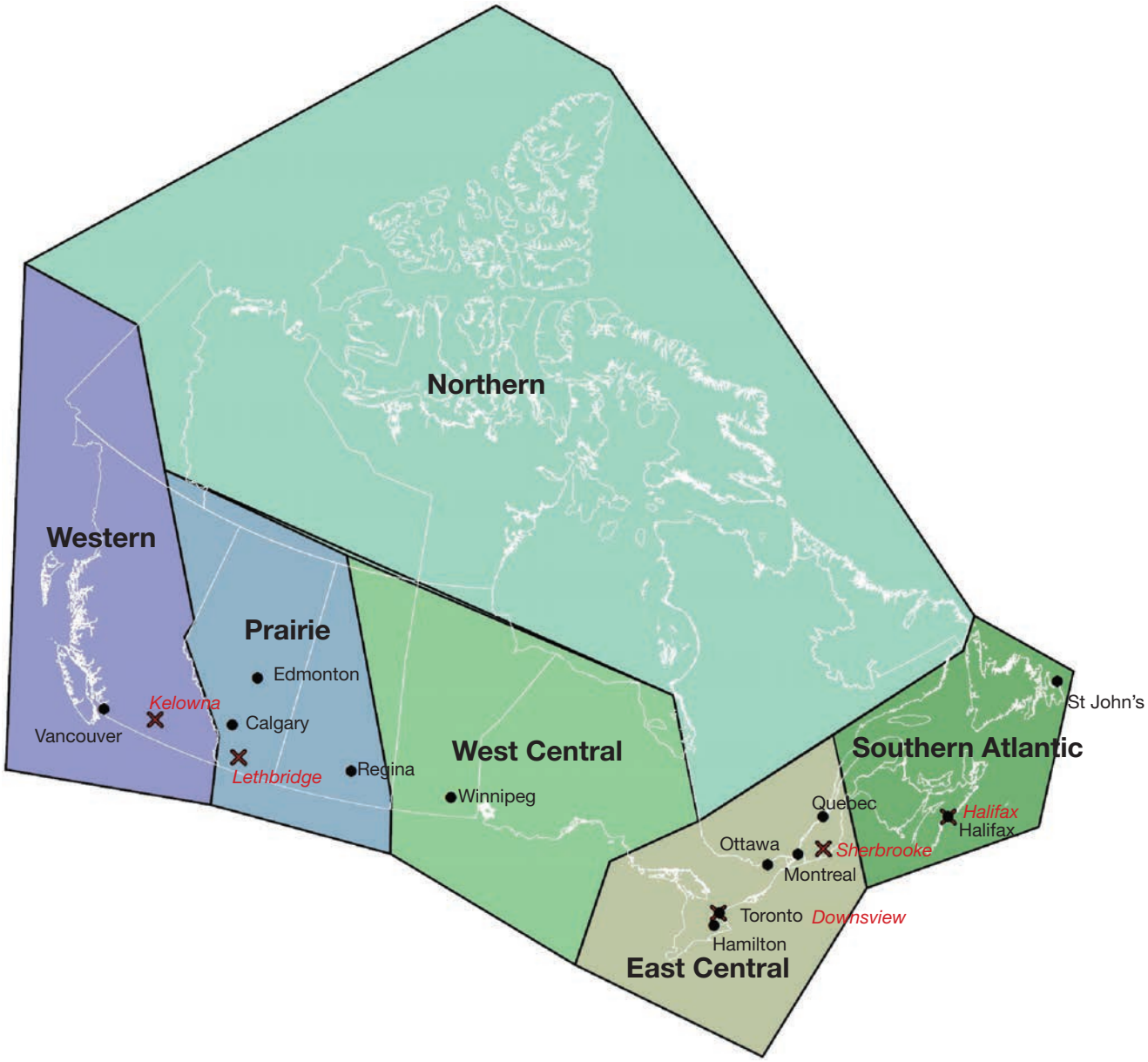

Figure 3. Map of the 6 airsheds in Canada across the provinces and territories, with locations of large cities (black circles) and MAPLE $PM_{2.5}$ monitoring sites (red Xs).

flagged missing person-years in the analytical file based on this requirement, and missing person-years were removed from the analysis. We required subjects to have filed tax returns 10 years prior to the cohort starting year (i.e., 1981 for the 1991 cohort, 1986 for the 1996 cohort, and 1991 for the 2001 cohort). An implication of this exposure-assignment protocol is that subjects must have been living in Canada 10 years prior to the beginning of their respective cohort's follow-up period. We thus excluded all subjects who immigrated to Canada during the 10 years prior to their cohort enrollment. In earlier work, we evaluated the sensitivity of cause-specific HRs to immigration status and time since immigration. HRs for the association with cardiovascular and cerebrovascular mortality with $PM_{2.5}$ were slightly but not significantly higher for immigrants relative to nonimmigrants in Canada, while no other differences were observed for other causes of death (Erickson et al. 2020). The implication from this work is that excluding recent immigrants was unlikely to introduce directional bias in our risk estimates.

Although several known and important risk factors for mortality were reported on the long-form census, many risk

factors were not recorded, such as smoking habits, BMI, or diet. We addressed the influence of these risk factors on air pollution risk estimates using data from the CCHS. We pooled several cycles of the CCHS (mCCHS cohort) for simultaneous analysis of the shape of the concentration–response association between $PM_{2.5}$ and nonaccidental mortality. The mCCHS analyses were stratified by CCHS cycle. We also examined several other causes of death, including cardiovascular mortality, cerebrovascular mortality, heart failure, ischemic heart disease, diabetes, nonmalignant respiratory disease, COPD and associated conditions, pneumonia, lung cancer, and kidney failure (ICD-10 codes described earlier).

We reported in the Phase 1 report a flattening of the all-cause mortality $PM_{2.5}$ relationship at intermediate concentration ranges. Although concentration distributions overlap across airsheds, we utilized a newly available healthcare access measure to evaluate its potential relevance to the shape of the concentration–response relationship. The proximity to healthcare variable measures the closeness of a person's home to local healthcare facilities: doctors and mental health specialists, dentists, offices of other health practitioners, outpatient care centers, and hospitals within a 3-kilometer network distance by car (Statistics Canada 2020). Proximity is measured by distance between the centroids of dissemination blocks which are an urban block or areas bounded by roads in a rural area. A simple gravity model weighs the number of nearby dissemination blocks containing healthcare facilities and the size of the services, by employment or revenue generation, and produces a normalized value from 0 to 1.

We attached this measure to the stacked cohort file through a postal code-dissemination block correspondence file produced by PCCF+. In cases where a postal code was not linked to a dissemination block, or if a dissemination block did not have a proximity estimate, we imputed the postal code proximity to healthcare value based on the mean values of similar, full postal codes, or more complete partial postal codes. After attaching the variable to the stacked cohort, we categorized all person-years according to quintile, and this five-category proximity variable was included in a restricted cubic spline analysis of nonaccidental death with 9-knots.

We split those who reside outside of a CMA–CA into those who live in rural (i.e., sparsely populated areas, 22,267,800 person-years) and nonrural areas (i.e., villages, small towns, 7,593,900 person-years), which can be assumed based on the second digit of a person's postal code. We ran a 9-knot restricted cubic spline for nonaccidental death using our regular covariates and this slightly altered community size variable. The RCS curve did not change in a meaningful way.

Shape of the Association Between $PM_{2.5}$ Exposure and Mortality A quantitative characterization of the shape of the concentration–response relationship between outdoor $PM_{2.5}$ concentrations and mortality can be useful for evaluating the health and economic benefits of proposed strategies to improve outdoor air quality. Cohort studies, such as those included in MAPLE are often used to determine this relationship. In such studies, information on major mortality risk factors such as age, sex, race, smoking, diet, exercise, and obesity are often included for each participant. Participants are assigned estimates of multiyear averages of outdoor concentrations of $PM_{2.5}$ at or near their homes. These concentrations are then related to mortality using proportional hazard models adjusting for available information on other risk factors (Cox 1972) and HRs were reported with Wald CIs.

To assess the shape of air pollution–mortality relationships, we typically relate the concentration of $PM_{2.5}$ to the logarithm of the hazard function, or instantaneous probability of death during follow-up, with a slope denoted by β. The hazard model (h) then has the form: $\log h(PM_{2.5}) = \beta(PM_{2.5})$. This form of model has previously been used to estimate excess deaths from exposure to outdoor $PM_{2.5}$ concentrations (U.S. EPA 2012). Some simple extensions of this linear model have been suggested, including $\log h(PM_{2.5}) = \beta\log(PM_{2.5})$, where the logarithm of concentration is used (Crouse et al. 2012; Krewski et al. 2009). Nonlinear models have been extended to include nonparametric representations of the association using natural (Thurston et al. 2016) or restricted (Crouse et al. 2015) cubic splines. More complex extensions have included smoothing splines (Di et al. 2017). In these cases, several spline variables $\{s_l(z),\ l = 1, \ldots, L\}$ are used to characterize the association: $\log h(PM_{2.5}) = \sum_{l=1}^{L} \beta_l s_l(z)$, for any concentration z, with the parameters $\{\beta_l,\ l = 1, \ldots, L\}$ determining the magnitude. The spline variables take different shapes over different intervals of concentration. This local smoothing property allows for highly complex shapes to be modeled.

We have selected RCS to flexibly model the association between outdoor concentrations of $PM_{2.5}$ and mortality (Harrell 2015). These regression-based splines require fewer computing resources compared with smoothing splines, a restriction that is necessary within the computing environment at Statistics Canada. The RCS has the form

$$RCS(z) = \beta_0 z + \sum_{l=1}^{K-2} \beta_l s_l(z),$$

for $K \geq 3$ with

$$s_l(z) = \left(\max\left(0, \frac{z-\lambda_l}{(\lambda_K-\lambda_1)^{2/3}}\right)\right)^3 - \left(\frac{\lambda_K-\lambda_l}{\lambda_K-\lambda_{K-1}}\right) \left(\max\left(0, \frac{z-\lambda_{K-1}}{(\lambda_K-\lambda_1)^{2/3}}\right)\right)^3 + \left(\frac{\lambda_{K-1}-\lambda_l}{\lambda_k-\lambda_{k-1}}\right)\left(\max\left(0, \frac{z-\lambda_K}{(\lambda_K-\lambda_1)^{2/3}}\right)\right)^3,$$

for K knot concentrations (λ_1, . . ., λ_K). The RCS is linear below λ_1 and above λ_K with continuous second derivatives at the K knots. The K–1 unknown parameters (β_0, . . ., β_{K-2}) are estimated within the Cox survival model framework by including (z,$s_1(z)$, . . ., $s_K(z)$) as K–1 variables in the survival model. The analyst must specify the number and location of the knots. Knot locations are based on percentiles of the $PM_{2.5}$ person-year distribution (Table 1). These are based on the recommendation given in the SAS macro *lgtphcurv9* that we use to create the RCS variables and fit them with the Cox survival model (Li et al. 2011).

Let $\hat{\boldsymbol{\beta}} = (\hat{\beta}_0, \ldots, \hat{\beta}_{K-2})'$ be a K–1 by 1 vector of parameter estimates with corresponding covariance matrix $\mathbf{V}$ and let $s(z) = (z, s_1(z), \ldots, s_{K-2}(z))'$. The estimate of the $\ln RCS(z)$ prediction is given by

$$\ln\widehat{RCS}(z) = \hat{\beta}'s(z) = \hat{\beta}_0 z + \sum_{l=1}^{K-2} \hat{\beta}_l s_l(z),$$

with uncertainty in the estimate given by $\hat{\sigma}(z) = s(z)'Vs(z)$. We summarize the information obtained from the fitted RCS model by its mean prediction at any concentration z, $\widehat{RCS}(z)$, and its 95% confidence interval: $\exp(\ln\widehat{RCS}(z) \mp 1.96 \times \hat{\sigma}(z))$.

Selecting the Number of Knots For all nonaccidental causes of death, we fit 16 RCS models based on 3 to 18 knots. We report the model predictions and 95% CIs in addition to two measures of fit: Akaike (AIC) and BIC, to examine the sensitivity of the shape of the $PM_{2.5}$–mortality association to the number of knots.

Because of computing time limitations, for all other analyses we developed a supervised search routine to reduce the number of RCS models that were fit. Initially we fit RCS models with 5, 8, 11, and 14 knots and identified the number of knots with the lowest BIC value. Suppose this value is 11 knots. Then we fit another four models with 9, 10, 12, and 13 knots, toggling the number of knots above and below 11. We then identify the number of knots with the lowest BIC value among the 8 models run and select this as our final model, unless the best model is 16 knots (first selecting 14 knots) and then running 12, 13, 15, and 16 knots. In that case we run another four models with 17, 18, 19, and 20 knots. If the lowest BCI is in this range then we stop, if not we run multiple sets of four models until we reach a minimum BIC value. We used the log likelihood ratio test to compare the fit of the RCS vs the linear model.

Incorporation of Counterfactual Concentration Natural cubic or smoothing splines are often used to describe the association between concentration and mortality. These splines are characterized by CIs increasing in width as concentrations deviate from the mean. RCS do not necessarily

Table 1. Knot Location Person-Year Percentiles

Knots	Location
3	5 50 95
4	5 35 65 95
5	5 27.5 50 72.5 95
6	5 23 41 59 77 95
7	2.5 18.3 34.2 50 65.8 81.7 98
8	1 15 29 43 57 71 85 99
9	2 14 26 38 50 62 74 86 98
10	2 12.7 23.3 34 44.7 55.3 66 76.7 87.3 98
11	2 11.6 21.2 30.8 40.4 50 59.6 69.2 78.8 88.4 98
12	2 10.7 19.5 28.2 36.9 45.6 54.4 63.1 71.8 80.5 89.3 98
13	2 10 18 26 34 42 50 58 66 74 82 90 98
14	9.39 16.8 24.2 31.5 38.9 46.3 53.7 61.1 68.5 75.9 83.2 90.6 98
15	2 8.9 15.7 22.6 29.4 36.3 43.1 50 56.9 63.7 70.6 77.4 84.3 91.1 98
16	2 8.4 14.8 21.2 27.6 34 40.4 46.8 53.2 59.6 66 72.4 78.8 85.2 91.6 98
17	2 8 14 20 26 32 38 44 50 56 62 68 74 80 86 92 98
18	2 7.6 13.3 18.9 24.6 30.2 35.9 41.6 47.2 52.8 58.5 64.1 69.8 75.4 81.1 86.7 92.4 98

have this property. To represent the RCS predictions and their uncertainty in a manner similar to natural or smoothing splines we made the following adjustment:

$$\ln\widehat{RCS}(z|z_{mean}) = \hat{\beta}'\big(s(z) - s(z_{mean})\big)$$
$$= \hat{\beta}_0(z - z_{mean}) + \sum_{l=1}^{K-2}\hat{\beta}_l\left(s_l(z) - s_l(z_{mean})\right)$$

with $\ln\widehat{RCS}(z|z_{mean}) = 0$. Spline predictions are also often presented with the HR prediction equaling one at the lowest observed concentration, z_{min}. We include this property by transformatting the RCS predictions in the following manner:

$$\ln\widehat{RCS}(z|z_{mean}) - \ln\widehat{RCS}(z_{min}|z_{mean}).$$

Given this characterization, the lower confidence limit on the RCS prediction will be less than one at z_{min}. We identify the highest concentration, *C*, for which the lower confidence limit is less than one.

Relative-Risk Functions Suitable for Health Benefits Analysis We present RCS mean predictions over the cohort concentration range and their 95% CIs. We set the mean prediction at the minimum concentration to one and a counterfactual concentration equaling the mean, at which the standard error (SE) of the prediction is zero. A characteristic of this formulation is that the width of the CIs increases as concentration deviates from the mean. We further identify the maximum concentration for which the lower confidence limit is less than one. The lower confidence limit on estimates of excess deaths will be less than zero for concentration ranges where the lower confidence limit on HR predictions is less than one. This calculation is based on a contrast between any concentration above the minimum and the minimum concentration, where it is assumed the HR at the minimum is one with zero uncertainty.

For a health benefits analysis, one is often interested in predicting the relative risk between any two concentrations, not just between a concentration above the minimum and the minimum itself. A benefits calculation incorporates the population attributable fraction (PAF), or proportion of total deaths attributable to any specific contrast in concentration, of the form:

$$PAF(z_C, z_F) = 1 - \exp\left\{-\left(\ln\widehat{RCS}(z_C) - \ln\widehat{RCS}(z_F)\right)\right\},$$

where z_C is a current concentration and $z_F < z_C$ is a future predicted concentration under a specified air quality mitigation scenario. We therefore need to determine an estimate of $\ln\widehat{RCS}(z_F) - \ln\widehat{RCS}(z_C)$ and its standard error. To do this we note that:

$$\ln\widehat{RCS}(z_C) - \ln\widehat{RCS}(z_F) = \hat{\beta}\big(s(z_C) - s(z_F)\big)$$

with standard error

$$\hat{\sigma}(z_F, z_C) = \sqrt{\big(s(z_C) - s(z_F)\big)'\,\hat{\mathbf{V}}\big(s(z_C) - s(z_F)\big)}.$$

Determining the difference in the log HR predictions between z_C and z_F only requires estimates of the respective predictions at each concentration, $\hat{\beta}'s(z_C)$ and $\hat{\beta}'s(z_F)$, values that can be obtained from figures typically reported in publications such as those in Figures 13–19 in this report. However, determining $\hat{\sigma}(z_F, z_C)$ requires estimates of each of the RCS variables ($s_0, \ldots, s_{K-2}$) and the individual elements of the covariance matrix $\hat{\mathbf{V}}$. Thus, the standard error of $\ln\widehat{RCS}(z)$ that could be obtained from the Figures 13–19 for example, is not sufficient to determine $\hat{\sigma}(z_F, z_C)$.

As an example application of risk predictions for health benefits analysis, the Global Burden of Disease 2019 (GBD 2020) uses a smoothing spline to characterize the magnitude, shape, and uncertainty in the association between air pollution concentrations and health outcomes within a Bayesian meta-analytic framework (GBD 2020). One thousand values are sampled from the posterior distribution of the spline coefficients. Using these values, 1,000 sets of the logarithm of relative-risk predictions are determined using a sequence of concentrations of interest. Then, 1,000 PAF values are created based on the difference in prediction between any two concentrations. We apply this method within our frequentist approach using the RCS by generating 1,000 realizations from a multivariate normal distribution with mean $\hat{\beta}$ and covariance matrix $\hat{\mathbf{V}}$, denoted by $ri = (r_{0,i}, \ldots, r_{K-2,i})'$, $i = 1, \ldots, 1{,}000$. We then construct: $r_i'(s(z_C) - s(z_F))$, $I = 1, \ldots, 1{,}000$ used to construct 1,000 estimates of the $PAF(z_C, z_F)$ for the concentration contrast (z_C, z_F), a quantity necessary for health benefits analysis.

Extending the SCHIF The best-fitting shape of the association estimated by splines may not be entirely suitable for risk assessment or health benefits analysis, due to potentially multiple variations in shape over different segments of the concentration distribution. That is, the spline maybe too *wiggly* even if it is constrained to be monotonically increasing (Pya and Wood 2015).

Our proposed approach to this challenge is to transform each of the 1,000 sets of predictions $r_i's(z_j)$, $j = 0, \ldots, J$ into an algebraic function that we suggest is suitable for benefits analysis. Our algebraic function is based on an extension of the SCHIF first proposed by Nasari and colleagues (2016) and

then generalized as the Global Exposure Mortality Model (GEMM) by Burnett and colleagues (2018). It is given by

$$r_i's(z_j) - r_i's(z_0) = \gamma_i \ln\left(\frac{z_j - z_0}{\delta_i} + 1\right) + \theta_i \ln\left(\frac{z_j - z_0}{\alpha_i} + 1\right) \left(1 + exp\left\{-\left(\frac{z_j - z_0 - \mu_i}{\tau_i}\right)\right\}\right)^{-1}$$

for $j = 1, \ldots, J$; $I = 1, \ldots, 1{,}000$. We fix the model prediction to $r_i's(z_0)$, the lnRCS value at $z = z_0$, in order for our model to closely approximate the RCS predictions at very low concentrations. We denote this new model as eSCHIF. The second eSCHIF term was proposed by Burnett and colleagues (2018). We have added an additional term, the first eSCHIF term, to extend their model to additional shapes. In particular, this new formulation models confidence intervals of mean predictions that increase in width as deviation in concentration from their mean increase.

By setting the counterfactual to the mean concentration, the RCS CIs widen as concentrations deviate from the mean. The eSCHIF is thus capable of modeling such a structure, while the original SCHIF or GEMM are not. The eSCHIF can model near-linear, supralinear, sublinear, sigmoidal, and nonmonotonic shapes. A specific nonmonotonic shape of interest is when some of the RCS relative-risk predictions decline with concentration over lower concentrations and then increase with higher concentrations. This pattern results in PAF values less than zero.

eSCHIF Parameter Estimation We use linear least squares to estimate the parameters (θ_i, γ_i) for specified values of $(\delta, \alpha, \mu, \tau)$. We first generate uniform, U, sampling distributions for $(\delta, \alpha, \mu, \tau)$ as:

$\delta \sim U(1, 3v)$

$\alpha \sim U(1, 3v)$

$\mu \sim U(-1, 1) \times v$

$\tau \sim U(0.05, 1) \times v.$

$v = z_j - z_o$, the range in concentrations to be modeled over. We use these sampling distributions as a method to create a mesh of parameter values needed for our estimation routine. These sampling specifications also permit a wide range in shapes of interest.

From these sampling distributions we generate a large number (1,000) of quadruples $(\delta^{(n)}, \alpha^{(n)}, \mu^{(n)}, \tau^{(n)})$, for $n = 1, \ldots, 1{,}000$ and then create two transformations of concentration ($T^{(1)}$ and $T^{(2)}$) for each n and z_j as

$$T^{(1)}_{(\delta^{(n)})}(z_j) = \ln\left(\frac{z_j - z_0}{\delta^{(n)}} + 1\right)$$

and

$$T^{(2)}_{(\alpha^{(n)},\mu^{(n)},\tau^{(n)})}(z_j) = \ln\left(\frac{z_j - z_0}{\alpha^{(n)}} + 1\right) \left(1 + exp\left\{-\left(\frac{z_j - z_0 - \mu^{(n)}}{\tau^{(n)}}\right)\right\}\right)^{-1}$$

and include these two variables in a linear regression with the response $r_i's(z_j) - r_i's(z_0)$, $j = 0, \ldots, J$. We then identify the values of $(\delta^{(n)}, \alpha^{(n)}, \mu^{(n)}, \tau^{(n)})$ that solicit the lowest log-likelihood value with corresponding estimates of (θ_i, γ_i) denoted by $(\hat{\theta}_i, \hat{\gamma}_i)$. Let the corresponding values of $(\delta^{(n)}, \alpha^{(n)}, \mu^{(n)}, \tau^{(n)})$ that minimize the log-likelihood be denoted by $(\hat{\delta}_i, \hat{\alpha}_i, \hat{\mu}_i, \hat{\tau}_i)$.

Then the eSCHIF is characterized by

$$\ln\left(eSCHIF_i(z_j)\right) = \hat{\gamma}_i \ln\left(\frac{z_j - z_0}{\hat{\delta}_i} + 1\right) + \hat{\theta}_i \ln\left(\frac{z_j - z_0}{\hat{\alpha}_i} + 1\right) \left(1 + exp\left\{-\left(\frac{z_j - z_0 - \hat{\mu}_i}{\hat{\tau}_i}\right)\right\}\right)^{-1}$$

for $j = 0, \ldots, J$; $i = 1, \ldots, 1{,}000$.

The uncertainty distribution of $PAF(z_C, z_F)$ based on the eSCHIF is obtained from the 1,000 values of

$$PAF_i(z_C, z_F) = 1 - exp\left\{-\hat{\gamma}_i\left(T^{(1)}_{(\hat{\delta}_i)}(z_C) - T^{(1)}_{(\hat{\delta}_i)}(z_F)\right) - \hat{\theta}_i\left(T^{(2)}_{(\hat{\alpha}_i,\hat{\mu}_i,\hat{\tau}_i)}(z_C) - T^{(2)}_{(\hat{\alpha}_i,\hat{\mu}_i,\hat{\tau}_i)}(z_F)\right)\right\}$$

$i = 1, \ldots, 1{,}000$, independent of $r_i's(z_0)$.

Incorporating Uncertainty in the Number and Location of RCS Knots The shape and uncertainty of RCS predictions is governed, in part, by the number and placement of the knots. We characterize the uncertainty in number and placement of knots by first fitting RCS curves by a series of number of knots from 3 to 18. We then create an *ensemble* RCS estimate by first defining the ensemble weight $\omega(\kappa)$ with κ denoting the knot locations that define the RCS. Let M_κ denote a measure of fit associated with knots κ, then

$$\omega(\kappa) = \exp\left(-\frac{1}{2}(M_\kappa - \min(M_\kappa))\right) / \sum_\kappa \exp\left(-\frac{1}{2}(M_\kappa - \min(M_\kappa))\right)$$

(Buckland et al. 1997). We then form lnRCS model predictions over the exposure range by 0.1-μg/m³ increments, denoted by $\{z_1, \ldots, z_N\}$, by simulating realizations proportionate to $1{,}000 \times \omega(\kappa)$. That is, the values of κ that yield better model predictions are more often represented in the 1,000 realizations. This approach incorporates uncertainty in both the number and location of the knots. To each of these 1,000 RCS realizations we fit the eSCHIF.

Standard Threshold Functions In addition to the eSCHIF for nonaccidental mortality we fit the standard threshold HR function:

$$THRES(z) = \exp(\beta_\rho z_\rho)$$

where $z_\rho = \max(0, z - \rho)$, for threshold concentrations ρ = 2.5, 3.0, 3.5, . . ., 10.0. Let $\hat{\beta}_\rho$ denote the estimate of β_ρ; $\hat{\sigma}_{\hat{\beta}_\rho}$, its associated standard error; $LL\rho$, the log-likelihood value; and $\omega(\rho) = \exp(LL_\rho - \min(LL_\rho)) / \sum_\rho \exp(LL_\rho - \min(LL_\rho))$, the model ensemble weight (Buckland et al. 1997). We form model predictions by sampling 1,000 realizations of normal variates with mean $\hat{\beta}_\rho$ and standard deviation $\hat{\sigma}_{\hat{\beta}_\rho}$ with the sample size for each value of ρ proportionate to $1{,}000 \times \omega(\rho)$. That is, the values of the threshold parameter ρ that represent better model predictions are more often represented in the 1,000 realizations. We graphically present the mean of the HR predictions among the 1,000 sets in addition to the 2.5 and 97.5 percentile values over the concentration range and identify the highest concentration, such that the 2.5 percentile value equals one.

Sensitivity Analyses In addition to the main analyses described earlier, we conducted several sensitivity analyses using a similar modeling approach. These analyses were designed to further investigate observations reported in the MAPLE Phase 1 report. In most cases, we evaluated both linear Cox proportional hazards models as well as the nonlinear shape of the association between $PM_{2.5}$ and mortality, described earlier, using fully adjusted models. In most cases, we focused on using the Stacked CanCHEC for these analyses, unless otherwise indicated.

First, to further investigate the attenuation of $PM_{2.5}$ HRs by O_3 and O_x that we reported in the MAPLE Phase 1 report, we considered a series of joint two-pollutant models, incorporating both $PM_{2.5}$ with O_3 and $PM_{2.5}$ with O_x, through linear and nonlinear models. Joint nonlinear models were fit using the number and position of knots obtained based on BIC model fit for each of the pollutants in the single-pollutant models. Similarly, we considered $PM_{2.5}$ models within tertiles of O_3 and O_x in both linear and nonlinear models for nonaccidental mortality.

Next, we evaluated associations between nonaccidental mortality and $PM_{2.5}$ within different regions of Canada. For this analysis, models were fitted by airshed, representing large areas of Canada (see Figure 3). This analysis was conducted to evaluate a flattening of the concentration–response relationship that we observed at midrange $PM_{2.5}$ concentrations in the MAPLE Phase 1 report. We hypothesized that this may have reflected regional variation in the composition of the air pollution mixture at these levels or unmeasured regional variation in mortality risk factors. We additionally evaluated whether any observed regional variation in concentration–mortality relationships could be explained by differential regional representation of immigrants, Indigenous respondents, or healthy older persons who are lost to follow-up.

Further, we explored the potential effect of regional variation in access to healthcare as another factor that may have led to regional variation in the shape of the concentration–mortality relationship. In these analyses we evaluated separate models excluding immigrants, Indigenous respondents, and persons >80 years, 60–79 years, and >60 years, where immigrants and Indigenous respondents were removed, and where populations were restricted to specific age groups. To assess the sensitivity of concentration–mortality relationships to regional variation in access to healthcare, we included in models a new measure of the closeness of a census dissemination block to any census dissemination block with a healthcare facility within a driving distance of 3 kilometers. We further conducted analyses with 1-year age strata to assess potential residual confounding within the 5-year age strata in our main models.

Finally, we evaluated model sensitivity to using different versions of applying $PM_{2.5}$ exposure to the models. Different moving averages (3- vs. 10-year moving averages) were applied, as well as a comparison between the older version of the $PM_{2.5}$ data (V4.NA.01) and the new version (V4.NA.02-MAPLE) (Appendix Tables A.6 and A.7; available on the HEI website).

SUMMARY OF FINDINGS

EXPOSURE ASSESSMENT

Table 2 provides an overview of the measurements made at each sampling site. Filter and scattering measurements were collected for 328 to 459 days at all locations, with the exception of Kelowna that collected measurements for 134 days. The variation in sampling is due to differing logistics associated with site deployment, disassembly dates, and instrument downtime for required maintenance. Site mean $PM_{2.5}$ concentrations are below 7 μg/m³, varying by less than a factor of two across all sites, with the highest concentration observed in Downsview (6.8 μg/m³) and the lowest in Kelowna (3.4 μg/m³). Larger variations are observed for major chemical constituents.

Table 2. Summary of Mean Filter-Based and Nephelometer Measurements at MAPLE Sampling Locations

	Downsview	Halifax	Kelowna	Lethbridge	Sherbrooke
Sampling Period (yyyy/mm)	2017/07 – 2019/08	2017/08 – 2019/08	2017/11 – 2019/03	2017/08 – 2019/08	2017/06 – 2019/08
Sampled days	435	435	134	328	459
Sampled filters	68	62	18	39	59
Sampled seasons[a]	S,F,W,Sp	S,F,W,Sp	F,W,Sp	S,F,W,Sp	S,F,W,Sp
Measurements (Mean ± SE)					
$PM_{2.5}$ (μg/m³)	6.8 ± 0.3	4.1 ± 0.2	3.4 ± 0.8	5.7 ± 1.2	5.5 ± 0.3
Sulfate (μg/m³)	1.19 ± 0.07	0.68 ± 0.04	0.13 ± 0.05	0.66 ± 0.05	1.35 ± 0.26
Nitrate (μg/m³)	0.47 ± 0.10	0.13 ± 0.01	0.03 ± 0.01	0.32 ± 0.07	0.14 ± 0.03
Ammonium (μg/m³)	0.37 ± 0.03	0.17 ± 0.02	0.05 ± 0.02	0.23 ± 0.03	0.20 ± 0.02
SIA (μg/m³)	2.0 ± 1.3	1.0 ± 0.7	0.2 ± 0.1	1.2 ± 0.8	1.7 ± 1.4
Black carbon (μg/m³)	0.82 ± 0.06	0.36 ± 0.03	0.16 ± 0.07	0.37 ± 0.06	0.49 ± 0.04
Residual matter (μg/m³)	2.5 ± 0.2	1.7 ± 0.2	1.1 ± 0.2	4.0 ± 1.4	2.8 ± 0.3
Dust (μg/m³)	0.67 ± 0.06	0.43 ± 0.06	0.30 ± 0.07	0.46 ± 0.07	0.32 ± 0.03
Sea salt (μg/m³)	0.55 ± 0.04	0.79 ± 0.05	0.29 ± 0.03	0.39 ± 0.06	0.49 ± 0.03
PM_{10} (μg/m³)	15.9 ± 1.7	8.6 ± 0.6	8.6 ± 2.8	9.7 ± 3.0	11.5 ± 0.8
$b_{sp,24hr,550nm}$ (Mm^{-1})[b]	38.6 ± 1.3	16.5 ± 0.5	17.2 ± 1.6	26.7 ± 1.8	24.9 ± 0.7
$b_{sp,overpass,550nm}$ (Mm^{-1})	27.9 ± 1.3	12.9 ± 0.5	12.2 ± 1.1	23.3 ± 2.1	17.1 ± 0.6
$AOD_{overpass,550nm}$	0.18 ± 0.01	0.13 ± 0.01	0.14 ± 0.02	0.14 ± 0.01	0.16 ± 0.02
$b_{sp,overpass}$ / $PM_{2.5,24hr}$ (MSE, m²/g)	3.12 ± 0.10	2.73 ± 0.18	n/a	2.96 ± 1.22	2.60 ± 0.09

[a] Sampled seasons are S = summer (June, July, August), F = fall (September, October, November), W = winter (December, January, February), and Sp = spring (March, April, May). $b_{sp,24hr}$ = total scatter over 24 hours; $b_{sp,overpass}$ = total scatter during satellite overpass; SIA = secondary inorganic aerosol.

[b] Particle light (550 nm) scattering coefficient in units of $10^6 m^{-1}$.

Table 3 shows a summary of mean coincident $PM_{2.5}$ mass and species concentrations from MAPLE and NAPS monitors in Downsview. Overall, both measurement methods exhibit a high degree of consistency. Sulfate is most consistent across both methods, with mean concentrations within 6%. MAPLE nitrate and ammonium concentrations are lower than those from NAPS, as expected due to loss of these semivolatile components. The main compounds used for mineral dust, magnesium, aluminum, and iron are overall consistent across both methods.

Figure 4 shows the average contribution of major chemical components to total $PM_{2.5}$ mass concentrations from the five measurement sites. The five major chemical components (secondary inorganic aerosol (SIA), residual matter, black carbon, sea salt, and dust) show pronounced heterogeneity across sampling sites. SIA (sum of sulfate, nitrate and ammonium) vary by an order of magnitude from as low as 0.2 μg/m³ in Kelowna, to moderate values in Halifax (1.0 μg/m³) and Lethbridge (1.2 μg/m³), to 2.0 μg/m³ in Downsview (Table 2). Differences reflect regional emission sources. Kelowna is a small city in the Western airshed

Table 3. Summary of $PM_{2.5}$ Mass and Chemical Species Concentrations from NAPS and MAPLE at the Downsview Sampling Site

Species	Concentration ± SE[a]	
	NAPS	MAPLE
$PM_{2.5}$ (μg/m³)[b]	6.51 ± 0.35	6.97 ± 0.42
Sulfate (μg/m³)	0.95 ± 0.06	1.01 ± 0.06
Nitrate (μg/m³)	0.71 ± 0.19	0.41 ± 0.12
Ammonium (μg/m³)	0.52 ± 0.07	0.35 ± 0.04
Sodium (μg/m³)	0.05 ± 0.01	0.14 ± 0.02
Magnesium (μg/m³)	0.01 ± 0.00	0.01 ± 0.00
Aluminum (ng/m³)[c]	15.5 ± 2.1	13.1 ± 2.5
Iron (ng/m³)[c]	55.4 ± 3.4	49.0 ± 3.8

[a] SE = standard error.

[b] NAPS $PM_{2.5}$ are daily coincident values from the Partisol sampler (NAPS reference method).

[c] NAPS aluminum and iron are from the near-total extraction for the inductively coupled plasma mass spectrometry analysis.

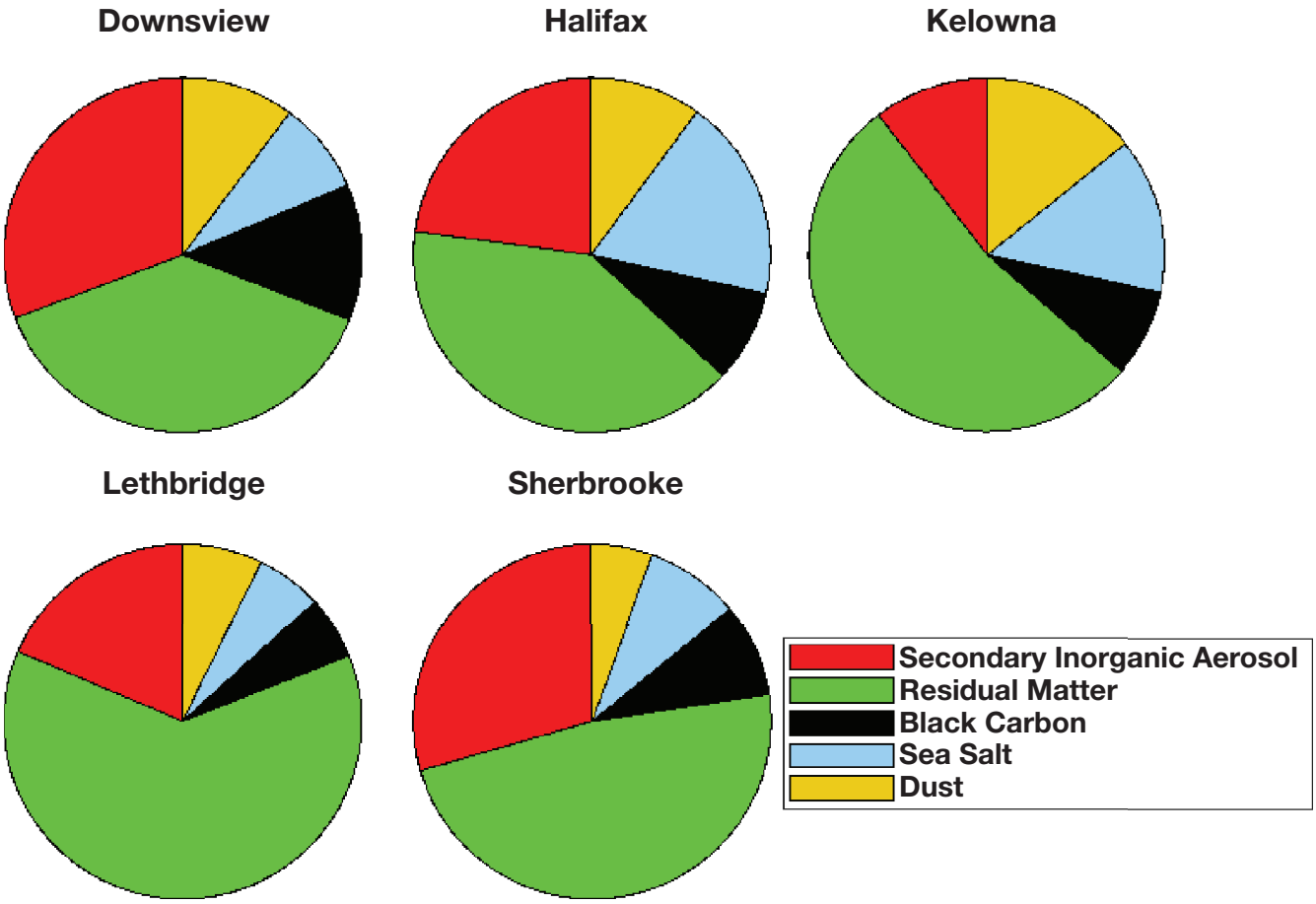

Figure 4. Average contribution of five major $PM_{2.5}$ chemical components to total $PM_{2.5}$ mass measured at MAPLE sampling sites in Downsview, Ontario (East Central Airshed); Halifax, Nova Scotia (Southern Atlantic Airshed); Kelowna, British Columbia (Western Airshed); Lethbridge, Alberta (Prairie Airshed); and Sherbrooke, Quebec (East Central Airshed).

surrounded by a natural environment that experiences limited local anthropogenic emissions of SIA precursors such as sulfur dioxide (SO_2) from industry and nitrogen oxides from combustion. Downsview is located within the East Central airshed inside the Greater Toronto Area, a large metropolitan area, near major sources of SIA precursors such as industrial SO_2 sources and nitrogen oxides from significant vehicular traffic. Sources of black carbon and organic matter may include combustion sources such as diesel and residential energy use. Sherbrooke is a small urban area, also located in the East Central airshed downwind of major urban and industrial emissions, that experiences slightly lower mean $PM_{2.5}$ concentrations than Downsview (5.5 vs. 6.8 μg/m^3), however site location and comparable contributions from major chemical components signify similar potential sources. Moderate $PM_{2.5}$ concentrations in Lethbridge (5.7 μg/m^3) within the Prairie airshed are driven by significant contributions from residual (organic) matter that could point toward forest fires as a dominant source of $PM_{2.5}$ in this region during the sampling period. Although lower overall concentrations of total $PM_{2.5}$ mass and chemical components were measured in Halifax, contributions similar to other urban sampling locations were observed with the exception of notably higher sea salt concentrations for this coastal city within the Southern Atlantic airshed.

Table 2 shows the MSE at 550 nm inferred from the measured scatter at satellite overpass time and the measured $PM_{2.5}$ mass. Site-mean values range from 2.6 m^2/g in Sherbrooke to 3.1 m^2/g in Downsview. As described in Bissonnette (2019), multiple linear regression was conducted on the relation of filter-dependent MSE with $PM_{2.5}$ composition to derive the MSE values for the five chemical components.

The resulting V4.NA.02.MAPLE dataset outperformed V4.NA.01 at collocated ground-based stations in long-term mean comparisons across the range of observed $PM_{2.5}$ (coefficient of determination (R^2) = 0.81 vs. R^2 = 0.71; RMSD = 1.5 μg/m^3 vs. RMSD = 1.9 μg/m^3) (Figure 5), as well as at low

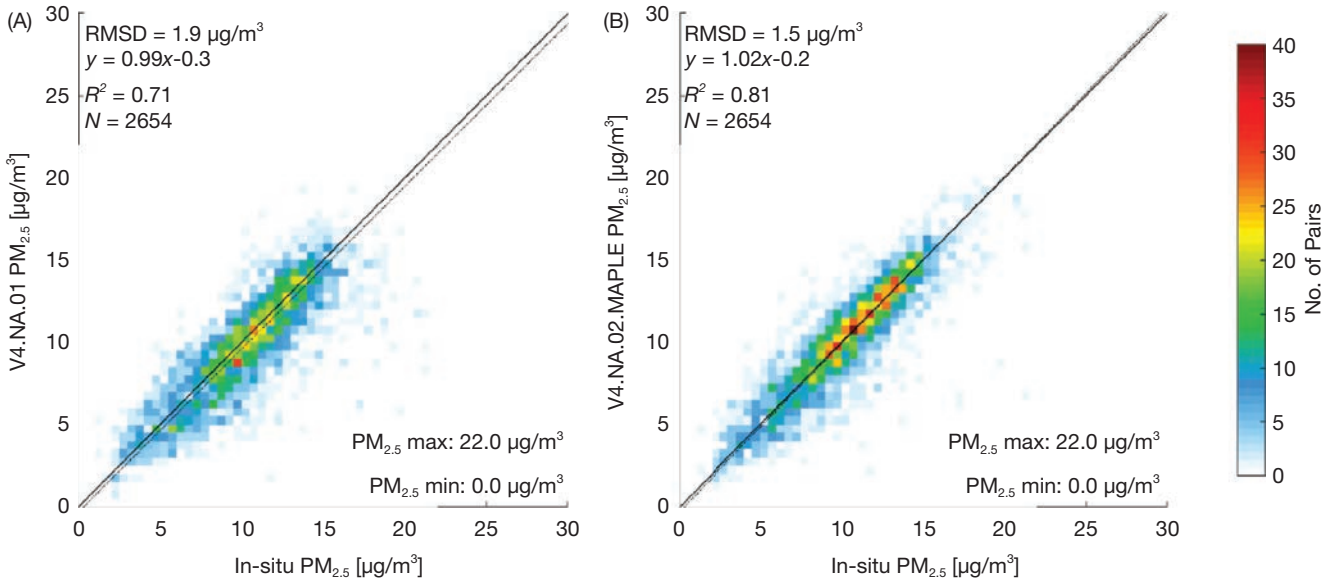

Figure 5. Comparison of mean $PM_{2.5}$ mass concentrations for 2000–2012 observed by in-situ ground-based monitors with (A) Phase 1 V4.NA.01 and (B) Phase 2 V4.NA.02-MAPLE satellite-derived $PM_{2.5}$ estimates for all North American monitor locations. Annotations include the root mean square difference (RMSD), line of best fit (y), coefficient of determination (R^2) and the number of points (N). See Figure 6 for Canadian locations only.

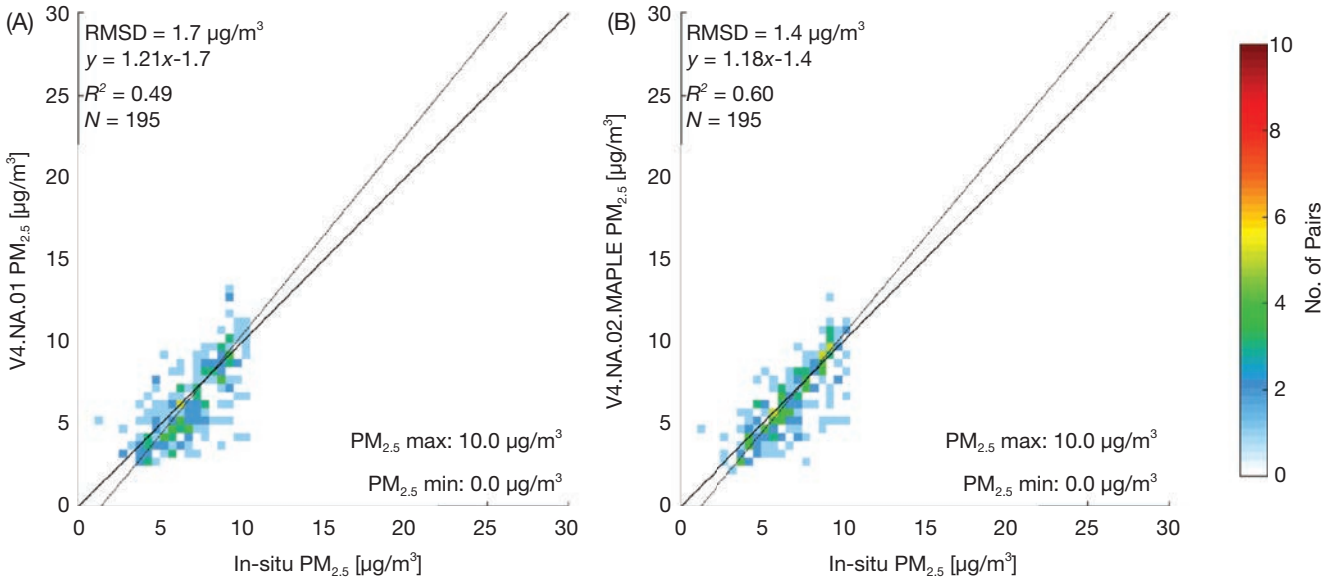

Figure 6. Comparison of mean $PM_{2.5}$ mass concentrations for 2000–2012 observed by in-situ ground-based monitors with (A) Phase 1 V4.NA.01 and (B) Phase 2 V4.NA.02-MAPLE satellite-derived $PM_{2.5}$ estimates for Canadian monitor locations and observed concentrations below 10 µg/m³. Annotations include the root mean square difference (RMSD), line of best fit (y), coefficient of determination (R^2) and the number of points (N).

concentrations at northern locations directly relevant to this study (e.g., for observed $PM_{2.5}$ <10 µg/m³ at Canadian sites (V4.NA.02.MAPLE vs V4.NA.01): R^2 = 0.60 vs. R^2 = 0.49; RMSD = 1.7 µg/m³ vs. RMSD = 1.4 µg/m³) (Figure 6).

Based on the V4.NA.02-MAPLE exposure estimates, mean estimates of $PM_{2.5}$ across Canada were relatively low in rural areas of the country (2–6 µg/m³) (Figure 7). In the largest cities, $PM_{2.5}$ estimates over the 1981–2015 average ranged

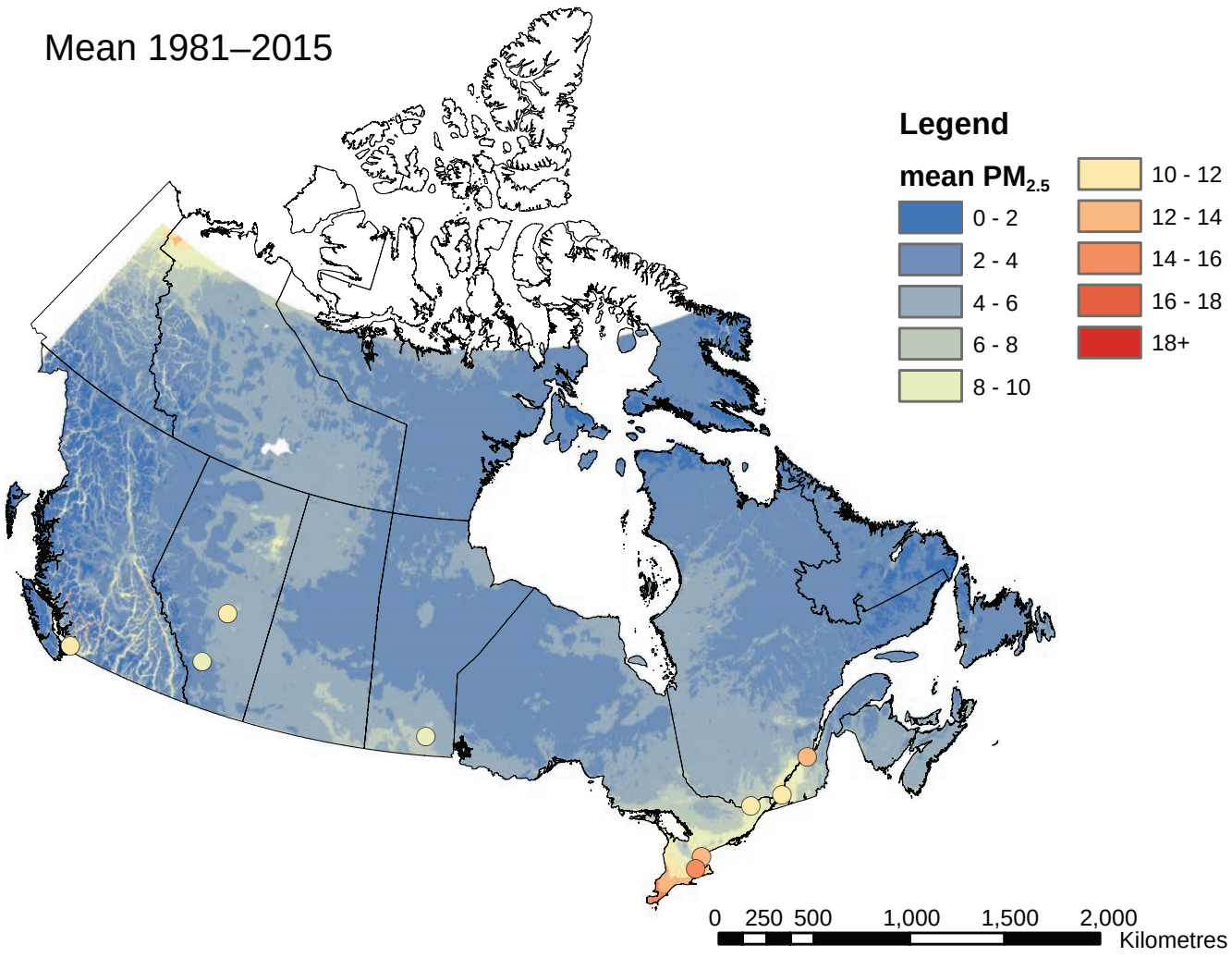

Figure 7. Estimates of fine particulate matter ($PM_{2.5}$) annual means averaged over the entire study period (1981–2015). City-level estimates for the largest cities are shown in the circles.

between 8 and 16 µg/m^3. When examining the change over time, estimates in rural and urban areas were notably higher during the first decade of the study (1981–1990) relative to later decades (Figure 8). The cities of Toronto, Hamilton, Quebec City and Vancouver had estimates in the highest range examined during the 1981–1990 period (18 µg/m^3).

A map of mean O_3 averaged across the entire study period is provided in Figure 9. In general, O_3 was highest in southern Ontario (e.g., Toronto and Hamilton), as well as in southern portions of Alberta (e.g., Calgary) and Saskatchewan (e.g., Regina). Spatial patterns of O_3 were similar across the decades of study (Figure 10).

The spatial distribution of O_x was similar to that of O_3, in that O_x was greatest in areas of southern Ontario and Alberta (Figure 11). It was also high in the downtown portions of major cities such as Toronto, Hamilton, Montreal, and Vancouver. Similar to O_3, the spatial distribution of O_x did not vary substantially across the decades included in the study (Figure 12).

National estimates of $PM_{2.5}$, O_x, and O_3 were applied to the cohorts in a time-varying manner, with estimates assigned in each year. Table 4 provides the distribution of $PM_{2.5}$, O_3, and O_x at the level of the person-year in each of the study cohorts. $PM_{2.5}$ estimates were overall slightly higher in increasingly older cohorts, likely because older cohorts include a greater proportion of estimates based on earlier years when concentrations were higher.

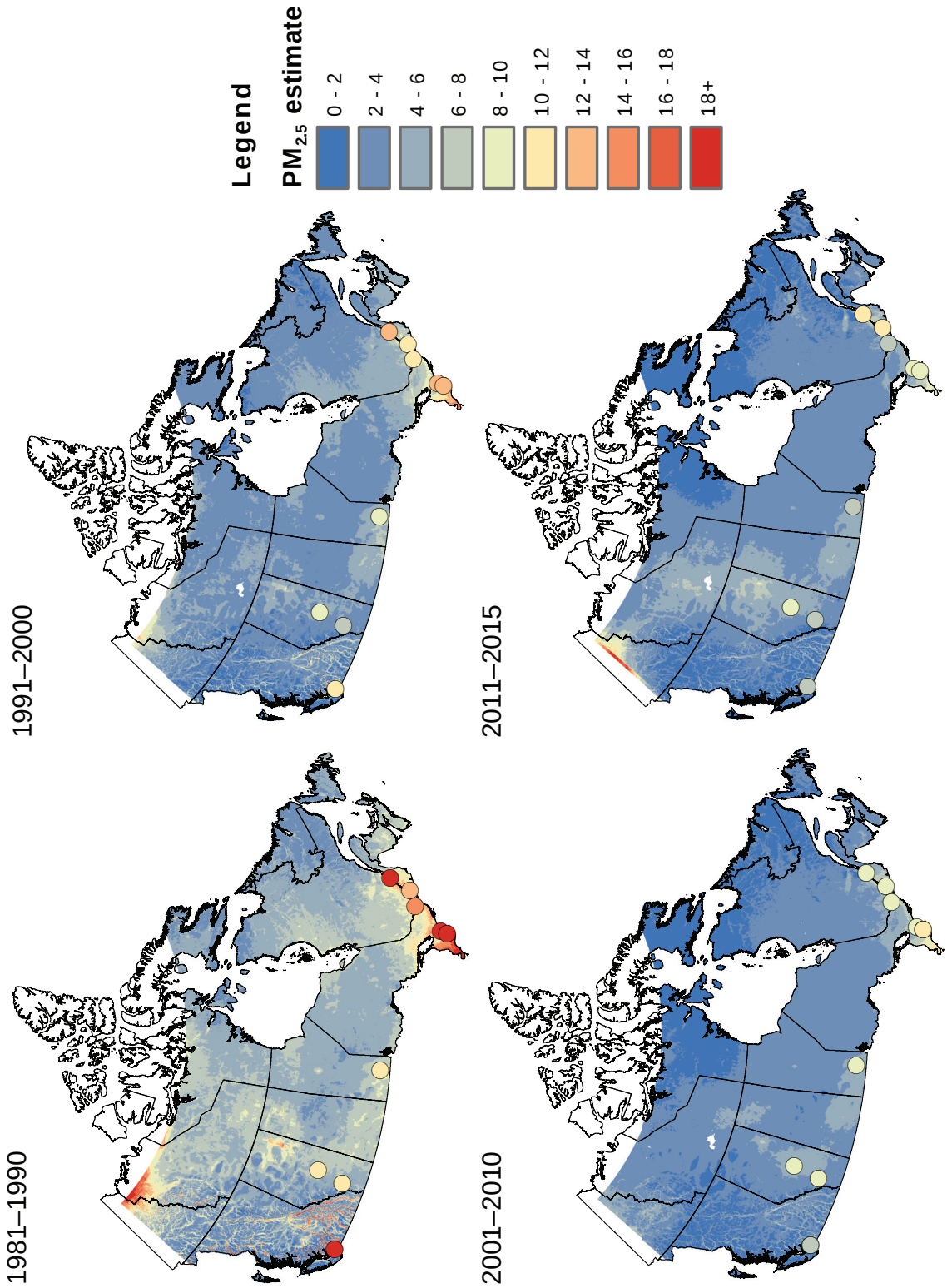

Figure 8. Estimates of fine particulate matter ($PM_{2.5}$) annual means averaged over decades within the study period (1981–1990, 1991–2000, 2001–2010, and 2011–2015).
City-level estimates for the largest cities are shown in the circles.

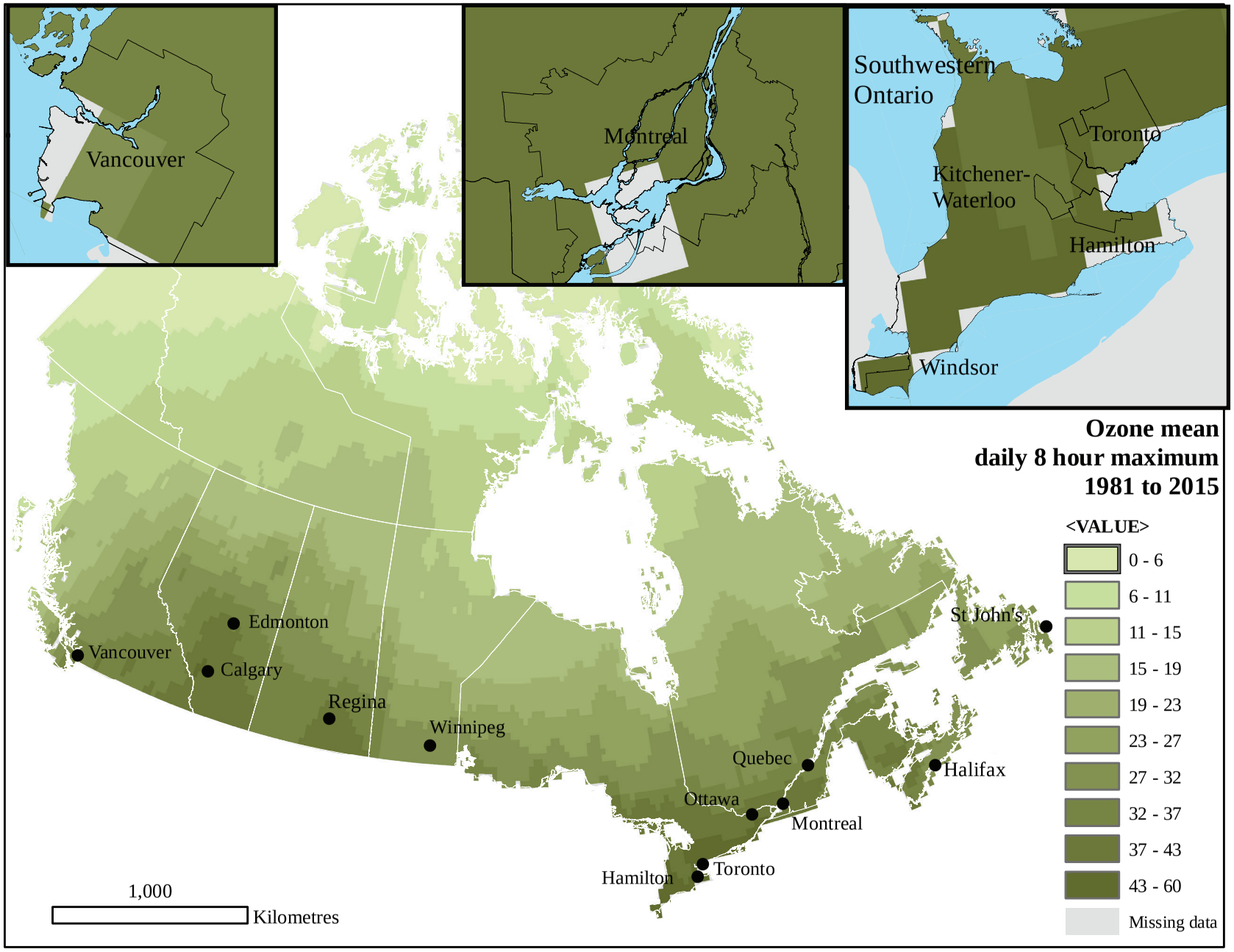

Figure 9. Estimates of O_3 annual means from 8-hour daily maxima, averaged over the entire study period (1981–2015). City-level estimates for the largest cities are shown in the insets.

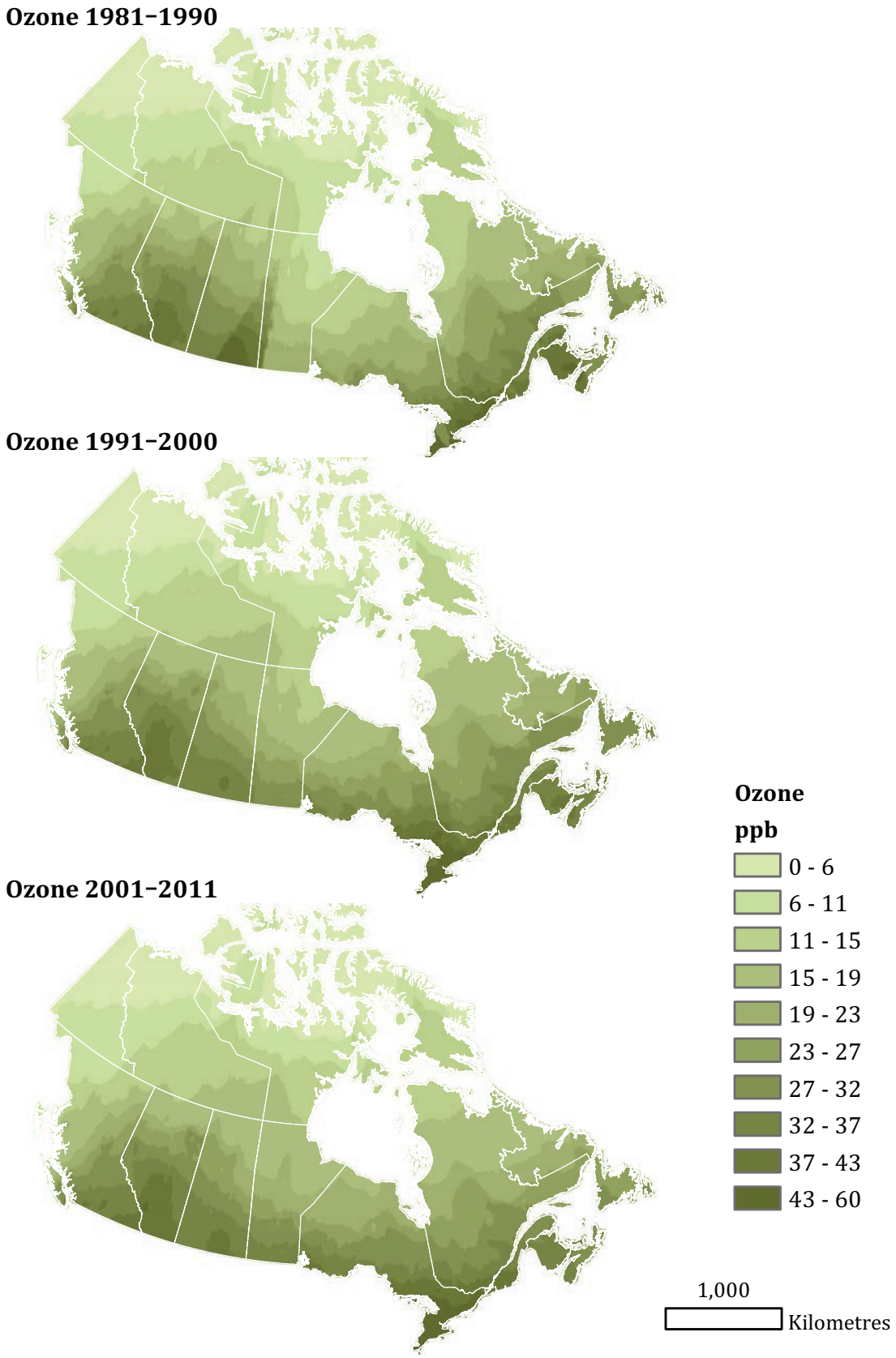

Figure 10. Estimates of O_3 annual means averaged over decades within the study period (1981–1990, 1991–2000, and 2001–2011).

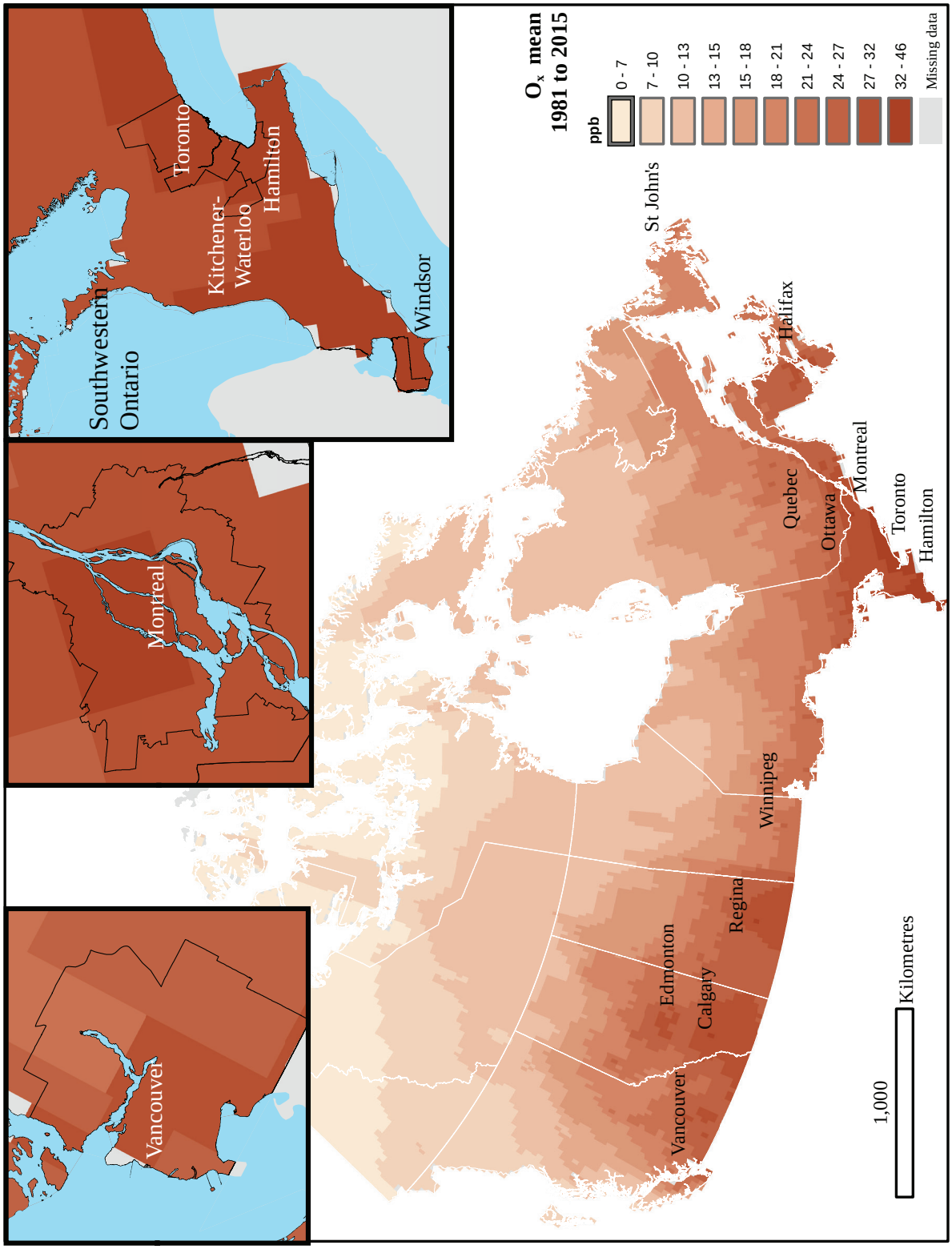

Figure 11. Estimates of O_x annual means calculated from annual O_3 and NO_2, averaged over the entire study period (1981–2015). City-level estimates for the largest cities are shown in the insets.

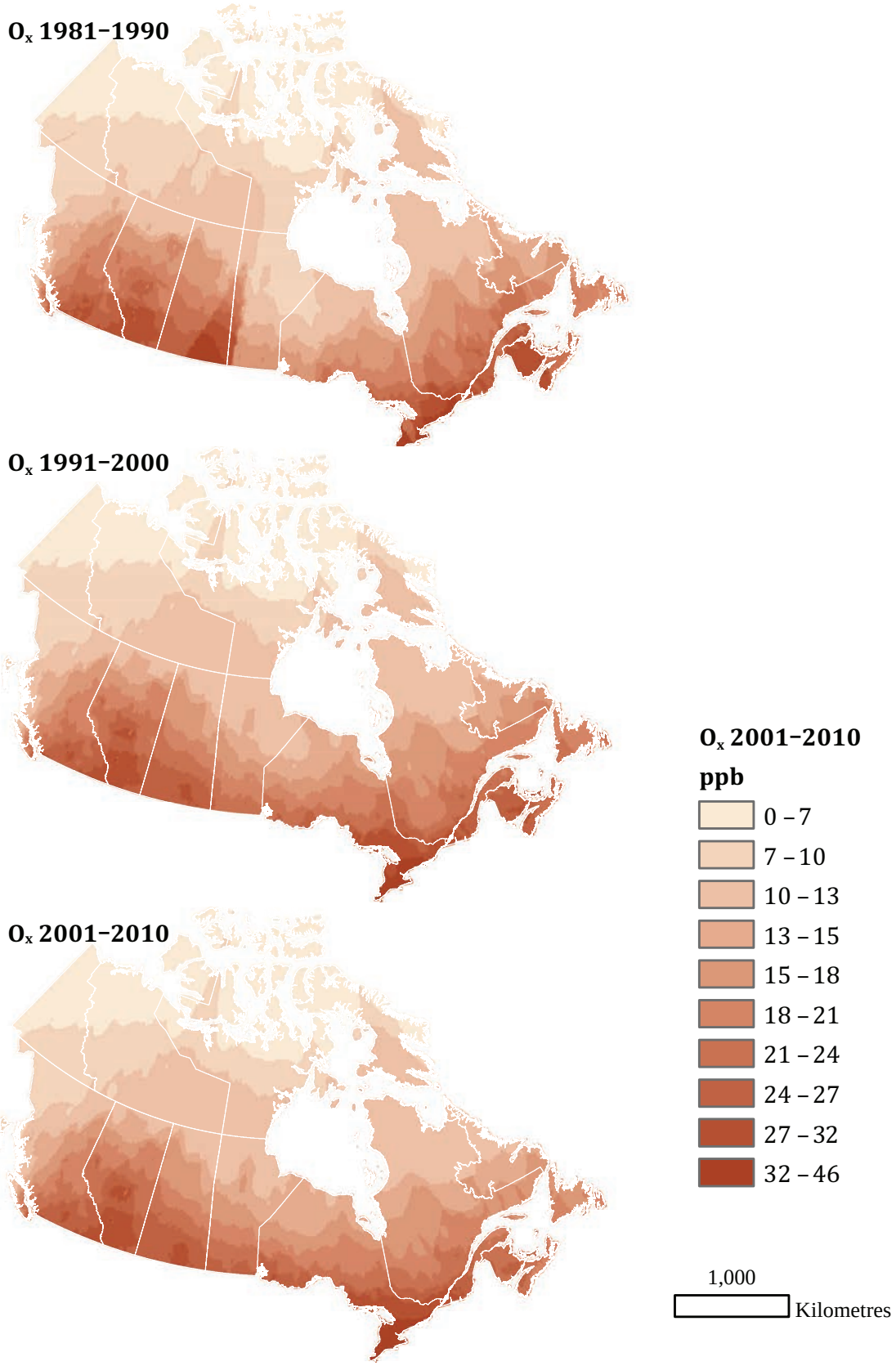

Figure 12. Estimates of O_x annual means averaged over decades within the study period (1981–1990, 1991–2000, and 2001–2011).

Table 4. Descriptive Statistics for $PM_{2.5}$, O_3, and O_x in all Cohorts for All Person-Years

Cohort / Pollutant[a]	Mean	SD	IQR	Minimum	5th	25th	50th	75th	95th	Maximum
Stacked CanCHEC										
$PM_{2.5}$	8.50	3.05	4.16	2.47	3.86	6.26	8.26	10.41	14.19	17.74
O_3	36.29	7.02	9.48	6.24	26.14	31.34	35.29	40.82	48.77	65.21
O_x	28.90	5.69	9.06	5.04	20.50	24.51	28.38	33.58	38.17	56.08
1991 CanCHEC										
$PM_{2.5}$	9.04	3.32	4.49	2.47	4.01	6.58	8.79	11.07	15.33	17.74
O_3	35.89	6.85	9.06	7.04	26.16	31.10	34.83	40.16	48.45	62.98
O_x	28.90	5.66	8.97	6.03	20.52	24.58	28.38	33.55	38.11	56.08
1996 CanCHEC										
$PM_{2.5}$	8.29	2.95	4.13	2.47	3.74	6.10	8.08	10.23	13.72	17.74
O_3	36.21	7.19	9.65	6.24	25.84	31.25	35.18	40.89	48.86	65.21
O_x	28.73	5.82	9.12	5.72	20.12	24.35	28.20	33.47	38.19	56.08
2001 CanCHEC										
$PM_{2.5}$	7.72	2.59	3.88	2.47	3.58	5.78	7.64	9.66	12.02	17.73
O_3	36.63	7.37	9.86	6.45	25.67	31.54	35.99	41.40	49.02	61.88
O_x	28.71	5.87	9.23	5.04	19.98	24.27	28.28	33.50	38.16	51.24
mCCHS										
$PM_{2.5}$	6.78	2.49	3.80	2.35	3.29	4.73	6.53	8.53	11.02	18.06
O_3	35.78	7.61	9.91	7.24	25.01	30.65	34.56	40.56	49.07	61.70
O_x	27.03	5.83	8.44	6.59	18.71	22.89	26.11	31.32	37.18	54.83

SD = standard deviation.

[a] Units are $\mu g/m^3$ for $PM_{2.5}$ and ppb for O_3 and O_x.

COHORTS: DESCRIPTIVE STATISTICS

CanCHEC Analytical Files: 1991, 1996, and 2001

Appendix Tables A.1 to A.3 (available on the HEI website) present descriptive statistics of each of the 1991, 1996, and 2001 CanCHEC analytical files, with Cox proportional HRs of nonaccidental mortality and mean exposures to $PM_{2.5}$, O_3, and O_x, among all model covariates.

Males tended to be assigned lower concentrations of all air pollutants than females in all three cohorts, although differences were very small (<0.1 $\mu g/m^3$ for $PM_{2.5}$). Mean exposure for $PM_{2.5}$ and O_x was higher with age at baseline in all three cohorts. Mean exposure for O_3 was lower for younger and older adults, but higher for middle-aged adults. Immigrants were consistently assigned higher concentrations than nonimmigrants. Subjects who identified themselves as visible minorities had higher assigned concentrations for all air pollutants than those who did not in the 1991 and 1996 cohorts. Subjects who identified themselves as Indigenous had lower concentrations than those who did not.

Exposure to $PM_{2.5}$ and O_x increased with educational attainment in all cohorts, while exposure to O_3 was highest in those with postsecondary education without a university degree. Exposure to O_3 and O_x increased with income. Exposure to $PM_{2.5}$ was highest in the 2nd income adequacy quintile. Subjects employed at the time of the survey had higher exposures than those who were unemployed. $PM_{2.5}$ exposure increased over the quintiles of the CAN-Marg dimensions of residential instability and ethnic concentration in all three cohorts.

Exposure to $PM_{2.5}$ generally increased with community size in the 1991 and 2001 cohorts, with no clear trends in the 1996 cohort. Of the six airsheds, the East Central contained the highest number of person-years and had the highest exposures for all air pollutants across all three cohorts.

CanCHEC Stacked Analytical File

Table 5 presents descriptive statistics of the Stacked CanCHEC, comprised of the 1991, 1996, and 2001 CanCHEC analytical files, with duplicates removed.

Table 5. Descriptive Statistics of the Stacked CanCHEC Analytical File with Cox Proportional HRs for Nonaccidental Mortality, and Outdoor Concentrations of $PM_{2.5}$, O_3, and O_x (10-year moving average with 1-year lag)

					$PM_{2.5}$ (μg/m³)		O_3 (ppb)		O_x (ppb)	
Characteristic	Person-Years[a]	HR[b]	95% CI		Mean	SD	Mean	SD	Mean	SD
Total	128,371,800	—	—	—	8.50	3.05	36.29	7.02	28.90	5.69
Sex										
Female	66,341,800	—	—	—	8.53	3.04	36.32	7.01	28.97	5.67
Male	62,030,100	—	—	—	8.47	3.07	36.26	7.03	28.83	5.71
Age (years)										
24–35	34,617,500	—	—	—	8.36	3.04	36.15	7.10	28.71	5.75
35–44	36,046,400	—	—	—	8.37	3.01	36.26	7.01	28.73	5.66
45–54	26,871,100	—	—	—	8.44	3.02	36.42	6.98	28.92	5.66
55–64	17,222,600	—	—	—	8.67	3.07	36.47	6.96	29.17	5.65
65–74	10,485,100	—	—	—	9.02	3.12	36.37	6.99	29.42	5.67
75–89	3,129,200	—	—	—	9.53	3.23	35.82	6.93	29.51	5.71
Immigrant status										
No (ref)	107,366,300	1.000	—	—	8.26	3.02	35.97	6.91	28.35	5.56
Yes	21,005,500	0.767	0.763	0.770	9.72	2.93	37.90	7.32	31.72	5.50
Income adequacy quintile										
Lowest (ref)	20,271,600	1.000	—	—	8.47	3.14	35.60	7.07	28.58	5.93
2nd	23,767,200	0.796	0.792	0.800	8.58	3.08	36.14	7.03	28.93	5.76
3rd	26,855,700	0.701	0.698	0.705	8.53	3.05	36.34	6.99	28.94	5.67
4th	28,350,300	0.626	0.623	0.630	8.50	3.02	36.49	6.99	28.97	5.61
Highest	29,127,100	0.534	0.531	0.537	8.44	3.00	36.64	7.01	29.00	5.55
Visible minority status										
No (ref)	119,997,100	1.000	—	—	8.45	3.06	36.30	6.99	28.76	5.65
Yes	8,374,700	0.830	0.822	0.838	9.24	2.89	36.17	7.39	30.88	5.96
Indigenous identity										
No (ref)	124,126,200	1.000	—	—	8.58	3.03	36.50	6.88	29.09	5.56
Yes	4,245,700	1.738	1.720	1.756	6.28	2.94	30.04	8.01	23.21	6.41
Employment status										
Employed (ref)	89,141,700	1.000	—	—	8.49	3.02	36.48	7.05	29.02	5.64
Unemployed	7,038,300	1.486	1.471	1.501	8.02	3.19	35.05	6.87	27.66	5.95
Not in labor force	32,191,800	1.639	1.631	1.647	8.66	3.12	36.02	6.93	28.84	5.75
Educational attainment										
< High school graduation (ref)	37,728,800	1.000	—	—	8.36	3.21	35.86	7.09	28.38	5.94
High school, with or without trades certification	47,533,900	0.812	0.809	0.816	8.46	3.04	36.34	7.04	28.79	5.64
Postsecondary nonuniversity	23,495,300	0.689	0.685	0.693	8.53	2.95	36.66	7.05	29.17	5.55
University degree	19,613,800	0.544	0.540	0.548	8.86	2.86	36.54	6.75	29.83	5.37

Continues next page

Table 5 (*Continued*). Descriptive Statistics of the Stacked CanCHEC Analytical File with Cox Proportional HRs for Nonaccidental Mortality, and Outdoor Concentrations of $PM_{2.5}$, O_3, and O_x (10-year moving average with 1-year lag)

					$PM_{2.5}$ (μg/m³)		O_3 (ppb)		O_x (ppb)	
Characteristic	Person-Years[a]	HR[b]	95% CI		Mean	SD	Mean	SD	Mean	SD
Occupational class										
Management (ref)	10,885,100	1.000	—	—	8.64	2.96	36.77	6.95	29.46	5.51
Professional	16,184,000	0.867	0.857	0.877	8.68	2.92	36.38	6.86	29.39	5.48
Skilled, technical, and supervisory	31,562,900	1.170	1.159	1.182	8.26	3.05	36.22	7.06	28.57	5.66
Semiskilled	31,876,800	1.313	1.300	1.326	8.48	3.06	36.48	7.13	28.95	5.73
Unskilled	9,777,200	1.538	1.521	1.556	8.31	3.14	35.89	7.23	28.35	5.95
Not applicable	28,085,900	1.922	1.904	1.941	8.72	3.11	36.05	6.87	28.90	5.73
Community Size (*n*)										
Pop: > 1,500,000 (ref)	36,383,800	1.000	—	—	10.12	2.43	37.25	5.94	32.06	4.54
Pop: 500,000 – 1,499,999	21,100,100	0.941	0.936	0.946	8.53	2.42	34.45	5.79	29.06	3.90
Pop: 100,000 – 499,999	23,408,700	1.018	1.013	1.023	9.07	3.22	39.49	8.19	30.36	6.34
Pop: 30,000 – 99,999	12,633,600	1.026	1.019	1.032	8.24	3.05	36.36	6.63	27.37	4.80
Pop: 10,000 – 29,999	4,983,800	1.034	1.024	1.044	6.73	2.69	32.74	7.36	24.34	5.42
Not a CMA or CA	29,861,700	1.037	1.031	1.042	6.48	2.71	34.48	6.93	25.21	5.03
Airshed										
Western (ref)	15,378,700	1.000	—	—	7.55	2.52	29.54	4.40	24.14	3.29
Prairie	16,688,100	0.947	0.940	0.954	6.36	1.89	32.24	4.38	26.08	3.65
West Central	7,417,000	1.041	1.032	1.050	6.47	1.97	29.17	3.96	23.76	3.57
Southern Atlantic	12,502,600	1.095	1.087	1.103	5.28	1.93	32.22	3.05	23.25	2.63
East Central	75,502,400	1.027	1.021	1.032	9.95	2.68	40.06	5.99	32.05	4.68
Northern	883,000	1.182	1.154	1.211	4.81	1.80	25.69	6.39	18.77	4.16
Urban form										
Active urban core (ref)	9,789,200	1.000	—	—	9.85	2.54	35.68	6.98	30.86	5.27
Transit-reliant suburb	8,276,800	0.942	0.934	0.950	10.27	2.46	35.66	6.20	31.74	4.86
Car-reliant suburb	52,819,500	0.871	0.865	0.876	9.41	2.71	37.39	6.83	30.89	5.06
Exurban	7,279,600	0.912	0.903	0.921	7.61	2.73	38.30	7.06	28.96	5.16
Not a CMA	50,206,800	0.945	0.939	0.951	7.12	3.00	35.06	7.09	25.94	5.26
Residential instability (CAN-Marg)										
Q1 (lowest) (ref)	29,568,200	1.000	—	—	8.05	3.11	37.83	7.26	29.35	5.84
Q2	33,703,000	1.002	0.996	1.007	8.06	3.08	36.85	7.42	28.47	5.78
Q3	26,187,300	1.000	0.994	1.006	8.42	3.13	35.18	7.08	28.09	5.91
Q4	22,745,900	1.004	0.998	1.009	9.09	2.89	35.76	6.42	29.27	5.45
Q5 (highest)	16,167,400	1.060	1.053	1.066	9.56	2.57	34.85	5.62	29.76	4.89
Dependence (CAN-Marg)										
Q1 (lowest) (ref)	21,194,400	1.000	—	—	8.54	3.12	35.36	7.39	28.99	6.09
Q2	21,610,100	0.969	0.962	0.976	8.79	3.03	36.23	7.00	29.33	5.62
Q3	20,965,400	0.963	0.957	0.970	9.04	3.02	37.16	7.14	29.88	5.54
Q4	27,313,100	0.952	0.946	0.958	8.72	3.02	36.89	7.23	29.20	5.55
Q5 (highest)	37,288,900	0.932	0.926	0.937	7.86	2.97	35.92	6.47	27.84	5.52

Continues next page

Table 5 (*Continued*). Descriptive Statistics of the Stacked CanCHEC Analytical File with Cox Proportional HRs for Nonaccidental Mortality, and Outdoor Concentrations of $PM_{2.5}$, O_3, and O_x (10-year moving average with 1-year lag)

Characteristic	Person-Years[a]	HR[b]	95% CI		$PM_{2.5}$ (μg/m³)		O_3 (ppb)		O_x (ppb)	
					Mean	SD	Mean	SD	Mean	SD
Material deprivation (CAN-Marg)										
Q1 (lowest) (ref)	26,776,400	1.000	—	—	8.48	2.83	37.50	6.97	29.63	5.34
Q2	27,472,900	1.057	1.050	1.063	8.85	2.87	37.31	7.24	29.48	5.46
Q3	25,619,000	1.077	1.071	1.083	8.73	2.97	36.68	7.17	29.21	5.48
Q4	21,604,900	1.110	1.104	1.117	8.75	3.02	35.66	6.98	28.98	5.81
Q5 (highest)	26,898,600	1.196	1.189	1.203	7.76	3.42	34.18	6.15	27.22	6.01
Ethnic concentration (CAN-Marg)										
Q1 (lowest) (ref)	39,063,200	1.000	—	—	7.30	2.90	36.10	6.87	27.27	5.31
Q2	31,068,600	1.019	1.014	1.024	8.36	2.96	36.87	7.16	28.79	5.54
Q3	22,368,600	1.016	1.010	1.021	8.74	2.96	35.79	7.28	29.08	5.85
Q4	18,766,500	1.029	1.023	1.035	9.63	2.82	36.26	6.94	30.48	5.57
Q5 (highest)	17,105,000	1.031	1.025	1.037	9.96	2.79	36.35	6.75	30.86	5.60

Ref = reference category; SD = standard deviation.

[a] Person-years are rounded to the nearest hundred for confidentiality reasons; sums may not add up to totals.

[b] HR for nonaccidental mortality relative to reference category stratified by age (5-year categories), sex, and immigrant status.

Similar to the individual cohorts, females in the stacked cohort had marginally higher air pollution estimates than males (i.e., 0.06 μg/m³ greater $PM_{2.5}$). Immigrants were also assigned higher concentrations than nonimmigrants for all air pollutants (1.46 μg/m³ greater $PM_{2.5}$). Subjects who identified themselves as visible minorities also had higher assigned concentrations for $PM_{2.5}$ and O_x than those who did not (0.79 μg/m³ greater $PM_{2.5}$). Exposure to O_3 and O_x increased marginally with income. Outdoor concentrations of $PM_{2.5}$ were greatest for those in the three middle-income quintiles.

Outdoor $PM_{2.5}$ concentrations increased over the quintiles of the CAN-Marg dimensions of residential instability and ethnic concentration. Outdoor $PM_{2.5}$ and O_x tended to increase with community size, with no clear trends for O_3 exposure. Of the six airsheds, the East Central contained the highest number of person-years and had the highest outdoor concentrations for all air pollutants. For example, the mean outdoor $PM_{2.5}$ concentration for the East Central airshed was 2.4 μg/m³ greater than the next-highest concentration (for the Western airshed).

Appendix Table A.4 (available on the HEI website) presents descriptive statistics of annual $PM_{2.5}$ estimates in the Stacked CanCHEC. The mean $PM_{2.5}$ estimates gradually decreased between 1991 (representing the mean of 1981 to 1990) of 12.2 μg/m³ and 2016 (representing the mean of 2006 to 2015) of 6.83 μg/m³.

CCHS Analytical File

Appendix Table A.5 presents descriptive statistics of the CCHS analytical cohort (mCCHS). Outdoor concentrations of all three air pollutants were slightly higher among women than men, immigrants, and people not identified as Indigenous. Subjects who defined themselves as visible minorities had higher assigned concentrations for $PM_{2.5}$ and O_x than those who did not. Outdoor air pollutant concentrations assigned to cohort members also tended to be higher among people ages 65 years and older. Being single, university educated, and in the poorest income quintile was associated with higher outdoor $PM_{2.5}$ concentrations. These relationships differ somewhat from those of the CanCHEC cohorts and likely reflect sampling differences for the CCHS, compared with the census. Subjects who were unemployed at the time of the interview were generally assigned lower outdoor $PM_{2.5}$ concentrations than those employed or not in the labor force.

Outdoor $PM_{2.5}$ concentrations increased over the quintiles of the CAN-Marg dimensions of residential instability and ethnic concentration. Concentrations of $PM_{2.5}$ and O_x tended to increase with community size, with the highest O_3 concentrations observed in communities with populations between 100,000 and 499,999. Similar to the previous cohorts, the East Central airshed contained the highest number of person-years and had the highest outdoor concentrations for all air pollutants.

EPIDEMIOLOGICAL ANALYSES

Main Analysis: Nonaccidental Mortality

Table 6 reports the HRs and 95% CIs for nonaccidental mortality for each CanCHEC cohort separately, the Stacked

Table 6. HRs for Nonaccidental Mortality in Fully Adjusted Models Among Different Cohorts (CanCHECs and mCCHS) for 10-Year Mean Outdoor $PM_{2.5}$ Concentrations[a]

Cohort	Deaths[b]	Coeff	SE	HR[c]	95% CI	
Stacked CanCHEC	1,253,300	0.0081	0.0005	1.084	1.073	1.096
1991 CanCHEC	531,300	0.0068	0.0008	1.070	1.053	1.086
1996 CanCHEC	537,400	0.0073	0.0008	1.076	1.058	1.094
2001 CanCHEC	401,000	0.0103	0.0011	1.109	1.086	1.132
mCCHS without behavior[d]	50,100	0.0116	0.0031	1.123	1.056	1.194
mCCHS with behavior[d]	50,100	0.0082	0.0031	1.086	1.021	1.155

[a] Fully adjusted models are stratified by sex, age (5-year categories), and recent immigrant status and are adjusted for income adequacy quintile, visible minority status, Indigenous identity, educational attainment, labor-force status, marital status, occupation, and ecological covariates of community size, airshed, urban form, and four dimensions of Can-Marg (instability, deprivation, dependency, and ethnic concentration). Stacked CanCHEC analyses were also stratified by the CanCHEC cohort, and mCCHS analyses were also stratified by the CCHS cycle.

[b] Deaths were rounded to the nearest 100 for confidentiality.

[c] HRs are presented as per 10-μg/m^3 increase.

[d] Behavioral covariates include additional adjustments for smoking, alcohol consumption, fruit and vegetable consumption, BMI, and exercise behavior.

CanCHEC cohort, and the mCCHS cohort (with and without behavioral covariates) per 10-μg/m^3 increase in $PM_{2.5}$ exposure. The largest cohort (the Stacked CanCHEC), representing nearly 1.3 million deaths, yielded an HR of 1.084 for nonaccidental mortality (95% CI: 1.073 to 1.096) per 10-μg/m^3 increase. For an IQR increase of 4.16 μg/m^3 in $PM_{2.5}$ mass concentration and for a mean nonaccidental death rate of 92.8/10,000 persons (over the 1991–2016 period for cohort participants ages 25–90), this HR corresponds to an additional 31.62/100,000 deaths (equivalent to an additional 7,848 deaths in Canada based on 2016 population counts). The HR from the 2001 CanCHEC was marginally higher than in previous CanCHEC cycles.

Use of the refined $PM_{2.5}$ (version 2-MAPLE) resulted in marginally stronger associations in the 1991 and 1996 CanCHECs and marginally weaker associations in the 2001 and mCCHS cohorts when compared with the version 1 exposure estimates that were used in the MAPLE Phase 1 report (Appendix Table A.6; available on the HEI website). As indicated in Crouse and colleagues (2020), the use of a 3-year moving average resulted in weaker associations between $PM_{2.5}$ and nonaccidental mortality than did a 10-year moving average (Appendix Table A.7).

The shape of the association between $PM_{2.5}$ and nonaccidental mortality is provided in Figure 13 for each of the 1991, 1996, and 2001 CanCHEC cohorts, using the RCS model with knots based on the minimum BIC model fit. In the 1991 and 1996 RCS models, a noticeable decline in HRs was observed between 5 and 10 μg/m^3, which was not observed in 2001. For each plot we identified the concentration at which the lower confidence limit of the function is <1 as an indication of the lowest adverse effect (mortality) level; this occurs at 4.0 μg/m^3 in the 1991 CanCHEC, 3.4 μg/m^3 in the 1996 CanCHEC, and 4.3 μg/m^3 in the 2001 CanCHEC.

Figure 14 shows the shape of the association between outdoor $PM_{2.5}$ concentrations and nonaccidental mortality for the Stacked CanCHEC cohort by the number of knots used in the RCS (3 to 18). The RCS predictions are sublinear for three and four knots but take on more complex shapes for five and more knots. The 5 to 18 knot-based RCS functions produced an uneven curve between 5 and 12 μg/m^3 with more complex curvature as the number of knots increased. Additional information on the fit is provided in the last row of panels in Figure 14. The −2 log-likelihood values decline with increasing number of knots as do the AIC values. The largest decline is observed from 8 to 9 knots. However, the BIC values increase from their minimum at 9 knots, suggesting additional knots may not be clearly improving the fit. The concentration, *C*, at which the lower confidence limit on the RCS predictions is <1 is also displayed by the number of knots (lower right panel Figure 14). The concentration is highest for four knots at C = 4.2 μg/m^3 and lowest for 9 and 10 knots at C = 2.8 μg/m^3. The concentration is relatively stable for knots number five and above (C = 2.8 μg/m^3 to C = 3.1 μg/m^3).

Using the likelihood-ratio test, we examine the strength of evidence that the RCS represented a statistically improved fit over the linear model. The likelihood ratio *P* value comparing the linear model to an RCS with 3 knots is P = 0.0082, for an RCS with 4 knots is P = 0.0183, and for all other numbers of knot (5 to 18) *P* values were <0.00001, suggesting that all RCS models examined displayed some

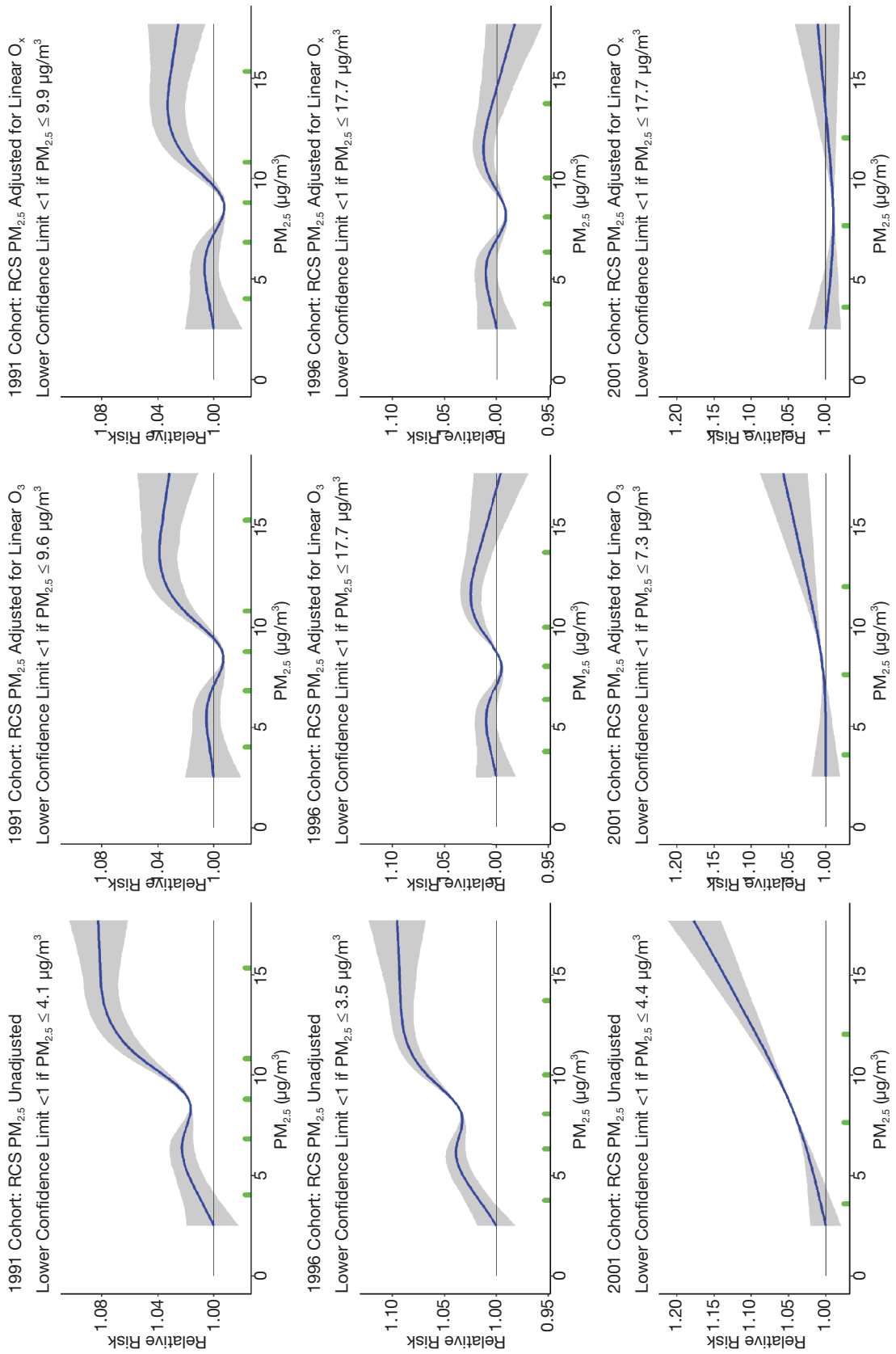

Figure 13. Predicted relative risk of nonaccidental mortality by $PM_{2.5}$ concentration (µg/m³) for the 1991, 1996, and 2001 CanCHEC cohorts. Predictions are **(left column)** unadjusted for either O_3 or O_x, **(center column)** adjusted for O_3, and **(right column)** adjusted for O_x. Mean predictions are displayed as solid blue lines with 95% CIs as grey-shaded areas. Green x-axis tick marks show RCS knot locations.

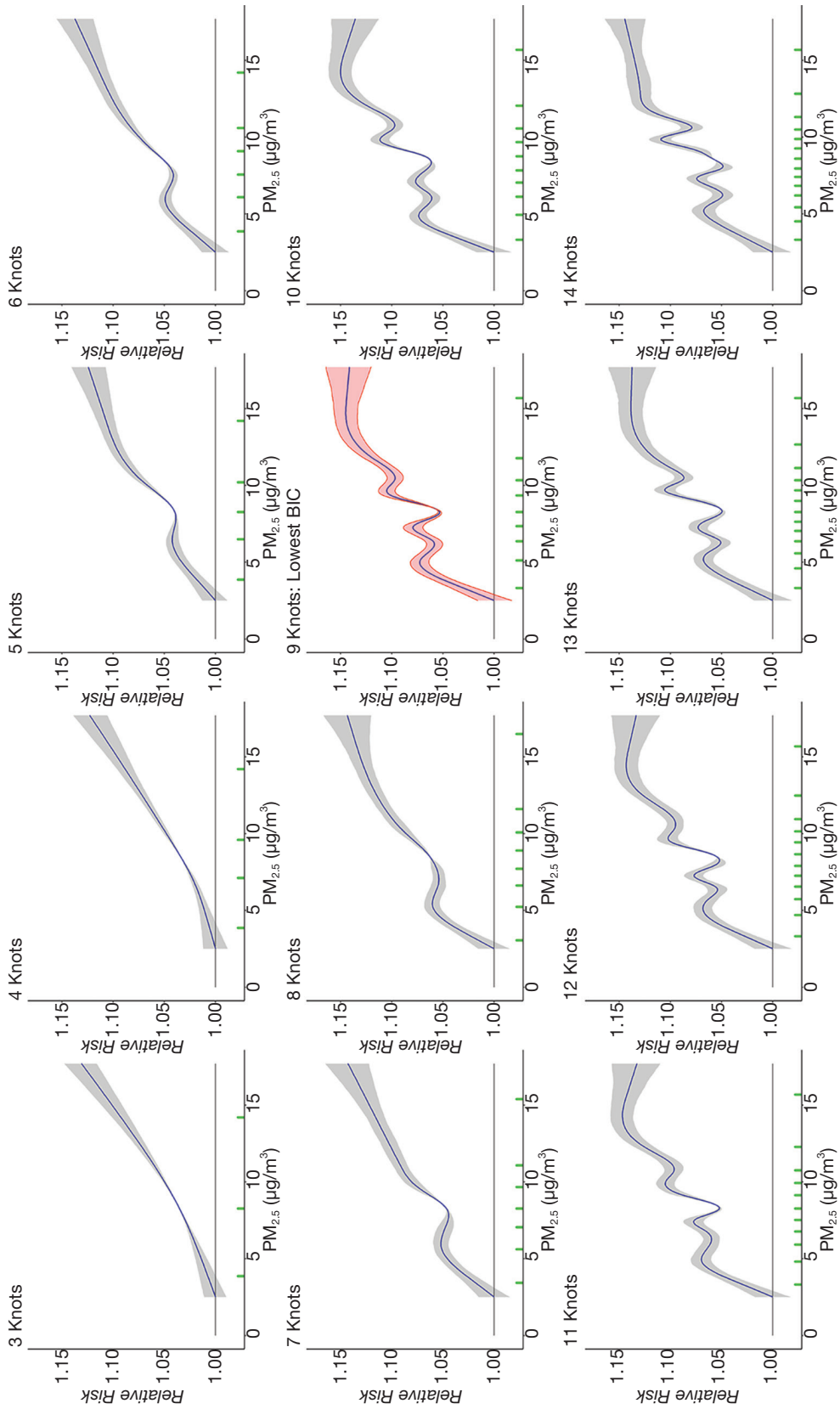

Figure 14. Predicted relative risk of nonaccidental mortality by $PM_{2.5}$ concentration (µg/m³) for the Stacked CanCHEC cohort by number of knots used in the RCS fit [3–18 knots; Rows 1–4]. Mean predictions are displayed as solid blue lines with 95% CIs as grey-shaded areas. Green x-axis tick marks show RCS knot locations. The pink curve at 9 knots has the lowest BIC value. From left to right the last row of panels shows −2 log-likelihood values, AIC, BIC, and the highest concentration below which the RCS lower confidence limit is less than one. *Figure continues next page.*

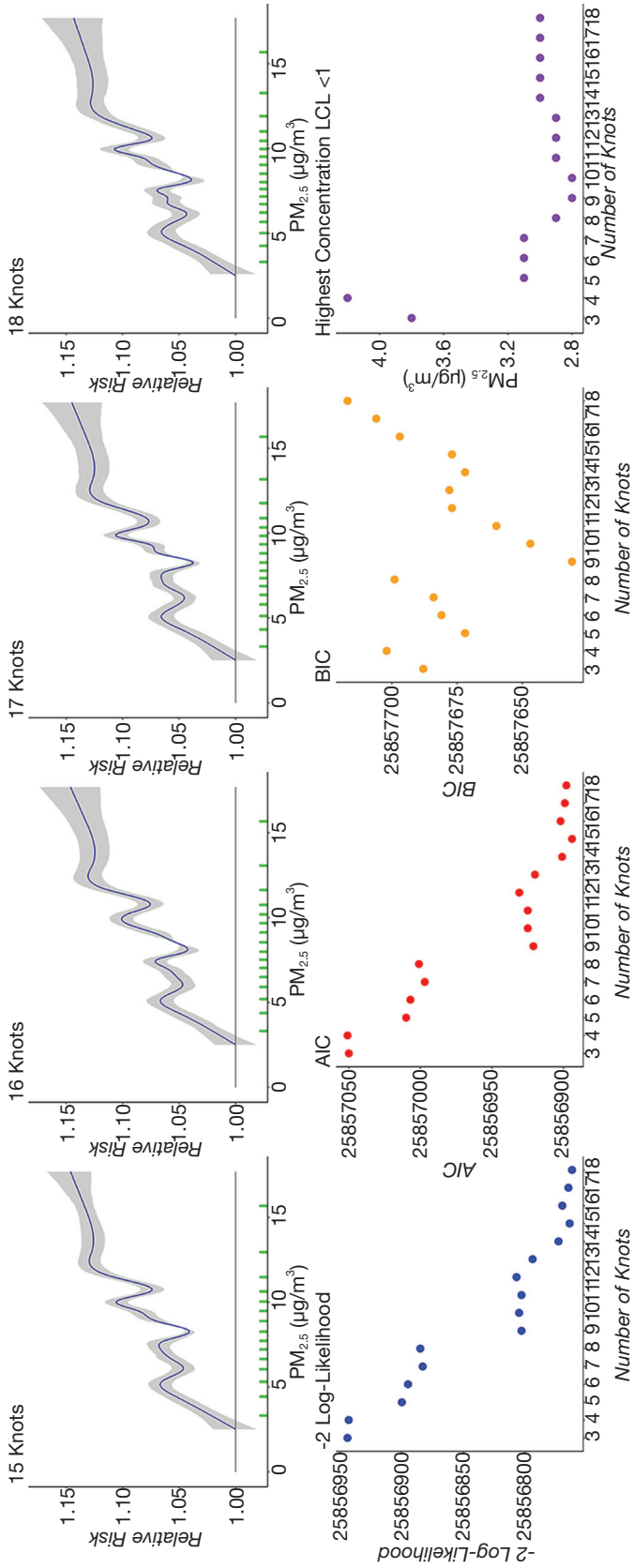

Figure 14. *(Continued).*

evidence of improved fit over the linear model. The likelihood ratio test is appropriate because all RCS models include a linear term, and thus the linear model is nested within each RCS model.

In the mCCHS cohort, the addition of behavioral covariates (i.e., smoking, alcohol consumption, fruit and vegetable consumption, BMI, and exercise behavior) attenuated the association, from HR = 1.123 (95% CI: 1.056 to 1.194) without covariates to HR = 1.086 (1.021 to 1.155) with covariates, (both per 10-μg/m^3 increase) (Table 6). Figure 15 illustrates the shape of the association for the mCCHS cohort, with and without adjustment for behavioral covariates. The shape of the curve was very similar between the two levels of adjustment, and the lower confidence limit was less than one at concentrations ≤3.6 μg/m^3 without behavioral covariate adjustment and ≤3.7 μg/m^3 with adjustment.

Main Analysis: Other Causes of Death

We determined HR estimates assuming a linear concentration model for cause-specific mortality per increase in 10-μg/m^3 exposure, for each CanCHEC cohort separately, the Stacked CanCHEC cohort, and the mCCHS cohort, with and without behavioral covariates (Table 7). For the Stacked CanCHEC cohort, we also produced RCS curves using BIC to determine model fitness for each of the causes of death (Figure 16):

- **Cardiovascular Disease** — In the stacked cohort (390,600 deaths), HRs in linear models were 1.163 (95% CI: 1.142 to 1.185, per 10-μg/m^3 increase). Similar associations were observed in other cohorts, but the model was not robust to adjustment for behavioral covariates in the mCCHS cohort (Table 7). The lower confidence limit for the RCS fit in the stacked cohort was less than one for $PM_{2.5}$ concentrations <3.5 μg/m^3 (Figure 16).
- **Cerebrovascular Disease** — In the stacked cohort (72,900 deaths), HRs in linear models were 1.105 (95% CI: 1.058 to 1.154, per 10-μg/m^3 increase). Similar associations were observed in the CanCHECs, but the 95% CI included one for the mCCHS cohort with and without behavior covariate adjustment (Table 7). The lower confidence limit for the RCS fit in the stacked cohort was less than one for $PM_{2.5}$ concentrations <10.8 μg/m^3 (Figure 16).
- **Heart Failure** — No significant associations were observed between heart failure mortality and exposure to $PM_{2.5}$ in any cohort examined (Table 7) with the lower confidence limit for the RCS fit in the stacked cohort being less than one for $PM_{2.5}$ concentrations <17.7 μg/m^3, the highest concentration examined (Figure 16).
- **Ischemic Heart Disease** — In the stacked cohort (215,700 deaths), HRs in linear models were 1.225 (95% CI: 1.195 to 1.255, per 10-μg/m^3 increase), and were significant in all cohorts examined, including after the addition of behavioral characteristics to mCCHS (Table 7). The lower confidence limit for the RCS fit in the stacked cohort was less than one for $PM_{2.5}$ concentrations <3.7 μg/m^3 (Figure 16).
- **Diabetes** — In the stacked cohort (41,100 deaths), HRs in linear models were 1.244 (95% CI: 1.173 to 1.319, per 10-μg/m^3 increase), were significant in all cohorts examined, and were robust to the addition of behavioral characteristics to mCCHS (Table 7). The lower confidence limit for the RCS fit in the stacked cohort was less than one for $PM_{2.5}$ concentrations <10.5 μg/m^3 (Figure 16).
- **Respiratory Disease** — In the stacked cohort (105,900 deaths), HR in linear models were 1.076 (95% CI: 1.037 to 1.118, per 10-μg/m^3 increase). Similar associations were observed in other cohorts, including mCCHS adjusted for behavioral covariates, except the 2001 CanCHEC (Table 7). The lower confidence limit for the RCS fit in the stacked cohort was less than one for $PM_{2.5}$ concentrations <3.8 μg/m^3 (Figure 16).
- **COPD** — In the stacked cohort (61,400 deaths), HRs in linear models were 1.059 (95% CI: 1.010 to 1.111, per 10-μg/m^3 increase), were robust to the addition of behavioral characteristics in mCCHS, but significant associations were not observed in the 1991 or 2001 CanCHECs (Table 7). The lower confidence limit for the RCS fit in the stacked cohort was less than one for $PM_{2.5}$ concentrations <4.5 μg/m^3 (Figure 16).
- **Pneumonia** — In the stacked cohort (25,600 deaths), HRs in linear models were 1.195 (95% CI: 1.110 to 1.287 per 10-μg/m^3 increase), but these associations were not consistent across the 2001 CanCHEC and the mCCHS cohorts (Table 7). The lower confidence limit for the RCS fit in the stacked cohort was less than one for $PM_{2.5}$ concentrations <4.1 μg/m^3 (Figure 16).
- **Lung Cancer** — No significant associations between lung cancer mortality and exposure to $PM_{2.5}$ were observed in any cohort examined (Table 7). In the RCS, the shape of the curve increased dramatically until 10-μg/m^3. The lower confidence limit for the RCS fit in the stacked cohort was less than one for $PM_{2.5}$ concentrations <17.7 μg/m^3, the highest concentration examined (Figure 16).
- **Kidney Failure** — No significant associations were observed between kidney failure mortality and exposure to $PM_{2.5}$ in any cohort examined (Table 7).

Sensitivity Analyses

Two-Pollutant Models: Joint Models with O_3 or O_x We considered a series of models where we added linear or RCS nonlinear terms for O_3. We also fit fully adjusted RCS models for $PM_{2.5}$, adjusting for a linear term of O_x.

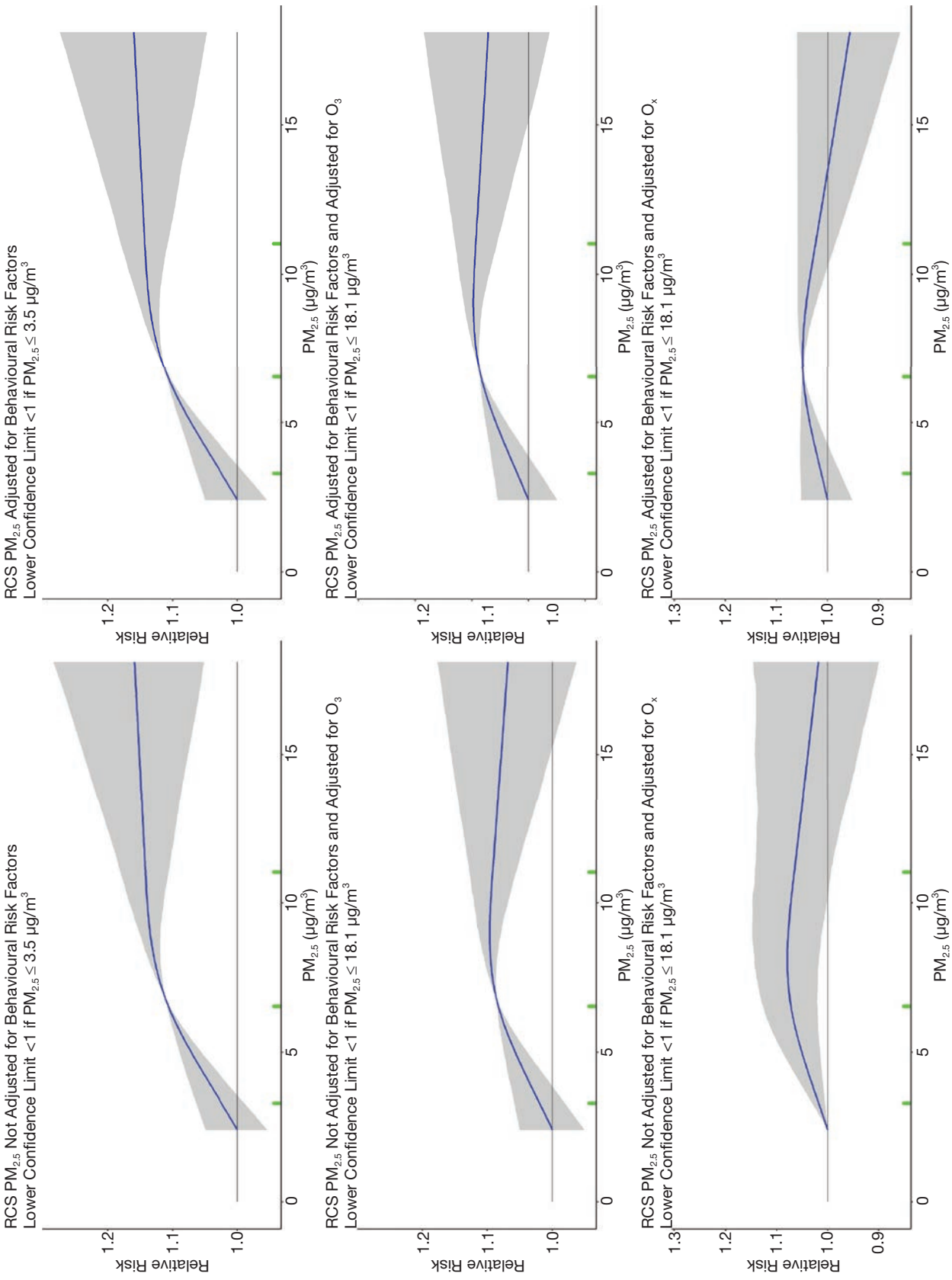

Figure 15. RCS-based predicted relative risk by $PM_{2.5}$ concentration (µg/m³) for the mCCHS cohort by: (left column) unadjusted and **(right column)** adjusted for behavioral covariates. Corresponding predictions adjusted for either O_3 **(middle row)** or O_x **(bottom row)** are also presented. Mean predictions are displayed as solid blue lines with 95% CIs as grey-shaded areas. Green x-axis tick marks show RCS knot locations.

Table 7. Cox Proportional HRs of Selected Causes of Death in Fully Adjusted Models Among Different CanCHEC Cohorts and mCCHS for Exposure to $PM_{2.5}$ During the Previous 10 Years[a]

Cause of Death / Cohort	Deaths[b] (*n*)	Coeff	SE	HR[c]	95% CI	
Cardiovascular						
Stacked CanCHEC	390,600	0.0151	0.0010	1.163	1.142	1.185
1991 CanCHEC	171,500	0.0139	0.0014	1.149	1.119	1.180
1996 CanCHEC	166,500	0.0151	0.0015	1.163	1.130	1.197
2001 CanCHEC	117,600	0.0161	0.0020	1.175	1.131	1.221
mCCHS without behavior[d]	14,800	0.0122	0.0057	1.130	1.010	1.264
mCCHS with behavior[d]	14,800	0.0082	0.0057	1.085	0.970	1.214
Cerebrovascular						
Stacked CanCHEC	72,900	0.0100	0.0022	1.105	1.058	1.154
1991 CanCHEC	32,100	0.0100	0.0032	1.108	1.041	1.178
1996 CanCHEC	30,900	0.0069	0.0035	1.071	1.001	1.147
2001 CanCHEC	21,800	0.0159	0.0046	1.172	1.071	1.282
mCCHS without behavior[d]	2,700	0.0004	0.0135	1.004	0.770	1.308
mCCHS with behavior[d]	2,700	−0.0014	0.0135	0.986	0.757	1.285
Heart failure						
Stacked CanCHEC	20,500	0.0041	0.0043	1.042	0.959	1.133
1991 CanCHEC	8,800	−0.0004	0.0061	0.996	0.884	1.123
1996 CanCHEC	8,800	0.0009	0.0066	1.009	0.886	1.149
2001 CanCHEC	6,400	0.0083	0.0086	1.086	0.918	1.286
mCCHS without behavior[d]	900	−0.0119	0.0249	0.888	0.545	1.448
mCCHS with behavior[d]	900	−0.0178	0.0249	0.837	0.513	1.364
Ischemic heart disease						
Stacked CanCHEC	215,700	0.0203	0.0013	1.225	1.195	1.255
1991 CanCHEC	96,000	0.0185	0.0018	1.203	1.161	1.246
1996 CanCHEC	91,600	0.0211	0.0020	1.235	1.189	1.284
2001 CanCHEC	63,600	0.0192	0.0026	1.212	1.151	1.276
mCCHS without behavior[d]	7,900	0.0248	0.0077	1.281	1.101	1.491
mCCHS with behavior[d]	7,900	0.0202	0.0078	1.224	1.051	1.424
Diabetes						
Stacked CanCHEC	41,100	0.0218	0.0030	1.244	1.173	1.319
1991 CanCHEC	17,100	0.0180	0.0044	1.198	1.098	1.307
1996 CanCHEC	18,300	0.0163	0.0046	1.176	1.075	1.287
2001 CanCHEC	13,600	0.0293	0.0058	1.340	1.196	1.501
mCCHS without behavior[d]	1,700	0.0492	0.0170	1.636	1.173	2.281
mCCHS with behavior[d]	1,700	0.0399	0.0170	1.491	1.068	2.081
Respiratory						
Stacked CanCHEC	105,900	0.0073	0.0019	1.076	1.037	1.118
1991 CanCHEC	43,100	0.0067	0.0029	1.069	1.011	1.131
1996 CanCHEC	45,900	0.0083	0.0029	1.087	1.026	1.151

Continues next page

Table 7 (*Continued*). Cox Proportional HRs of Selected Causes of Death in Fully Adjusted Models Among Different CanCHEC Cohorts and mCCHS for Exposure to $PM_{2.5}$ During the Previous 10 Years[a]

Cause of Death / Cohort	Deaths[b] (*n*)	Coeff	SE	HR[c]	95% CI	
2001 CanCHEC	35,400	0.0059	0.0037	1.061	0.988	1.140
mCCHS without behavior[d]	4,800	0.0250	0.0102	1.284	1.051	1.568
mCCHS with behavior[d]	4,800	0.0220	0.0102	1.246	1.020	1.523
COPD						
Stacked CanCHEC	61,400	0.0057	0.0024	1.059	1.010	1.111
1991 CanCHEC	25,800	0.0025	0.0036	1.025	0.956	1.099
1996 CanCHEC	26,300	0.0101	0.0038	1.106	1.027	1.191
2001 CanCHEC	19,300	0.0048	0.0049	1.050	0.954	1.155
mCCHS without behavior[d]	2,800	0.0388	0.0133	1.473	1.135	1.912
mCCHS with behavior[d]	2,800	0.0355	0.0133	1.426	1.098	1.852
Pneumonia						
Stacked CanCHEC	25,600	0.0178	0.0038	1.195	1.110	1.287
1991 CanCHEC	11,500	0.0182	0.0053	1.200	1.082	1.331
1996 CanCHEC	10,900	0.0200	0.0059	1.221	1.087	1.371
2001 CanCHEC	7,600	0.0082	0.0080	1.085	0.927	1.271
mCCHS without behavior[d]	900	−0.0012	0.0231	0.988	0.629	1.553
mCCHS with behavior[d]	900	−0.0029	0.0231	0.972	0.618	1.528
Lung cancer						
Stacked CanCHEC	129,200	−0.0011	0.0017	0.989	0.957	1.022
1991 CanCHEC	54,700	−0.0035	0.0025	0.966	0.920	1.013
1996 CanCHEC	54,800	−0.0002	0.0026	0.998	0.948	1.051
2001 CanCHEC	41,800	0.0050	0.0033	1.051	0.986	1.121
mCCHS without behavior[d]	5,400	0.0017	0.0095	1.017	0.845	1.224
mCCHS with behavior[d]	5,400	−0.0024	0.0094	0.977	0.812	1.175
Kidney failure						
Stacked CanCHEC	15,000	−0.0034	0.0050	0.966	0.876	1.067
1991 CanCHEC	6,200	0.0021	0.0074	1.021	0.883	1.181
1996 CanCHEC	6,600	−0.0044	0.0077	0.957	0.824	1.112
2001 CanCHEC	4,800	0.0087	0.0099	1.091	0.899	1.324
mCCHS without behavior[d]	600	−0.0189	0.0290	0.828	0.470	1.461
mCCHS with behavior[d]	600	−0.0256	0.0290	0.774	0.439	1.368

[a] Fully adjusted models are stratified by sex, age (5-year categories), and recent immigrant status and are adjusted for income adequacy quintile, visible minority status, Indigenous identity, educational attainment, labor-force status, marital status, occupation, and ecological covariates of community size, airshed, urban form, and four dimensions of CanMarg (instability, deprivation, dependency, and ethnic concentration). Stacked CanCHEC analyses were also stratified by the CanCHEC cohort, and mCCHS analyses were also stratified by the CCHS cycle.

[b] Deaths were rounded to the nearest 100 for confidentiality.

[c] HRs are presented as per 10-$\mu g/m^3$ increase.

[d] Behavioral covariates include additional adjustment for smoking, alcohol consumption, fruit and vegetable consumption, BMI, and exercise behavior.

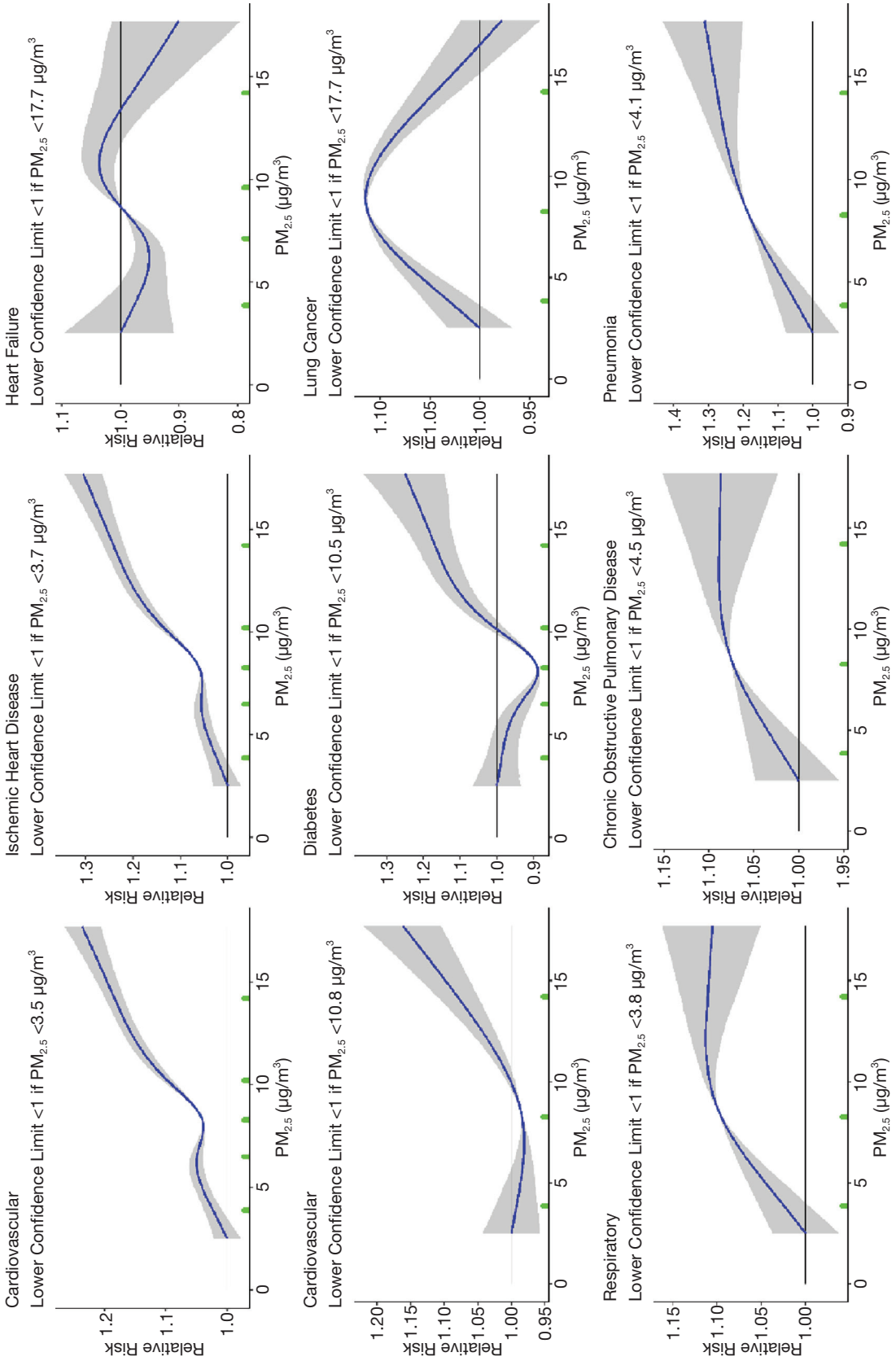

Figure 16. RCS-based predicted relative risk by $PM_{2.5}$ concentration (µg/m³) for the Stacked CanCHEC cohort by cause of death. Mean predictions are displayed as solid blue lines with 95% CIs as grey-shaded areas. Green x-axis tick marks show RCS knot locations.

Adjusting for O_3 attenuated the HR estimates for the association between outdoor $PM_{2.5}$ and nonaccidental mortality. Specifically, in the Stacked CanCHEC adjusting for O_3, the HR for $PM_{2.5}$ (per 10-µg/m³ increase) was 1.039 (95% CI: 1.027 to 1.051) (Table 8) compared with 1.084 (1.073 to 1.096) in models not adjusting for O_3 (Table 6). In the 1996 CanCHEC and mCCHS cohorts, $PM_{2.5}$ was not associated with nonaccidental mortality after adding O_3. After adding a linear O_3 term to the RCS for $PM_{2.5}$ in the Stacked CanCHEC, we observed the highest concentration for which the RCS lower confidence limit was less than one, at 2.9 µg/m³ (Figure 17), a value similar to that based on the unadjusted model of 2.8 µg/m³. Similarly, when a nonlinear RCS O_3 fit was added to the RCS for $PM_{2.5}$, this concentration remained the same at 2.9 µg/m³. However, the magnitude of the relative-risk predictions was smaller after O_3 adjustment and was similar for either linear or RCS O_3 model specifications. The RCS for O_3 was relatively flat for concentrations below 40 ppb (Figure 17). Nonlinear associations with the other cohorts are provided in the Appendix Figure E.1, available on the HEI website.

The addition of O_3, either as a linear or the RCS model, greatly attenuated associations between outdoor $PM_{2.5}$ concentrations and cardiovascular mortality. In the Stacked CanCHEC, the HR for $PM_{2.5}$ decreased to 1.048 (95% CI: 1.027 to 1.070) when O_3 was included in the model (Table 9) compared with 1.163 (1.142 to 1.185) in the model excluding O_3 (Table 7). When a linear O_3 term was added to the RCS model for the relationship between $PM_{2.5}$ and cardiovascular mortality, the 95% CI included the null throughout most of the range of $PM_{2.5}$ concentrations (Figure 17). The same was true when a nonlinear O_3 term was added to the RCS (Figure 17). Increased HRs for O_3 were evident, but only for concentrations above approximately 24 ppb.

The CIs spanned an HR of 1.0 for the association between outdoor $PM_{2.5}$ concentrations and respiratory mortality in the stacked cohort after adjusting for O_3 (Table 9 and Figure 17), although there was some suggestion of an elevated HR. Similarly, the concentration–response curves suggested some tendency for increased HRs, although with wide uncertainty intervals. There was little evidence of an association between O_3 and respiratory mortality in the linear model. The RCS revealed a complex association with increases below 50 ppb and then a marked decline above 50 ppb (Figure 17).

Table 8. Cox Proportional HRs of Nonaccidental Mortality in Fully Adjusted Models in CanCHEC Cohorts and mCCHS, with Both $PM_{2.5}$ and O_3 Together in the Same Model[a,b]

Cohort	Deaths[c] (*n*)	Pollutant	Coeff	SE	HR[d]	95% CI	
Stacked CanCHEC	1,253,300	$PM_{2.5}$	0.0038	0.0006	1.039	1.027	1.051
		O_3	0.0036	0.0002	1.036	1.032	1.041
1991 CanCHEC	531,300	$PM_{2.5}$	0.0040	0.0009	1.041	1.023	1.059
		O_3	0.0024	0.0003	1.024	1.018	1.031
1996 CanCHEC	537,400	$PM_{2.5}$	0.0017	0.0009	1.017	0.999	1.036
		O_3	0.0045	0.0003	1.046	1.040	1.053
2001 CanCHEC	401,000	$PM_{2.5}$	0.0033	0.0012	1.033	1.010	1.057
		O_3	0.0054	0.0004	1.056	1.048	1.064
mCCHS without behavior[e]	50,100	$PM_{2.5}$	0.0064	0.0035	1.066	0.995	1.142
		O_3	0.0036	0.0011	1.036	1.014	1.059
mCCHS with behavior[e]	50,100	$PM_{2.5}$	0.0016	0.0035	1.016	0.948	1.089
		O_3	0.0045	0.0011	1.046	1.024	1.070

[a] HRs are given for each pollutant in two-pollutant models. HRs scaled to IQRs are provided in Appendix Table D.1.

[b] Fully adjusted models are stratified by sex, age (5-year categories), and recent immigrant status and are adjusted for income adequacy quintile, visible minority status, Indigenous identity, educational attainment, labor-force status, marital status, occupation, and ecological covariates of community size, airshed, urban form, and four dimensions of Can-Marg (instability, deprivation, dependency, and ethnic concentration). mCCHS analyses were also stratified by CCHS cycle.

[c] Deaths were rounded to the nearest 100 for confidentiality.

[d] HRs are presented as per 10-µg/m³ increase.

[e] Behavioral covariates include additional adjustment for smoking, alcohol consumption, fruit and vegetable consumption, BMI, and exercise behavior.

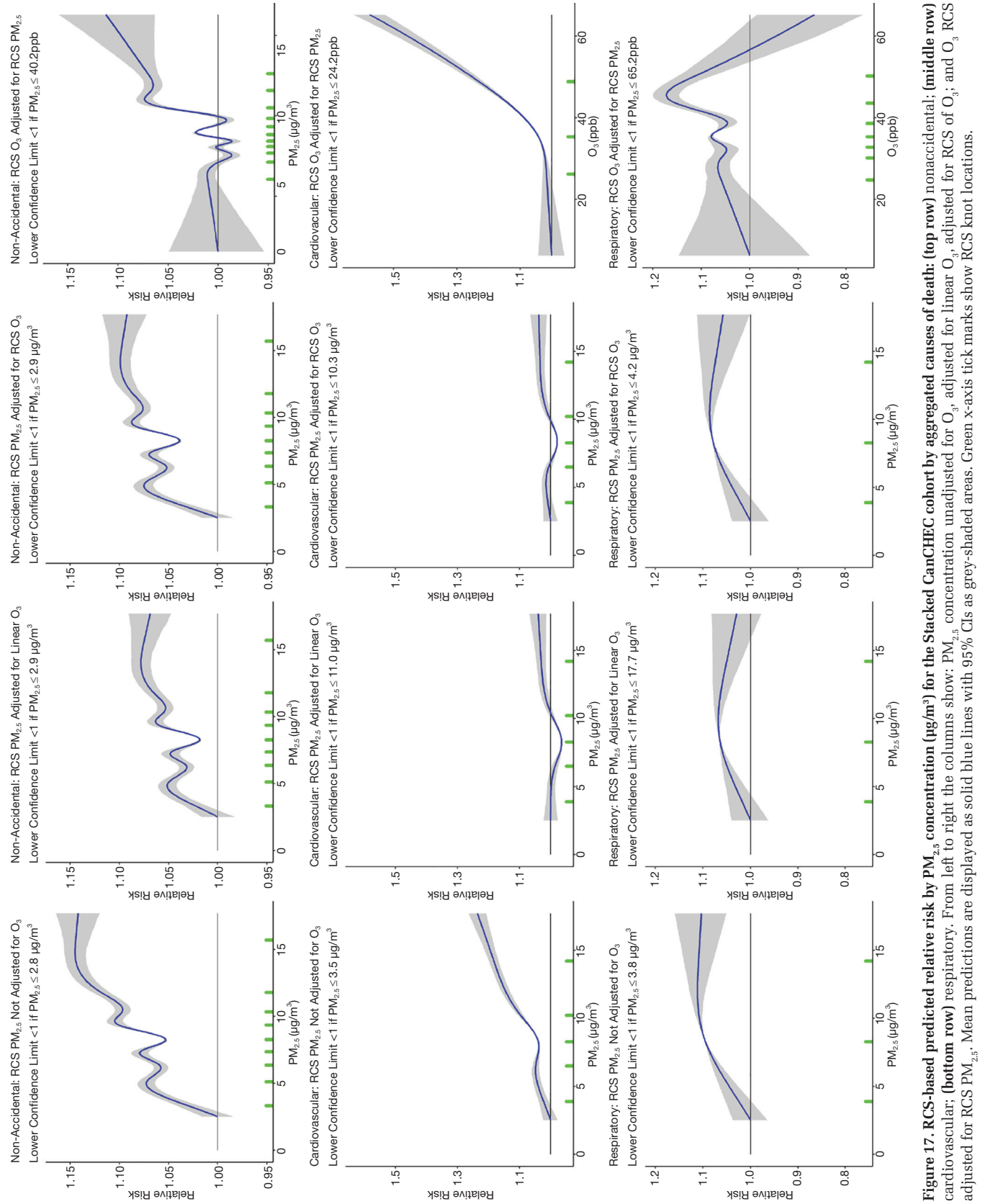

Figure 17. RCS-based predicted relative risk by $PM_{2.5}$ concentration (µg/m³) for the Stacked CanCHEC cohort by aggregated causes of death: (top row) nonaccidental; **(middle row)** cardiovascular; **(bottom row)** respiratory. From left to right the columns show: $PM_{2.5}$ concentration unadjusted for O_3; adjusted for linear O_3; adjusted for RCS of O_3; and O_3 RCS adjusted for RCS $PM_{2.5}$. Mean predictions are displayed as solid blue lines with 95% CIs as grey-shaded areas. Green *x*-axis tick marks show RCS knot locations.

The addition of a linear term for O_x in two-pollutant linear models resulted in the further attenuation of the association between $PM_{2.5}$ and nonaccidental mortality (in the Stacked CanCHEC HR = 1.022; 95% CI: 1.010 to 1.035) (Table 10). After adding O_x, the association was no longer significant in the 1996 and 2001 CanCHECs or mCCHS cohorts. When O_x was added as a linear term in the RCS $PM_{2.5}$ model, the highest concentration for which the RCS lower confidence limit was less than one was at 2.9 μg/m³ (Figure 18), similar to the single-pollutant model at 2.9 μg/m³. Nonlinear associations with the other CanCHEC cohorts are provided in Appendix Figure C.1; available on the HEI website.

In two-pollutant linear models, the addition of O_x attenuated the association between $PM_{2.5}$ and cardiovascular mortality (in the Stacked CanCHEC, HR = 1.024; 95% CI: 1.002 to 1.047) (Table 11). When O_x was added as a linear term to the RCS model the lower confidence limit was less than one throughout most of the range of $PM_{2.5}$ concentrations (Figure 18).

Table 9. Cox Proportional HRs of all Causes of Mortality in Fully Adjusted Models in the Stacked CanCHEC, Using Both $PM_{2.5}$ and O_3 Jointly in the Same Model[a,b]

Cause of Death	Deaths[c] (*n*)	Pollutant	Coeff	SE	HR[d]	95% CI	
Nonaccidental	1,253,300	$PM_{2.5}$	0.0038	0.0006	1.039	1.027	1.051
		O_3	0.0036	0.0002	1.036	1.032	1.041
Cardiovascular	390,600	$PM_{2.5}$	0.0047	0.0011	1.048	1.027	1.070
		O_3	0.0088	0.0004	1.092	1.084	1.997
Cerebrovascular	72,900	$PM_{2.5}$	–0.0010	0.0025	0.990	0.944	1.039
		O_3	0.0093	0.0009	1.098	1.079	1.117
Heart failure	20,500	$PM_{2.5}$	0.0267	0.0047	1.306	1.192	1.431
		O_3	–0.0199	0.0017	0.820	0.793	0.847
Diabetes	41,100	$PM_{2.5}$	–0.0038	0.0034	0.962	0.901	1.028
		O_3	0.0205	0.0012	1.228	1.199	1.257
Ischemic heart disease	215,700	$PM_{2.5}$	0.0051	0.0014	1.053	1.024	1.082
		O_3	0.0127	0.0005	1.135	1.124	1.147
Lung cancer	129,200	$PM_{2.5}$	0.0084	0.0019	1.088	1.049	1.128
		O_3	–0.0079	0.0007	0.924	0.912	0.936
Respiratory	105,900	$PM_{2.5}$	0.0027	0.0021	1.027	0.985	1.070
		O_3	0.0039	0.0007	1.040	1.025	1.055
COPD	61,400	$PM_{2.5}$	–0.0021	0.0027	0.979	0.929	1.032
		O_3	0.0066	0.0010	1.068	1.048	1.088
Pneumonia	25,600	$PM_{2.5}$	0.0142	0.0041	1.152	1.063	1.250
		O_3	0.0032	0.0015	1.032	1.002	1.063
Kidney Failure	15,000	$PM_{2.5}$	0.0065	0.0056	1.067	0.957	1.190
		O_3	–0.0082	0.0020	0.921	0.886	0.958

[a] HRs are given for each pollutant in two-pollutant models. HRs scaled to IQRs are provided in Appendix Table D.2; available on the HEI website.

[b] Fully adjusted models are stratified by sex, age (5-year categories), and recent immigrant status and are adjusted for income adequacy quintile, visible minority status, Indigenous identity, educational attainment, labor-force status, marital status, occupation, and ecological covariates of community size, airshed, urban form, and four dimensions of Can-Marg (instability, deprivation, dependency, and ethnic concentration).

[c] Deaths were rounded to the nearest 100 for confidentiality.

[d] HRs are presented as per 10-μg/m³ increase.

Table 10. Cox Proportional HRs of Nonaccidental Mortality in Fully Adjusted Models in CanCHEC Cohorts and mCCHS with Both $PM_{2.5}$ and O_x Together in the Same Model[a,b]

Cohort	Deaths[c] (*n*)	Pollutant	Coeff	SE	HR[d]	95% CI	
Stacked CanCHEC	1,253,300	$PM_{2.5}$	0.0022	0.0006	1.022	1.010	1.035
		O_x	0.0053	0.0003	1.054	1.048	1.060
1991 CanCHEC	531,300	$PM_{2.5}$	0.0031	0.0009	1.032	1.013	1.050
		O_x	0.0034	0.0004	1.035	1.026	1.044
1996 CanCHEC	537,400	$PM_{2.5}$	<0.0001	0.0010	1.000	0.981	1.020
		O_x	0.0064	0.0005	1.066	1.056	1.075
2001 CanCHEC	401,000	$PM_{2.5}$	0.0003	0.0013	1.003	0.978	1.028
		O_x	0.0081	0.0006	1.084	1.073	1.096
mCCHS without behavior[e]	50,100	$PM_{2.5}$	0.0038	0.0040	1.039	0.965	1.118
		O_x	0.0061	0.0016	1.062	1.029	1.096
mCCHS with behavior[e]	50,100	$PM_{2.5}$	−0.0005	0.0038	0.995	0.924	1.071
		O_x	0.0068	0.0016	1.070	1.037	1.105

[a] HRs are given for each pollutant in two-pollutant models. HRs scaled to IQRs are provided in Appendix Table D.3; available on the HEI website.

[b] Fully adjusted models are stratified by sex, age (5-year categories), and recent immigrant status and are adjusted for income adequacy quintile, visible minority status, Indigenous identity, educational attainment, labor-force status, marital status, occupation, and ecological covariates of community size, airshed, urban form, and four dimensions of Can-Marg (instability, deprivation, dependency, and ethnic concentration). Stacked CanCHEC were also stratified by CanCHEC year, and mCCHS analyses were also stratified by CCHS cycle.

[c] Deaths were rounded to the nearest 100 for confidentiality.

[d] HRs are presented as per 10-μg/m³ increase.

[e] Behavioral covariates include additional adjustment for smoking, alcohol consumption, fruit and vegetable consumption, BMI, and exercise behavior.

In two-pollutant linear models using the Stacked CanCHEC, the addition of O_x rendered the association between $PM_{2.5}$ and respiratory mortality nonsignificant (Table 11). When O_x was added as a linear term in the RCS Model, the highest concentration for which the RCS lower confidence limit was below one was 17.7 μg/m³ (Figure 18).

Two Pollutant Models: Models Within Tertiles of O_3 or O_x To further examine the effect of O_3 and O_x on $PM_{2.5}$ HRs, we also examined the linear and nonlinear associations between $PM_{2.5}$ exposure and nonaccidental mortality within tertiles of O_3 and O_x in the Stacked CanCHEC. The mean exposure within each O_3 and O_x tertile is shown in Table 12.

For tertiles of O_3, the association between $PM_{2.5}$ and nonaccidental mortality was lowest in the middle O_3 tertile (HR = 1.041; 95% CI: 1.020 to 1.062 per 10-μg/m³ increase) (Table 13). Among tertiles of O_x, the significant association between $PM_{2.5}$ and nonaccidental mortality was limited to the highest tertile of O_x (HR = 1.086; 1.064 to 1.108 per 10-μg/m³ increase) (Table 14). An inverse association was observed in the lowest tertile of O_x and no association was observed in the middle tertile of O_x.

The shape of the association between $PM_{2.5}$ and nonaccidental mortality varied by O_3 and O_x tertile (Figure 19). The highest concentration for which the RCS lower confidence limit was less than one varied from 3.2 μg/m³ for the second O_3 tertile to 9.0 μg/m³ for the first O_3 tertile — and from 3.2 μg/m³ for the third O_x tertile to 17.7 μg/m³ for the first O_x tertile.

Threshold Models To examine the sensitivity of the exposure–response relationship to exposure level we considered several threshold levels, below which we truncated exposures and assumed no increased risk. Specifically, we fit fully adjusted threshold models for nonaccidental mortality in the Stacked CanCHEC for $PM_{2.5}$ using threshold values from 2.5 μg/m³ to 11.0 μg/m³ by 0.5-μg/m³ increments. Note that the threshold model with a threshold concentration of 2.5 μg/m² is equivalent to the linear model because the minimum concentration is 2.5 μg/m³.

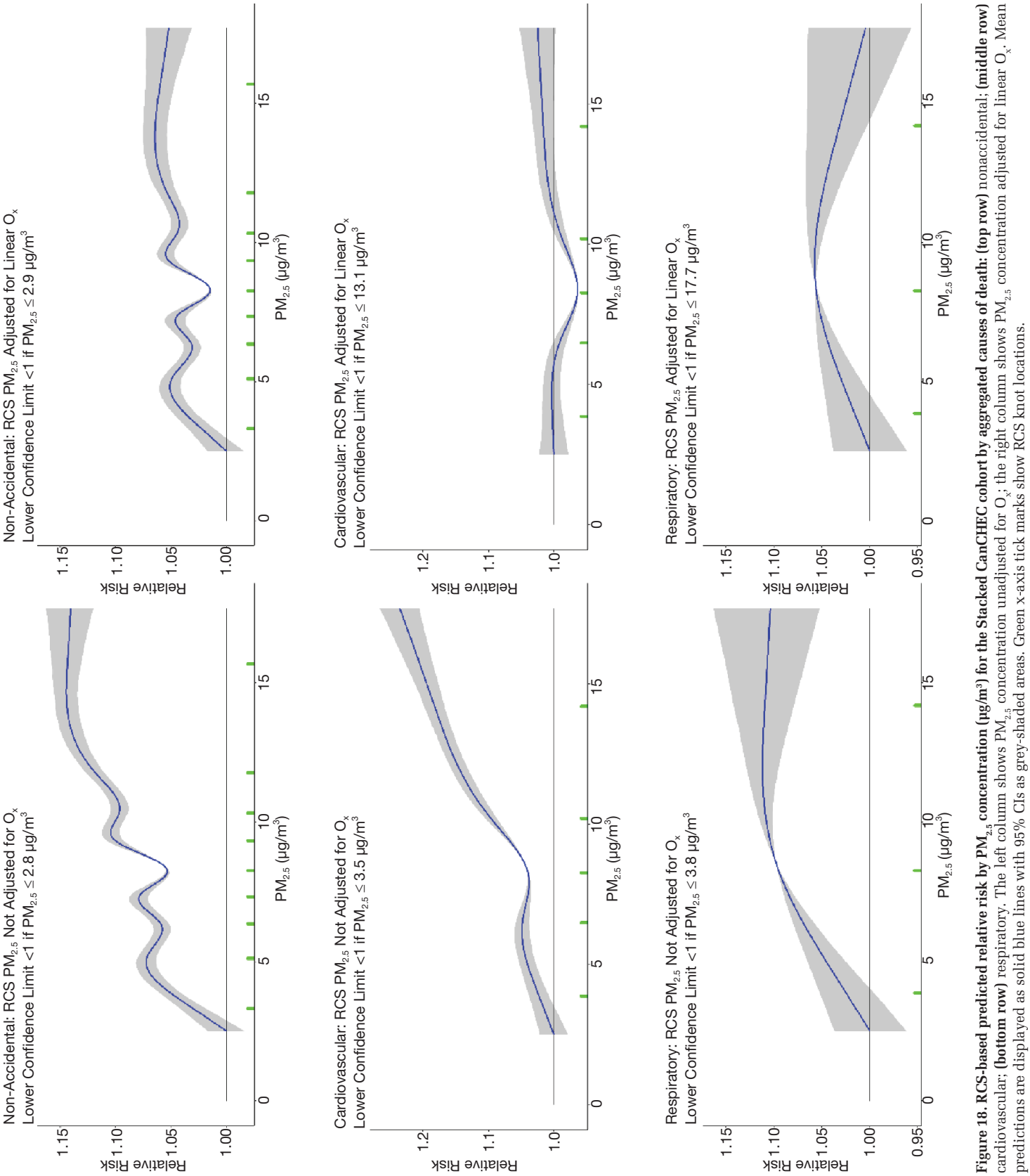

Figure 18. RCS-based predicted relative risk by $PM_{2.5}$ concentration (µg/m³) for the Stacked CanCHEC cohort by aggregated causes of death: (top row) nonaccidental; **(middle row)** cardiovascular; **(bottom row)** respiratory. The left column shows $PM_{2.5}$ concentration unadjusted for O_x; the right column shows $PM_{2.5}$ concentration adjusted for linear O_x. Mean predictions are displayed as solid blue lines with 95% CIs as grey-shaded areas. Green x-axis tick marks show RCS knot locations.

Table 11. Cox Proportional HRs of All Causes of Mortality in Fully Adjusted Models in the Stacked CanCHEC With Both $PM_{2.5}$ and O_x Together in the Same Model[a,b]

Cause of Death	Deaths[c] (*n*)	Pollutant	Coeff	SE	HR[d]	95% CI	
Nonaccidental	1,253,300	$PM_{2.5}$	0.0022	0.0006	1.022	1.010	1.035
		O_x	0.0053	0.0003	1.054	1.048	1.060
Cardiovascular	390,600	$PM_{2.5}$	0.0024	0.0011	1.024	1.002	1.047
		O_x	0.0116	0.0005	1.123	1.112	1.135
Cerebrovascular	72,900	$PM_{2.5}$	−0.0014	0.0026	0.986	0.937	1.037
		O_x	0.0105	0.0012	1.110	1.084	1.138
Heart failure	20,500	$PM_{2.5}$	0.0358	0.0049	1.431	1.299	1.575
		O_x	−0.0296	0.0023	0.744	0.711	0.779
Diabetes	41,100	$PM_{2.5}$	−0.0115	0.0036	0.891	0.831	0.956
		O_x	0.0287	0.0017	1.333	1.290	1.377
Ischemic heart disease	215,700	$PM_{2.5}$	0.0011	0.0015	1.011	0.982	1.040
		O_x	0.0175	0.0007	1.191	1.175	1.208
Lung cancer	129,200	$PM_{2.5}$	0.0090	0.0020	1.095	1.053	1.138
		O_x	−0.0090	0.0009	0.914	0.897	0.930
Respiratory	105,900	$PM_{2.5}$	0.0010	0.0022	1.010	0.967	1.055
		O_x	0.0056	0.0010	1.058	1.037	1.079
COPD	61,400	$PM_{2.5}$	−0.0061	0.0029	0.941	0.889	0.995
		O_x	0.0106	0.0013	1.112	1.083	1.141
Pneumonia	25,600	$PM_{2.5}$	0.0175	0.0044	1.191	1.094	1.298
		O_x	0.0003	0.0021	1.003	0.963	1.045
Kidney failure	15,000	$PM_{2.5}$	0.0124	0.0059	1.132	1.008	1.271
		O_x	−0.0139	0.0027	0.870	0.825	0.918

[a] HRs are given for each pollutant in two-pollutant models. HRs scaled to IQRs are provided in Appendix Table D.4; available on the HEI website.

[b] Fully adjusted models are stratified by sex, age (5-year categories), and recent immigrant status and are adjusted for income adequacy quintile, visible minority status, Indigenous identity, educational attainment, labor-force status, marital status, occupation, and ecological covariates of community size, airshed, urban form, and four dimensions of Can-Marg (instability, deprivation, dependency, and ethnic concentration).

[b] Deaths were rounded to the nearest 100 for confidentiality.

[c] HRs are presented as per 10-μg/m^3 increase.

Table 12. Mean $PM_{2.5}$ Exposure Within Each O_3 and O_x Tertile, 10-Year Moving Averages

	N[a]	Mean $PM_{2.5}$ (μg/m^3)	SD	Minimum	Maximum
O_3					
Tertile 1	42,804,100	29.01	3.12	6.24	32.67
Tertile 2	42,775,700	35.46	1.79	32.67	38.76
Tertile 3	42,792,000	44.41	3.90	38.76	65.21
O_x					
Tertile 1	42,790,600	22.72	2.52	5.04	25.65
Tertile 2	42,790,600	28.46	1.73	25.65	31.72
Tertile 3	42,790,600	35.52	2.37	31.72	56.08

SD = standard deviation.

[a] Person-years were rounded to the nearest 100 for confidentiality.

Table 13. Cox Proportional HRs of Mortality in Fully Adjusted Models in the Stacked CanCHEC for All Causes of Death, for $PM_{2.5}$ Within Tertiles of O_3[a]

Cause of Death/O_3 Tertile	Deaths[b] (*n*)	Coeff	SE	HR[c]	95% CI	
Nonaccidental						
Lowest	400,400	0.0087	0.0012	1.091	1.065	1.118
Middle	419,600	0.0040	0.0010	1.041	1.020	1.062
Highest	433,300	0.0095	0.0010	1.099	1.078	1.120
Cardiovascular						
Lowest	128,700	0.0087	0.0021	1.091	1.047	1.137
Middle	128,000	0.0029	0.0018	1.030	0.994	1.066
Highest	133,900	0.0162	0.0017	1.175	1.136	1.216
Cerebrovascular						
Lowest	24,800	–0.0041	0.0049	0.959	0.872	1.055
Middle	22,900	–0.0034	0.0042	0.967	0.890	1.050
Highest	25,200	0.0084	0.0040	1.088	1.005	1.177
Heart failure						
Lowest	7,300	0.0019	0.0089	1.019	0.856	1.212
Middle	7,400	0.0210	0.0076	1.233	1.062	1.431
Highest	5,800	0.0247	0.0086	1.280	1.082	1.515
Ischemic heart disease						
Lowest	68,900	0.0163	0.0029	1.177	1.113	1.245
Middle	70,800	0.0049	0.0024	1.050	1.002	1.100
Highest	76,000	0.0165	0.0023	1.180	1.128	1.234
Diabetes						
Lowest	13,700	0.0005	0.0068	1.005	0.879	1.149
Middle	12,700	–0.0133	0.0060	0.875	0.779	0.984
Highest	14,800	0.0150	0.0052	1.162	1.050	1.287
Respiratory						
Lowest	34,000	0.0216	0.0043	1.241	1.140	1.351
Middle	35,900	0.0021	0.0036	1.021	0.952	1.096
Highest	36,000	0.0034	0.0034	1.034	0.967	1.106
COPD						
Lowest	20,000	0.0226	0.0054	1.254	1.127	1.394
Middle	21,500	–0.0006	0.0045	0.994	0.910	1.085
Highest	19,900	–0.0014	0.0045	0.987	0.904	1.077
Pneumonia						
Lowest	8,600	0.0149	0.0082	1.160	0.988	1.363
Middle	8,300	0.0151	0.0071	1.163	1.013	1.336
Highest	8,700	0.0128	0.0071	1.137	0.989	1.307
Lung cancer						
Lowest	40,400	0.0210	0.0038	1.234	1.146	1.330
Middle	46,700	0.0124	0.0031	1.132	1.065	1.202
Highest	42,000	0.0067	0.0031	1.069	1.005	1.136
Kidney failure						
Lowest	5,000	0.0160	0.0112	1.173	0.943	1.460
Middle	5,000	0.0129	0.0095	1.138	0.945	1.370
Highest	5,000	–0.0057	0.0092	0.944	0.788	1.132

[a] Fully adjusted models are stratified by sex, age (5-year categories), and recent immigrant status and are adjusted for income adequacy quintile, visible minority status, Indigenous identity, educational attainment, labor-force status, marital status, occupation, and ecological covariates of community size, airshed, urban form, and four dimensions of Can-Marg (instability, deprivation, dependency, and ethnic concentration).

[b] Deaths were rounded to the nearest 100 for confidentiality.

[c] HRs are presented as per 10-μg/m^3 increase.

Table 14. Cox Proportional HRs of Mortality in Fully Adjusted Models in the Stacked CanCHEC for all Causes of Death, for $PM_{2.5}$ Within Tertiles of O_x[a]

Cause of Death/Tertile of O_x	Deaths[b] (*n*)	Coeff	SE	HR[c]	95% CI	
Nonaccidental						
Lowest	422,400	−0.0111	0.0012	0.895	0.874	0.917
Middle	402,300	0.0006	0.0011	1.006	0.985	1.027
Highest	428,600	0.0082	0.0010	1.086	1.064	1.108
Cardiovascular						
Lowest	132,200	−0.0097	0.0021	0.908	0.871	0.946
Middle	122,700	−0.0042	0.0019	0.959	0.924	0.995
Highest	135,800	0.0145	0.0018	1.156	1.116	1.196
Cerebrovascular						
Lowest	25,600	−0.0271	0.0049	0.763	0.693	0.839
Middle	21,900	−0.0087	0.0045	0.917	0.839	1.001
Highest	25,300	0.0154	0.0041	1.167	1.076	1.265
Heart failure						
Lowest	7,800	−0.0114	0.0087	0.892	0.751	1.058
Middle	6,800	0.0494	0.0081	1.639	1.399	1.921
Highest	5,900	0.0128	0.0087	1.137	0.958	1.349
Ischemic heart disease						
Lowest	69,600	−0.0024	0.0029	0.976	0.922	1.033
Middle	68,200	−0.0082	0.0025	0.922	0.877	0.969
Highest	77,800	0.0135	0.0023	1.144	1.094	1.197
Diabetes						
Lowest	14,800	−0.0237	0.0067	0.789	0.691	0.900
Middle	11,800	−0.0338	0.0064	0.713	0.629	0.808
Highest	14,500	0.0094	0.0055	1.098	0.986	1.223
Respiratory						
Lowest	36,800	−0.0007	0.0042	0.993	0.914	1.078
Middle	34,800	0.0040	0.0038	1.040	0.966	1.120
Highest	34,200	0.0002	0.0037	1.002	0.932	1.076
COPD						
Lowest	21,700	0.0008	0.0053	1.008	0.908	1.118
Middle	20,500	−0.0021	0.0048	0.980	0.892	1.075
Highest	19,200	−0.0075	0.0047	0.927	0.845	1.017
Pneumonia						
Lowest	8,900	−0.0071	0.0082	0.932	0.793	1.095
Middle	8,000	0.0171	0.0074	1.187	1.028	1.371
Highest	8,600	0.0301	0.0072	1.352	1.173	1.558
Lung cancer						
Lowest	44,000	0.0012	0.0037	1.012	0.941	1.089
Middle	43,900	0.0209	0.0033	1.232	1.156	1.314
Highest	41,200	−0.0003	0.0033	0.997	0.935	1.063
Kidney failure						
Lowest	5,300	−0.0141	0.0111	0.869	0.699	1.079
Middle	4,700	0.0199	0.0101	1.221	1.002	1.487
Highest	5,000	−0.0025	0.0096	0.976	0.809	1.177

[a] Fully adjusted models are stratified by sex, age (5-year categories), and recent immigrant status and are adjusted for income adequacy quintile, visible minority status, Indigenous identity, educational attainment, labor-force status, marital status, occupation, and ecological covariates of community size, airshed, urban form, and four dimensions of Can-Marg (instability, deprivation, dependency, and ethnic concentration).

[b] Deaths were rounded to the nearest 100 for confidentiality.

[c] HRs are presented as per 10-μg/m^3 increase.

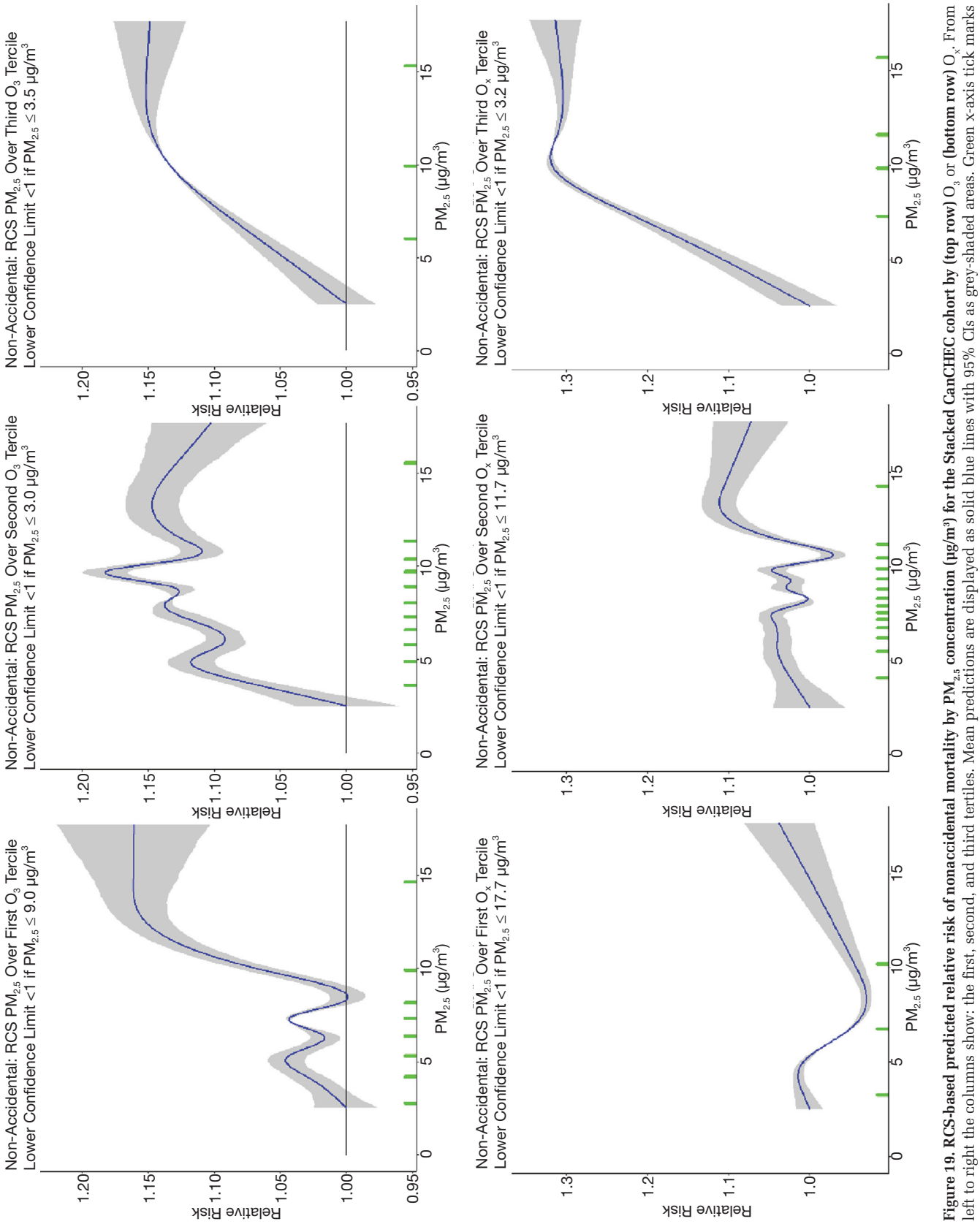

Figure 19. RCS-based predicted relative risk of nonaccidental mortality by $PM_{2.5}$ concentration (µg/m³) for the Stacked CanCHEC cohort by (top row) O_3 or (bottom row) O_x. From left to right the columns show: the first, second, and third tertiles. Mean predictions are displayed as solid blue lines with 95% CIs as grey-shaded areas. Green x-axis tick marks show RCS knot locations.

The −2 log-likelihood values monotonically increase from a minimum for the linear model (threshold = 2.5 μg/m^3) to a threshold concentration of 5.0 μg/m^3. These values then decrease to a threshold concentration of 8.0 μg/m^3 and then increase for threshold concentrations from 8.5 μg/m^3 to 11.0 μg/m^3 (Figure 20A). The −2 log-likelihood value at threshold concentrations of 2.5 μg/m^3 and 8.0 μg/m^3 were identical (Table 15). Threshold models with threshold values of 3.0 μg/m^3, 3.5 μg/m^3, and 8.0 μg/m^3 did not differ significantly from the linear model ($P \geq 0.05$). These threshold values lie below the −2 log-likelihood value of the linear model plus 3.84 (purple dashed line, Figure 20A). All other threshold values represent models that were not a significant improvement in fit over the linear model, using the likelihood ratio test.

The ensemble model-based threshold distribution estimates (Figure 20B) were bimodal, with most values near either 2.5 μg/m^3 or 8.0 μg/m^3. The mean ensemble predictions (Figure 20C) were sublinear with the lower 95% CI equaling one from 2.5 μg/m^3 to 8.0 μg/m^3. For comparison purposes, the RCS fit is also presented in Figure 20C. The RCS mean predictions are larger in magnitude than the mean ensemble of threshold models and clearly a better fit with a much lower −2 log-likelihood value (Figure 20A). However, the wide ensemble-based threshold model CIs likely reflect the increasing RCS predictions from 2.5 μg/m^3 to 4.5 μg/m^3 and then a declining trend in RCS predictions between 4.5 μg/m^3 and 8.0 μg/m^3.

Regional (Airshed) Differences

In the MAPLE Phase 1 report and in the RCS curves for the Stacked CanCHEC nonaccidental mortality (Figure 14), we observed a flattening in the middle concentration range (~5–10 μg/m^3). We hypothesized that this may have been due to regional variation in the air pollution mixture or uncontrolled regional variation in mortality risk factors. Given the size of the Stacked CanCHEC cohort, we therefore investigated this in separate analyses within each of the six airsheds. Population characteristics and mortality by cause for each airshed is shown in Table 16. Specifically, in the Stacked CanCHEC, the association between nonaccidental mortality and $PM_{2.5}$ was assessed using linear (Table 16) and nonlinear RCS (Figure 21) models within each of the six airsheds: Prairie, West Central, East Central, Western, Southern Atlantic, and Northern. Note that all analyses are based on a 10-year moving average exposure window, during which time participants may have lived within multiple airsheds. Exposures, therefore, reflect the person-years for those who either lived in that given year or died within each airshed. In these analyses, airshed was assigned in each year of follow-up based on postal codes.

Very different HRs were obtained within the different airsheds in Canada. In linear models, protective associations were obtained for the West Central and Prairie airsheds (Table 16). The associations between $PM_{2.5}$ and nonaccidental mortality were relatively low (HRs ~1.05) but significant for East Central and Western airsheds (Table 16). In contrast, the associations between $PM_{2.5}$ and nonaccidental mortality were very high for the two airsheds with the lowest $PM_{2.5}$ estimates (Table 5). In the Southern Atlantic airshed ($PM_{2.5}$ mean = 5.28 μg/m^3), the HR estimate was 1.359 (95% CI: 1.293 to 1.427 per 10-μg/m^3 increase) (Table 16). Similarly, in the Northern airshed ($PM_{2.5}$ mean = 4.81 μg/m^3), the HR estimate was 1.414 (1.110 to 1.801 per 10-μg/m^3 increase).

In the nonlinear RCS models, we observed differences in the shapes of associations (Figure 21, Appendix Figure C.2; available on the HEI website.). The Southern Atlantic, East Central, and Western airshed RCSs displayed an increasing concentration–response at lower concentrations, while we observed little association at lower concentrations for the Northern airshed (Figure 21). However, the West Central and Prairie airsheds displayed patterns similar to each other that were much different than the other airshed patterns. In both West Central and Prairie airsheds the mean relative-risk predictions increased, then flattened out, sharply decreased, and then sharply increased over the concentration range. We evaluated potential explanations for this regional variability in sensitivity analyses, described in the next section.

Sensitivity Analyses Related to Regional Variation in Concentration–Response Relationships

Regional Representation In the Phase 1 report we suggested that variation in the composition of the air pollution mixture (as characterized by oxidant gases or particle–oxidant gas interactions) may play a role in explaining the flattening of the concentration–mortality relationship. Given the indications of regional variation in the concentration–mortality shapes as being largely responsible for the flattening of the national concentration–response relationship shape detailed earlier in this report, we conducted several sensitivity analyses to assess factors unrelated to exposure that may influence this regional variation.

Our sensitivity analysis evaluating whether variation in access to healthcare may have affected the shape of the concentration–mortality relationship indicated that adjustment for healthcare access did not affect the shape of the relationship or remove the dip present at intermediate (~5–10 μg/m^3) concentrations (Figure 22).

Given that there is regional variation in several population characteristics (Table 16), such as the proportion of Indigenous respondents, we conducted regional sensitivity analyses (Table 17). Deaths (by cause) counts for visible minority and Indigenous residents in the Stacked canCHEC are provided in Table 18. Specifically, we evaluated whether regional variation

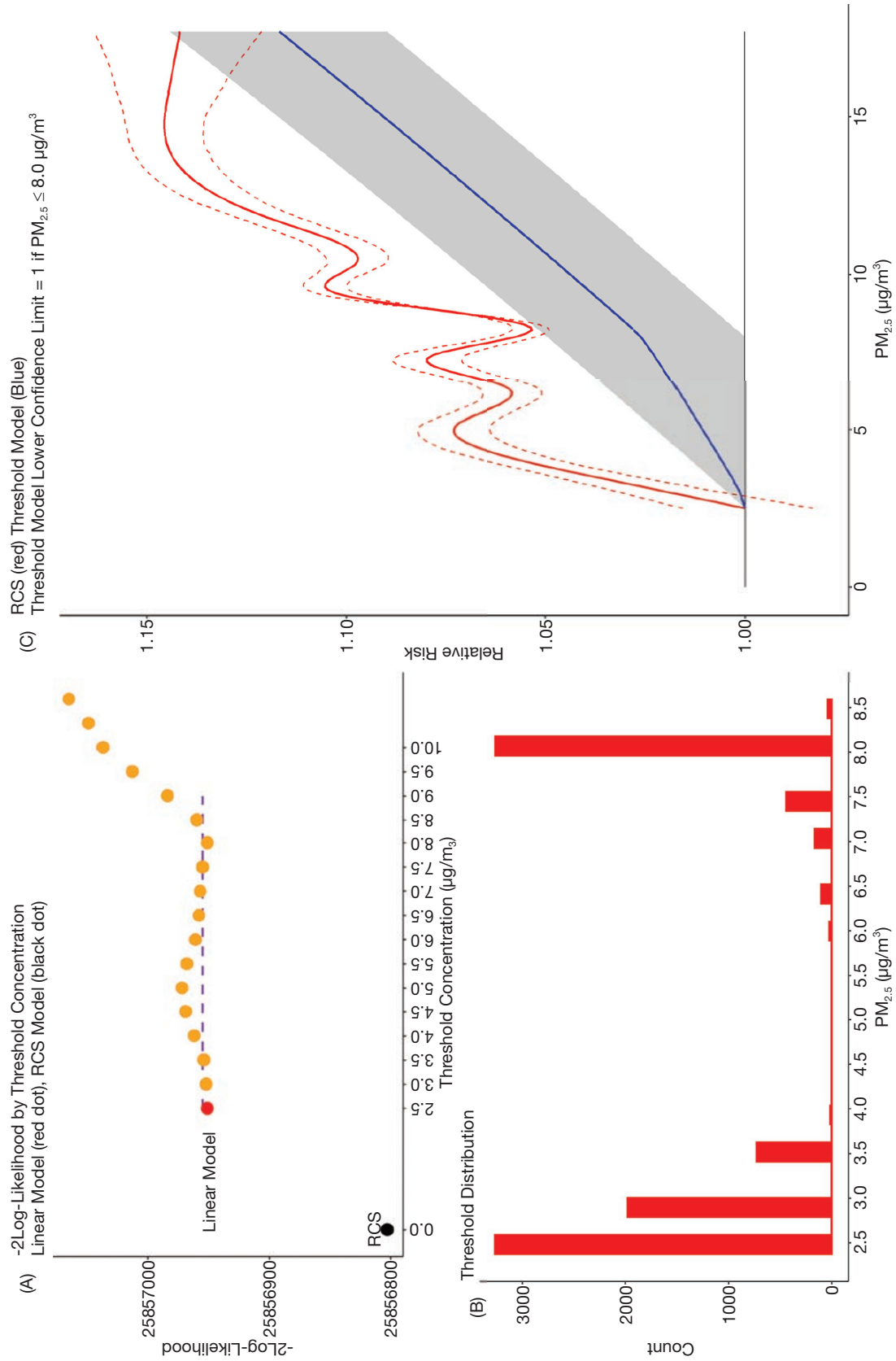

Figure 20. Threshold model comparisons with linear and RCS models. (A) –2 log-likelihood values (orange dots) by threshold concentration; threshold concentrations for models representing statistically significantly improved fit ($P < 0.05$; orange dots lying below purple dashed line) over the linear model (red dot) using the likelihood-ratio test; and RCS – 2 log-likelihood value (black dot). **(B)** Distribution of estimated threshold values under the ensemble model. **(C)** Predicted relative risk by $PM_{2.5}$ concentration (µg/m³) for nonaccidental mortality in the Stacked CanCHEC cohort; mean predictions (solid red line) and 95% CIs (dashed red lines).

Table 15. Threshold Model Results by Threshold $PM_{2.5}$ Concentration for Nonaccidental Mortality in Fully Adjusted Models in the Stacked Cohort for Exposure to $PM_{2.5}$ During the Previous 10 Years[a]

Threshold $PM_{2.5}$ Concentration ($\mu g/m^3$)	Coeff	SE	–2 Log-Likelihood	Ensemble Weight
2.5	0.00806	0.000542	25,856,951	0.326023
3.0[b]	0.00806	0.000543	25,856,952	0.197743
3.5[b]	0.00805	0.000544	25,856,954	0.072746
4.0	0.00794	0.000547	25,856,962	0.001332
4.5	0.00787	0.000551	25,856,969	4.02E-05
5.0	0.00789	0.000557	25,856,972	8.98E-06
5.5	0.00808	0.000565	25,856,968	6.63E-05
6.0	0.00836	0.000575	25,856,961	0.002197
6.5	0.00865	0.00059	25,856,958	0.009845
7.0	0.00896	0.000609	25,856,957	0.016232
7.5	0.00936	0.000635	25,856,955	0.044122
8.0[b]	0.00994	0.000667	25,856,951	0.326023
8.5	0.01031	0.000707	25,856,960	0.003622
9.0	0.01038	0.000756	25,856,984	2.23E-08
9.5	0.01032	0.000815	25,857,013	1.12E-14
10.0	0.01038	0.000889	25,857,037	6.90E-20

[a] Fully adjusted models are stratified by sex, age (5-year categories), and recent immigrant status and are adjusted for income adequacy quintile, visible minority status, Indigenous identity, educational attainment, labor-force status, marital status, occupation, and ecological covariates of community size, airshed, urban form, and four dimensions of Can-Marg (instability, deprivation, dependency, and ethnic concentration).

[b] Threshold model concentrations that did not differ significantly from the linear model ($P \geq 0.05$).

Table 16. Airshed Characteristics, Proportion of Visible Minority and Indigenous Residents, and Death Counts for All Causes of Death in the Stacked CanCHEC

	Airshed					
	Western	Prairie	West Central	Southern Atlantic	East Central	Northern
Population characteristics (%)						
Indigenous identity	4.63	6.26	13.63	2.22	1.27	27.67
Visible minority	11.15	6.18	5.45	1.49	6.62	4.14
Deaths (*n*) by cause of death[a]						
Nonaccidental	156,500	138,000	73,500	129,300	749,200	6,900
Cardiovascular	49,800	45,900	24,000	40,800	228,200	1,900
Cerebrovascular	10,800	8,000	4,600	7,500	41,500	400
Heart failure	3,000	2,700	1,200	2,400	11,200	100
Diabetes	5,200	4,100	3,400	4,600	23,600	200
Ischemic heart disease	24,500	25,500	12,900	21,900	129,800	1,000
Lung cancer	14,500	12,300	6,600	14,200	80,700	900
Respiratory	13,800	12,100	5,900	11,100	62,200	700
COPD	8,000	7,000	3,300	6,900	35,700	500
Pneumonia	3,800	2,800	1,500	2,400	14,900	100
Kidney failure	1,400	1,800	1,000	1,800	8,900	100

[a] Deaths were rounded to the nearest 100 for confidentiality.

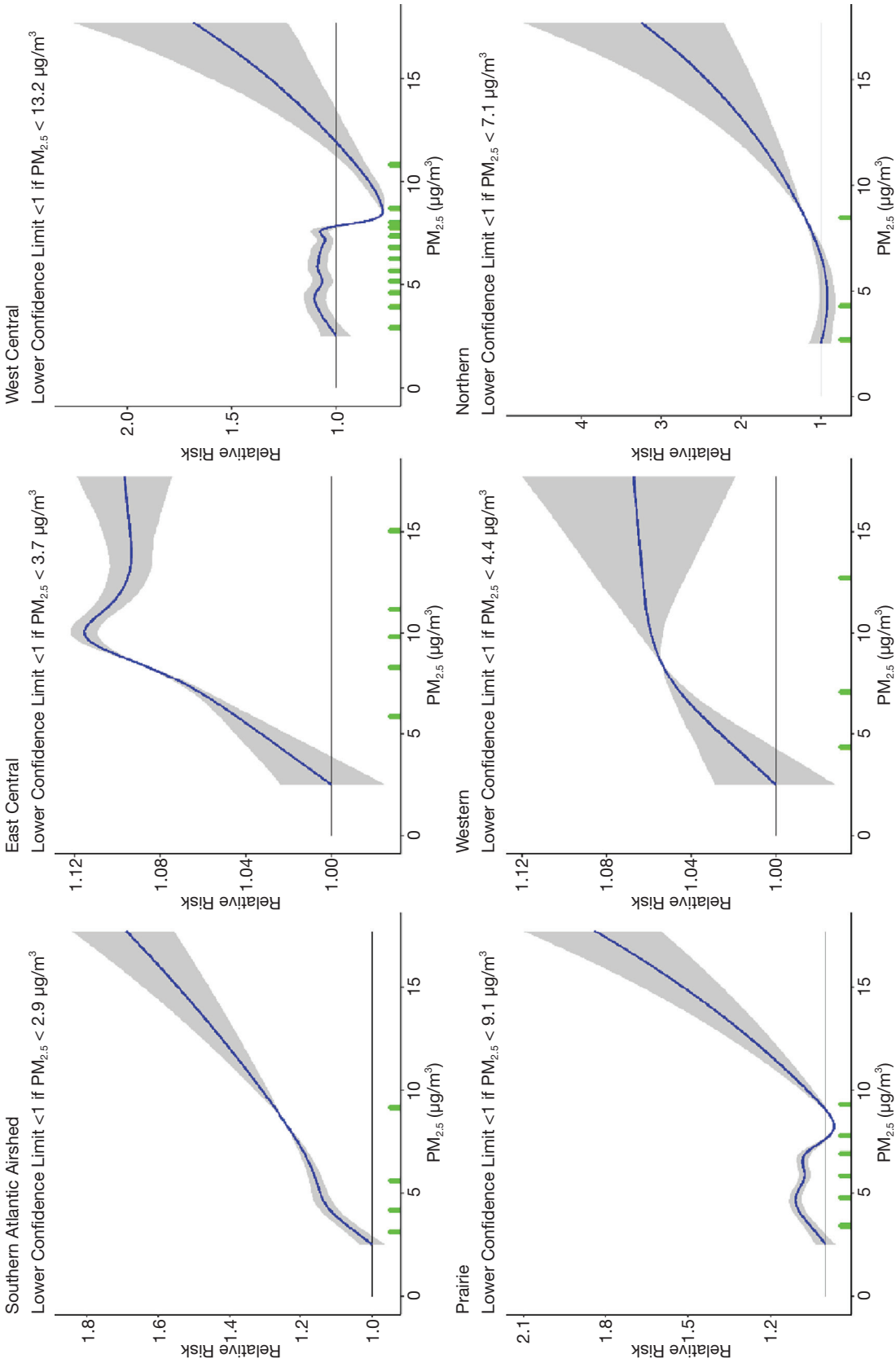

Figure 21. Predicted relative risk by $PM_{2.5}$ concentration (µg/m³) for the Stacked CanCHEC cohort by airshed. Mean predictions are displayed as solid blue lines with 95% CIs as grey-shaded areas. Green x-axis tick marks show RCS knot locations.

in the shape of the concentration–mortality relationship may be due to differential regional representations of immigrants or Indigenous respondents. Results indicate, however, that the flattening of the relationship persisted after exclusion of these populations (Figure 23). Further, we explored regional variation in the proportion of healthy older persons who are lost to follow-up as an additional potential explanation for the observed flattening. Here we evaluated separate models excluding immigrants, Indigenous respondents, and persons >80 years, 60–79 years, and >60 years. In all such sensitivity analyses the dip persisted in the Prairie and West Central airsheds, but it was not present nor were the curves sensitive to exclusion in the other airsheds.

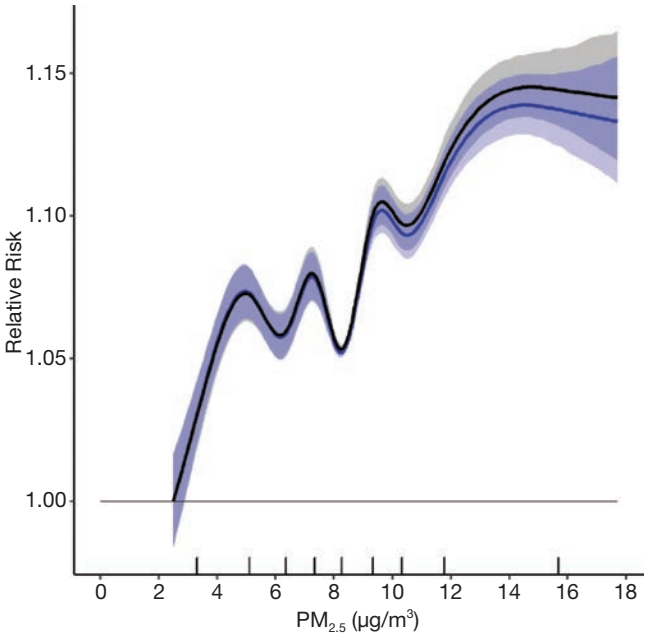

Figure 22. RCS predictions over $PM_{2.5}$ concentration range based on 9 knots with and without adjustment for proximity to healthcare resources. Mean and uncertainty bounds with adjustment (blue line and blue-shaded area) and without adjustment (black line and grey-shaded area).

To address potential residual confounding within the 5-year age strata in our main models, we conducted an additional sensitivity analysis using 1-year age strata (Figure 24). Results indicate highly similar relationships when using 1-year age strata, compared with the 5-year strata included in our main models.

Sensitivity of the Nonaccidental Mortality–$PM_{2.5}$ Association to Removal of Person-Years Above Selected Concentrations

We examined the nonaccidental mortality–$PM_{2.5}$ association shape sensitivity to the removal of person-years from $PM_{2.5}$ at or above selected concentrations. We selected 12 µg/m³ as it is the current U.S. National Ambient Air Quality Standard and 10 µg/m³ as it is the current Canadian and World Health Organization guideline. Restricting person-years to $PM_{2.5}$ concentrations below 12 µg/m³ removed 13% of person-years and 10% of deaths compared with the full cohort, while 30% of person-years and 28% of deaths were removed when person-years were restricted to $PM_{2.5}$ concentrations less than 10 µg/m³. Results of linear models for these restricted cohorts are presented in Table 19. HRs and the lower 95% confidence limit was greater than one for the 12-µg/m³ restriction, while the HR was slightly above one with a confidence limit spanning one for the 10-µg/m³ restriction. Given the spatial patterns in $PM_{2.5}$ concentrations and the regional variation in

Table 17. Cox Proportional HRs of Nonaccidental Mortality in Fully Adjusted Models in the Stacked CanCHEC, for $PM_{2.5}$ Within Each Airshed in Canada (see Figure 3)[a]

Airshed	Deaths[b] (*n*)	Coeff	SE	HR[c]	95% CI	
East Central	749,200	0.0056	0.0007	1.057	1.044	1.072
Prairie	138,000	<–0.0001	<–0.0001	0.901	0.862	0.941
Southern Atlantic	129,300	0.0306	0.0025	1.359	1.293	1.427
West Central	73,500	<–0.0001	<–0.0001	0.774	0.717	0.836
Western	156,500	0.0052	0.0016	1.053	1.021	1.086
Northern	6,900	0.0347	0.0123	1.414	1.110	1.801

[a] Fully adjusted models are stratified by sex, age (5-year categories), and recent immigrant status and are adjusted for income adequacy quintile, visible minority status, Indigenous identity, educational attainment, labor-force status, marital status, occupation, and ecological covariates of community size, airshed, urban form, and four dimensions of Can-Marg (instability, deprivation, dependency, and ethnic concentration).

[b] Deaths were rounded to the nearest 100 for confidentiality.

[c] HRs are presented as per 10-µg/m³ increase.

Table 18. Number of Deaths of Visible Minority and Indigenous Residents for All Causes of Death in the Stacked CanCHEC

Cause of Death	Deaths (*n*)	
	Visible Minorities	Indigenous
Nonaccidental	46,800	38,700
Cardiovascular	14,200	10,900
Cerebrovascular	3,200	1,900
Heart failure	600	600
Diabetes	2,400	3,000
Ischemic heart disease	7,400	6,200
Lung cancer	3,500	3,500
Respiratory	3,200	3,600
COPD	1,200	1,800
Pneumonia	1,000	1,000
Kidney failure	800	700

[a] Deaths were rounded to the nearest 100 for confidentiality.

the shape and magnitude of the concentration–mortality relationship described earlier, interpretation of these restricted cohorts is complex, as the restrictions lead to different cohorts with geographic representation and covariate distributions that differ from the full cohort.

For each set of person-year restrictions we also identified the number of RCS knots that minimized the BIC (8 for <12 μg/m³ and 6 for <10 μg/m³) and plotted the mean predictions with their corresponding uncertainty intervals in Figure 25.

The RCS mean predictions were similar for the full cohort and the cohort that was restricted to person-years with <12 μg/m³ of $PM_{2.5}$ exposure for $PM_{2.5}$ concentrations less than 10 μg/m³ (Figure 25). Over the 10 to 12 μg/m³ concentration range, the full cohort RCS was slightly larger in magnitude compared with the <12 μg/m³ restricted cohort, suggesting that person-years ≥12 μg/m³ were contributing to a positive association with nonaccidental mortality in defining the curve below 12 μg/m³. This relationship was observed to a much greater extent in the RCS predictions for the cohort restricted to person-years with <10 μg/m³ of $PM_{2.5}$ exposure, suggesting that $PM_{2.5}$ concentrations ≥10 μg/m³ were clearly contributing to positive associations with mortality. In all three curves, a steep increase was observed from the minimum concentration of 2.5 μg/m³ to 5 μg/m³. For the full cohort and the <12 μg/m³ restricted cohort the RCS predictions flattened over the 5 to 9 μg/m³ range and then increased above 9 μg/m³. A similar increase was observed for the <10 μg/m³ restricted cohort followed by a clear decline in the magnitude of predictions over the 5 to 9 μg/m³ concentration interval. Above 9 μg/m³ the <10 μg/m³ cohort RCS increased.

These results suggest that a positive association exists for concentrations >9 μg/m³, however, it is unclear whether these data support a positive association in the 5 to 9 μg/m³ concentration interval.

Extended SCHIF

The basis of our eSCHIF model is using 1,000 series of simulated RCS predictions over the concentration range and fitting the two-variable eSCHIF function to these predictions. We therefore require that the simulation-based predictions and corresponding standard errors are similar to those obtained using standard methods. To evaluate this requirement, we compared the mean predictions and their 95% CIs between methods based on using $\hat{\beta}'s(z_j), j = 1, \ldots, J$ to represent the mean predictions at a sequence of concentrations z_j, $j = 1, \ldots, J$ and $\hat{\beta}'s(z_j) \mp 1.96 \times \hat{\sigma}(z_j), j = 1, \ldots, J$ to represent the 95%

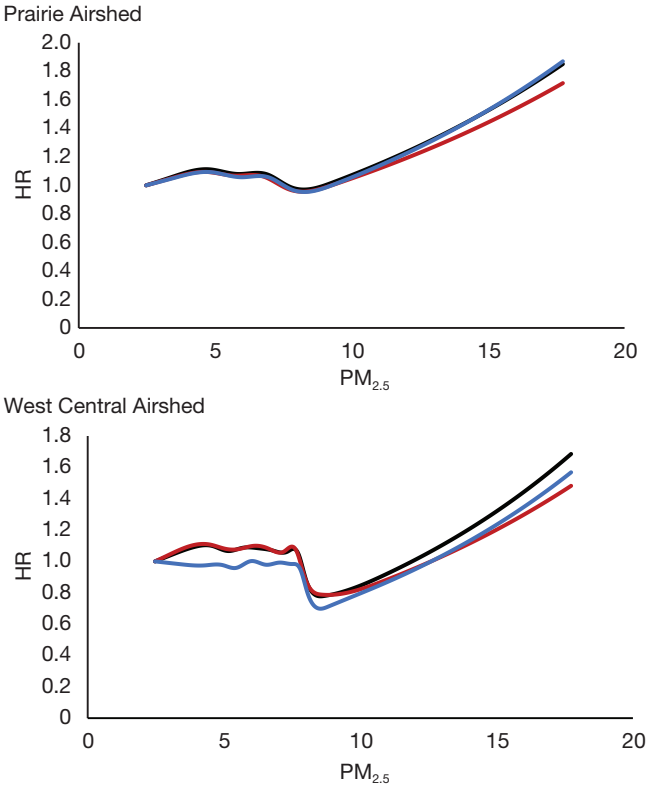

Figure 23. RCS sensitivity analyses for nonaccidental mortality in the Stacked CanCHEC, using BIC on the fully adjusted model for the best-fitting spline for two airsheds that show a large dip in the concentration–response shape and removal of population groups for which linkage to mortality may have been less complete. Black line: full cohort; red line: immigrants removed from cohort; blue line: Indigenous respondents removed from cohort.

CI to the average, 0.025, and 0.975 percentiles of $r_i' s(z_j)$, $i = 1, \ldots, 1{,}000$ for $j = 0, \ldots, J$ (Figure 26A), for an RCS using three knots for nonaccidental mortality in the 2001 cohort. The corresponding $PAF(z_{j+1}, z_j)$ estimates are presented in Figure 26B. These two approaches yield very similar results, and we conclude that 1,000 randomly generated values of the distribution of $\hat{\beta}$ provide an acceptable approximation to the standard method of estimating mean and CI relative risk and PAF predictions.

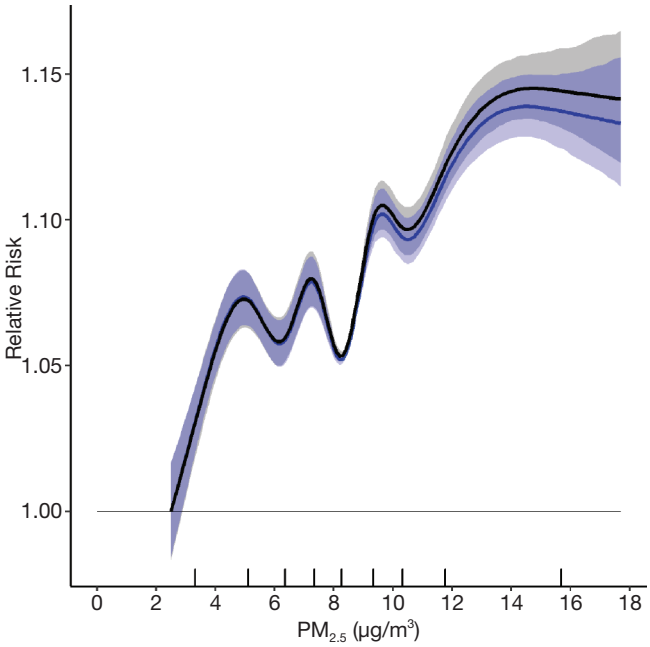

Figure 24. RCS predictions over $PM_{2.5}$ concentration range based on 9 knots specifying age as 1-year or 5-year strata. Mean and uncertainty bounds with 1- and 5-year strata (blue line and blue-shaded area) (black line and grey-shaded area).

We now illustrate the eSCHIF model with four examples. The first is based on the 2001 cohort where the RCS model that minimized the BIC contained three knot values. The mean RCS predictions over the concentration range from $z_0 = 2.5$ µg/m³ to the 99.9th percentile concentration $z_j = 15.0$ µg/m³ by 0.1-µg/m³ increments are displayed in Figure 27A, in addition to the average of the 1,000 eSCHIF predictions at each concentration and the corresponding 0.025 and 0.975 percentiles. In this example, we suggest that the eSCHIF provides a reasonable approximation to the (well-behaved) monotonically increasing mean RCS predictions in addition to the monotonically increasing CIs. The corresponding $PAF(z_{j+1}, z_j)$ results are displayed in Figure 27B, based on a 0.1-µg/m³ change in concentration throughout the concentration range. The RCS-based $PAF(z_{j+1}, z_j)$ mean values are constant below the first and above the last (third) knot values because the RCS is linear over these ranges. Note that even though the lower confidence limit of the RCS is less than one when $z < 4.5$ µg/m³, the lower confidence limit on the $PAF_i(z_{j+1}, z_j)$ is greater than zero, suggesting that there is some evidence that any reduction in concentration is associated with reductions in attributable deaths.

As our second example, we consider the 2001 cohort RCS for $PM_{2.5}$ after adjustment for the RCS of O_3 (Figure 28A), again with three knots. The mean RCS predictions are approximately one for $z < 4.5$ µg/m³ with the upper confidence limit declining with concentration below the mean concentration of 7.7 µg/m³ and then increasing above this concentration. The lower confidence limit of the PAF is less than zero for concentrations less than 7.7 µg/m³ for both the RCS and eSCHIF (Figure 28B). Again, our eSCHIF model provides a close approximation to both RCS relative risk predictions and PAF predictions.

In the first two examples, the RCS model provides a reasonable relative risk function for use in benefits analysis. In such cases transforming the eSCHIF is not necessary.

Table 19. Cox Proportional $PM_{2.5}$ HRs of Mortality in Fully Adjusted Models in the Stacked CanCHEC for Selected Person-Year Restrictions[a]

Person-Year Restriction	Person-Years (millions)	Deaths (millions)	Coeff	SE	HR[b]	95% CI	
None	128.37	1.25	0.00806	0.0005421	1.084	1.072	1.096
$PM_{2.5}$ <12 µg/m³	111.85	1.12	0.00604	0.0007006	1.062	1.048	1.077
$PM_{2.5}$ <10 µg/m³	90.02	0.90	0.00068	0.0008930	1.007	0.989	1.025

[a] Fully adjusted models are stratified by sex, age (5-year categories), and recent immigrant status and are adjusted for income adequacy quintile, visible minority status, Indigenous identity, educational attainment, labor-force status, marital status, occupation, and ecological covariates of community size, airshed, urban form, and four dimensions of Can-Marg (instability, deprivation, dependency, and ethnic concentration).

[b] HRs are presented as per 10-µg/m³ increase.

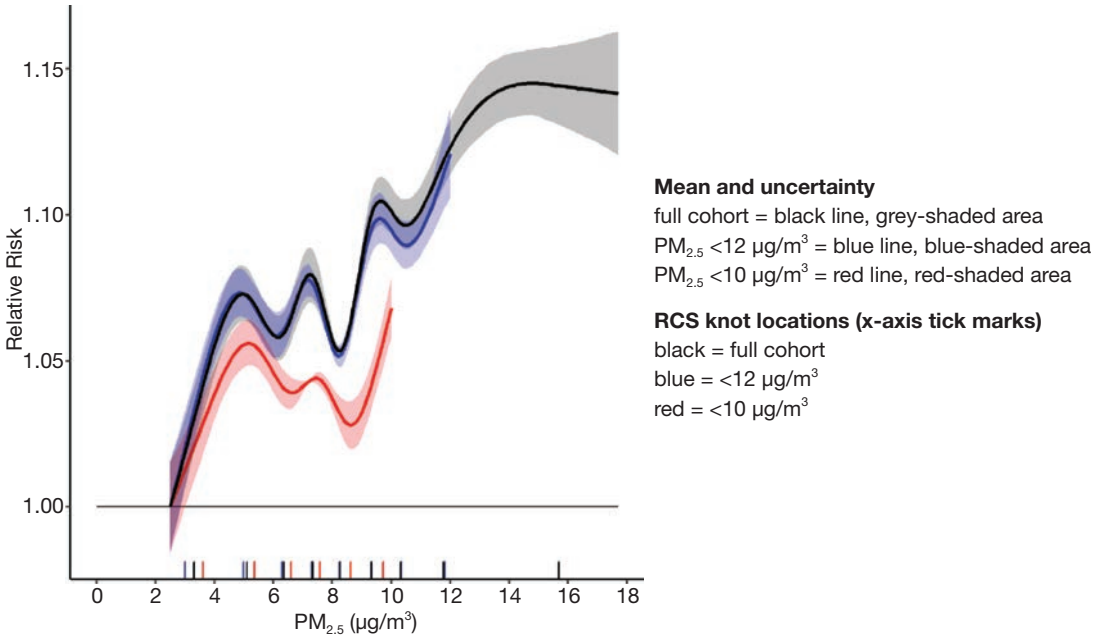

Figure 25. RCS predictions for nonaccidental mortality over the $PM_{2.5}$ concentration range for the full cohort, person-years with $PM_{2.5}$ <12 µg/m³, and person-years with $PM_{2.5}$ <10 µg/m³.

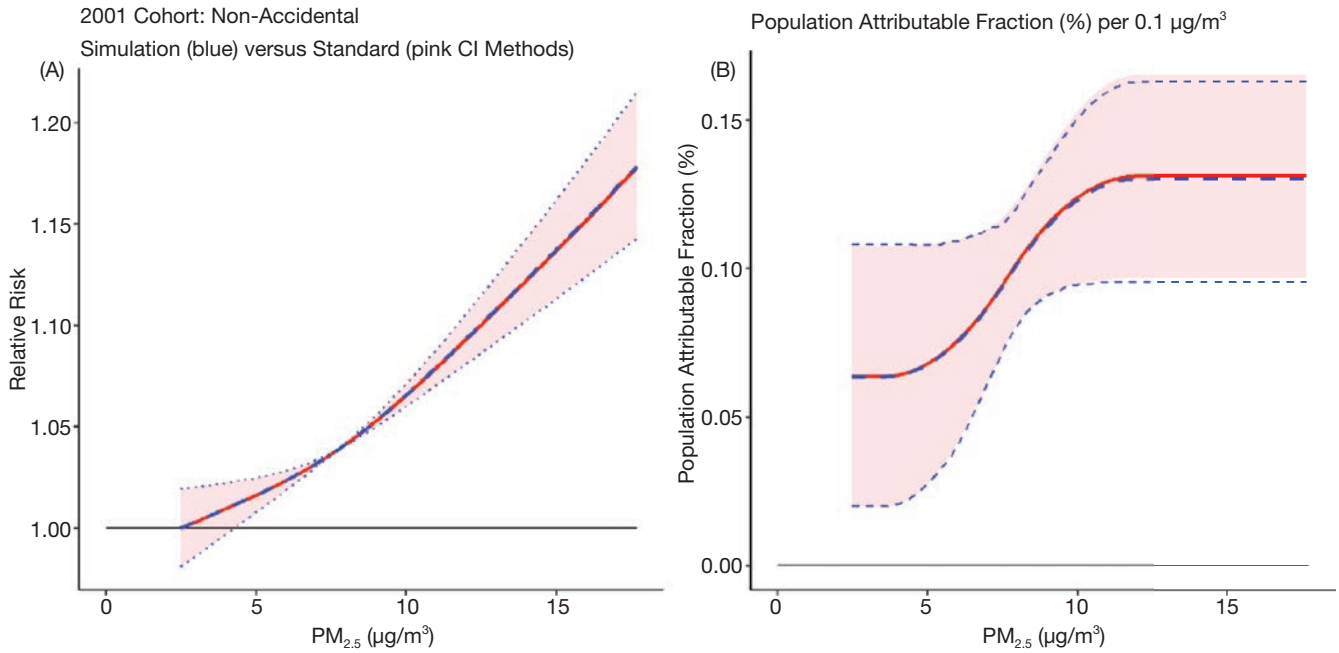

Figure 26. Comparison of standard and simulation-based methods to determine mean and 95% confidence intervals. (A) Relative risk estimates and **(B)** PAF Estimates (%) per 0.1-µg/m³ are also presented. Mean and 95% CI: Standard = dashed red line and pink-shaded area; Simulated = dashed blue line and blue dotted lines

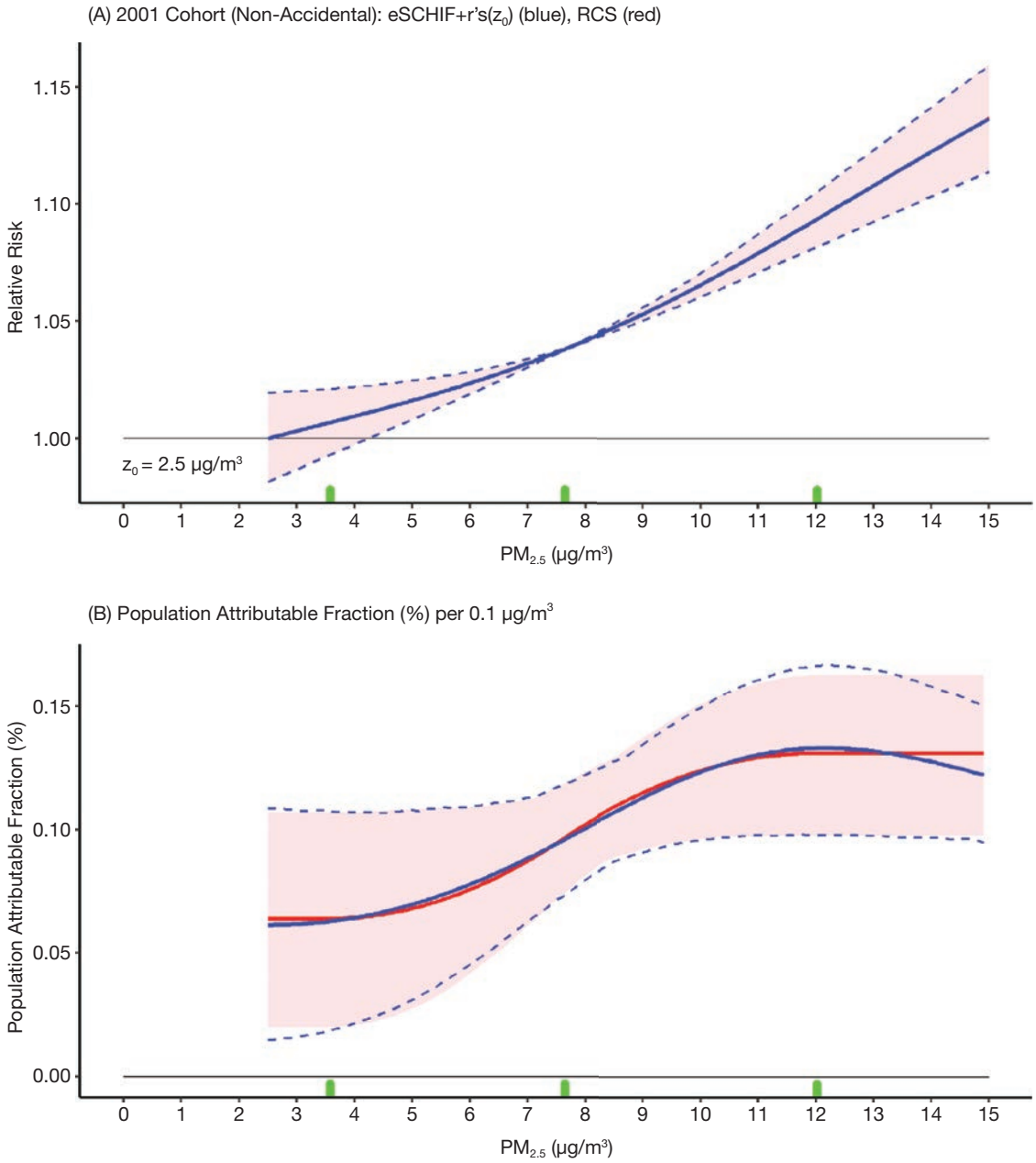

Figure 27. 2001 cohort nonaccidental death RCS mean relative risk predictions over the $PM_{2.5}$ concentration range, with eSCHIF relative risk predictions. (A) Relative risk estimates; **(B)** PAF estimates. Mean and 95% CI: RCS = solid red line and pink-shaded area; eSCHIF = solid blue line and dashed blue lines. Green x-axis tick marks show RCS knot locations.

However, in our third example such a transformation is likely desirable. The example is nonaccidental mortality in the stacked cohort, where a more complex RCS relationship between the relative risk and $PM_{2.5}$ concentrations is observed (Figure 29A). The eSCHIF average predictions are much smoother than the RCS mean predictions, displaying a supralinear association. The eSCHIF CIs widen as concentration deviates from the mean, as do the RCS CIs. The eSCHIF-based PAF average estimates are also much smoother than those based on the RCS (Figure 29B). The eSCHIF-based PAF lower confidence limit is near zero from approximately 5 µg/m³ to 7 µg/m³, suggesting lower and uncertain marginal benefits for exposure reductions in this concentration range. This observation is supported

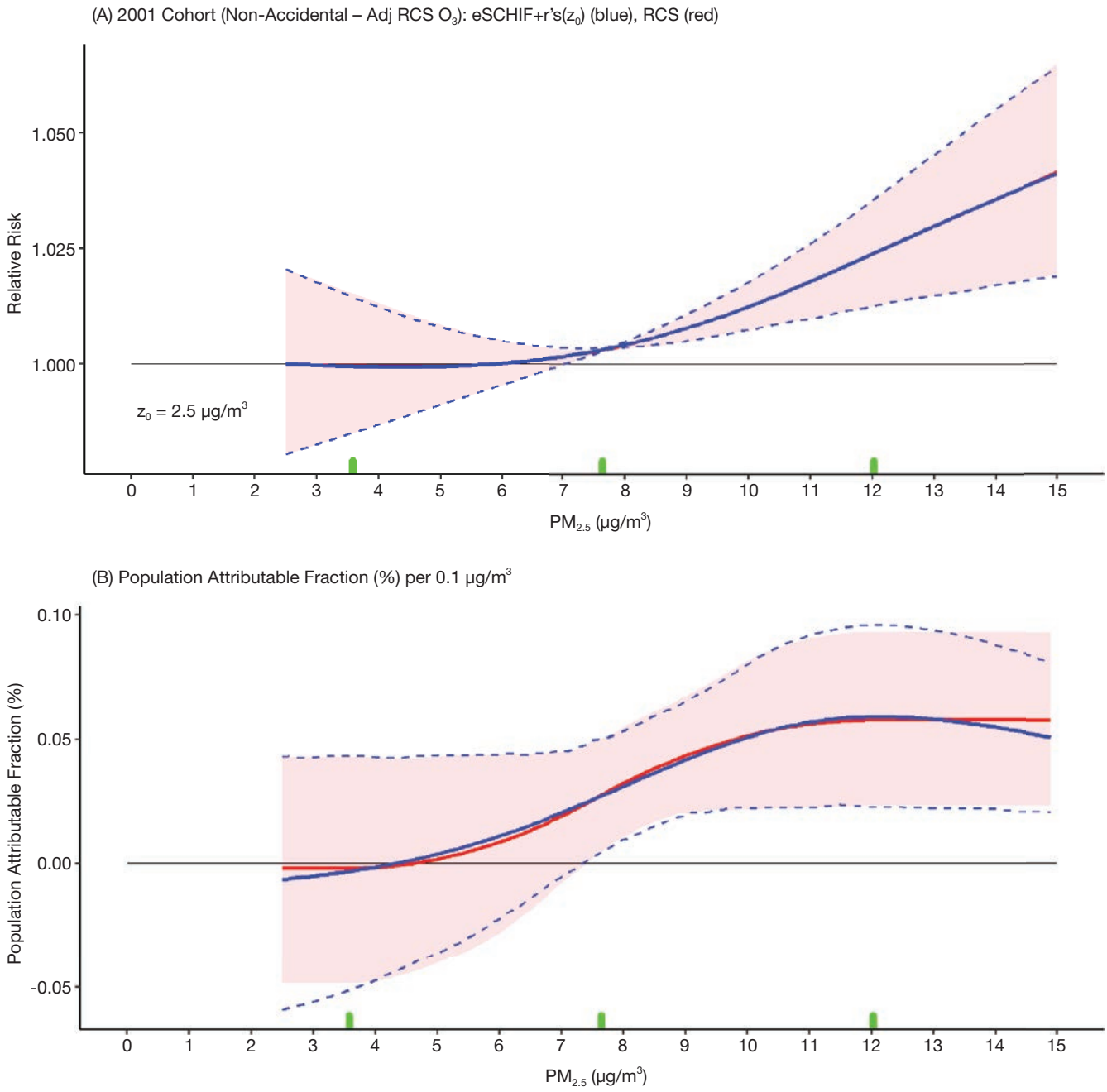

Figure 28. 2001 cohort nonaccidental death RCS mean relative risk predictions adjusted for O_3 over the $PM_{2.5}$ concentration range, with eSCHIF relative risk predictions. (A) Relative risk estimates; **(B)** PAF estimates. Mean and 95% CI: RCS = solid red line and pink-shaded area; eSCHIF = solid blue line and dashed blue lines. Green x-axis tick marks show RCS knot locations.

by the ensemble of threshold models (Figure 20). However the eSCHIF-based PAF predictions suggest larger benefits from reductions in the 2.5 to 5 µg/m³ concentration range, thus differing from the ensemble of threshold models. We also note that the RCS model is a much better predictor in these data than the linear model or any threshold model examined. Finally, both the RCS- and eSCHIF-based PAF display uncertain predictions at the highest concentrations (>15 µg/m³), with lower confidence limits overlapping zero.

We illustrate the use of an ensemble of RCS predictions with nonaccidental mortality in the stacked cohort. We ran

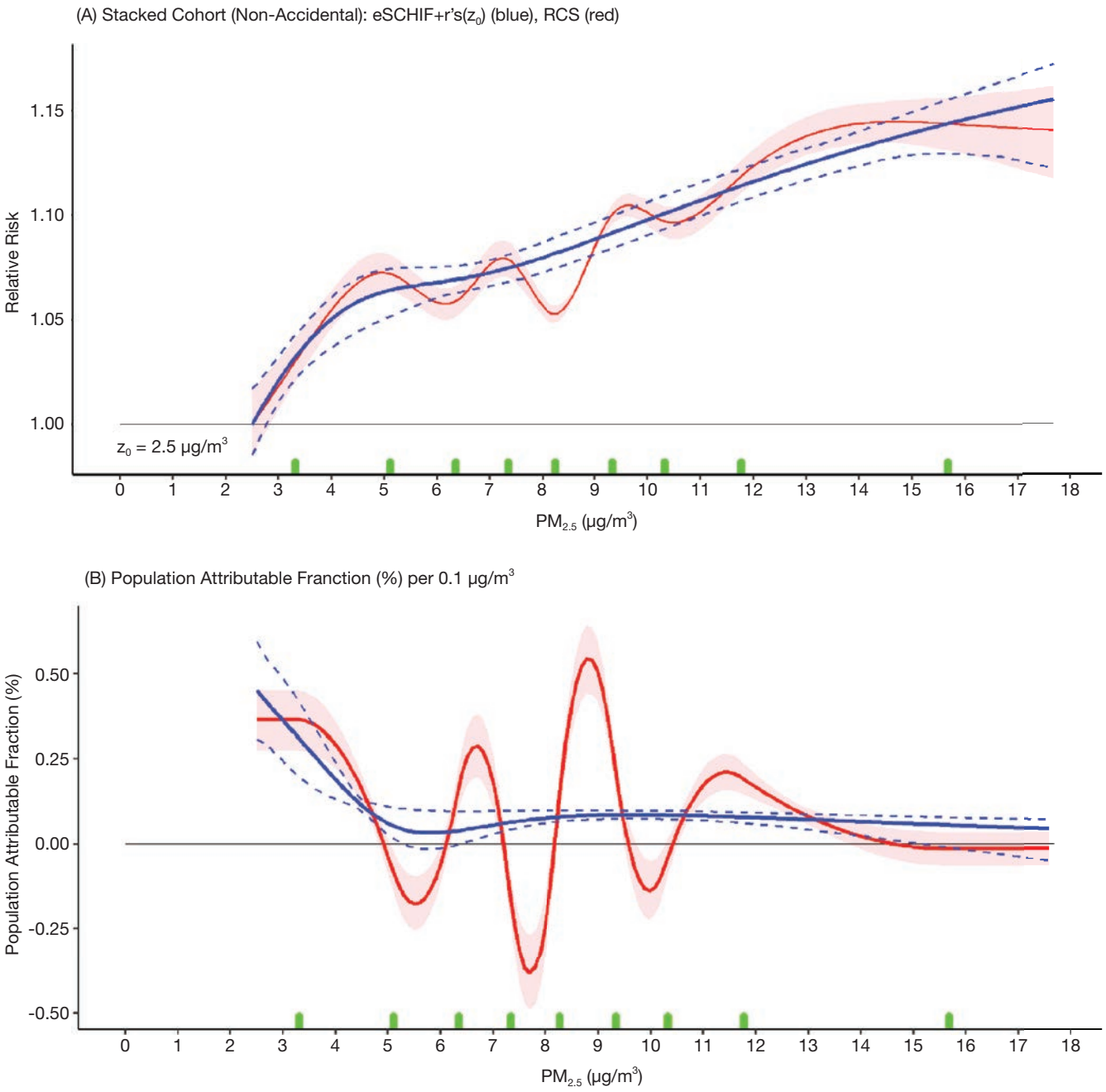

Figure 29. Stacked cohort nonaccidental death RCS (9 knots) mean relative risk predictions over the $PM_{2.5}$ concentration range, with eSCHIF relative risk predictions. (A) Relative risk estimates; (B) PAF estimates. Mean and 95% CI: RCS = solid red line and pink-shaded area; eSCHIF = solid blue line and dashed blue lines. Green x-axis tick marks show RCS knot locations.

16 RCS models with 3 to 18 knots. Using the AIC as the measure of fit, 2.4% of the 1,000 simulated realizations were assigned to 14 knots, 79.0% to 15 knots, 1.4% to 16 knots, 6.5% to 17 knots, and 10.7% to 18 knots. All other numbers of knots were assigned zero weight. The eSCHIF average predictions (Figure 30A) provide a smooth representation of the ensemble-based RCS predictions with a corresponding smoother PAF fit (Figure 30B). The eSCHIF fit of the ensemble of RCS displays a pattern similar to those of the eSCHIF based on the minimum BIC RCS fitting criteria (9 knots) displayed in Figure 29, suggesting some robustness of the eSCHIF to the method of determining the 1,000 RCS predictive curves.

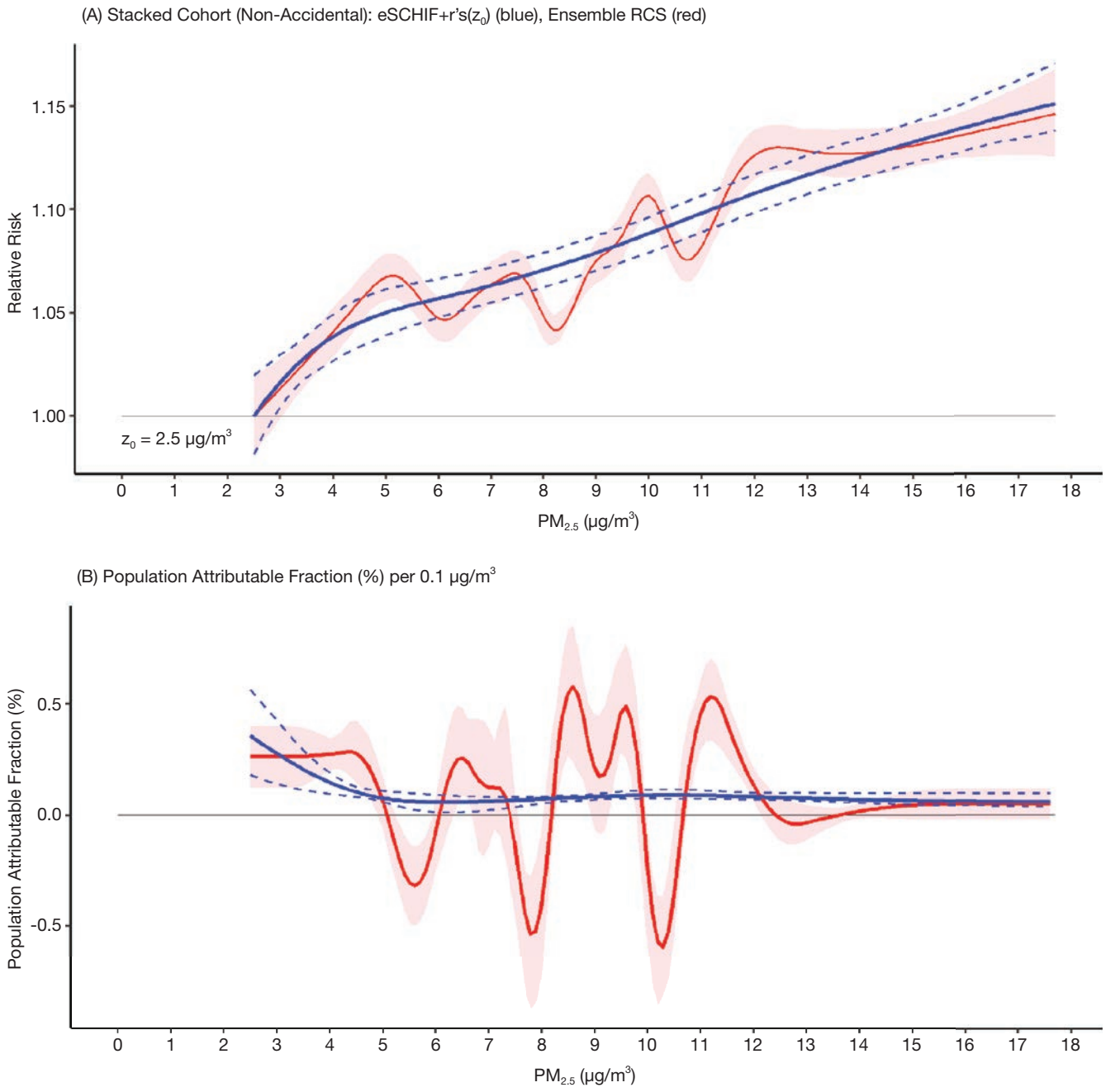

Figure 30. Stacked cohort nonaccidental death ensemble RCS mean relative risk predictions over the $PM_{2.5}$ concentration range, with eSCHIF relative risk predictions. (A) Relative risk estimates; (B) PAF estimates. Mean and 95% CI: RCS = solid red line and pink-shaded area; eSCHIF = solid blue line and dashed blue lines.

DISCUSSION

The MAPLE project has provided enhanced estimates of associations between nonaccidental and cause-specific mortality and exposure to $PM_{2.5}$, based on a large, stacked cohort of 7.1 million unique respondents to three cycles of the Canadian census, each representing about 20% of the entire population of Canada. These results further refine previous estimates provided in the Phase 1 MAPLE report. In this Phase 2 report, duplicate respondents in more than one CanCHEC cycle were removed and $PM_{2.5}$ exposure models were updated using data derived from a series of new collocated measurements of $PM_{2.5}$ and AOD collected at five sites across Canada. These measurements, which were used to develop refined models based on

remote sensing, include the GEOS-Chem, land use information, and ground measurements that were tailored to the estimation of low $PM_{2.5}$ concentrations. Additional analyses using the refined exposure estimates and selected mortality causes were also conducted with the mCCHS cohort.

CONCENTRATION–RESPONSE RELATIONSHIPS FOR NONACCIDENTAL MORTALITY

We observed consistent positive associations between $PM_{2.5}$ concentrations and nonaccidental mortality in all of the cohorts examined. In our Stacked CanCHEC analyses, which included nearly 1.3 million nonaccidental deaths, each 10-μg/m^3 increment in outdoor $PM_{2.5}$ concentration corresponded to an HR of 1.084 (95% CI: 1.073 to 1.096). In nonlinear models using RCS, mean predictions were greater than one for all concentrations that predicted at the minimum concentrations. Using an ensemble of threshold models, the mean prediction was greater than one for all observed concentrations, but the lower 95% confidence limit was greater than one only for concentrations greater than 8.0 μg/m^3. The mCCHS cohort analyses complemented those of CanCHEC by providing information on the shapes of concentration–response relationships between $PM_{2.5}$ and nonaccidental and selected mortality causes, with and without adjustment for behavioral covariates including smoking, BMI, fruit and vegetable consumption, exercise, and alcohol use. Although there was some attenuation evident in linear models with the inclusion of the behavioral covariates, this attenuation varied by cause of death (Table 7). Further, we found that the inclusion of these covariates led to no discernable differences in the shapes of the concentration–response curves and in the concentration (3.6–3.7 μg/m^3) at which the lower 95% confidence limits of the HRs were above one. Similar to our findings in the Phase 1 report, these results suggest that these individual-level variables were unlikely to be important confounders of the relationship between outdoor $PM_{2.5}$ concentrations and mortality at the very low observed concentrations. Given the similar population representativeness of the CanCHEC and mCCHS cohorts, these results and our inclusion of many individual-scaled socioeconomic and demographic characteristics in the CanCHEC, which likely capture variation in health outcomes attributed to health behavior, also suggest no strong confounding from behavioral factors in the CanCHEC analyses.

The $PM_{2.5}$–nonaccidental mortality relationship estimated using the eSCHIF suggests a supralinear form (Figure 29). This shape was similarly reported in previous work on the 1991 CanCHEC (Crouse et al. 2012, 2015) and 2001 CanCHEC (Pinault et al. 2017) cohorts, as well as in the pooled CanCHEC results presented in the Phase 1 report (and in Pappin et al. 2019). We have extended the analyses presented in the Phase 1 report, where no lower threshold was detected, for the mean of the association between $PM_{2.5}$ and nonaccidental mortality, specifically, the concentration of 2.5 μg/m^3 (the minimum value assigned to respondents in the cohort). This minimum effect (mortality) level was also substantially lower than the minimum measured concentrations in studies conducted in other countries. For example, the National Health Interview Survey Cohort had a minimum value of 7.6 μg/m^3 (Pope et al. 2018) and the American Cancer Society Cancer Prevention II Cohort had a minimum value of 6.7 μg/m^3 (Turner et al. 2016). However, we did detect some uncertainty in the threshold concentration with the best-fitting threshold values for the minimum concentration (2.5 μg/m^3) and a concentration of 8 μg/m^3. This was most likely due to the dip in the risk relationship for concentrations near 8 μg/m^3.

From a statistical perspective, the wiggles in relative-risk predictions for nonaccidental deaths may be due to a combination of the large number (1.25 million) of deaths, the use of RCS that do not have additional smoothing parameters, the large number of knots (9) with a limited range between knots (~1 μg/m^3), and a pattern in the data displaying a marked increase in risk at low concentrations, followed by a slight decline, and then followed by an increase in risk. Relatively small improvements in prediction can warrant inclusion of additional spline knots when the numbers of death are very large. The limited range between knots can force RCS predictions to oscillate over small ranges in concentration. For example, RCS predictions become increasingly wiggly as the number of knots increases and the concentration range between knots decreases (Figure 14). We suggest that use of smoothing splines, such as thin-plate splines where a smoothing parameter is estimated from the data, be considered in future work. These smoothing splines may be able to reduce the wiggle-ness of relative risk predictions. However, we also suggest that the eSCHIF is specifically designed to smooth out these wiggles yet preserve the general concentration–response relationship as described by the RCS.

We examined the sensitivity of the shape of the nonaccidental mortality–$PM_{2.5}$ association to the removal of person-years above selected concentrations. Removing person-years with $PM_{2.5}$ exposure at or above 12 μg/m^3 and 10 μg/m^3 indicated that the higher concentrations were contributing to a positive association with nonaccidental mortality. However, a steep increase was observed from the minimum concentration of 2.5 μg/m^3 to 5 μg/m^3 in all curves, further suggesting adverse effects on mortality at concentrations as low as 2.5 μg/m^3. Additional analyses described later indicated that regional variation in the concentration–mortality relationship are likely contributing to the overall shape, including the flattening within the midrange of the concentration distribution. Sensitivity analyses designed to identify reasons for this complex shape are described later in the regional variation section.

Compared with prior research and results presented in the MAPLE Phase 1 report, our estimates in this analysis are also based on longer-term exposure estimates (i.e., 10 years of prior exposure) using new estimates of $PM_{2.5}$ that are based on

a refined methodology, resulting in reduced evaluation errors with ground monitors and improved performance at low concentrations specifically. These new estimates were derived from a series of new collocated measurements of $PM_{2.5}$ and AOD that provided some new insights on aerosol MSE, and that were used to refine models based on remote sensing, GEOS-Chem, land use information, and ground data. These enhancements and their application to backcasted exposures are likely to have reduced exposure measurement error when compared with prior CanCHEC and CCHS analyses.

CONCENTRATION–RESPONSE RELATIONSHIPS FOR OTHER CAUSES OF DEATH

In addition to nonaccidental mortality, we also examined the shapes of concentration–response relationships for other causes of death using the Stacked CanCHEC (and for selected causes with sufficient numbers of deaths in the mCCHS). These included cardiovascular, cerebrovascular, heart failure, ischemic heart disease, diabetes, respiratory, COPD, pneumonia, and lung cancer mortality. Of the specific causes examined, $PM_{2.5}$ concentrations were strongly and consistently associated with ischemic heart disease, respiratory disease, and to a somewhat lesser degree for cardiovascular disease and diabetes. These findings suggest, not unexpectedly, that our all-cause mortality findings were driven by these major causes of death in Canada. There was less consistency between the CanCHEC and mCCHS findings and across specific CanCHEC cohorts for several of the other causes. This potentially reflects small differences in the overall population representation of the cohorts, variation in disease management over time, or both, as well as generally less robust associations for several specific causes of death. Specifically, associations were observed in CanCHEC but not in the mCCHS for cerebrovascular disease, while associations for COPD mortality were observed in the Stacked CanCHEC and mCCHS but not in the 1991 or 2001 CanCHEC cohorts alone. Similarly, associations for pneumonia mortality were observed in the Stacked CanCHEC analysis but were not consistent across the 2001 CanCHEC and the mCCHS cohorts. No significant associations were found between exposure to $PM_{2.5}$ and lung cancer, heart failure, or kidney failure.

REGIONAL VARIATIONS AND SENSITIVITY TO ADJUSTMENT FOR OXIDANT GASES

Additional analyses were conducted to examine possible explanations for the observed dip in the concentration–response curve for $PM_{2.5}$ and nonaccidental mortality in the middle of the $PM_{2.5}$ distribution that was first observed in the Phase 1 report and then in these analyses. The dip was observed for nonaccidental deaths in the 1991 and 1996 cohorts but not in the 2001 cohort (Figure 13). However, the dip was present in the stacked cohort when RCS were fit with five or more knots (Figure 14). The dip was not present in the mCCHS however (Figure 15). Both the 2001 CanCHEC and mCCHS cohorts started follow-up in 2001. This is also the period when better data support was available for our $PM_{2.5}$ prediction model, including ground-monitoring and remote-sensing data. The dip was present in cardiometabolic causes of death such as all cardiovascular, ischemic heart disease, heart failure, stroke, and diabetes. No such dip was observed in lung-related disease such as lung cancer, all respiratory, COPD, and pneumonia (Figure 16).

To further explore the causes of the dip, we fit RCS to each of the six airsheds separately (Figure 21). Next, we examined possible confounding and effect modification by oxidant gases (i.e., O_3 – Figure 17 and O_x – Figure 18) to evaluate how these pollutants may affect the concentration–response curves for $PM_{2.5}$. Taken together, the results of these analyses suggest that there is important spatial variation in the strength and shape of associations between $PM_{2.5}$ and mortality across Canada. Specifically, $PM_{2.5}$ concentrations were positively associated with nonaccidental mortality in the East Central, Southern Atlantic, Western, and Northern airsheds. However, associations were not observed except at relatively high concentrations (~12 $\mu g/m^3$ and above) for the Prairie and the West Central airsheds, where there was even some evidence of inverse relationships. The dip in the national concentration–response curve therefore appeared to be explained by similar patterns observed in these areas. These findings cannot be explained by $PM_{2.5}$ mass concentrations, as these overlapped between all the airsheds, but they may be attributable to unrecognized population differences, unmeasured confounders (i.e., factors that are causes of mortality and are causally or noncausally associated with outdoor $PM_{2.5}$ concentrations), or spatial differences in particle composition, air pollution mixtures, or interactions between pollutants. With respect to unmeasured confounders, it is not clear which variables could have been considered beyond those already included in the analyses. The most likely candidates would be ecological variables (e.g., neighborhood-level factors), rather than individual-level factors as individual-level characteristics are not likely to be strongly related to outdoor $PM_{2.5}$ concentrations (e.g., if an individual starts smoking or has a BMI increase, it doesn't affect the long-term outdoor $PM_{2.5}$ concentration). This is supported by our analyses with individual-level characteristics that include BMI and smoking.

Our sensitivity analyses for evaluating the potential role of regional variation in healthcare access or in differential representation of population characteristics (age, immigrants, Indigenous respondents) indicated that results were insensitive to an adjustment for healthcare access or to removal of specific population subgroups. Although other unmeasured population factors may still vary among regions, our additional evaluation of regional variation and sensitivity to copollutant adjustment supports a potential role for regional variation in the pollutant mixture composition.

As $PM_{2.5}$ is a complex mixture that varies across both space and time, it is not altogether surprising to observe spatial differences in the shapes of concentration–response curves for $PM_{2.5}$, simply because these populations are not exposed to the same thing (despite similarity in measured $PM_{2.5}$ mass concentrations). More work is needed to understand how $PM_{2.5}$ composition and pollutant interactions affect long-term health risks. Our findings for O_x and O_3 suggest that oxidant gases may be particularly important. Specifically, O_x was more strongly associated with mortality than was $PM_{2.5}$ mass for several outcomes examined in the stacked cohort (i.e., nonaccidental mortality, diabetes, ischemic heart disease, respiratory mortality, and COPD; Table 11), and the shapes of concentration–response relationships between $PM_{2.5}$ and nonaccidental, cardiovascular, and respiratory mortality were clearly influenced by O_x (Figure 18). For cardiovascular outcomes in particular, $PM_{2.5}$ was most strongly associated with mortality when O_x was higher (Table 14).

Collectively, these findings further support the notion that the long-term health effects of $PM_{2.5}$ are spatially heterogeneous and suggest that outdoor O_x concentrations should be considered in combination with $PM_{2.5}$ as there may be important interactions between these pollutants. Although the nature of these possible interactions require further research to fully elucidate, this finding is consistent with our previous results (Weichenthal et al. 2017), which suggested that the chronic health effects of $PM_{2.5}$ mass concentrations are enhanced in the presence of oxidant gases. As noted earlier, this pattern could be explained by a direct action of O_x on the lungs, or O_x could simply be an efficient marker of harmful air pollution mixtures reflecting spatial variations in atmospheric processes or sources that can have an effect on particle toxicity (e.g., particle aging or oxidation of organic components). Ultimately, we cannot conclusively explain the observed heterogeneity in $PM_{2.5}$–mortality associations in our current study, but our findings strongly suggest that important spatial differences do exist and that oxidant gases (or particle–oxidant gas interactions) may play a role in explaining this variation. Future work should examine this possibility, as it may allow for more efficient regulatory interventions if we can predict where $PM_{2.5}$ mass concentrations are expected to pose the greatest threat to public health, or which sources may be most relevant.

Although our study was strengthened by the use of a Stacked CanCHEC with 7.1 million respondents with individual socioeconomic and demographic indicators, there are some limitations arising from the use of such cohorts. First, CanCHEC excludes the institutional population on census day, and those not enumerated by the census. Although the CanCHECs are largely representative of the population of Canada, they tend to be slightly healthier than the overall Canadian population (Tjepkema et al. 2020). This may be heightened by our exclusion criteria, which tend to remove person-years associated with marginalized groups. The mCCHS, on the other hand, is based on the CCHS survey, which is not totally representative of the entire population of Canada, as the sampling frame for the survey is designed to produce estimates at a health-region level (Sanmartin et al. 2016). Second, in all cohorts, individual covariates are collected only at the time of the census or survey, while it is acknowledged that many of these characteristics are likely to change over the follow-up period. Third, postal codes reported on tax files are used to assign air pollution exposures and neighborhood covariates. Postal codes may not always represent the location of a person's residence, such as when the postal code represents a post office box or the address of a relative. One analysis of the CCHS has indicated that postal codes in tax files do represent the location of the residence in 92.9% of cases (Bérard-Chagnon 2017). Accuracy in assignment of residential location using postal codes is relatively high for urban postal codes, within about 500 meters of a person's home, although it may be more distant in rural areas (Khan et al. 2018). However, $PM_{2.5}$ is more spatially uniform in rural areas of Canada relative to urban areas, which may mitigate some of this possible misclassification in rural regions.

Based on a Stacked CanCHEC, individual CanCHECs, and the mCCHS cohorts, we report associations between nonaccidental mortality and exposures to $PM_{2.5}$ at concentrations above 2.5 $\mu g/m^3$, corresponding to the minimum $PM_{2.5}$ concentrations assigned to the cohort. We also report associations between $PM_{2.5}$ and death due to cardiovascular disease, ischemic heart disease, cerebrovascular disease, diabetes, nonmalignant respiratory disease, COPD, and pneumonia, as well as minimum $PM_{2.5}$ concentrations, above which we observe a significant association for these causes. Future work will apply our eSCHIF methodology to other international cohorts, to determine if associations observed are consistent in other regions of the world.

DATA SHARING

Approved researchers can access the CanCHECs in Research Data Centres and in the Federal Research Data Centre. Information on the Research Data Centre program, including the application process and guidelines, are available at *https://www.statcan.gc.ca/en/microdata/data-centres*.

ACKNOWLEDGMENTS

We would like to thank the Canadian Urban Environmental Health Research Consortium for providing postal code level O_3 surfaces to support multipollutant modeling and for creating the 5-km and 10-km buffered estimates of $PM_{2.5}$. We would also like to thank Dr. Hong Chen for his support in running the SCHIF codes and Drs. Alain Robichaud and Richard Menard for developing the O_3 model used to calculate the O_x estimates used in these analyses.

REFERENCES

Apte JS, Marshall JD, Cohen AJ, Brauer M. 2015. Addressing global mortality from ambient $PM_{2.5}$. Environ Sci Technol 49:8057–8066.

Beelen R, Raaschou-Nielsen O, Stafoggia M, Jovanovic Andersen Z, Weinmayr G, Hoffman B, et al. 2014. Effects of long-term exposure to air pollution on natural-cause mortality: An analysis of 22 European cohorts within the multicenter ESCAPE project. Lancet 383:785–795.

Bérard-Chagnon J. 2017. Comparison of place of residence between the T1 Family File and the Census: Evaluation using record linkage. Statistics Canada Demographics Documents, Catalogue no. 91F0015M —No. 13ISSN 205-996X ISBN 978-0-660-08112-0.

Bissonnette P. 2019. SYRUP: A Novel Inversion Method for Aerosol Size-Distribution Properties from Optical and Chemical Measurements of $PM_{2.5}$. MSc thesis, Dalhousie University, Halifax, Canada. Available: *https://dalspace.library.dal.ca/xmlui/handle/10222/76202* [accessed 24 June 2021].

Blomberg A, Mudway I, Svensson M, Hagenbjörk-Gustafsson A, Thomasson L, Helleday R, et al. 2003. Clara cell protein as a biomarker for ozone-induced lung injury in humans. Eur Respir J22:883–888.

Bratsch SG. 1989. Standard Electrode Potentials and Temperature Coefficients in Water at 298.15 K. J Phys Chem Ref Data 18:1–21. Available: *https://www.nist.gov/sites/default/files/documents/srd/jpcrd355.pdf* [accessed 24 June 2021].

Broeckaert F, Arsalane K, Hermans C, Bergamaschi E, Brustolin A, Mutti A, et al. 2000. Serum clara cell protein: A sensitive biomarker of increased lung epithelium permeability caused by ambient ozone. Environ Health Perspect 108:533–537.

Buckland ST, Burnham KP, Augustin NH. 1997. Model selection: An integral part of inference. Biometrics 53:603–618.

Burnett R, Chen H, Szyszkowicz M, Fann N, Hubbell B, Pope CA 3rd, et al. 2018. Global estimates of mortality associated with long-term exposure to outdoor fine particulate matter. Proc Natl Acad Sci USA 115:9592–9597.

Cabada JC, Rees S, Takahama S, Khlystov A, Pandis SN, Davidson CI, et al. 2004. Mass size distributions and size resolved chemical composition of fine particulate matter at the Pittsburgh supersite. Atmospheric Environment 38:3127–3141.

Christidis T, Erickson AC, Pappin AJ, Crouse DL, Pinault LL, Weichenthal SA, et al. 2019. Low concentrations of fine particle air pollution and mortality in the Canadian Community Health Survey cohort. Environ Health 18:84.

Christidis T, Labrecque-Synnott F, Pinault L, Saidi A, Tjepkema M. 2018. Analytical studies: Methods and references — The 1996 CanCHEC: Canadian Census Health and Environment Cohort Profile. In: Statistics Canada. Ottawa, Ontario, Canada:Health Statistics Division.

Ciencewicki J, Trivedi S, Kleeberger SR. 2008. Oxidants and the pathogenesis of lung diseases. J Allergy Clin Immunol 122:456–468.

Cox DR. 1972. Regression Models and Life Tables. J Royal Stat Soc B 34:187–220.

Crobeddu B, Aragao-Santiago L, Bui LC, Boland S, Squiban AB. 2017. Oxidative potential of particulate matter 2.5 as predictive indicator of cellular stress. Environ Pollut 230:125–133.

Crouse DL, Christidis T, Erickson A, Pinault L, Martin RV, Tjepkema M, et al. 2020. Evaluating the sensitivity of $PM_{2.5}$-mortality associations to the spatial and temporal scale of exposure assessment at low particle mass concentrations. Epidemiology 31:168–176.

Crouse DL, Peters PA, Hystad P, Brook JR, van Donkelaar A, Martin RV, et al. 2015. Ambient $PM_{2.5}$, O_3, and NO_2 exposures and associations with mortality over 16 years of follow-up in the Canadian Census Health and Environment Cohort (CanCHEC). Environ Health Perspect 123:1180–1186.

Crouse DL, Peters PA, van Donkelaar A, Goldberg MS, Villeneuve PJ, Brion O, et al. 2012. Risk of nonaccidental and cardiovascular mortality in relation to long-term exposure to low concentrations of fine particulate matter: A Canadian national-level cohort study. Environ Health Perspect 120:708–714.

Crouse DL, Philip S, van Donkelaar A, Martin RV, Jessiman B, Peters PA, et al. 2016. A new method to jointly estimate the mortality risk of long-term exposure to fine particulate matter and its components. Sci Rep 6:18916.

Davy PM, Tremper AH, Nicolosi Eleonora MG, Quincey P, Fuller GW. 2017. Estimating particulate black carbon concentrations using two offline light absorption methods applied to four types of filter media. Atmos Environ; doi:10.1016/j.atmosenv.2016.12.010.

Di Q, Wang Y, Zanobetti A, Wang Y, Koutrakis P, Choirat C, et al. 2017. Air pollution and mortality in the Medicare population. N Engl J Med 376:2513–2522.

Environment Canada. National Air Pollution Surveillance (NAPS) Program. 2013. Available: *https://www.canada.ca/en/environment-climate-change/services/air-pollution/monitoring-networks-data/national-air-pollution-program.html* [accessed 12 June 2019].

Erickson AC, Brauer M, Christidis T, Pinault L, Crouse DL, van Donkelaar A, et al. 2019. Evaluation of a method to indirectly adjust for unmeasured covariates in the association between fine particulate matter and mortality. Environ Res 175:108–116.

Erickson AC, Christidis T, Pappin A, Brook JR, Crouse DL, Hystad P, et al. 2020. Disease assimilation: The mortality impacts of fine particulate matter on immigrants to Canada. Health Rep 3:14–26.

Fellegi IP, Sunter AB. 1969. A theory for record linkage. J Am Stat Assoc 64:1183–1210.

Finès P, Pinault L, Tjepkema M. 2017. Analytical studies: Methods and reference — Imputing postal codes to analyze ecological variables in longitudinal cohorts: Exposure to particulate matter in the Canadian Census Health and Environment Cohort Database. In: Statistics Canada. Ottawa, Ontario, Canada:Health Statistics Division.

GBD 2019 Risk Factors Collaborators. 2020. Global burden of 87 risk factors in 204 countries and territories, 1990–2019: A systematic analysis for the Global Burden of Disease Study 2019. Lancet 396:1223–1249.

Georas SN, Rezaee F. 2014. Epithelial barrier function: at the front line of asthma immunology and allergic airway inflammation. J Allergy Clin Immunol 134:509–520.

Gordon DL, Janzen M. 2013. Suburban nation? Estimating the size of Canada's suburban population. J Archit Plan Res 30:197–220.

Hand JL. Malm WC. 2007. Review of aerosol mass scattering efficiencies from ground-based measurements since 1990. J Geophys 112:16203.

Harrel JFE. 2015. Regression modeling strategies. Available: *https://link.springer.com/book/10.1007%2F978-3-319-19425-7* [accessed 10 June 2021].

Hystad P, Setton E, Cervantes A, Poplawski K, Deschenes S, Brauer M, et al. 2011. Creating national air pollution models for population exposure assessment in Canada. Environ Health Perspect 119:1123–1129.

Khan S, Pinault L, Tjepkema M, Wilkins R. 2018. Positional accuracy of geocoding from residential postal codes versus full street addresses. Health Rep 29:3–9.

Kienast K, Knorst M, Lubjuhb S, Muller-Quernheim J, Ferlinz R. 1994. Nitrogen dioxide-induced reactive oxygen intermediates production by human alveolar macrophages and peripheral blood mononuclear cells. Arch Environ Health 49:246–250.

Lakey PSJ, Berkemeier T, Tong H, Arangio AM, Lucas K, Pöschl U, et al. 2016. Chemical exposure-response relationship between air pollutants and reactive oxygen species in the human respiratory tract. Sci Rep 6:32916.

Latimer RNC, Martin RV. 2019. Interpretation of measured aerosol mass scattering efficiency over North America using a chemical transport model. Atmos Chem Phys 19:2635–2653.

Li R, Hertzmark E, Louie M, Chen L, Spiegelman D. 2011. The SAS LGTPHCURV9 Macro. Available: *https://cdn1.sph.harvard.edu/wp-content/uploads/sites/271/2012/09/lgtphcurv9_7-3-2011.pdf* [accessed 13 January 2022].

Li T, Zhang Y, Wang J, Xu D, Yin Z, Chen H, et al. 2018. All-cause mortality risk associated with long-term exposure to ambient $PM_{2.5}$ in China: A cohort study. Lancet Public Health 3:e470–e477.

Matheson FI, Dunn JR, Smith KLW, Moineddin R, Glazier RH. 2012. Development of the Canadian Marginalization Index: A new tool for the study of inequality. Can J Public Health 103:S12–16.

McNeille J, Snider G, Weagle CL, Walsh B, Bissonnette P, Stone E, et al. 2020. Large global variations in measured airborne metal concentrations driven by anthropogenic sources. Sci Rep 10:21817.

Meng J, Li C, Martin R, van Donkelaar A, Hystad P, Brauer M. 2019. Estimated long-term (1981–2016) concentrations of ambient fine particulate matter across North America from chemical transport modeling, satellite remote sensing and ground-based measurements. Environ Sci Technol 53:5071–5079.

Nasari MM, Szyszkowicz M, Chen H, Crouse D, Turner MC, Jerrett M, et al. 2016. A class of non-linear exposure-response models suitable for health impact assessment applicable to large cohort studies of ambient air pollution. Air Qual Atmos Health 9:961–972.

Pappin AJ, Christidis T, Pinault LL, Crouse DL, Tjepkema M, Erickson AC, et al. 2019. Examining the shape of the association between low levels of fine particulate matter and mortality across three cycles of the Canadian Census Health and Environment Cohort. Environ Health Perspect 127:107008; doi:10.1289/EHP5204.

Peters PA, Tjepkema M, Wilkins R, Finès P, Crouse DL, Chan PC, et al. 2013. Data resource profile: 1991 Canadian Census Cohort. Int J Epidemiol 42:1319–1326.

Pinault L, Finès P, Labrecque-Synnott F, Saidi A, Tjepkema M. 2016a. Analytical studies: Methods and references — The Canadian Census Tax-Mortality Cohort: A 10-year follow-up. In: Statistics Canada. Ottawa, Ontario, Canada:Health Statistics Division.

Pinault L, Tjepkema M, Crouse DL, Weichenthal S, van Donkelaar A, Martin RV, et al. 2016b. Risk estimates of mortality attributed to low concentrations of ambient fine particulate matter in the Canadian Community Health Survey Cohort. Environ Health 15:18.

Pinault L, Weichenthal S, Crouse DL, Brauer M, Erickson A, van Donkelaar A, et al. 2017. Associations between fine particulate matter and mortality in the 2001 Canadian Census Health and Environment Cohort Environ Res 159:406–415.

Pope CA 3rd, Burnett RT, Thun MJ, Calle EE, Krewski D, Ito K, et al. 2002. Lung cancer, cardiopulmonary mortality, and long-term exposure to fine particulate air pollution. J Am Med Assoc 287:1132–1141.

Pope CA 3rd, Ezzati M, Cannon J, Allen R, Jerrett M, Burnett R. 2018. Mortality risk and $PM_{2.5}$ air pollution in the USA: An analysis of a national prospective cohort. Air Qual Atmos Health 11:245–252.

Pun VC, Kazemiparkouhi F, Manjourides J, Suh HH. 2017. Long-term $PM_{2.5}$ exposure and respiratory, cancer, and cardiovascular mortality in older U.S. adults. Am J Epidemiol 186:961–969.

Pya N, Wood SN. 2015. Shape-constrained additive models. Stat Comput 25:543–559.

Rattanavaraha W. 2011. The reactive oxidant potential of different types of aged atmospheric particles: An outdoor chamber study. Atmos Environ 45:3848–3855.

Robichaud A, Ménard R. 2014. Multi-year objective analyses of warm season ground-level ozone and $PM_{2.5}$ over North America using real-time observations and the Canadian operational air quality models. Atmos Chem Phys 14:1769–1800.

Robichaud A, Ménard R, Zaitseva Y, Anselmo D. 2016. Multi-pollutant surface objective analyses and mapping of air quality health index over North America. Air Qual Atmos Health 9:743–759.

Safari A, Daher N, Shafer MM, Schauer JJ, Sioutas C. 2014. Global perspective on the oxidative potential of airborne particulate matter: A synthesis of research findings. Environ Sci Technol 48:7576–7583.

Sanmartin C, Decady Y, Trudeau R, Dasylva A, Tjepkema M, Finès P, et al. 2016. Linking the Canadian Community Health Survey and the Canadian Mortality Database: An enhanced data source for the study of mortality. Health Rep 27:10–18.

Snider G, Weagle CL, Martin RV, van Donkelaar A, Conrad K, Cunningham D, et al. 2015. SPARTAN: A global network to evaluate and enhance satellite-based estimates of ground-level particulate matter for global health applications. Atmos Meas Tech Discuss 7:7569–7611.

Snider G, Weagle CL, Murdymootoo KK, Ring A, Ritchie Y, Stone E, et al. 2016. Variation in global chemical composition of $PM_{2.5}$: Emerging results from SPARTAN. Atmos Chem Phys 16:9629–9653.

Statistics Canada. 2003. 2001 Census dictionary (reference products: 2001 census – archived (Cat No. 92-378-XIE). In: Statistics Canada. Ottawa, Ontario, Canada:Health Statistics Division.

Statistics Canada. 2005. Canadian community health survey: Public use microdata file, 2003. In: Statistics Canada. Ottawa, Ontario, Canada:Health Statistics Division.

Statistics Canada. 2016. Low-income lines: What they are and how they are created. Income Research Paper Series (Cat No. 75F0002M-No.002). In: Statistics Canada. Ottawa, Ontario, Canada:Health Statistics Division.

Statistics Canada. 2017a. Postal code conversion file plus (PCCF+) version 6D, August 2015 postal codes. In: Statistics Canada. Ottawa, Ontario, Canada:Health Statistics Division.

Statistics Canada. 2017b. Social Data Linkage Environment (SDLE): Expanding Data Potential. Available: *https://www.statcan.gc.ca/eng/sdle/index* [accessed 28 January 2019].

Statistics Canada. 2020. Proximity Measures Database – Early Release. Available: *https://www150.statcan.gc.ca/n1/pub/17-26-0002/172600022020001-eng.htm* [accessed 16 May 2021].

Thurston GD, Ahn J, Cromar KR, Shao Y, Reynolds HR, Jerrett M, et al. 2016. Ambient particulate matter air pollution exposure and mortality in the NIH-AARP Diet and Health cohort. Environ Health Perspect 124:484–490.

Tjepkema M, Christidis T, Bushnik T, Pinault L. 2020. Cohort profile: The Canadian Census Health and Environment Cohorts (CanCHECs). Health Rep 30:18–26.

Turner MC, Jerrett M, Pope CA 3rd, Krewski D, Gapstur SM, Diver WR, et al. 2016. Long-term ozone exposure and mortality in a large prospective study. Am J Respir Crit Care Med 193:1134–1142.

U.S. EPA (United States Environmental Protection Agency). 2012. Regulatory Impact Analysis for the Final Revisions to the National Ambient Air Quality Standards for Particulate Matter. EPA-452/R-12-005 December. Research Triangle Park, NC:Office of Air Quality Planning and Standards, Health and Environmental Impacts Division.

van Donkelaar A, Martin RV, Brauer M, Hsu NC, Kahn RA, Levy RC, et al. 2016. Global estimates of fine particulate matter using a combined geophysical-statistical method with information from satellites, models, and monitors. Environ Sci Technol 50:3762–3773.

van Donkelaar A, Martin RV, Li C, Burnett RT. 2019. Regional estimates of chemical composition of fine particulate matter using a combined geoscience-statistical method with information from satellites, models, and monitors. Environ Sci Technol 53:2595–2611.

van Donkelaar A, Martin RV, Spurr RJD, Burnett RT. 2015. High resolution satellite-derived $PM_{2.5}$ from optical estimation and geographically weighted regression over North America. Environ Sci Technol 49:10482–10491.

Weichenthal S, Pinault L, Burnett R. 2017. Impact of oxidant gases on the relationship between outdoor fine particulate air pollution and nonaccidental, cardiovascular, and respiratory mortality. Sci Rep 7:Article no. 16401.

Wilkins R, Tjepkema M, Mustard CM, Choiniere R. 2008. The Canadian census mortality follow-up study, 1991 through 2001. Health Rep 19:25–43.

Yin P, Brauer M, Cohen A, Burnett RT, Liu J, Liu Y, et al. 2017. Long-term fine particulate matter exposure and nonaccidental and cause-specific mortality in a large national cohort of Chinese men. Environ Health Perspect 125:117002.

HEI QUALITY ASSURANCE STATEMENT

The conduct of this study was subjected to independent audits by RTI International staff members Dr. Linda Brown and Dr. Prakash Doraiswamy. These staff members are experienced in quality assurance (QA) oversight for air quality monitoring, chemical transport modeling, use of satellite data, and epidemiological methods and analysis. The RTI QA oversight team also included statistician Dr. David Wilson who reviewed the statistical methods and accompanying codes.

The QA oversight program consisted of an initial onsite audit of the research study for conformance to the study protocol and standard operating procedures and a final remote audit of the final report and the data processing steps. The onsite audit was performed by Drs. Brown and Doraiswamy. The final remote audit was performed by Drs. Brown, Doraiswamy, and Wilson. The dates of the audits and reviews are listed below.

Audit 1: Onsite Audit at an External Facility Nearby Statistics Canada in Ottawa, Canada, August 23–24, 2018

The auditors conducted an in-person audit in Ottawa, Canada, at an external facility due to security restrictions at Statistics Canada. The audit reviewed the following study components: progress reports, personnel and staff, internal quality assurance procedures, air quality data processing and documentation, health data processing and quality checks, and backup procedures. Program codes were inspected to verify proper documentation. The codebook for the analytic file was examined. The audit included an observation of selected scripts. No actual script executions were observed due to restrictions on connection to Statistics Canada from an external location. No errors were noted during the audit, but recommendations were made for ensuring proper documentation for field and lab log sheets (e.g., including detailed documentation with reason and signature when modifying previously recorded values), updating study plan and quality plan, documenting codes and documenting procedures, checks and assumptions related to model development, and QA/QC. The audit was conducted at an external location not affiliated with any of the research team members and therefore did not include an inspection of facilities or equipment.

Audit 2: Final Remote Audit, March – June 2022

The final remote audit consisted of two parts: (1) review of the final project report, and (2) audit of data processing steps. The review of the final report focused on ensuring that the methods are well documented and the report is easy to understand. The review also examined if the report highlighted key study findings and limitations. The data audit included (1) a remote live demonstration of selected data processing codes, and (2) the review of the codes for data reduction, processing and analysis, and model development. This specific portion of the audit was restricted to the key components of the study and associated findings. Selected codes for exposure assessment and epidemiological model development were sent to RTI. No raw data were sent to RTI due to data confidentiality restrictions.

The codes were reviewed at RTI to verify, to the extent feasible, linkages between the various scripts, confirmation of the models reported, and verification of key tables. The codes appear to be largely consistent with the models described in the report and followed the overall model development procedure described. The auditors identified a couple of discrepancies whose impact on the overall study findings are anticipated to be negligible. The values themselves could not be generated at RTI due to unavailability of the input data.

The remote live demonstration included a real-time execution of selected codes generating key tables and figures in the report. Values generated by the codes during the real-time demonstration matched the values in the report. Except for the couple of discrepancies, no major quality-related issues were identified from the review of the codes and the report.

Recommendations were made to address noted discrepancies, add clarifying statements for some findings, and general edits for improved clarity.

A written report was provided to HEI. The QA oversight audit demonstrated that the study was conducted according to the study protocol. The final report, except as noted in the comments and recommended corrections, appears to be representative of the study conducted.

Linda Morris Brown, MPH, DrPH, Epidemiologist, Quality Assurance Auditor

Prakash Doraiswamy, PhD, Air Quality Specialist, Quality Assurance Auditor

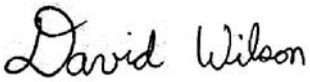

David Wilson, PhD, Statistician, Quality Assurance Auditor

June 07, 2022

MATERIALS AVAILABLE ON THE HEI WEBSITE

Appendices A through C and Additional Materials A and B contain supplemental material not included in the main report. They are available on the HEI website at *www.healtheffects.org/publications.*

Appendix A. Tables

Appendix B. Tables with Hazard Ratios Rescaled by IQR

Appendix C. Figures

Additional Materials A. Collection of Measurements at MAPLE/SPARTAN Sites

Additional Materials B. Sensitivity of Estimates of Excess Deaths Attributable to $PM_{2.5}$ Exposure in Canada Due to Form of Relative Risk Model and Characterization of Low Concentration Uncertainty

ABOUT THE AUTHORS

Michael Brauer is a professor at The University of British Columbia School of Population and Public Health — Occupational and Environmental Health Division and an affiliate professor and principal research scientist at the Institute for Health Metrics and Evaluation at the University of Washington. He also holds associate appointments in the Division of Respiratory Medicine and the Institute for Resources, Environment and Sustainability at The University of British Columbia. He has an ScD from Harvard University. His research focuses on linkages between the built environment and human health, with specific interest in transportation-related and biomass air pollution, the global health effects of air pollution, and relationships among multiple exposures mediated by urban form and population health. He has conducted monitoring and epidemiological studies throughout the world and served on numerous advisory committees (e.g., World Health Organization, Climate and Clean Air Coalition, the U.S. National Academies, Royal Society of Canada).

Jeffrey R. Brook is an assistant professor at the University of Toronto Dalla Lana School of Public Health and Scientific Director of the Canadian Urban Environmental Health Research Consortium. He has a PhD from the University of Michigan and 25 years of experience as an Environment Canada scientist working at the science–policy interface. He is one of Canada's leading experts in air quality for his substantial contributions in air pollution health research. Dr. Brook has led scientific assessments to inform policy nationally and internationally and advised multiple stakeholder groups on shaping policy. He has led a variety of multidisciplinary research teams in government, government–academic partnerships, and academia.

Tanya Christidis is a research analyst at Statistics Canada. She has a BSc and MSc in health studies and gerontology and a PhD in urban planning from the University of Waterloo.

Yen Chu is a research coordinator at The University of British Columbia School of Population and Public Health — Occupational and Environmental Health Division. Dr. Chu has a PhD from the University of Minnesota.

Dan L. Crouse is a research associate at the University of New Brunswick, Department of Sociology and the New Brunswick Institute for Research, Data, and Training. He has a PhD from McGill University. His research bridges knowledge on the environmental and social determinants of health. Dr. Crouse has been involved in a number of studies investigating the effect of ambient air pollution exposure on adverse health outcomes, including the risk of mortality, adverse birth outcomes, and incidence of cancer.

Anders Erickson is an epidemiologist with the Office of the Provincial Health Officer at the Ministry of Health in British Columbia. He has a PhD from the University of Victoria. He was previously a postdoctoral fellow at The University of British Columbia School of Population and Public Health — Occupational and Environmental Health Division. His work focuses on environmental risk factors including the social determinants of disease.

Perry Hystad is an associate professor at the Oregon State University School of Biological and Population Health Sciences. He has a PhD from The University of British Columbia. He is the program coordinator for the environmental health program and principal investigator of the Spatial Health Lab. Dr. Hystad's research uses spatial exposure-assessment methods to determine the chronic health effects associated with exposure to air pollution. He is developing new methods to assess environmental exposures for large population-based studies using new technologies and big-data approaches.

Chi Li is a postdoctoral fellow at University of California, Berkeley, and was previously a graduate student at the Dalhousie University Atmospheric Composition Analysis Group. He has a PhD from Dalhousie University.

Randall V. Martin is a professor at Washington University in St. Louis, Department of Energy, Environmental & Chemical Engineering, and was previously a professor at the Dalhousie University Department of Physics and Atmospheric Science. He is also a research associate at the Harvard-Smithsonian Center for Astrophysics. He has a PhD from Harvard University. His research focuses on characterizing atmospheric composition to inform effective policies surrounding major environmental and public health challenges ranging from air quality to climate change. He leads a research group at the interface of satellite remote sensing and global modeling, with applications that include population exposure for health studies, top-down constraints on emissions, and analysis of processes that affect atmospheric composition.

Jun Meng is a postdoctoral fellow at the University of California, Los Angeles, and was previously a graduate student with the Dalhousie University Atmospheric Composition Analysis Group. He has a PhD from Dalhousie University. His work focuses on the use of GEOS-Chem to study the sectoral contribution of anthropogenic emissions to regional and global $PM_{2.5}$ and its health effects.

Amanda J. Pappin is a scientific evaluator at Health Canada. She previously held postdoctoral fellowships at Statistics Canada and Health Canada. Dr. Pappin holds a BEng and PhD in Environmental Engineering from Carleton University.

Lauren Pinault is a senior research analyst in the Health Analysis Division at Statistics Canada, in Ottawa. Her research focuses on health effects from environmental benefits and hazards using large, national cohorts from census and survey data, as well as on questions of environmental justice. She has a BSc in Biology (Ecology) from the University of Ottawa, an MSc in Forest Ecology and Management from the University of New Brunswick, and a PhD in Biological Sciences (Global Health) from Brock University.

Michael Tjepkema is a principal researcher in the Health Analysis Division at Statistics Canada. He has been the lead investigator of the Canadian Census Health and Environment Cohorts (CanCHEC) since 2007. He has a MPH from the University of Toronto. His research focuses on health equity, record linkage, and geographic concepts.

Aaron van Donkelaar is a research associate with the Dalhousie University Atmospheric Composition Analysis Group. He is also a visiting research associate at Washington University in St. Louis. He has a PhD from Dalhousie University. His research combines satellite retrievals, chemical transport model simulations, and ground-based observations to estimate fine aerosol concentrations around the world. Dr. van Donkelaar's work continues to provide valuable insight into exposure-related health effects in regions both with and without ground-based monitoring capabilities.

Crystal Weagle was a postdoctoral fellow in the Dalhousie University Atmospheric Composition Analysis Group with a leading role in SPARTAN. She has a PhD from Dalhousie University.

Scott Weichenthal is an assistant professor at the McGill University Department of Epidemiology, Biostatistics, and Occupational Health. He has a PhD from McGill University. His research is focused on understanding the effect of the built environment on air pollution exposures in urban areas as well as the short- and long-term health effects of air pollution exposures.

Richard T. Burnett is a private consultant specializing in mathematically characterizing the magnitude and shape of the association between adverse health outcomes and exposure to outdoor air pollution. He has a PhD from Queens University. Dr. Burnett previously was a senior research scientist at Health Canada.

OTHER PUBLICATIONS RESULTING FROM THIS RESEARCH

Christidis T, Erickson AC, Pappin AJ, Crouse DL, Pinault LL, Weichenthal SA, et al. 2019. Low concentrations of fine particle air pollution and mortality in the Canadian Community Health Survey cohort. Environ Health 18:84; doi:10.1186/s12940-019-0518-y.

Crouse DL, Christidis T, Erickson A, Pinault L, Martin RV, Tjepkema M, et al. 2020. Evaluating the sensitivity of $PM_{2.5}$–mortality associations to the spatial and temporal scale of exposure assessment at low particle mass concentrations. Epidemiology 31:168–176; doi:10.1097/EDE.0000000000001136.

Erickson AC, Brauer M, Christidis T, Pinault L, Crouse DL, van Donkelaar A, et al. 2019. Evaluation of a method to indirectly adjust for unmeasured covariates in the association between fine particulate matter and mortality. Environ Res 175:108–116; doi:10.1016/j.envres.2019.05.010.

Erickson AC, Christidis T, Pappin A, Brook JR, Crouse DL, Hystad P, et al. 2020. Disease assimilation: The mortality impacts of fine particulate matter on immigrants to Canada. Health Reports 3:14–26; doi:10.25318/82-003-x202000300002-eng.

Latimer RNC, Martin RV. 2019. Interpretation of measured aerosol mass scattering efficiency over North America using a chemical transport model. Atmos Chem Phys 19:2635–2653; doi:10.5194/acp-19-2635-2019.

Meng J, Li C, Martin R, van Donkelaar A, Hystad P, Brauer M. 2019. Estimated long-term (1981–2016) concentrations of ambient fine particulate matter across North America from chemical transport modeling, satellite remote sensing and ground-based measurements. Environ Sci Technol 53:5071–5079; doi:10.1021/acs.est.8b06875.

Pappin AJ, Christidis T, Pinault LL, Crouse DL, Tjepkema M, Erickson AC, et al. 2019. Examining the shape of the association between low levels of fine particulate matter and mortality across three cycles of the Canadian Census Health and Environment Cohort. Environ Health Perspect 127:107008; doi:10.1289/EHP5204.

Pinault L, Brauer M, Crouse DL, Weichenthal S, Erickson A, van Donkelaar A, et al. 2018. Diabetes status and susceptibility to the effects of $PM_{2.5}$ exposure on cardiovascular mortality in a national Canadian cohort. Epidemiology 29:784–794; doi:10.1097/EDE.0000000000000908.

Pinault L, Tjepkema M, Crouse DL, Weichenthal S, van Donkelaar A, Martin RV, et al. 2016. Risk estimates of mortality attributed to low concentrations of ambient fine particulate matter in the Canadian Community Health Survey cohort. Environ Health 15:18; doi:10.1186/s12940-016-0111-6.

Pinault L, Weichenthal S, Crouse DL, Brauer M, Erickson A, van Donkelaar A, et al. 2017. Associations between fine particulate matter and mortality in the 2001 Canadian Census Health and Environment Cohort. Environ Res 159:406–415; doi:10.1016/j.envres.2017.08.037.

Research Report 212, *Mortality–Air Pollution Associations in Low Exposure Environments (MAPLE): Phase 2*, M. Brauer et al.

INTRODUCTION

Ambient air pollution is an important contributor to the global burden of disease (GBD 2020; HEI 2020). Although levels of air pollution have declined over the past 50 years in many high-income countries, several studies published in the last decade reported associations between risk of mortality and long-term exposure to particulate matter ≤2.5 µm in aerodynamic diameter ($PM_{2.5}$*) at low concentrations (Beelen et al. 2014; Crouse et al. 2012, 2015; Hales et al. 2012; Pinault et al. 2016). To inform future risk assessment and regulation, it is important to confirm whether associations with adverse health effects continue to be observed as air pollution levels decline further. Determining the shape of the concentration–response curve at low concentrations is also key to identifying levels of exposure with minimal health risks. Thus, HEI initiated a research program on health effects at low concentrations.

In 2016, HEI funded three studies under Request for Applications (RFA) 14-3, *Assessing Health Effects of Long-Term Exposure to Low Levels of Ambient Air Pollution*, to explore the health effects associated with exposures to low concentrations of air pollution using large cohorts and administrative databases (e.g., census, health insurance claims). Dr. Brauer's study, *Mortality–Air Pollution Associations in Low Exposure Environments (MAPLE)*, focused on a nationally representative cohort of approximately nine million people in Canada. Additional information about the RFA and the two other studies that were conducted in the United States and Europe is included in the Preface. It should be noted that all three study teams are conducting additional analyses to harmonize their approaches to the maximum extent possible. Through this collaboration, the teams aim to (1) evaluate concentration–response thresholds, (2) share analytical techniques and identify common statistical methods (e.g., a common set of covariates across the studies), and (3) determine strengths, weaknesses, and common findings of the three studies. That work is expected to be completed in 2022.

The current MAPLE study is the second of two phases. In November 2019, HEI published *Research Report 203: Mortality–Air Pollution Associations in Low Exposure Environments (MAPLE): Phase 1*, along with a Commentary by HEI's Low-Exposure Epidemiology Studies Review Panel (Brauer et al. 2019). That Report and Commentary summarized and discussed analyses and findings produced through the first half of Dr. Brauer's study. The present Commentary focuses on the research and findings produced during the second phase, recognizing that this work builds on the Phase 1 analyses.

This Commentary was prepared by HEI's Low-Exposure Epidemiology Studies Review Panel, which was convened to review these three HEI-funded studies, and by members of HEI's Scientific Staff. The Commentary includes the scientific and regulatory background for the research, a summary of the study's approach and key results, and the Panel's evaluation of the Investigator's Report. This Commentary is intended to aid HEI sponsors and the public by highlighting the strengths and limitations of the study and by placing the Investigators' Report into scientific and regulatory context.

SCIENTIFIC AND REGULATORY BACKGROUND

Setting ambient air quality standards at levels considered adequate to protect public health is central to programs designed under the U.S. Clean Air Act, the European Union Ambient Air Quality Directives, and similar measures around the world. Although the process for setting such standards varies, all contain several common components:

- Identifying, reviewing, and synthesizing the scientific evidence on sources, exposures, and health effects of air pollution
- Conducting risk and policy assessments to estimate public health effects likely to be seen at various levels of the standards

Dr. Michael Brauer's 4-year study, "Identifying the shape of the association between long-term exposure to low levels of ambient air pollution and the risk of mortality: An extension of the Canadian Census Health and Environment Cohort using innovative data linkage and exposure methodology," began in April 2016. Total expenditures were $2,065,564. The draft Phase 2 Investigators' Report from Brauer and colleagues was received for review in December 2020. A second revised report, received in October 2021, was accepted for publication in January 2022. During the review process, HEI's Low-Exposure Epidemiology Studies Review Panel and the investigators had the opportunity to exchange comments and to clarify issues in both the Investigators' Report and the Panel's Commentary.

* A list of abbreviations and other terms appears at the end of this volume.

- Identifying and setting standards based on risk assessments
- Monitoring air quality to identify areas that do not meet the standards
- Implementing air quality interventions to meet the standards by reducing the concentrations to which people are exposed

In September 2021, the World Health Organization (WHO) updated its 2005 Global Air Quality Guidelines after extensive research and deliberation. The new Air Quality Guidelines set ambitious targets for air pollutants of worldwide importance, including $PM_{2.5}$, nitrogen dioxide (NO_2), and ozone (O_3). Although the Air Quality Guidelines are not legally binding, they will influence air quality policy across the globe for years to come. The recommended limits for long-term exposure are as follows (WHO 2021):

- $PM_{2.5}$: annual mean of 5 μg/m^3
- NO_2: annual mean of 10 μg/m^3
- O_3: peak season 8-hour mean of 60 μg/m^3

SETTING AIR QUALITY STANDARDS IN THE UNITED STATES

The U.S. Clean Air Act requires that in setting the National Ambient Air Quality Standards (NAAQS), the U.S. Environmental Protection Agency (U.S. EPA) Administrator reviews all available science and sets the NAAQS for all major (criteria) pollutants (e.g., particulate matter, NO_2, and O_3) at a level "requisite to protect the public health with an adequate margin of safety." In practice, that review has had two principal steps:

1. Synthesis and evaluation of all available science in what is now called an Integrated Science Assessment. This document reviews the widest range of exposure, dosimetry, toxicological, mechanistic, clinical, and epidemiological evidence. It then—using a predetermined set of criteria (U.S. EPA 2015)—draws on all lines of evidence to determine whether the exposure is causal, likely to be causal, or suggestive of being causal for a series of health outcomes.
2. Assessment of the risks based on that science is then conducted in a Risk and Policy Assessment. This additional analysis draws on the Integrated Science Assessment to identify the strongest evidence—most often from human clinical and epidemiological studies—of the lowest concentrations at which health effects are observed, the likely implications of such concentrations for adverse health outcomes across the population, and the degree to which the newest evidence suggests that there are health effects observed below the then current NAAQS for a particular pollutant.

The Risk and Policy Assessment also examines the uncertainties around estimates of health effects and the shape of the concentration–response curve, especially at concentrations near and below the then current NAAQS. Although a range of possible shapes for the curve is considered, including whether there is a threshold at a concentration below which effects are not likely, the U.S. EPA's conclusions in these reviews thus far have not found evidence of such thresholds (although studies to date have not always had the statistical power to detect one) (U.S. EPA 2004, 2013). Also, although the standard is set under the Clean Air Act at "a level requisite to protect public health with an adequate margin of safety," it has been understood that there are likely additional, albeit more uncertain, health effects of exposure to air pollution concentrations below the NAAQS.

Both documents are subjected to extensive public comments and review by the Clean Air Scientific Advisory Committee, which was established under the U.S. Clean Air Act. The Committee is charged with peer reviewing the documents, which includes advising the Administrator on the strength and uncertainties in the science and making the decision whether to retain or change the NAAQS. The current NAAQS for long-term exposure to $PM_{2.5}$, NO_2, and O_3 are as follows (*https://www.epa.gov/criteria-air-pollutants/naaqs-table*):

- $PM_{2.5}$: annual mean averaged over 3 years of 12 μg/m^3
- NO_2: annual mean of 53 ppb (approximately 100 μg/m^3)
- O_3: 3–year average peak season 8-hour mean of 70 ppb (approximately 140 μg/m^3)

SETTING AIR QUALITY STANDARDS IN CANADA

Air quality policy in Canada is broadly directed by the Canadian Environmental Protection Act of 1999, a federal regulation that aims to prevent pollution and protect the environment and human health. However, multiple levels of government collectively share responsibility in developing specific policies and managing air pollution. They are led by the Canadian Council of Ministers of the Environment (CCME), an intergovernmental organization of Ministers from federal, provincial, and territorial governments (Health Canada 2016).

In 2012, the CCME collaborated with industry, nongovernmental, and Indigenous organizations to develop and implement an Air Quality Management System. As part of this system, new Canadian Ambient Air Quality Standards (CAAQS) replaced the older Canada Wide Standards for several ambient air pollutants. The CAAQS were adopted across Canada, except for Quebec, with decreasing target concentrations set for 2015, 2020, and 2025. Risk of adverse health effects is the primary consideration in setting CAAQS, but technology, economics, and societal concerns are also considered (Health Canada 2016). The current 2020 CAAQS for long-term exposure to $PM_{2.5}$, NO_2, and O_3 are as follows (CCME 2021):

- $PM_{2.5}$: annual mean averaged over 3 years of 8.8 μg/m^3
- NO_2: annual mean of 17 ppb (approximately 33 μg/m^3)

- O_3: 3–year average peak season 8-hour mean of 62 ppb (approximately 124 μg/m^3)

Although CAAQS are nonlegally binding goals, air quality is actively managed. Local governments within individual *air zones* and regional *airsheds* monitor air quality with four management levels—green, yellow, orange, and red. Each level corresponds to increasing pollutant concentration targets up to the CAAQS at the red level. The four levels also have increasingly strict mitigation strategies, ranging from industrial and mobile emissions controls to individual consumer incentives, with the goal of discouraging emissions so ambient concentrations remain below the CAAQS (CCME 2021).

EVALUATING ASSOCIATIONS BELOW CURRENT AIR QUALITY STANDARDS AND GUIDELINES

As the quality and availability of data on air pollution concentrations improved over the first decade of this century, emerging research from Canada and New Zealand suggested that associations between PM and mortality could be observed down to concentrations well below the NAAQS of 12 μg/m^3 (Crouse et al. 2012; Hales et al. 2012). Using standard statistical methods, these studies found robust associations, with some evidence of larger effects at the lowest concentrations of $PM_{2.5}$. However, neither study examined associations with NO_2 or O_3 exposure, and some potential individual-level confounding variables were unavailable. If replicated in other populations and by other investigators, such findings could change the basis for future determinations of the levels to set the NAAQS and other air quality standards.

At the same time, the findings of these previous studies from Canada and New Zealand suggested several questions:

- Would the results be robust to the application of more sophisticated statistical methods, including nonlinear and causal inference models?
- Could other important determinants of population health not accounted for in prior studies—including lifestyle factors such as smoking, health status, access to medical care, and differences in air pollution sources and time–activity patterns—modify or confound the associations?
- What might be the effects of co-occurring pollutants on health effect associations at low ambient concentrations?

As described in the Preface, these important questions were the basis for RFA 14–3. After a rigorous selection process, the Research Committee recommended the study by Brauer and colleagues for funding because it used a large representative sample of the Canadian population, aimed to develop new methods for concentration–response modeling in health assessments, and built on prior work by an experienced research team.

SUMMARY OF APPROACH AND METHODS

The overall objective of the MAPLE study was to characterize the relationship between long-term exposure to low ambient concentrations of $PM_{2.5}$ and nonaccidental mortality in a representative sample of the adult Canadian population. The investigators developed fine-scale satellite-based $PM_{2.5}$ exposure estimates for North America from 1981 to 2016. They then applied epidemiological analyses to estimate the shape of the concentration–response relationship and the lowest $PM_{2.5}$ concentration of detectable health effects. Here we describe the overall approach and methods of the MAPLE study.

STUDY OBJECTIVES

To estimate ambient $PM_{2.5}$ concentrations, the investigators proposed to

1. Develop and apply annual average satellite-derived $PM_{2.5}$ estimates for North America at 1 km × 1 km spatial resolution for years 2000–2016
2. Evaluate $PM_{2.5}$ estimates using insight gained from comparisons of colocated measurements of $PM_{2.5}$ and aerosol optical depth (AOD) with chemical transport model (GEOS–Chem) simulations of that relationship
3. Use a combination of geophysical and statistical methods, together with land use information, to further refine the above $PM_{2.5}$ estimates
4. Use available $PM_{2.5}$, PM_{10}, and total suspended PM monitoring data in Canada from 1981–1999, to scale the 1 km × 1 km exposure estimates back in time annually from 1981–1999 and produce high-resolution exposure estimates over the entire 1981–2016 study period
5. Make the above refined $PM_{2.5}$ estimates available to other studies that cover Canada and the United States for incorporation into their analyses

To examine the concentration–response relationship between $PM_{2.5}$ exposure and risk of nonaccidental mortality, investigators proposed to:

1. Use five cohorts linked to mortality, vital statistics, and tax records through December 31, 2016
    a. Three Canadian Census Health and Environment Cohort (CanCHEC) cycles (1991, 1996, and 2001)
    b. A CanCHEC cohort combining all three cycles
    c. A pooled Canadian Community Health Survey (CCHS) cohort that contained detailed information on health behaviors
2. Examine the shape of the association between long-term exposure to ambient concentrations of $PM_{2.5}$ and mortality in all five cohorts by using
    a. Restricted cubic splines (RCS)
    b. A standard threshold approach

c. An extended version of the Shape Constrained Health Impact Functions (SCHIF) to identify the lowest concentration for which there is evidence of a positive association with mortality

The study was completed in two phases, with the Phase 1 Report (Brauer et al. 2019) providing interim results to inform ongoing review of the NAAQS for $PM_{2.5}$. In Phase 2, the investigators refined some of their methods, tackled additional aspects of the analysis, and omitted methods shown to be insufficiently robust during Phase 1 (Commentary Table).

METHODS AND STUDY DESIGN

Study Population

The investigators used a nationally representative sample of the adult Canadian population, ages 25–89 years, and followed them for up to 25 years. They created four census-based cohorts and one survey-based cohort, including approximately 7.6 million people, and recorded nearly 1.4 million deaths (Commentary Figure 1). Three CanCHEC cohorts comprised randomly selected participants who completed the mandatory long-form census. This census contains detailed individual-level sociodemographic information, such as education, income, and ethnicity. A Stacked CanCHEC cohort merged all CanCHEC cycles into a single cohort with duplicate respondents removed. The survey-based CCHS cohort comprised randomly selected participants to complete one of the CCHS health surveys between 2001 and 2012. In addition to the sociodemographic information in CanCHEC, the CCHS includes information on health status and behaviors such as smoking.

Survey data were linked to Statistics Canada's Social Data Linkage Environment from survey date through December 31, 2016, which provided residential histories via annual tax records and dates and causes of death. Participants were

Commentary Table. Analytic Approaches in the MAPLE Study

	Phase 1	Phase 2
Use of CanCHEC Cohorts for Overall Analysis	Cohort-specific analyses and meta-analyses	Cohort-specific and pooled cohort analyses with duplicates removed (see Commentary Figure 1)
Linking CanCHEC and CCHS Participants to Death Records	Probabilistic and deterministic linkage	Deterministic only linkage
$PM_{2.5}$ Exposure Modeling	Developed a high-resolution exposure model using single daily satellite observations	Improved the model with multiple daily satellite observations and colocated ground measurements
$PM_{2.5}$ Exposure Windows and Lag Time	1-, 3-, and 8-year moving average with a 1-year lag	10-year moving average with a 1-year lag based on analysis showing larger effect estimates for longer moving averages
$PM_{2.5}$ Exposure Assignment for Person–Years with Missing Postal Codes	Imputed as the national population-weighted average exposure	Imputed based on the population-weighted average exposure from nearby postal codes
Covariate Adjustment	Directed Acyclic Graph informed (group-level covariates only), fully adjusted (included group- and individual-level covariates), and indirectly adjusted for health behaviors	Fully adjusted only
Evaluation of the Concentration–Response Shape	RCS, SCHIF	RCS, extended SCHIF, and threshold
Copollutant Analysis	Linear HR models adjusted for NO_2, O_3, and O_x	Linear HR models adjusted for O_3 and O_x, stratified by O_3 and O_x tertiles and nonlinear model adjustment for linear O_3 and O_x
Additional Sensitivity Analyses	With and without immigrants included	Exclusion of person-years with $PM_{2.5}$ exposure >U.S. and Canadian air quality standards, and mortality risk by regional airshed

O_x = gaseous pollutant oxidant capacity.

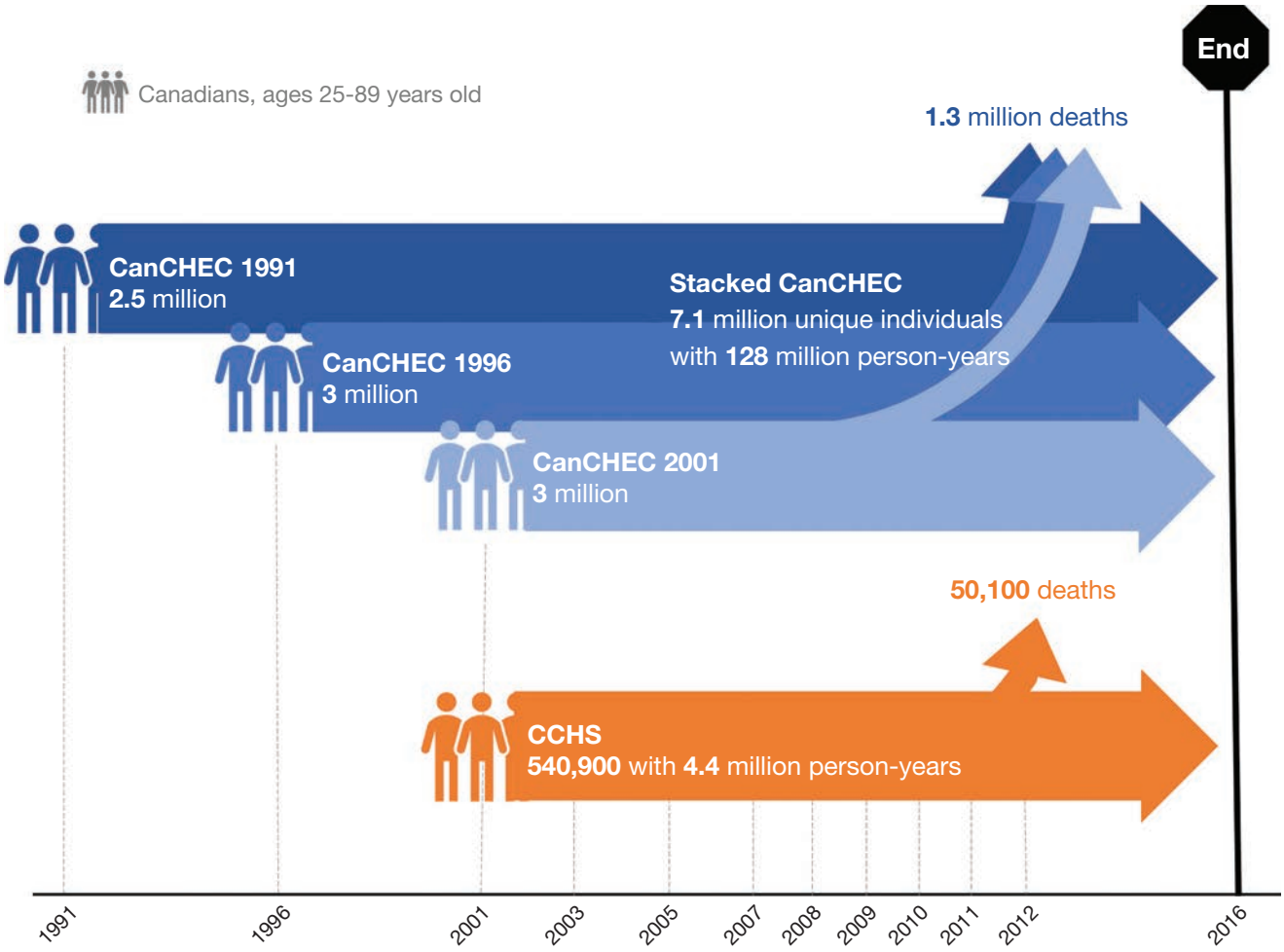

Commentary Figure 1. MAPLE study cohorts. The five cohorts included CanCHEC 1991, CanCHEC 1996, CanCHEC 2001, Stacked CanCHEC, and CCHS. The Stacked CanCHEC and CCHS cohorts included groups of respondents that entered the study in different census or survey years (dashed lines). Participants were followed until death or the end of the study.

excluded if they had immigrated less than 10 years prior, turned 90 years old during follow-up, or had no recorded postal code with which to assign exposure. Due to these exclusions and the noninstitutionalized representation of CanCHEC, the study sample was slightly healthier than Canada's general population as evidenced by lower mortality rates, particularly for older individuals (Tjepkema et al. 2019). All data linkages and analyses were conducted at Statistics Canada's secure Research Data Centers by approved researchers with government security clearance.

Exposure Assessment

$PM_{2.5}$ Model Brauer and colleagues developed high resolution (1 km^2) annual average ambient $PM_{2.5}$ concentration estimates for North America for 1981 to 2016. The method combined remote sensing of AOD with the GEOS-Chem chemical transport model, land use information, and ground-monitoring data. First, multiple daily satellite measurements of AOD from the moderate resolution imaging spectroradiometer (MODIS) were inversely weighted by error, then converted to geophysical $PM_{2.5}$ concentrations using GEOS-Chem model simulations (van Donkelaar et al. 2019). To evaluate the conversion in regions of low $PM_{2.5}$ concentrations, the investigators collected colocated ground measurements of $PM_{2.5}$, aerosol scatter, and AOD at five sites (in five different airsheds) with low concentrations of air pollution across Canada. Sites included Halifax, Nova Scotia; Sherbrooke, Quebec; Downsview, Ontario; Lethbridge, Alberta; and Kelowna, British Columbia, and were added to the Surface Particulate Matter Network (SPARTAN).

Next, they used geographically weighted regression to merge the satellite-derived geophysical estimates with average monthly ground monitoring measurements (Canadian

National Air Pollution Surveillance and U.S. EPA Air Quality System Data Mart) to produce hybrid $PM_{2.5}$ estimates for the years 2000 through 2016. Because few AOD data exist before 2000, the investigators used historic ground measurements of $PM_{2.5}$, PM_{10}, and total suspended PM to *backcast*, or simulate, satellite-based estimates from 1981 through 1999 (Meng et al. 2019).

Copollutant Models To estimate the effect of $PM_{2.5}$ on mortality in the presence of important copollutants, the investigators estimated ambient NO_2, O_3, and gaseous pollutant oxidant capacity (O_x) concentrations. One hundred m^2-resolution NO_2 concentrations for 2006 were previously derived via land use regression modeling that incorporated ground monitoring, satellite (10 km^2), and land use data (Hystad et al. 2011). Warm season (May–September) 8-hour daily maximum O_3 concentrations were estimated using chemical transport modeling of monitoring data at spatial resolutions of 21 km^2 (2002–2009) and 10 km^2 (2010–2015) (Pappin et al. 2019; Robichaud and Ménard 2014; Robichaud et al. 2016). NO_2 and O_3 concentrations were backcasted to all study years using time-series analysis of ground monitoring measurements obtained in 24 large cities (Weichenthal et al. 2017). O_x was calculated as a weighted average of O_3 and NO_2 following a formula used by Weichenthal and colleagues (2017).

Exposure Assignment For each study year (1981–2016), individual residential, geocoded postal codes were assigned to the nearest 1 km^2 grid of estimated ambient concentration of $PM_{2.5}$. NO_2 and O_3 exposure was assigned to postal codes based on the geographically nearest time-series data point. Brauer and colleagues accounted for changes in postal codes over time and for residential mobility. Exposure assignment to urban postal codes provided locational accuracy within about 150 meters, whereas greater uncertainty existed when assigning exposure to rural postal codes, which are accurate within a 1–5 kilometer range (Khan et al. 2018). Missing postal codes were imputed for 2.1% of the person-years, with exposure assigned based on the population-weighted average of postal codes that had at least two characters in common with the postal codes of adjacent nonmissing person-years. To assess long-term exposure, the investigators used a 10-year moving average with a 1-year lag. The lag ensured that exposure temporally preceded recorded deaths.

Health Assessment

Associations with Mortality To assess $PM_{2.5}$ exposure with the rate of nonaccidental total- and cause-specific mortality, the investigators conducted Cox proportional hazards regression on all five cohorts. This linear modeling method calculates a hazard ratio (HR), which describes the risk of mortality associated with $PM_{2.5}$ exposure, compared with the baseline risk in the study population, while controlling for potential individual- and area-level confounding characteristics. In this Commentary, HRs were reported per interquartile range (IQR), or 75th versus 25th percentile, increase in $PM_{2.5}$ exposure with 95% confidence intervals (CI). Person-years before the census and after year of death were excluded from the analysis.

Cause-specific outcomes were selected partly based on similar studies (e.g., Global Burden of Disease project) to facilitate comparison and determined using International Classification of Disease, 10th edition (ICD–10) codes. Selected outcomes were cardiovascular mortality, cerebrovascular mortality, heart failure, ischemic heart disease, diabetes (types 1 and 2), nonmalignant respiratory disease, chronic obstructive pulmonary disease (COPD), pneumonia, lung cancer, and kidney failure. Models were adjusted for numerous individual-level variables (e.g., income, minority [not white], Indigenous identity, education, marital status, employment, and occupation) and community-level variables (community size, airshed, urban form, and four Canadian Marginalization Index dimensions). Models were stratified by 5-year age groups, sex, and immigrant status. Analyses of the CCHS cohort were further adjusted for individual-level health behavior variables (smoking, alcohol consumption, fruit and vegetable consumption, body mass index, and exercise behavior). Given the multiple years that participants could enter the Stacked CanCHEC and CCHS cohorts, analyses of these were also stratified by census or survey year.

Concentration–Response Function To examine the shape of the association, and to identify the lowest $PM_{2.5}$ concentration at which a positive association with mortality was observed, Brauer and colleagues applied three nonlinear modeling approaches—RCS, extended SCHIF, and standard threshold (see Sidebar). In RCS modeling (Harrell 2015), the investigators tested 3 to 18 knots (i.e., 16 models) and selected the model with the lowest Bayesian Information Criterion, a measure of fit. Next, the investigators applied a novel extension of the SCHIF model (Burnett et al. 2018; Nasari et al. 2016), which they deemed more suitable for health impact assessments. For the RCS and extended SCHIF, the HR was fixed to one (e.g., no association) at the minimum $PM_{2.5}$ concentration of 2.5 $\mu g/m^3$, meaning that the risk of mortality associated with all higher concentrations was compared with the risk at the minimum concentration. The 95% CIs for RCS and extended SCHIF were computed to reflect the uncertainty in high- and low-level exposure estimates relative to the mean $PM_{2.5}$ concentration, becoming wider as $PM_{2.5}$ concentrations deviated from the mean. Finally, the standard threshold model was applied to identify levels of exposure with no detectible health effects. They evaluated threshold values ranging from 2.5 to 10 $\mu g/m^3$ and identified the most probable thresholds using a weighted

Modeling the Shape of the Concentration–Response Function

Brauer and colleagues used three nonlinear modeling approaches to evaluate the shape of the association between ambient $PM_{2.5}$ exposure and nonaccidental mortality. Unlike a *linear* model where the change in risk of mortality for a unit increase in $PM_{2.5}$ is constant across all exposure concentrations, nonlinear models allow the association to fluctuate. Allowing fluctuation is important because many biological responses to toxicants do not follow a linear relationship outside of narrow concentration ranges (Klassen 2019). The Sidebar Figure shows hypothetical example curves derived from the models described here.

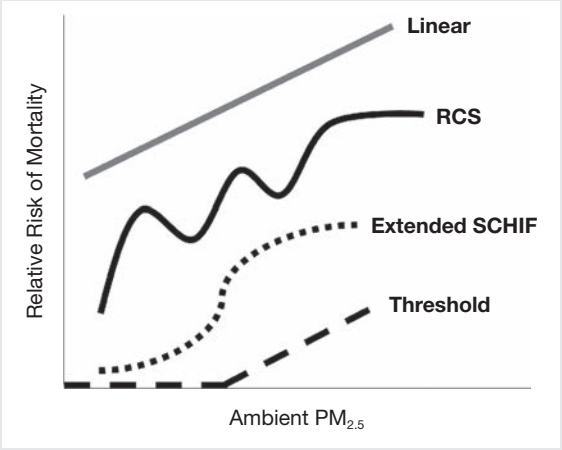

- **RCS** allows for highly complex curves. Splines represent smoothly connected piecewise polynomials and take on different shapes over different intervals of $PM_{2.5}$ exposure; they are connected by knots, or points where the curve changes shape. A disadvantage of RCS is that the curve can become so complex that it is biologically implausible or exceedingly difficult to interpret.
- The **extended SCHIF** incorporates RCS predictions, but places constraints on the shape so that it is consistent with known biological concentration–response curves. Therefore, error-prone data that produce highly complex, or wiggly, RCS curves would be smoothed into a near-linear, sublinear (e.g., U-shaped), supralinear (e.g., inverted U-shaped), sigmoidal (e.g., S-shaped), or simpler non-monotonic (e.g., areas of decreasing response) curve. This approach ensures that public health risks can be interpreted and communicated.
- **Threshold** models assume that there is a level of $PM_{2.5}$ exposure between 0 and the threshold value where mortality is not affected. Above the threshold value, $PM_{2.5}$ is associated with mortality and the concentration–response curve can take on a variety of shapes. The MAPLE study applied a linear model beyond the threshold. These models are commonly used in toxicology (and pharmacology) where a specific concentration of toxicant (or drug) is required to elicit a target effect.

ensemble method. Under all three modeling scenarios, they reported the lowest $PM_{2.5}$ concentration for which the HR 95% CI lower limit was greater than or equal to one; this concentration was defined as the lowest concentration with observed adverse health effects.

Sensitivity Analyses The investigators assessed the association between $PM_{2.5}$ and mortality and restricted the analysis to person-years with <10 and <12 μg/m³ of exposure to evaluate whether the association persisted below these concentrations. The cutoff value of 10 μg/m³ corresponded to the CAAQS and WHO Air Quality Guidelines prior to 2020 and 2021, respectively. The cutoff value of 12 μg/m³ corresponded to the current U.S. NAAQS. They also examined associations controlling for, and stratified by tertiles of, copollutants O_3 and O_x. Finally, they examined the association and shape of the concentration–response function across six geographic regions with distinct atmospheric conditions known as airsheds: Northern, Western, Prairie, West Central, East Central, and Southern Atlantic (Commentary Figure 2). Population density is highest in the East Central, and lowest in the West Central and Northern airsheds.

Commentary Figure 2. Airsheds of Canada. The associations between $PM_{2.5}$ and mortality were also examined by airshed because regional geographical features and weather conditions influence ambient air quality.

SUMMARY OF FINDINGS

EXPOSURE ESTIMATION RESULTS

Between 1981 and 2015, average annual $PM_{2.5}$ concentrations ranged from 8 to 16 μg/m³ in Canada's largest cities, but only from 2 to 6 μg/m³ in rural areas. The highest annual $PM_{2.5}$ concentration, 18 μg/m³, was observed in the cities of Toronto, Hamilton, Quebec, and Vancouver between 1981 and 1990. Over the next 25 years, $PM_{2.5}$ concentrations declined. For example, in the Stacked CanCHEC cohort, the 10-year average assigned exposure was 12.2 μg/m³ in 1991, but just 6.8 μg/m³ in 2016. Similarly, the average assigned exposure for CanCHEC 1991, 1996, and 2001, and CCHS were 9.0, 8.3, 7.7, and 6.8 μg/m³, respectively. The highest and lowest assigned exposure concentrations for the Stacked CanCHEC overall were 17.7 and 2.5 μg/m³, respectively, with similar high and low concentrations among all individual cohorts (see Investigators' Report Table 4 for complete descriptive statistics).

The chemical composition of $PM_{2.5}$ varied widely across the colocated sampling sites in the five different regional airsheds. The $PM_{2.5}$ composition variability reflected differences in natural and anthropogenic sources of PM. O_3 and O_x concentrations also varied by regional airshed and were highest in southern areas. Compared with Phase 1, Brauer and colleagues noted improved performance using the refined Phase 2 exposure models. For example, when comparing $PM_{2.5}$ concentrations estimated from the model with those measured at ground monitors across the North America, a higher R^2 (0.81 vs. 0.71) and lower root mean square deviation (1.5 vs. 1.9 μg/m³) were achieved in Phase 2.

HEALTH ASSESSMENT RESULTS

$PM_{2.5}$ was Associated with Increased Mortality in Linear Models Ambient long-term $PM_{2.5}$ exposure was associated with increased nonaccidental mortality. The investigators observed similar results across all five cohorts. In the CCHS cohort, adjustment for individual-level health behaviors elicited similar, but attenuated associations. The investigators theorized that after adjusting for the numerous individual- and community-level variables, health behaviors might not be important confounders at the low $PM_{2.5}$ exposure concentrations observed in this study population. Therefore, health assessment results presented here will focus primarily on the Stacked CanCHEC cohort given that it had the largest sample size and longest follow-up.

In the Stacked CanCHEC cohort an IQR increase (4.16 μg/m³) in $PM_{2.5}$ exposure was associated with a 3% rise in the total nonaccidental mortality rate (HR per IQR: 1.034; 95% CI: 1.030–1.039) (Commentary Figure 3). When scaled to the average annual total nonaccidental mortality rate over the entire 25-year study period (1991–2016), this HR corresponded to about 32 additional deaths for every 100,000 people each year with a 4.16-μg/m³ increase in $PM_{2.5}$ exposure. In reference to the 2016 Canadian population, this was equivalent to 7,848 additional deaths annually. In cause-specific analyses, ambient long-term $PM_{2.5}$ exposure was associated with increased mortality due to cardiovascular, ischemic heart, and cerebrovascular diseases, diabetes, pneumonia, respiratory disease, and COPD (Commentary Figure 3), with the largest association for diabetes. The associations with kidney failure and lung cancer were consistent with the null; these two causes of death were less common in the population. The association with heart failure was also consistent with the null given the confidence interval.

Nonlinear Concentration–Response Function The RCS models suggested that the shape of the association between $PM_{2.5}$ and total nonaccidental mortality was nonlinear, with a statistically significantly better fit than the linear model. In the Stacked CanCHEC cohort the RCS with 9 knots was selected and showed that the relative risk of mortality increased rapidly with increasing $PM_{2.5}$ concentration from the minimum observed concentration of 2.5 until about 5 μg/m³, plateaued with undulations to about 8 μg/m³, and increased again at higher concentrations (Commentary Figure 4). In other words, although the HR (e.g., a single point on the curve) is generally higher for any given higher concentration of $PM_{2.5}$ when compared with the minimum exposure, the largest increases in the HR (e.g., change in the curve) occurs at lower concentration ranges. In the RCS curve, the lowest $PM_{2.5}$ concentration for which the 95% CI lower limit of the HR was ≥1 was 2.8 μg/m³.

The extended SCHIF model showed a similar but smoothed concentration–response curve compared with the RCS in the Stacked CanCHEC cohort, demonstrating a rapid increase from $PM_{2.5}$ of 2.5 to 5 μg/m³, and then increasing approximately linearly at an intermediate rate thereafter (Commentary Figure 4). Results for the threshold analysis in the Stacked CanCHEC were not conclusive. Specifically, the HR was greater than one even at the lowest level exposure of 2.5 μg/m³, but the 95% CI lower limit did not exceed one until a threshold of 8 μg/m³ was reached. Above 8 μg/m³, the slope was steeper for the threshold model compared with the RCS and extended SCHIF. Model fit (using the likelihood statistic) was equal for models with thresholds of 2.5 and 8 μg/m³, and all threshold models demonstrated inferior fit compared with the RCS model. Overall, the three nonlinear modeling approaches all suggested that there may be no safe level of $PM_{2.5}$ exposure given the minimum observed exposure concentration in this study of 2.5 μg/m³.

Cause-specific analyses of the concentration–response curve in the Stacked CanCHEC cohort using RCS generally showed increased risk of mortality across the observed $PM_{2.5}$ concentration ranges (see Investigators' Report Figure 16). However, this was not the case for heart failure, lung cancer, or diabetes. The concentration–response curve for heart

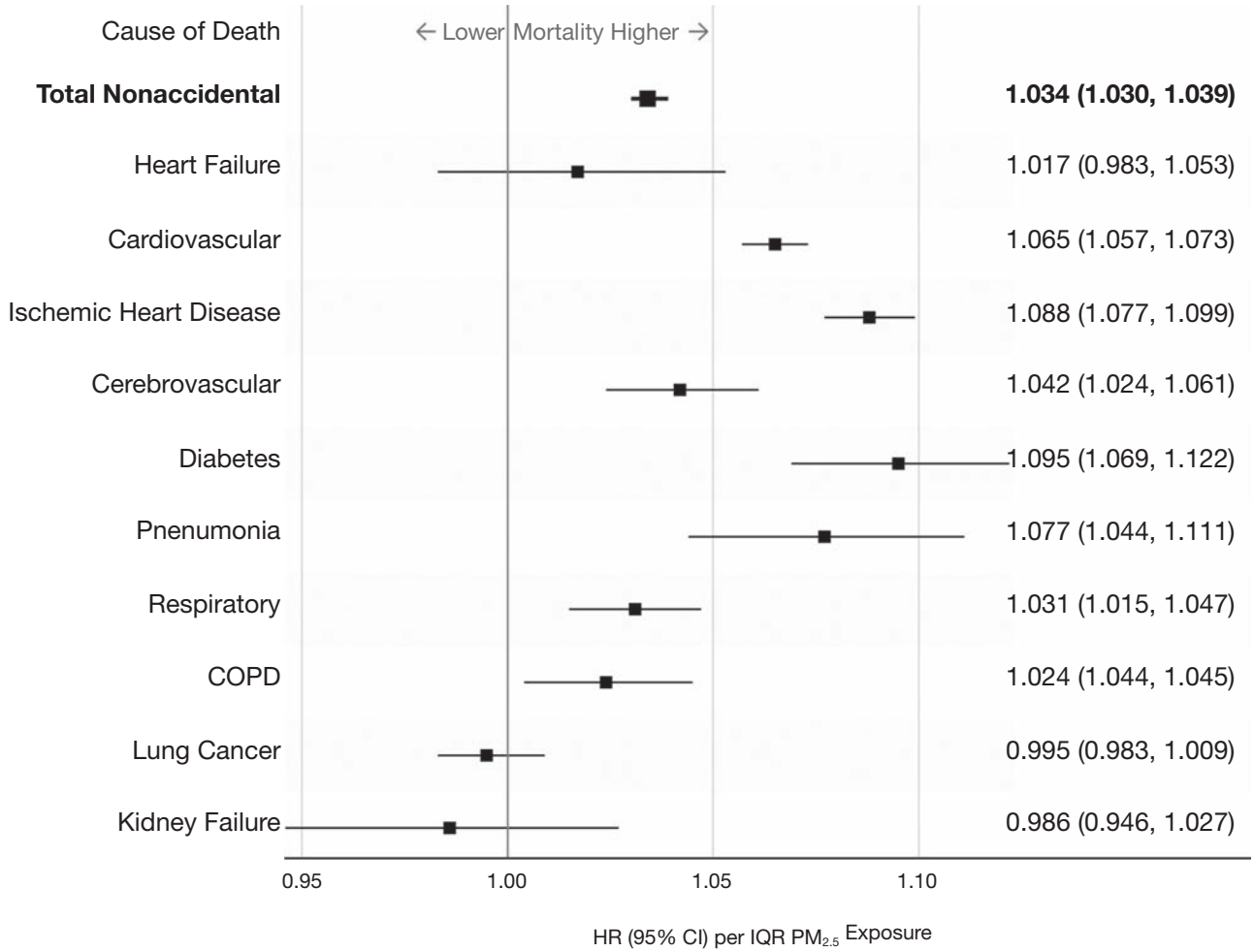

Commentary Figure 3. Ambient $PM_{2.5}$ exposure and nonaccidental mortality in the Stacked CanCHEC cohort. Ambient $PM_{2.5}$ exposure with a 10-year moving average and 1-year lag was associated with higher total nonaccidental and select cause-specific mortality rates using a linear model and controlling for individual- and community-level sociodemographic variables.

failure hovered near the null, and for lung cancer showed an increased risk until a peak at 8 µg/m³, and then decreased. The concentration–response curve for diabetes demonstrated a decreased risk until 8 µg/m³, and then increased.

Associations Below U.S. NAAQS When restricting the analyses of the Stacked CanCHEC to person-years with exposure below the U.S. NAAQS for annual average $PM_{2.5}$ exposure of 12 µg/m³, similar results were observed when compared with the full cohort. Specifically, the linear model showed that $PM_{2.5}$ exposure was associated with total nonaccidental mortality, although the HR was slightly smaller compared with the full cohort. The concentration–response curve using RCS showed a nearly identical relative risk of mortality with the full cohort for $PM_{2.5}$ concentrations from 2.5 to 8 µg/m³, and a slightly lower relative risk through <12 µg/m³ (see Investigators' Report Table 19 and Figure 25). However, when restricting the analyses of the Stacked CanCHEC to person-years with exposure below the previous CAAQS of 10 µg/m³, $PM_{2.5}$ was not significantly associated with total nonaccidental mortality. The concentration–response curve using RCS showed a similar rapid increase in the relative risk of mortality for $PM_{2.5}$ concentrations from 2.5 to 4 µg/m³, but no further increased relative risk from 4 to <10 µg/m³. The investigators suggested that higher $PM_{2.5}$ concentrations contributed to the observed positive associations with mortality. They also noted that the interpretation of these results was challenging because the restrictions compromised the representativeness of the cohorts. Specifically, the <12 and <10 cutoffs excluded 13% and 30% of person-years and 10% and 28% of deaths, respectively. Therefore, these restricted cohorts were not representative of the original Stacked CanCHEC and thus not representative of the Canadian adult population.

Copollutants Weaken the Association Inclusion of copollutants O_3 or O_x in two-pollutant models with $PM_{2.5}$ weakened

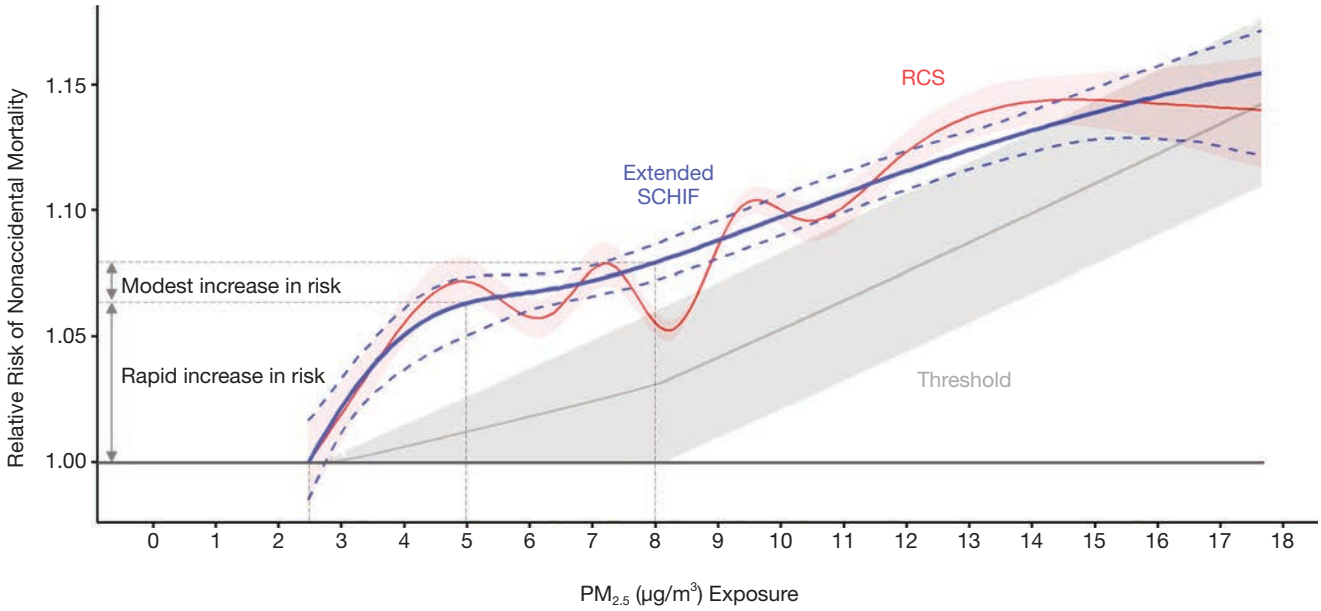

Commentary Figure 4. Concentration–response curves for ambient $PM_{2.5}$ exposure and relative risk of nonaccidental mortality in the Stacked CanCHEC cohort. The RCS and extended SCHIF 95% CIs are wider at low and high $PM_{2.5}$ levels to reflect greater uncertainty in the hazard ratio at these levels of exposure relative to the mean concentration. (Adapted from Investigators' Report Figures 20 and 29.)

the associations between $PM_{2.5}$ exposure and total nonaccidental mortality in the Stacked CanCHEC cohort (O_3-adjusted HR per IQR: 1.016; 95% CI: 1.011–1.021; O_x-adjusted HR per IQR: 1.096; 95% CI: 1.091–1.101). Two-pollutant nonlinear models that included O_3 or O_x flattened the concentration–response curves for $PM_{2.5}$ exposure and total nonaccidental mortality in the Stacked CanCHEC cohort.

Airsheds and Copollutants Modify the Association Analyses of different regional airsheds across Canada revealed considerable variation in the association and shape of the concentration–response curve by place. In the Stacked CanCHEC, $PM_{2.5}$ concentration–response curves using RCS for the East Central, Southern Atlantic, Western, and Northern airsheds varied in shape but generally showed increases in total nonaccidental mortality across $PM_{2.5}$ concentrations. In contrast, the Prairie and West Central airsheds showed minimal increased mortality for $PM_{2.5}$ concentrations from 2.5 to 5 μg/m³ and then an inverse association with mortality for $PM_{2.5}$ concentrations from 5 to 8 μg/m³ (see Investigators' Report Table 16 and Figure 21). Further sensitivity analyses that adjusted for proximity to healthcare resources or excluded immigrants, Indigenous people, or older age groups suggested that the variation was not due to differences in population characteristics or healthcare access by regional airshed. Instead, Brauer and colleagues hypothesized that the regional variation in the $PM_{2.5}$–mortality relationship could be due to differences in PM chemical composition and pollutant mixtures, including copollutants O_3 and O_x, which are known to vary over space and time. In addition, stratified analyses found larger associations between $PM_{2.5}$ and nonaccidental mortality in the highest O_3 or O_x exposure terciles. As such, they recommended that future studies evaluate interactions between mixtures of $PM_{2.5}$ chemical constituents and $PM_{2.5}$ with other copollutants.

EVALUATION BY THE HEI LOW-EXPOSURE EPIDEMIOLOGY STUDIES REVIEW PANEL

EVALUATION OF STUDY DESIGN AND APPROACH

The MAPLE Study examined whether long-term low-level air pollution exposure was associated with nonaccidental death among five population-based cohorts comprising 7.6 million Canadian adults. The investigators combined information from satellites, ground monitors, and models to estimate fine-scale $PM_{2.5}$ concentrations across Canada between 1981 and 2016. They assigned 10-year moving average exposure with a 1-year lag using complete residential histories and followed people for up to 25 years. Long-term $PM_{2.5}$ exposure was associated with increased risk of total nonaccidental mortality, including deaths caused by several cardiovascular and respiratory-related diseases and by diabetes. The MAPLE cohort included 20% of noninstitutionalized adults and was geographically representative of the Canadian population. Overall, the collection and analysis of such high-quality and comprehensive data over more than two decades was a major accomplishment.

This study addressed important research gaps in understanding the health effects of low-level ambient air pollution. Regulators want to know whether tightening $PM_{2.5}$ standards below current levels might benefit public health. The U.S. EPA's 2019 Integrated Science Assessment asserted that the scientific evidence supported a nonthreshold, linear association between $PM_{2.5}$ and adverse health effects, with limited and uncertain evidence of a supralinear shape at lower $PM_{2.5}$ concentrations (U.S. EPA 2019). Consequently, the U.S. EPA invited information on the shape of the concentration–response curve, particularly at concentrations below 8 μg/m³. Because Canada boasts some of the cleanest ambient air quality globally with a large proportion of the population who experience low exposures (HEI 2017), it was an ideal setting to address these research questions. Indeed, half of all person-years in the Stacked CanCHEC cohort were estimated to have $PM_{2.5}$ exposures at concentrations less than 8.26 μg/m³ averaged over the entire study period, and a quarter were below 6.26 μg/m³. These exposures were lower than those seen in most prior studies (Chen and Hoek 2020), enabling Brauer and colleagues to evaluate the lower end of the concentration–response curve.

Evaluation of Air Pollution Models and Exposure Estimation

The investigators developed highly detailed $PM_{2.5}$ exposure models that incorporated information from ensemble satellite measurements, atmospheric modeling, government and supplemental ground monitor measurements, and land use. Phase 2 refinements to the exposure models demonstrably improved the exposure estimation. Although the investigators incorporated new colocated measurements at five sites with lower ambient air pollution, data remained sparse across rural, less polluted areas. The Panel appreciated that the investigators acknowledged this potential measurement error given the MAPLE study's emphasis on capturing low $PM_{2.5}$ exposure concentrations. Favorably, the epidemiological analyses were weighted more toward highly populated areas in cities and near the U.S. border with less exposure measurement error. Yet it is uncertain how exposure measurement error may have affected analyses that focused on the lower observed exposure ranges, particularly in mostly rural regional airsheds with no major cities.

Evaluation of Epidemiological Analysis

A major strength of this study was the thorough epidemiological analysis. The analysis of the concentration–response curve was impressive, using three different nonlinear modeling techniques. The investigators assessed cause-specific mortality, adjusted for copollutants O_3 and O_x, and analyzed findings by regional airshed. They also conducted sensitivity analyses that restricted the cohort to people with $PM_{2.5}$ exposures below the current U.S. and former Canadian standards of 12 and 10 μg/m³, respectively. Analyses were applied to the five cohorts, allowing them to compare results across different time periods, length of follow-up, and with different covariate adjustments.

Although all methods consistently showed associations of increased mortality with greater $PM_{2.5}$ levels, the Panel was unclear about how to interpret findings from some of the statistical methods, including the lowest $PM_{2.5}$ concentration at which the lower confidence limit of the HR was greater than or equal to one, and uncertainty estimates for the extended SCHIF. For the former, it is unclear how statistically appropriate and robust this approach is for estimating a potential threshold, as discussed further below. For the latter, the RCS simulations used as input for the extended SCHIF model were not clearly frequentist or Bayesian, thus the statistical properties of the uncertainty estimates and how they relate to standard approaches is unclear. Further details on the rationale and limitations of these methods would have improved the report. Despite this, the standard statistical approaches that were used reached similar substantive conclusions.

DISCUSSION OF THE FINDINGS AND INTERPRETATION

Brauer and colleagues found that long-term low-level ambient $PM_{2.5}$ exposures averaged over ten years, with a 1-year lag were associated with an increased risk of total nonaccidental mortality, as well as for several specific causes. The increased risk for total, respiratory-, and cardiovascular-related mortality is consistent with a recent meta-analysis (Chen and Hoek 2020), and the increased risk for diabetes mortality was recently reported in large U.S.-based cohort studies (Bowe et al. 2019; Lim et al. 2018). However, the lack of an association between $PM_{2.5}$ and lung cancer conflicts with prior research that demonstrated relatively consistent positive associations (Ciabattini et al. 2021; Pope et al. 2002).

Shape of the Concentration–Response Function

The investigators observed a rapid increase in mortality risk for person-years exposed to long-term $PM_{2.5}$ concentrations between 2.5 μg/m³ and 5 μg/m³ in both the RCS and extended SCHIF curves. Between $PM_{2.5}$ concentrations of 5 and 8 μg/m³, the RCS concentration–response curve demonstrated only a modest increase in the mortality risk where the slope of the curve was shallower. Mortality risk increased at an intermediate rate and was approximately linear for the RCS and extended SCHIF models above 8 and 5 μg/m³, respectively. The supralinear curve at low concentrations and near linearity at higher concentrations is consistent with concentration–response curves estimated in a recent study of over 325,000 Europeans with average $PM_{2.5}$ exposures below 25 μg/m³ (Brunekreef et al. 2021; Strafoggia et al. 2022; Strak et al. 2021) and in a study that combined

41 cohorts with varying levels of exposure from across the globe (Burnett et al. 2018).

The immediate rise in mortality risk from the minimum $PM_{2.5}$ concentration of 2.5 μg/m³ suggests that there is no threshold for adverse health effects given the observed data. This is consistent with the investigators' threshold model analysis in which a conclusive threshold value could not be determined. The investigators approximated a threshold value by reporting the $PM_{2.5}$ concentration (2.8 μg/m³) at which the 95% CI lower limit exceeded one in the RCS curve. However, the Panel was unclear on how to interpret this metric. The approach as implemented does not account for the uncertainty in the HR at the minimum exposure concentration. Therefore, it does not estimate the uncertainty for the difference in the mortality risk at a given exposure concentration compared with the minimum exposure concentration, thereby preventing a robust statistical assessment with regard to the presence of a threshold. The absence of evidence for a threshold is consistent with most prior studies that evaluated thresholds (Chen and Hoek 2020). This reinforces that we currently have no evidence of a $PM_{2.5}$ concentration below which there is no association with health effects. Further, the investigators' health impact analysis projected that $PM_{2.5}$ reductions within the 2.5 to 5 μg/m³ range would benefit the largest proportion of the sample population. Overall, evidence from this study supports the 2021 WHO Air Quality Guidelines of 5 μg/m³ and suggests that achieving ambient $PM_{2.5}$ concentrations below 5 μg/m³ where the curve demonstrates supralinearity could prevent premature mortality.

The segment of the RCS concentration–response curve in the middle $PM_{2.5}$ concentration range between 5 and 8 μg/m³ demonstrated a shallower slope relative to segments of the curve in lower and higher concentration ranges. The RCS curve also demonstrated up-and-down undulations in this middle concentration range. These results imply that incremental reductions within this middle range may not yield substantial health benefits. However, this segment of the RCS curve must be interpreted cautiously due to its inconsistency with prior evidence and lack of biological plausibility. The investigators concluded that the undulations in the RCS curves were partly due to the large sample size which statistically favored many knots, resulting in an RCS curve that is likely under-smoothed relative to the true unknown curve. Due to different results for the individual cohorts, which can serve as a proxy for different results over time, the investigators also suggested that undulations in the curve may be due to lower data quality prior to 2001. The Panel noted that it is possible that the undulating portion of the RCS curve is a true reflection of the data and potentially due to complex features such as exposure measurement error and aggregation of heterogeneous responses to air pollution across different populations and spatial regions. When evaluating potential sources of error, the study's large sample size and concomitant statistical power also imply that bias, more so than precision, should be considered when interpreting these results.

In analyses restricting the cohort to 10-year $PM_{2.5}$ exposure below the current NAAQS (12 μg/m³) and the former CAAQS and WHO Air Quality Guidelines (10 μg/m³), the investigators found that compared with the full cohort, there were lower associations for person-years below 12 μg/m³, and that there was no evidence of a positive association below 10 μg/m³ when using linear models. However, the concentration–response curves for the <10 μg/m³, <12 μg/m³, and full cohorts all demonstrated similar steep increases in mortality for exposure concentrations <5 μg/m³. The investigators suggested that the observed associations at low to moderate concentrations in the full cohort were strongly influenced by the inclusion of person-years with higher $PM_{2.5}$ exposure. The Panel disagreed with this interpretation given the use of flexible RCS models in which adjacent segments of the curve generally do not overly influence each other. The investigators noted that restricting the analyses to person-years with these lower exposure concentrations changed the cohort composition, raising potential concerns about differences in associations across populations or locations. Therefore, the actual health benefits of achieving lower $PM_{2.5}$ exposures across the entire country remain uncertain, although likely beneficial. The linear model results in this study were inconsistent with a recent study that analyzed a subsample of older U.S. adults with 1-year $PM_{2.5}$ exposures below 12 μg/m³ (Dominici et al. 2022) and with a meta-analysis that evaluated results for groups of studies with successively lower mean exposure (Chen and Hoek 2020); those studies showed larger effect estimates among people with lower exposures. A possible explanation for this discrepancy is the flatter slope segment of the concentration–response curve in the current study, which spanned concentrations 5 to 8 μg/m³. If analyses restricted person-years to below 5 μg/m³, the steeper slope portion of the concentration–response curve might have resulted in a larger effect estimate in the linear model.

Differences in Associations Due to PM Composition and Pollutant Mixtures

The RCS concentration–response curves generally increased across $PM_{2.5}$ concentrations for four of the airsheds. In contrast, the concentration–response curves for the Prairie and West Central airsheds showed only small increased mortality risk with subtle undulations for low $PM_{2.5}$ concentrations, followed by decreased risk near 8 μg/m³. These results were mirrored in the linear models where $PM_{2.5}$ was associated with lower risk of mortality in the Prairie and West Central airshed. Thus, it is possible that the Prairie and West Central airsheds were responsible for driving the low slope and undulating segment in the overall curve for Canada. Although the investigators adjusted for a wide range

of individual level and spatial covariates and performed sensitivity analyses to control for disparate demographic makeup and healthcare access, residual confounding could be responsible for the regional variation. Regional heterogeneity across North America, but not in Europe, has previously been reported in a meta-analysis of long-term $PM_{2.5}$ exposure and mortality (Chen and Hoek 2020). Consequently, aggregating data across certain geographic regions might have limitations unless the underlying cause of the heterogeneity can be determined. In the end, the investigators hypothesized that regional variation may partly be attributed to regional differences in $PM_{2.5}$ composition. This notion is supported by the varied chemical composition of the colocated sampling measurements in five of the airsheds. It is also supported by prior research indicating that individual $PM_{2.5}$ chemical components vary by geography and in elicited adverse health effects (Dai et al. 2014; Davis et al. 2011; Lippmann et al. 2013). In this study the colocated measurements only served as a supplemental input to the exposure modeling and were not used in the health analysis directly. Note also that the regional variation is unlikely to be solely due to differences in the concentrations of copollutants O_3 and O_x as the Prairie and West Central airsheds had distributions of these pollutants similar to the other airsheds.

Although the effects of $PM_{2.5}$ chemical composition in the MAPLE study were speculative, the results showed that adjusting for copollutants O_3 and O_x attenuated the association between $PM_{2.5}$ and mortality, and inclusion of these copollutants in the nonlinear models flattened the RCS concentration–response curves. This result is consistent with the findings from numerous previous studies (Dominici et al. 2022; U.S. EPA 2019). In stratified analyses, the largest effect sizes were observed for $PM_{2.5}$ and mortality in the highest O_3 and O_x tertiles, suggesting that these gases play an important role in determining the adverse health effects of $PM_{2.5}$. Recent studies in Europe and the United States indicated that NO_2 was also an important copollutant (Brunekreef et al. 2021; Dominici et al. 2022). Brauer and colleagues assessed NO_2 exposure but did not evaluate it in the MAPLE study Phase 2, given the Phase 1 results demonstrating minimal effect of adjusting for NO_2 on the association between $PM_{2.5}$ and mortality. Note that these multipollutant results must be interpreted in light of the fact that O_3, O_x, and NO_2 were estimated at coarser spatial resolutions than $PM_{2.5}$. Given the sensitivity of the association between $PM_{2.5}$ and mortality to copollutants O_3 and O_x, it will be important to investigate this issue in future studies.

Generalizability of the Findings

The size of the study populations was unprecedented and allowed detailed investigations for the questions at hand. The Panel noted that despite the large size of the MAPLE cohort, the results might not be generalizable to the Canadian population as a whole. Although the response and data linkage rates were high for both the CanCHEC and CCHS cohorts, successive steps in assembling cohort data incrementally reduced inclusivity and generalizability. Census quality reports indicate that 4% of the Canadian population are not enumerated in CanCHEC and tend to be younger, mobile, low income, homeless, or Indigenous peoples (Tjepkema et al. 2019). After imputation, 90% of person-years were linked to a valid postal code. Because this linkage is based on tax records, unlinked person-years are presumably associated with lower income. Explicit exclusion criteria was more likely to remove immigrants and older individuals, and implicit exclusion criteria by way of missing data were more likely to remove minorities, Indigenous peoples, and individuals who were unemployed or lived in rural and Northern communities. Because socioeconomically disadvantaged subsets of the population might be more susceptible to both exposure and the adverse health effects of poor ambient air quality (Deguen and Zmirou-Navier 2010; Hajat et al. 2015), it is important to keep in mind that results from this study might portray a more optimistic scenario than the reality.

CONCLUSIONS

The MAPLE study aimed to characterize the association between nonaccidental mortality and long-term exposure to ambient $PM_{2.5}$ concentrations lower than most of the world. Brauer and colleagues developed fine-scale satellite-, monitor-, and model-based $PM_{2.5}$ exposure estimates across North America from 1981 to 2016. They applied comprehensive epidemiological analyses in a large representative sample of Canadian adults to identify the shape of the concentration–response curve and the lowest $PM_{2.5}$ concentration at which associations with health effects could be detected.

The study demonstrated that 10-year $PM_{2.5}$ exposures were associated with increased total and cause-specific mortality. Given the minimum observed exposure of 2.5 $\mu g/m^3$, the findings support a nonthreshold, supralinear concentration–response curve.

The Panel commended the investigators' impressive accomplishments and agree that the results show a positive association with mortality even at $PM_{2.5}$ concentrations below the current U.S. ambient air quality standard of 12 $\mu g/m^3$. Yet they noted that uncertainty remains in how to interpret some of the results, including the low-slope segment of the RCS concentration–response curve for middle concentration ranges and differences by regional airshed. The influence of individual PM chemical components, copollutants, and residual confounding on the results remains uncertain. Further interpretation of findings and further description for some of the nonstandard statistical methods would have enhanced the report. Future work is warranted to build on

the MAPLE study findings, including analyses of PM composition, multipollutant models, and further refinement of concentration–response curve methods.

ACKNOWLEDGMENTS

The HEI Review Committee is grateful to the Low-Exposure Epidemiology Studies Review Panel for their thorough review of the study. The Committee is also grateful to Hanna Boogaard for oversight of the study; to Eleanne van Vliet, Annemoon van Erp, and Martha Ondras for assistance with review of the report; to Eva Tanner for assistance with review of the report and in preparing its Commentary; to Carol Moyer for editing of this Report and its Commentary; and to Hope Green and Kristin Eckles for their roles in preparing this Research Report for publication.

REFERENCES

Beelen R, Raaschou-Nielsen O, Stafoggia M, Andersen ZJ, Weinmayr G, Hoffmann B, et al. 2014. Effects of long-term exposure to air pollution on natural-cause mortality: An analysis of 22 European cohorts within the multicentre ESCAPE project. Lancet 383:785–795; doi:10.1016/S0140-6736(13)62158-3.

Bowe B, Xie Y, Yan Y, Al-Aly Z. 2019. Burden of cause-specific mortality associated with $PM_{2.5}$ air pollution in the United States. JAMA Netw Open 2:e1915834; doi:10.1001/jamanetworkopen.2019.15834.

Brauer M, Brook JR, Christidis T, Chu Y, Crouse DL, Erickson A, et al. 2019. Mortality–Air Pollution Associations in Low-Exposure Environments (MAPLE): Phase 1. Research Report 203. Boston, MA:Health Effects Institute.

Brunekreef B, Strak M, Chen J, Andersen ZJ, Atkinson R, Bauwelinck M, et al. 2021. Mortality and Morbidity Effects of Long-Term Exposure to Low-Level $PM_{2.5}$, BC, NO_2, and O_3: An Analysis of European Cohorts in the ELAPSE Project. Research Report 208. Boston, MA:Health Effects Institute.

Burnett R, Chen H, Szyszkowicz M, Fann N, Hubbell B, Pope CA 3rd, et al. 2018. Global estimates of mortality associated with long-term exposure to outdoor fine particulate matter. Proc Natl Acad Sci USA 115:9592–9597; doi:10.1073/pnas.1803222115.

CCME (Canadian Council of Ministers of the Environment). 2021. Canada's Air. Available: *https://ccme.ca/en/air-quality-report* [accessed 4 November 2021].

Chen J, Hoek G. 2020. Long-term exposure to PM and all-cause and cause-specific mortality: A systematic review and meta-analysis. Environ Int 143:105974; doi.org/10.1016/j.envint.2020.105974.

Ciabattini M, Rizzello E, Lucaroni F, Palombi L, Boffetta P. 2021. Systematic review and meta-analysis of recent high-quality studies on exposure to particulate matter and risk of lung cancer. Environ Res 196:110440; doi.org/10.1016/j.envres.2020.110440.

Crouse DL, Peters PA, Hystad P, Brook JR, van Donkelaar A, Martin RV, et al. 2015. Ambient $PM_{2.5}$, O_3, and NO_2 exposures and associations with mortality over 16 years of follow-up in the Canadian census health and environment cohort (CanCHEC). Environ Health Perspect 123:1180–1186; doi:10.1289/ehp.1409276.

Crouse DL, Peters PA, van Donkelaar A, Goldberg MS, Villeneuve PJ, Brion O, et al. 2012. Risk of non-accidental and cardiovascular mortality in relation to long-term exposure to low concentrations of fine particulate matter: A Canadian national-level cohort study. Environ Health Perspect 120:708–714; doi:10.1289/ehp.1104049.

Dai L, Zanobetti A, Koutrakis P, Schwartz JD. 2014. Associations of fine particulate matter species with mortality in the United States: A multicity time-series analysis. Environ Health Perspect 122:837–842; doi.org/10.1289/ehp.1307568.

Davis JA, Meng Q, Sacks JD, Dutton SJ, Wilson WE, Pinto JP. 2011. Regional variations in particulate matter composition and the ability of monitoring data to represent population exposures. Sci Total Environ 409:5129–5135; doi.org/10.1016/j.scitotenv.2011.08.013.

Deguen S, Zmirou-Navier D. 2010. Social inequalities resulting from health risks related to ambient air quality—A European review. Eur J Public Health 20:27–35; doi:10.1093/eurpub/ckp220.

Dominici F, Zanobetti A, Schwartz J, Braun D, Sabath B, Xiao Wuet. 2022. Assessing Adverse Health Effects of Long-Term Exposure to Low Levels of Ambient Air Pollution: Implementation of Causal Inference Methods. Research Report 211. Boston, MA:Health Effects Institute.

Global Burden of Disease (GBD) 2019 Risk Factors Collaborators. 2020. Global burden of 87 risk factors in 204 countries and territories, 1990–2019: A systematic analysis for the Global Burden of Disease Study 2019. Lancet 396:1223–1249; doi:10.1016/S0140-6736(20)30752-2.

Hajat A, Hsia C, O'Neill MS. 2015. Socioeconomic disparities and air pollution exposure: A global review. Curr Environ Health Rep 2:440–450; doi:10.1007/s40572-015-0069-5.

Hales S, Blakely T, Woodward A. 2012. Air pollution and mortality in New Zealand: Cohort study. J Epidemiol Community Health 66:468–473; doi:10.1136/jech.2010.112490.

Harrell Jr FR. 2015. Regression Modeling Strategies, 2nd edition. Switzerland:Springer International Publishing,

Health Canada. 2016. Human Health Risk Assessment for Ambient Nitrogen Dioxide. Ottowa, ON:Health Canada.

HEI (Health Effects Institute). 2017. State of Global Air 2017: A Special Report on Global Exposure to Air Pollution and Its Disease Burden. Special Report. Boston, MA:Health Effects Institute.

HEI (Health Effects Institute). 2020. State of Global Air 2020. Special Report. Boston, MA:Health Effects Institute.

Hystad P, Setton E, Cervantes A, Poplawski K, Deschenes S, Brauer M, et al. 2011. Creating national air pollution models for population exposure assessment in Canada. Environ Health Perspect 119:1123–1129; doi:10.1289/ehp.1002976.

Khan S, Pinault L, Tjepkema M, Wilkins R. 2018. Positional accuracy of geocoding from residential postal codes versus full street addresses. Health Rep 29:3–9. PMID: 29465738.

Klassen C. 2019. Casarett & Doull's Toxicology: The Basic Science of Poisons, 9th edition. New York:McGraw-Hill Education.

Krewski D, Jerrett M, Burnett RT, Ma R, Hughes E, Shi Y, et al. 2009. Extended follow-up and spatial analysis of the American Cancer Society study linking particulate air pollution and mortality. Res Rep Health Eff Inst 140:5–114; discussion 115–36.

Lim CC, Hayes RB, Ahn J, Shao Y, Silverman DT, et al. 2018. Association between long-term exposure to ambient air pollution and diabetes mortality in the U.S. Environ Res 165:330–336; doi.org/10.1016/j.envres.2018.04.011.

Lippman M, Chen L, Gordon T, Ito K, Thurston G.D. 2013. National Particle Component Toxicity (NPACT) Initiative: Integrated Epidemiologic and Toxicologic Studies of the Health Effects of Particulate Matter Components. Research Report 177. Boston, MA:Health Effects Institute.

Meng J, Li C, Martin R, van Donkelaar A, Hystad P, Brauer M. 2019. Estimated long-term (1981–2016) concentrations of ambient fine particulate matter across North America from chemical transport modeling, satellite remote sensing and ground-based measurements. Environ Sci Technol 53:5071–5079; doi:10.1021/acs.est.8b06875.

Nasari MM, Szyszkowicz M, Chen H, Crouse D, Turner MC, Jerrett M, et al. 2016. A class of non-linear exposure-response models suitable for health impact assessment applicable to large cohort studies of ambient air pollution. Air Qual Atmos Health 9:961–972; doi:10.1007/s11869-016-0398-z.

Pappin AJ, Christidis T, Pinault LL, Crouse DL, Brook JR, Erickson A, et al. 2019. Examining the shape of the association between low levels of fine particulate matter and mortality across three cycles of the Canadian Census Health and Environment Cohort. Environ Health Perspect 127:107008; doi:10.1289/EHP5204.

Pinault L, Tjepkema M, Crouse DL, Weichenthal S, van Donkelaar A, Martin RV, et al. 2016. Risk estimates of mortality attributed to low concentrations of ambient fine particulate matter in the Canadian community health survey cohort. Environ Health 15:18–31; doi:10.1186/s12940-016-0111-6.

Pope CA 3rd, Burnett RT, Thun MJ, Calle EE, Krewski D, Ito K, et al. Lung cancer, cardiopulmonary mortality, and long-term exposure to fine particulate air pollution. JAMA 287:1132–1141; doi:10.1001/jama.287.9.1132.

Robichaud A, Ménard R. 2014. Multi-year objective analyses of warm season ground-level ozone and $PM_{2.5}$ over North America using real-time observations and Canadian operational air quality models. Atmos Chem Phys 14:1769–1800; doi:10.5194/acp-14-1769-2014.

Robichaud A, Ménard R, Zaïtseva Y, Anselmo D. 2016. Multi-pollutant surface objective analyses and mapping of air quality health index over North America. Air Qual Atmos Health 9:743–759; doi:10.1007/s11869-015-0385-9.

Stafoggia M, Oftedal B, Chen J, Rodopoulou S, Renzi M, Atkinson RW, et al. 2022. Long-term exposure to low ambient air pollution concentrations and mortality among 28 million people: results from seven large European cohorts within the ELAPSE project. Lancet Planet Health 16:E9–E19. Available: *https://doi.org/10.1016/S2542-5196(21)00277-1*.

Strak M, Weinmayr G, Rodopoulou S, Chen J, de Hoogh K, Andersen ZJ, et al. 2021. Long-term exposure to low level air pollution and mortality in eight European cohorts within the ELAPSE project: Pooled analysis. BMJ 374:n1904. Available: *http://dx.doi.org/10.1136/bmj.n1904*.

Tjepkema M, Christidis T, Bushnik T, Pinault L. 2019. Cohort profile: the Canadian Census Health and Environment Cohorts (CanCHECs). Health Rep 30:18–26; doi:10.25318/82-003-x201901200003-eng.

U.S. EPA (Environmental Protection Agency). 2013. Integrated Science Assessment (ISA) for Ozone and Related Photochemical Oxidants. EPA/600/R-10/076F. Washington, DC:U.S. Environmental Protection Agency.

U.S. EPA (Environmental Protection Agency). 2019. Integrated Science Assessment (ISA) for Particulate Matter. EPA/600/R-19/188. Washington, DC:U.S. Environmental Protection Agency.

U.S. EPA (Environmental Protection Agency). 2015. Preamble to the Integrated Science Assessments (ISA). EPA/600/R-15/067. Washington, DC:U.S. Environmental Protection Agency.

U.S. EPA (Environmental Protection Agency). 2004. Vol I. PM Air Quality Criteria Document. Washington, DC:U.S. Environmental Protection Agency.

van Donkelaar A, Martin RV, Li C, Burnett RT. 2019. Regional estimates of chemical composition of fine particulate matter using a combined geoscience-statistical method with information from satellites, models, and monitors. Environ Sci Technol 53:2595–2611. Available: *https://doi.org/10.1021/acs.est.8b06392*.

Weichenthal S, Pinault LL, Burnett RT. 2017. Impact of oxidant gases on the relationship between outdoor fine particulate air pollution and nonaccidental, cardiovascular, and respiratory mortality. Sci Rep 7:16401; doi:10.1038/s41598-017-16770-y.

WHO (World Health Organization). 2021. WHO Global Air Quality Guidelines. Particulate Matter ($PM_{2.5}$ and PM_{10}), Ozone, Nitrogen Dioxide, Sulfur Dioxide and Carbon Monoxide. Geneva:World Health Organization.

ABBREVIATIONS AND OTHER TERMS

AERONET	Aerosol Robotic Network
AIC	Akaike information criterion
AOD	aerosol optical depth
BIC	Bayesian information criterion
BMI	body mass index
CA	census agglomeration
CAAQS	Canadian Ambient Air Quality Standards
CAN-Marg	Canadian Marginalization Index
CanCHEC	Canadian Census Health and Environment Cohort
CCHS	Canadian Community Health Survey
CCME	Canadian Council of Ministers of the Environment
CI	confidence interval
CMA	census metropolitan area
COPD	chronic obstructive pulmonary disease
ESCAPE	European Study of Cohorts for Air Pollution Effects
eSCHIF	extended shape constrained health impact function
GBD	global burden of disease
GEMM	Global Exposure Mortality Model
GEOS-Chem	GEOS-Chem chemical transport model
HR	hazard ratio
ICD	International Classification of Disease
IQR	interquartile range
MAPLE	Mortality–Air Pollution Associations in Low Exposure Environments
mCCHS	CCHS mortality cohort
MSE	mass scattering efficiency
NAAQS	National Ambient Air Quality Standards
NAPS	National Air Pollution Surveillance
NO_2	nitrogen dioxide
O_3	ozone
O_x	gaseous pollutant oxidant capacity
PAF	population attributable fraction
PCCF+	Postal Code Conversion File Plus
PM	particulate matter
$PM_{2.5}$	particulate matter ≤2.5 µm in aerodynamic diameter
R^2	coefficient of determination
RCS	restricted cubic splines
RFA	request for applications
RMSD	room mean square difference
SCHIF	shape constrained health impact function
SD	standard deviation
SE	standard error
SIA	secondary inorganic aerosol
SO_2	sulfur dioxide
SPARTAN	Surface PARTiculate mAtter Network
TSP	total suspended particulate matter
U.S. EPA	U.S. Environmental Protection Agency
WHO	World Health Organization

RELATED HEI PUBLICATIONS

Number	Title	Principal Investigator	Date
Research Reports			
211	Assessing Adverse Health Effects of Long-Term Exposure to Low Levels of Ambient Air Pollution: Implementation of Causal Inference Methods	F. Dominici	2022
208	Mortality and Morbidity Effects of Long-Term Exposure to Low-Level $PM_{2.5}$, BC, NO_2, and O_3: An Analysis of European Cohorts in the ELAPSE Project	B. Brunekreef	2021
203	Mortality–Air Pollution Associations in Low-Exposure Environments (MAPLE): Phase 1	M. Brauer	2019
200	Assessing Adverse Health Effects of Long-Term Exposure to Low Levels of Ambient Air Pollution: Phase 1	F. Dominici	2019
193	Particulate Air Pollutants, Brain Structure, and Neurocognitive Disorders in Older Women	J-C. Chen	2017
192	Multicenter Ozone Study in older Subjects (MOSES): Part 1. Effects of Exposure to Low Concentrations of Ozone on Respiratory and Cardiovascular Outcomes	M.W. Frampton	2017
187	Causal Inference Methods for Estimating Long-Term Health Effects of Air Quality Regulations	C.M. Zigler	2016
183	Development of Statistical Methods for Multipollutant Research	B.A. Coull	2015
142	Air Pollution and Health: A European and North American Approach	K. Katsouyanni	2009
140	Extended Follow-Up and Spatial Analysis of the American Cancer Society Study Linking Particulate Air Pollution and Mortality	D. Krewski	2009
139	Effects of Long-Term Exposure to Traffic-Related Air Pollution on Respiratory and Cardiovascular Mortality in the Netherlands: The NLCS-AIR Study	B. Brunekreef	2009
Special Report			
	Reanalysis of the Harvard Six Cities Study and the American Cancer Society Study of Particulate Air Pollution and Mortality	Health Effects Institute	2000

Copies of these reports can be obtained from HEI; PDFs are available for free downloading at www. healtheffects.org/publications.

HEI BOARD, COMMITTEES, and STAFF

Board of Directors

Richard A. Meserve, Chair *Senior of Counsel, Covington & Burling LLP; President Emeritus, Carnegie Institution for Science; former Chair, U.S. Nuclear Regulatory Commission*

Enriqueta Bond *President Emerita, Burroughs Wellcome Fund*

Jo Ivey Boufford *President, International Society for Urban Health*

Homer Boushey *Emeritus Professor of Medicine, University of California–San Francisco*

Michael T. Clegg *Professor of Biological Sciences, University of California–Irvine*

Jared L. Cohon *President Emeritus and Professor, Civil and Environmental Engineering and Engineering and Public Policy, Carnegie Mellon University*

Stephen Corman *President, Corman Enterprises*

Martha J. Crawford *Operating Partner, Macquarie Asset Management*

Michael J. Klag *Dean Emeritus and Second Century Distinguished Professor, Johns Hopkins Bloomberg School of Public Health*

Alan I. Leshner *CEO Emeritus, American Association for the Advancement of Science*

Catherine L. Ross *Regents' Professor and Harry West Professor of City and Regional Planning and Civil and Environmental Engineering, and Director of the Center for Quality Growth and Regional Development, Georgia Institute of Technology*

Karen C. Seto *Frederick Hixon Professor of Geography and Urbanization Science, Yale School of the Environment*

Research Committee

David A. Savitz, Chair *Professor of Epidemiology, School of Public Health, and Professor of Obstetrics and Gynecology, Alpert Medical School, Brown University*

Jeffrey R. Brook *Assistant Professor, University of Toronto, Canada*

Amy H. Herring *Sara & Charles Ayres Professor of Statistical Science and Global Health, Duke University*

Barbara Hoffmann *Professor of Environmental Epidemiology, Institute of Occupational, Social, and Environmental Medicine, University of Düsseldorf, Germany*

Heather A. Holmes *Associate Professor, Department of Chemical Engineering, University of Utah*

Neil Pearce *Professor of Epidemiology and Biostatistics, London School of Hygiene and Tropical Medicine, United Kingdom*

Ana Rule *Assistant Professor and Director, Environmental Exposure Assessment Laboratories, Department of Environmental Health and Engineering, Johns Hopkins School of Public Health*

Ivan Rusyn *Professor, Department of Veterinary Integrative Biosciences, Texas A&M University*

Evangelia (Evi) Samoli *Associate Professor of Epidemiology and Medical Statistics, Department of Hygiene, Epidemiology and Medical Statistics, School of Medicine, National and Kapodistrian University of Athens, Greece*

Gregory Wellenius *Professor, Department of Environmental Health, Boston University School of Public Health*

Review Committee

Melissa Perry, Chair *Professor and Chair, Department of Environmental and Occupational Health, George Washington University Milken Institute School of Public Health*

Sara D. Adar *Associate Professor and Associate Chair, Department of Epidemiology, University of Michigan School of Public Health*

Kiros Berhane *Professor and Chair, Department of Biostatistics, Mailman School of Public Health, Columbia University*

HEI BOARD, COMMITTEES, and STAFF

Michael Jerrett *Professor and Chair, Department of Environmental Health Sciences, Fielding School of Public Health, University of California–Los Angeles*

Frank Kelly *Henry Battcock Chair of Environment and Health and Director of the Environmental Research Group, Imperial College London School of Public Health, United Kingdom*

Jana B. Milford *Professor, Department of Mechanical Engineering and Environmental Engineering Program, University of Colorado–Boulder*

Jennifer L. Peel *Professor of Epidemiology, Colorado School of Public Health and Department of Environmental and Radiological Health Sciences, Colorado State University*

Eric J. Tchetgen Tchetgen *Luddy Family President's Distinguished Professor, Professor of Statistics and Data Science, The Wharton School, University of Pennsylvania*

Officers and Staff

Daniel S. Greenbaum *President*

Robert M. O'Keefe *Vice President*

Ellen K. Mantus *Director of Science*

Donna J. Vorhees *Director of Energy Research*

Annemoon M. van Erp *Deputy Director of Science*

Thomas J. Champoux *Director of Science Communications*

Jacqueline C. Rutledge *Director of Finance and Administration*

Jason Desmond *Deputy Director of Finance and Administration*

Emily Alden *Corporate Secretary*

Amy Andreini *Communications Assistant*

Palak Balyan *Consulting Staff Scientist*

Hanna Boogaard *Consulting Principal Scientist*

Aaron J. Cohen *Consulting Principal Scientist*

Dan Crouse *Senior Scientist*

Robert M. Davidson *Staff Accountant*

Philip J. DeMarco *Compliance Manager*

Kristin C. Eckles *Senior Editorial Manager*

Elise G. Elliott *Staff Scientist*

Hope Green *Editorial Project Manager*

Yi Lu *Staff Scientist*

Lissa McBurney *Senior Science Administrator*

Janet I. McGovern *Executive Assistant*

Martha Ondras *Research Fellow*

HEI BOARD, COMMITTEES, and STAFF

Pallavi Pant *Senior Scientist*
Allison P. Patton *Senior Scientist*
Quoc Pham *Science Administrative Assistant*
Anna S. Rosofsky *Senior Scientist*
Robert A. Shavers *Operations Manager*
Eva Tanner *Staff Scientist*

HEALTH
EFFECTS
INSTITUTE

75 Federal Street, Suite 1400
Boston, MA 02110, USA
+1-617-488-2300
www.healtheffects.org

RESEARCH
REPORT

Number 212
July 2022